A clinical and ultrastructural investigation of the cornea in keratoconus

A thesis submitted to Cardiff University for the degree of

Doctor of Philosophy

By

Abdullah A. M. Assiri B.Sc. (Optom)

School of Optometry & Vision Sciences

Cardiff University

November 2005

ProQuest LLC
789 East Eisenhower Parkway
P.O. Box 1346
Ann Arbor, MI 48106-1346

Abstract

The cornea is the transparent part at the front of the eyeball that works as a window to the world, and acts as a strong barrier protecting the inner eye against infection and trauma. Keratoconus is a corneal disease that progressively causes topographical alteration of the cornea as a result of thinning, and consequently leads to impaired vision.

The purpose of this thesis was to study keratoconus and the possible structural mechanism by which the cornea becomes misshapen by a number of techniques, ranging from the epidemiological to the structural. In doing so it was aimed to provide new information that might help us better understand the overall concept of keratoconus and the loss of vision due to corneal shape changes.

First, population study of keratoconus was undertaken in Saudi Arabia to see how people there are affected. The influence of ethnic origin on the incidence rate and severity of keratoconus has been suggested to be of significant importance. Investigation of the incidence rate, onset age and associated signs and symptoms of patients with keratoconus was carried out. The results showed that the incidence rate and severity of keratoconus in Asir Province, Saudi Arabia is high with an early onset and more rapid progress to the severe disease stage at a young age. This, I propose, high lights the influence of genetic and/or environmental factor(s) in the aetiology of keratoconus.

Due to the unpredictable nature of keratoconus progression, the best contact lens design is also difficult to predict. Therefore, in this study several lens designs were used to assess the correlation between Rigid Gas Permeable (RGP) lens design and keratoconus severity, and to assess the relationship between the optimum lens choice and the keratometric readings in order to improve the speed of lens fitting. The results showed that the Tricurve lens design with 9 mm diameter is the best at first, regardless of the stage of disease.

Regular and Steep McGuire lens designs with 8.6 mm diameter are a suitable second option. However, in the advance stage, the McGuire Steep lens design is more effective than the McGuire Regular and Tricurve designs. The Percon lens design with a 9.4 mm diameter is suitable for some cases in the early stages of the disease. The results also showed that the initial back optic zone radius for Tricurve lens design may be based on the average keratometric reading. For Regular and Steep McGuire lens designs, lens selection should base on the steepest keratometric reading. However, in moderate and advanced stages it may be selected on the average keratometric reading. For the Percon lens design, it may be based on the flattest keratometric reading.

The work then moved on to the laboratory to try and understand the role that Bowman's layer might play in the corneal shape changes that yield vision loss in keratoconic eyes. Breaks in Bowman's layer in keratoconus have been reported in the literature. Investigation in Bowman's layer of keratoconus corneas obtained after surgery using different microscopes revealed that the changes are not limited to the apical cone only, but extent to the periphery of the cornea especially in the advanced stage of keratoconus. This might explain postoperative keratoconus reoccurrences in some patients. Although the topographical map is usually used in trephination, it was found here that the topographical features alone failed to indicate the full extent of the progress of keratoconus towards the corneal periphery.

In an attempt to more fully understand the link between corneal ultrastructure and shape change light and transmission electron microscopy was used to investigate the internal fine structure of the corneas of a strain of mice the (SPARC-deficient mice) that are predisposed to corneal shape changes. This revealed thin corneas with a slightly larger collagen fibril diameter, with a normal appearance of proteoglycans. Furthermore, a sharp decrease in collagen fibril number density was observed across the thickness of the stroma. It is postulated that the structural matrix changes might weaken the cornea and lead to ectasia.

A controlling influence on corneal shape in humans is thought to be the circumferential ring or annulus of collagen fibrils at the limbus. Some preliminary published evidence is consistent with the possibility of a limbal annulus in the mouse cornea, but its presence has not been proven. Therefore, high-angle X-ray diffraction was used to investigate the orientation of collagen fibrils throughout the whole cornea in the mouse. The study revealed that the preferred alignment of collagen fibrils at the centre of the cornea was mainly in the vertical meridian. This is not the situation in the human cornea where an orthogonal arrangement predominates. The study also demonstrated the presence of a limbal annulus of circumferential collagen fibrils at the edge of the cornea in the mouse as is the case in humans. Further, the current study discovered that the collagen fibril orientation in the corneas of mice predisposed to shape changes (SPARC-null and JKC strains) was often altered compared to that from normal cornea. The data suggest that structural abnormalities in the stromal fibrillar matrix might be influential underlying reasons for topographic changes in the animal models.

DEDICATION

I dedicate this work to my late father and to my love mother who have spent whole life together nurturing in me the love, faith and ability to learn and study.

I dedicate this work also to my wife *Jamilah* who scarified a lot throughout the period of my study. She is a wonderful wife, a great mother and a reliable fellow.

My appreciation extends to my love children

Riyadh, Ghadah, Raghadh, Talah and the cheerful little boy *Ibrahim* for being with me always. My life without them is meaningless.

To father-in-law the late *Ibrahim Hussein.*

To my love brothers and sisters and all other relatives and friends.

Acknowledgements

First and foremost, I must praise and thank constantly almighty Allah (God) for giving me countless grace that helps me to complete this work.

I must sincerely thank my supervisor Dr. Andrew J. Quantock for his positive guidance, enthusiasm and invaluable suggestions and encouragement during the course of this research. Andrew has been a nice supervisor, always modest, helpful, appreciative of my personality, and I was able to speak with him by any way and at any time.

The same sincere thank go to my co-supervisor Prof. Keith M. Meek for his keenness, invaluable suggestions, support and comments. In summary, it has been an amusement and honour to know and work with them.

I would like to express my deep, sincere thanks to Dr. Robert D. Young for his honest friendship and excellent help. Robert's willingness to help and share his experience in microscopy and for reading and commenting on my first draft is appreciated and gratefully acknowledged. I also express my deep, sincere thanks to Dr. Paul J Murphy for his guidance, and help with my clinical work. I am grateful too to my advisors Prof. Stuart Hodson and Prof. Tim Wiss.

Sincere thanks to Dr. Saeed Akhtar from the Biophysics Laboratory, Dr. Ac Hann from the Bioscience Laboratory and Dr. Mark Kerb from the Cavendish Laboratory Cambridge University for their excellent technical assistance with microscopes, and to the staff of the Daresbury synchrotron for their help.

Sincere thanks are due also to Drs. Sally Hayes, Craig Boote and Che Connon for their help with analysis of X-ray diffraction. Sally's attitude and kind help are

honestly appreciated. I would like to thank all of my colleagues of the biophysics research group. I also extend my thanks to all the academic staff, the secretaries in the Optometry and Vision Sciences School and the library staff. It has been really enjoyable, and a wonderful time in my life during the period of my PhD study.

I am indebted to all of my collaborators who provide the human and mouse tissues Dr. Mike Wride from the Cell and Molecular biology unit, Prof. Masayoshi Tachibana from Saitama Cancer Centre, Japan, Dr. Steven Tuft from Moorefields Eye Hospital, London, Dr. Arun Brahma from Manchester Eye Hospital, Manchester, and Dr. Shigeru Kinoshita from Kyoto Prefectural University of Medicine, Japan.

Deep thanks and appreciation to my sincere friend Dr. Turki Al-Mubrad from King Saud University for his honest friendship help and continued advice. Thanks a lot to "Abu-Ziyadh" Mohammad Aba-Hussein because I feel happy when I see him. Mohammad is always joking and makes the time fun.

Furthermore, I would like to express my sincere gratitude to all brothers and sisters in Cardiff for their support, co-operation, patience and help during my leadership of Saudi community, especially Dr. Hussein Al-Gahtani.

Extended gratitude goes to the Cultural Bureau in London, especially to Abdullah Al-Nasser, Cultural Attaché for his support and advice throughout the period of my study.

Finally, I am deeply indebted to my family for their continued support especially brother Ahmed (Abu-Muath) who has been looking after my family in Saudi Arabia during the period of my study.

CONTENTS

List of Figures

List of Tables

General Introduction

1.1 Sight and gross structure of the mammalian eye.

Vision is considered to be the most important of the five senses of the animal kingdom since it enables a spatial perception of the surrounding world. The eye enables animals to see and interpret the shapes, colours, and dimensions of objects by processing the light rays that enter it. It acts as an ocular window to vertebrates and other seeing creatures, helping them survive in the environments in which they live. Psychologically, the bright eye expresses the human personality and conveys emotions such as love, happiness and fun; conversely the dark eye expresses hastiness, sadness and pain.

Anatomically, the eyeball is situated in the anterior part of the orbital cavity, closer to the roof than the base, and nearer the lateral rather than medial wall. Externally, there are three pairs of extraocular muscles responsible for movement and the rotation of both eyes: two horizontal recti, two vertical recti, and two oblique muscles. Rectus muscles originate at an annular structure of connective tissue at the rear of the orbit called the annulus of Zinn. They pass forward and insert themselves into the sclera a few millimeters posterior to the limbus. The superior oblique attaches superomedially to the optic foramen just outside the tendinous ring and inserts into the sclera posterior to the equator of

the eyeball. Its counterpart is the inferior oblique, which arises from the floor of the orbit just posterior to the orbital margin and lateral to the nasolacrimal canal. This muscle inserts into the sclera at the posteriolateral aspect of the eyeball.

The eyeball is a fluid-filled globe that is not completely spherical, and is made up of two main outer parts of different size placed one in front of the other. The front, smaller segment is transparent, forms about 17% of the whole surface and is called the cornea. The structure and function of the cornea is the subject of this thesis and is described in greater detail in section 1.4. The back, larger segment, the sclera, is opaque and forms about 83% of the eyeball.

Three outer coats enclose the refractive media of the eye. The outermost, protective tunic, as mentioned, is made up of the sclera and the cornea. The middle coat is mainly vascular, consisting of the choroid, ciliary body, and iris. The retina or the neural coat is a tissue that lines two-third of the innermost wall of the eye. It contains the essential photoreactive nervous elements, the rods high at the periphery and the cones highly concentrated at the fovea inside the macula. Cones are responsible for colours and day vision, whereas rods are responsible for night vision. Finally, the optic nerve consists of gathered bundles of nerve fibres located at the posterior pole and extending to the visual cortex of the brain. The gross structure of the eye is shown diagrammatically in figure 1.1.

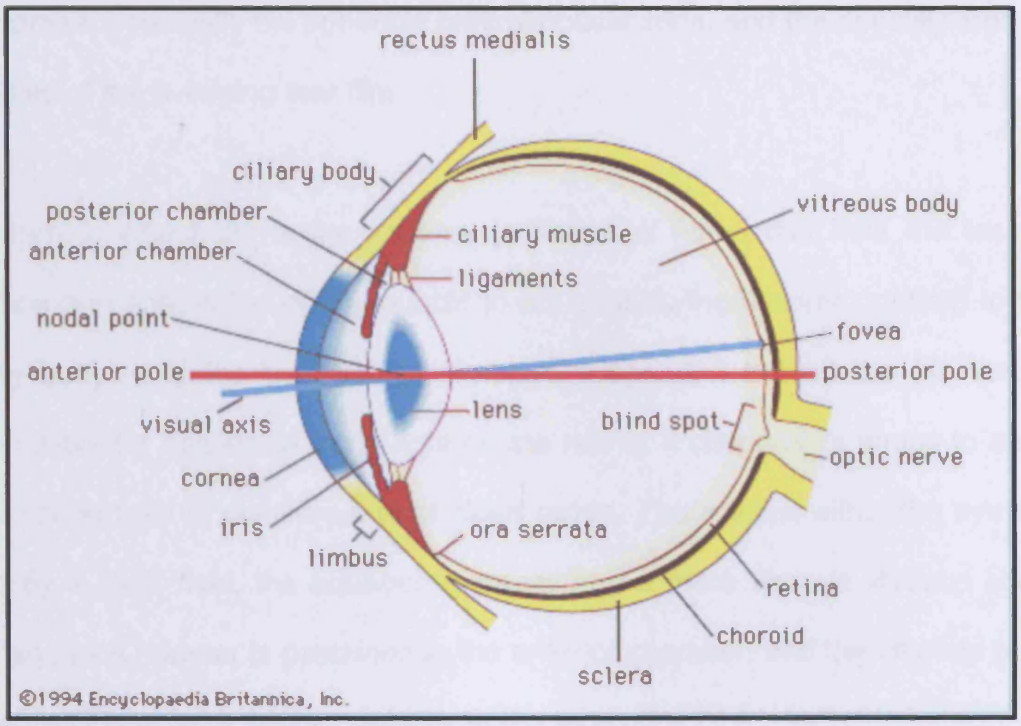

Figure 1.1: *Schematic diagram showing the different structures of the human eye. Source: Website: www.icat.ncsu.edu/ projects/retina/archive.htm.*

1.1.1 Optical apparatus.

The visual system is made up of predominantly transparent structures. The cornea is the first tissue encountered by a ray of light entering the eye. It is mainly responsible for protecting the eye and refracting light as it enters the eye. The main optical function of the cornea is to act as the principal refractive component, accounting for some 70% (40-45 D) of the eye's total refractive power. The refractive requirements are met by the regular anterior curvature of

the cornea, especially the spherical central optical zone, and the optically smooth qualities of the overlying tear film.

The lens is attached via the zonules (a series of fibres that hold the lens in position and enable the ciliary muscle to act on it during accommodation) to the ciliary body. It is the transparent structure suspended behind the iris that is responsible for helping to focus light on the retina. It changes its shape to allow clear vision both at distance and at close range. The spaces within the eye are filled by a clear fluid, the aqueous humour, and a more viscous vitreous body. The aqueous humour is contained in the anterior chamber, and the vitreous body is located in the large space posterior to the lens.

The iris functions as a diaphragm, modifying the amount of light entering the eye by adjusting the size of the pupil. It dilates in conditions of low light intensity to permit more light into the eye. On the other hand, in bright light the iris constricts to reduce the amount of light that enters the eye.

An image of external objects is formed on the retina at the highly specialised portion called the fovea. The optic nerve carries the information from the retina as electrical signals and delivers it to the posterior cortex in the brain where the information is interpreted as a visual image.

1.2 Dimensions of the cornea.

The cornea's outline is not circular, its thickness is not uniform, and its radius of curvature is not constant. It is recognised that the normal cornea is an avascular tissue with a smooth, convex anterior surface, which in humans, appears elliptical being typically 11.7 mm wide in the horizontal meridian and 10.6 mm in the vertical. It has a concave inner surface which appears circular and is about 11.7 mm in diameter. This difference is due to the greater overlap of the sclera and conjunctiva above and below the cornea than in the lateral and nasal portions of the cornea. Further, the cornea is more curved in the vertical than the horizontal meridian, giving rise to astigmatism with the rule. In the late decades of life, the horizontal meridian becomes more curved than in young individuals, giving rise to astigmatism against the rule. The latter is thought to be due to the lids exerting pressure on the cornea (Wilson, 1982) or the cornea becoming more flat at around the age of 30, which suggests that accommodation may have some effect on the corneal shape as a result of aging (Pierscionek, 2001).

The axial thickness of the human cornea at its centre is 0.52 mm (Donaldson, 1966; Maurice, 1969) with a peripheral thickness of 0.67 mm. In its centre third, "the optical zone", the radius of curvature of the anterior surface is about 7.8 mm and that of the posterior 6.5 mm. Unequal radii occur because the anterior and posterior radii are not concentric, and thickness increases towards the periphery of the cornea. The anterior surface of the peripheral cornea is more flattened than the central cornea.

The cornea's structure gives some indication of the diverse functional demands upon the tissue. It must be transparent, refract light, contain the intraocular pressure, and serve as a strong barrier protecting the inner structures of the eye against infection and trauma. Each of these functions is provided by a highly specialised substructural organisation. The resistance of the cornea, which provides a protective layer and resists ocular pressure, is due to the collagenous components of the stroma. The transparency of the corneal stroma is achieved by the regularity and fineness of its collagen fibrils and the closeness and homogeneity of their packing (Maurice, 1957).

1.3 Human corneal structure.

The cornea is composed of five layers named, from anterior to posterior, the epithelium, Bowman's layer, the stroma, Descemet's layer, and the endothelium (figure 1.2). Each is described in more detail below.

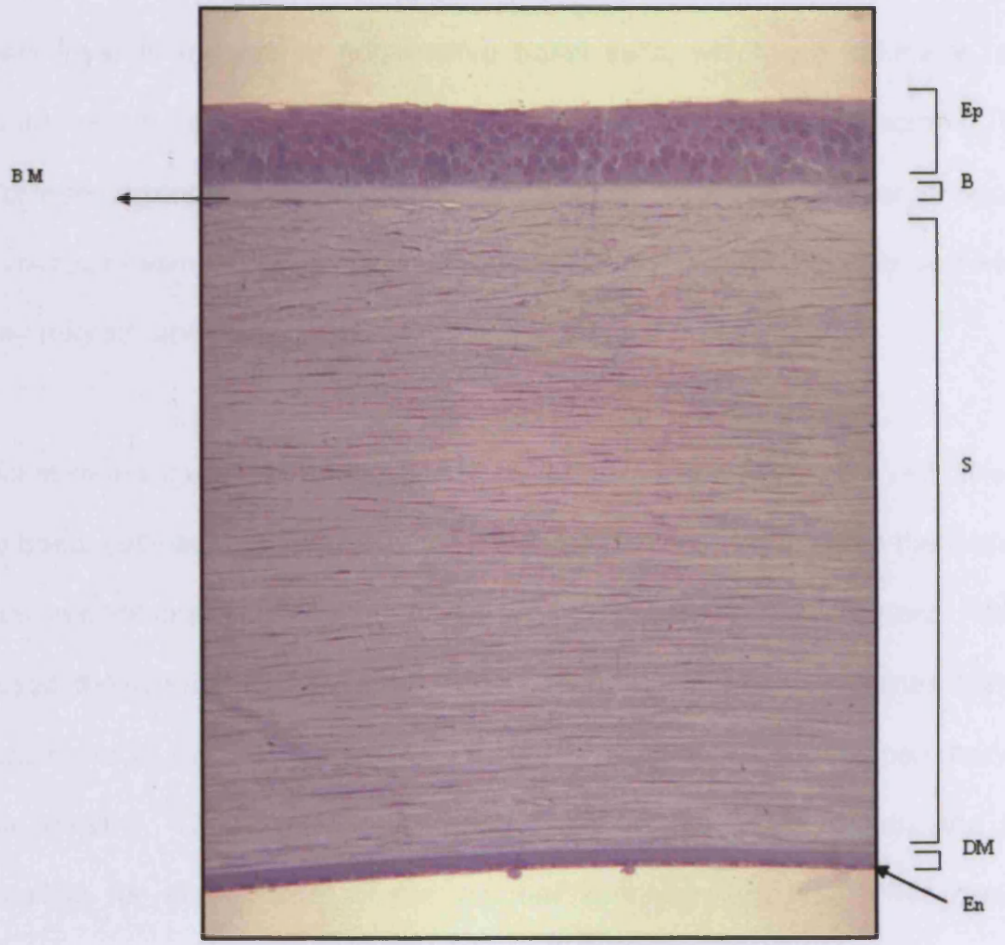

Figure 1.2: *Low-power light micrograph showing layers of the human cornea. Epithelium (Ep), Basement Membrane (BM), Bowman's layer (BL), stroma (L), Descemet's membrane (DM) and endothelium (En).* ***Source****: Website: www.city.ac.uk/biolabs/tissie.*

1.3.1 Epithelium.

The outermost surface of the cornea is a non-keratinised, stratified squamous epithelium, which is five to seven cells thick in the central region and more at the periphery. It constitutes approximately 10% of the total corneal thickness. The

deepest layer is formed by germinative basal cells, which are columnar, and attached to the underlying basement membrane by hemidesmosomes. The middle layer is made up of polygonal, wing shaped cells that are interconnected by numerous desmosomes and become increasingly flattened, thinner and wider as they migrate anteriorly.

Epithelial renewal used to be thought to be achieved through simple cell division of the basal cells across the entire cornea which then moved towards the corneal surface and desquamated into the tear film. However, Thoft and Friend (1983) proposed the X-Y-Z hypothesis, which suggests that the central cornea cannot depend on local mitosis, but requires a net influx of cells from the periphery to remain healthy. These stem cells are located in the limbal region and are responsible for the renewal of the corneal epithelium (Kruse, 1994; Zieske, 1994).

The outermost surface of the epithelium, in contact with the tears, is covered with microplicae and microvilli (Sheldon, 1956). Pfister (1973) suggests that these may facilitate the adsorption of mucin to improve the wettability of the cell surface and increase the stability of the tear film. Hemidesmosoms and anchoring filaments connect the basal epithelial cells to the basal lamina (Bron et al., 1997), and these adhere to Bowman's layer via anchoring fibril complexes containing type VII collagen (Bergmanson, 2001).

1.3.2 Bowman's layer.

Bowman's layer was initially thought to be a specialised corneal membrane. However, it is now described as a modified region of the anterior stroma. Some observers believe that the epithelium has a role in the laying down and maintaining Bowman's layer (Kuwabara, 1978). A recent study using transmission electron microscopy (TEM) has shown that lower mammals have a thin layer whereas higher mammals have a thick Bowman's layer (Hayashi et al. 2002).

Bowman's layer is narrow, acellular, homogeneous, and 8-12 μm thick in humans, immediately subjacent to the basal lamina of the corneal epithelium. Ultrastructurally, it consists of fine collagen fibrils (24–27 nm in diameter) of uniform size, embedded in an extrafibrillar matrix. In the proximal region of this layer, the fibrils become progressively more ordered in their orientation, blending and interweaving with the fibrils of the anterior stroma. Additionally, small pores, about 0.5 -1.5 μm in diameters, which appear to penetrate Bowman's sheet, are seen on the epithelial aspect of Bowman's layer (Komai and Ushiki, 1991).

1.3.3 Corneal Stroma.

The corneal stroma constitutes approximately 90% of the corneal thickness, and this contribution gradually increases from the centre towards the periphery. Basically, the corneal stroma consists of collagen fibrils embedded in a gel consisting of water, non-fibril forming collagens, proteoglycans, glycoproteins,

other soluble proteins, and inorganic salts. Elongated cells called keratocytes are arranged in a regular clockwise spiralling pattern throughout the full stromal thickness (Muller et al., 1995). The collagen fibrils lie in 200-300 parallel lamellae at the cornea's centre, and 500 lamellae at the periphery (Maurice, 1957; Hamada, 1974). Collagen fibrils in each lamella run parallel to each other and to the surface of the cornea, but are rotated with respect to fibrils in adjacent lamellae (figure 1.3). Moreover, they are of a very similar diameter and are relatively uniformly spaced. Anteriorly, stromal lamellae are thinner, narrow and follow an intertwining path, while posteriorly they are thicker, flatter and wider and less interwoven (Hogan et al., 1971; Maurice, 1984).

Figure 1.3: *lamellar surface of the stromal cornea. Collagen fibrils of each bundle run in the same direction.* ***Source****: IOVS (Komai and Ushiki, 1991).*

With regard to the keratocytes, they are located between lamellae, but their distribution in the stroma may not be as random as was first thought. Muller et al. (1995) found keratocytes arranged in a regular clockwise spiralling pattern throughout the full stromal thickness. Estimation of keratocyte number in the adult human cornea suggests the cornea contains 2.4 million keratocytes. Their highest density is found anteriorly and decreases towards the posterior stroma, but a small increase in cell density has also been noticed immediately anterior to Descemet's layer (Petroll et al., 1995). Keratocytes play an important role in wound healing, and are a reserve source of glycogen (Watsky, 1995).

1.3.4 Descemet's membrane.

Descemet's membrane is the basement membrane of the endothelium. Its thickness in humans ranges from 3 μm at birth to 20 μm in adults. Anatomically, it is divided into two parts. The anterior is the fetal or oldest part, 3-4 μm thick at birth and is banded. In contrast, the posterior postnatal part is uniform in texture, has a homogeneous appearance under microscopy, and grows with age at a rate of approximately 1 μm per decade (Johnson et al., 1982). The periphery of an adult's Descemet's membrane often reveals pockets of local thickening known as Hassal-Henle warts, which sometimes are noted centrally in the cornea. This condition is known as corneal guttata, and occasionally affects the health of the endothelial cell in the case of abnormal endothelial basement membrane synthesis (Bergmanson et al., 1999). This is known as Fuchs' endothelial dystrophy.

1.3.5 Endothelium.

The corneal endothelium is formed of a single layer of cubical cells, and is 5 μm thick. Sectioned en face, the endothelial cells appear predominantly hexagonal in shape and are small in youth, but become polymorphic and large in adulthood. Normally, the cells' density decreases with age (2987-5632 cells/mm^2 at birth and 2000-2500 cells/mm^2 at 80 years of age (Shaw et al., 1978)) for the following reasons: first, the cells do not divide after birth; and second, when an endothelial cell dies, the neighbouring cells spread out laterally to cover the surface made bare by the departing cell in order to maintain the essential function of the endothelial layer in maintaining deturgesence and thus transparency of the cornea. These events lead to an increased variation in the shape of cells. It is believed that the functional limit of the corneal endothelium is approximately 700-1000 cells/mm^2 (Bergmanson, 2001). Another function of the endothelial layer is to regulate the fluid entering the cornea from the aqueous via an active bicarbonate ion pump (Hodson, 1997). The lateral walls of corneal endothelial cells show extensive interdigitations. As mentioned by Bergmanson (2001), these interdigitations increase the surface area of the cell, and are one reason why the endothelial cell can expand laterally when required. The cells contain a high density of mitochondria and endoplasmic reticulum, which are hallmarks of metabolically active cells.

1.4 Features and structure of the limbus.

The limbus forms an intermediate zone between the transparent cornea and the opaque sclera. It plays an important role in the nourishment of the peripheral cornea and contains the pathways of aqueous humour outflow. Its vertical meridian is wider than its horizontal meridian. The limbus is defined anteriorly by a line between the peripheral extremes of Bowman's layer and Descemet's membrane, and posteriorly by a line from the scleral spur perpendicular to the tangent of the external surface of the globe (Hogan et al., 1971).

Externally, the limbal epithelium has a similar structure to the corneal epithelium, except that it has a larger number of cells (Hogan et al., 1971). It contains subpopulation of epithelial stem cells which are located at the basal zone of the epithelial limbal layer (Schermer et al., 1986; Bukusoglu and Zieske, 1988; Zieske, 1994).

Internally, limbal collagen fibril diameters are larger than those in the corneal stroma (Borcherding et al., 1975). The same authors also noticed a marked fall in the proteoglycan keratan sulphate, with the appearance of dermatan sulphate and hyaluronic acid towards the limbus. The small curvature of the cornea (7.8 mm) changes to a larger curvature (13 mm) in the sclera at the limbus. Maurice (1969) suggests that due to changes in curvature at the limbus, the circumferential strength will be at least twice that in neighbouring regions. Newton and Meek (1998a and 1998b) have found that preferentially, collagen

fibrils align orthogonally along the vertical and horizontal meridians throughout the width of the corneal stroma until 1-2 mm at the periphery. As a population they run circumferentially at the limbus to form an uneven annulus. This annulus is characterised by a narrower width in the superior sector than the inferior sector. These authors also revealed also that the greatest density of collagen fibrils is at the superior margin rather than the inferior margin.

1.5 Comparative aspects of human and mouse cornea.

In mammals, the thickness of each layer of the cornea increases gradually from smaller animals, like mice and rats, to the larger animals like cattle and human. Bowman's layer in lower species is scarcely visible but is easily seen in primates. Hayashi at al. (2002) carried out comprehensive observations of the corneas of nine different species of the animal kingdom using transmission and scanning electron microscopy. They reported that in mice Bowman's layer can be scarcely seen, rather the collagen fibril arrangement is random and slightly meandering in appearance and the layer lacks a clear boundary with stroma. However, Quantock et al. (2005) argued that the rat and mouse did not have true Bowman's layer that is anatomically and functionally similar to that in humans. Bowman's layer in humans is up to 12 μm thick and is a random tightly packed meshwork of collagen fibrils is visible.

Of course, there are clear differences between humans and mice in relation to the aging process, sexual maturity, gestation, body weight, ocular dimensions

and anatomical and physiological features, with typical details presented in table 1.1.

Species characteristics	Mouse	Human
General		
Body weight	≈ 25g in adult	≈ 60 kg
Life span	≈ 18 months	≈ 70 years
Gestation	21 days	9 months
Sexual maturity	≈ 6 weeks	≈ 15 years
Ocular		
Eye dimension	≈ 2.9 mm	≈ 24 mm
Position	Lateral	Centrally
Visual field	Large	Slight narrow
Cornea		
Curvature radius	1.4 mm	7.7 mm
Thickness of Bowman's layer	0.8 µm	10 – 12 µm
Thickness of stroma + Bowman's layer	100 µm	340 µm
Thickness of Descemet's layer	5 µm	6 µm at centre ≈19 µm at periphery
Collagen fibril diameter	20-30 nm	20-30 nm

Table 1.1: *A comparison of species characteristics between mouse and human. Source: Systematic evaluation of the mouse eye (Smith et al. 2002; Hayashi et al. 2002; Schmucker and Schaeffel, 2004; Dr. Nathan Hill, personal communication, 2006).*

A major consideration when extrapolating mice studies to the human situation cornea is the aging process. Perez-Gomez et al. (2000) used confocal microscopy to examine the central corneas of 119 normal subjects with an age range of 11–80 years and concluded the following: (i) Keratocyte density

decreases with age, (ii) endothelial cell density decreases and endothelial polymegethism increases with age, and (iii) folds occur in the posterior stroma, and guttata occur in the endothelium in the later decades of life. No comparable data exists for mice. Song et al. (2003), however, have indicated that neonatal changes in corneal stromal thickness, light scattering and keratocyte density occur in mice in the neonatal period, but that after about 3 weeks of age changes are only minimal. In all studies described in this thesis, the corneas of adult mice between the ages of 14 and 54 weeks are used.

1.6 Corneal collagen.

Collagen is a major structural protein in the body, present in the majority of species throughout the animal kingdom, including all vertebrates. All forms of collagen are made up of three left-handed polypeptide chains, and these chains, are coiled in a right-handed direction about a common axis to form the rope-like collagen molecule. Thus, the collagen molecule has a triple-helical structure, and was defined by Burgeson, (1988) as "an extracellular structural protein whose functional properties depend upon a triple-helical domain". There are around 27 different collagen types currently known in the eye and these can be categorised into three families according to their structural properties: (1) fibrous collagen types I, II, III, V, and XI (Kadler et al., 1996); (2) FACIT (fibril associated collagens with interrupted triple helices) that modify interactive properties and associate with the surface of collagen fibrils (these include types IX, XII, XIV, XVI, XX and XIX (Koch et al., 2001)); and, (3) non-fibrous collagen types such as

IV, VI, VII, VIII, IX, and X (Sandberg-Lall et al., 2000). Collagen type I constitutes the majority of the solid substance in the stromal cornea and sclera, although there are also collagen types III, V, VI, VIII and XII. Collagen types IV, VII, XII, XIV and XX are found in the cornea too. As can be seen in table 1.2, Michelacci (2003) summarised the different collagen types and their locations in vertebrate corneas.

Type	Localisation
I	Stroma
II	Development stroma (epithelium)
III	Inflammation, wound healing
IV	Basement membranes
V	Stroma
VI	Stroma
VII	Basement membrane (epithelium)
VIII	Basement membrane (Descemet)
IX	Developing stroma (epithelium)
XII	Stroma (endothelium origin)
XIII	Stroma (posterior two third)
XIV	Stroma
XVII	Developing stroma (hemdesmosomes)
XVIII	Basement membrane (epithelium)
XX	Epithelial layer

Table 1.2: *Locations of different collagens types in vertebrate corneas.* ***Source:*** *Modified from Brazilian Journal of Medical and Biological Research (Michelacci, 2003).*

1.7 Corneal Proteoglycans.

Proteoglycans (PGs) are a heterogeneous family of molecules composed of a core protein domain to which glycosaminoglycans (GAGs) are covalently linked as side chains (Hassell et al., 1986). GAGs are large carbohydrates that are composed of repeating disaccharide units and occur in four main forms.

According to their GAG side chains PGs are classified into keratan sulphates representing 50% of the total GAG content in the stroma, chondroitin sulphate representing 30%, and dermatan sulphate about 20% (Scott and Bosworth, 1990). Core proteins of the PGs are identified in the corneal stroma. Keratan sulphate PGs consist mainly of lumican (Blochberger et al., 1992), keratocan (Corpuz et al., 1996), mimecan/ osteoglycin (Funderburgh et al., 1997) and fibromodulin (Oldberg et al., 1989). Chondroitin/dermatan sulphate GAGs are complexed mainly to the PGs decorin and biglycan (Funderburgh et al., 1998). PGs interact in a specific way to help control the maintenance of the stromal ultrastructure of the cornea (Scott and Haigh, 1988; Li et al., 1992). Further, the changed expression and disarranged distribution of these PGs and collagen fibrils observed during corneal wound healing backs up the possibility of structurally important interaction between the PGs and the collagens (Scott, 1988; Tanihara et al., 2002). The proteoglycan types and their concentrations in the different structures of the cornea are shown in table 1.2.

Corneal structure	Proteoglycan types and their level		
	Keratan S	Heparan S	Chondroitin S
Epithelium	low	Low	High
Bowman's	Low	High at interface with epithelium	Low
Stroma	high	Low	Low
Descemet's	Low	High at interface with endothelium	Low
Endothelium	Low	Low	High
Keratocyte	Low	Low	High

Table 1.3: *Distributions of proteoglycan types and their concentration in each structure of the cornea.* ***Source****: Cornea J (Bairaktaris, 1998).*

1.8 Maintenance of the shape of the cornea.

Even though the biomechanical properties of the human cornea play a very important role in its shape, resistance, and transparency this is still not clearly understood. Clearly the normal cornea must maintain its dimensions and a stable shape for good vision. Cellular layers (epithelium and endothelium) have few mechanical properties, and therefore do not likely contribute significantly to the corneal strength. Descemet's layer is quite a strong resistant sheet due to its resilience, but it does not come under tension until the adjoining stroma is fully extended (Jue and Maurice, 1986). It is widely accepted therefore, that the biomechanical properties of the cornea are largely determined by the corneal stroma, and are a summation of many factors related to the lamellae structure. Some of these are discussed below including optical lamination and collagen fibril arrangement, lamellar cohesion and tensile strength (Maurice, 1999), plus normal swelling pressure and internal pressure as a result of physiological hydration (Hodson, 1997):

1.8.1 Optical lamination.

Ultrastructurally, many microscopical studies have been conducted to investigate the morphologic structures of the corneal stroma. These studies agree that the anterior third of the stroma is characterised by thinner lamellae, comprising a few straight and many undulating collagen bundles which run obliquely to the surface of the cornea. In the posterior two-thirds of the stroma, the lamellae are more regular, running parallel to the surface of the cornea and become wider and

thicker (Maurice and Monroe., 1990; Komai and Ushiki., 1991; Radner et al., 1998a; Radner and Mallinger., 2002). However, more controversial is the nature of the anterioposterior interlacing between the lamellae which, together with proteoglycan components, may play an important role in maintaining the shape of the cornea.

1.8.2 Cohesive strength.

Maurice (1999) has observed that the layers of the stroma, whether anterior or posterior, do not separate or pull apart when the tissue is placed in water. He alludes to the presence of elements or interlamellae which bind the lamellae together, even though there is no interweaving in the posterior stroma. Muller et al. (2001) suggest that the more closely packed lamellae make the anterior stroma more resistant to edema than the posterior stroma, because the large interlamellar spaces allow for greater swelling. However, Radner and Mallinger (2002) claim that the lamellae split in an anterioposterior direction as well as horizontally into branches and are interlaced by crossing fissures between the branches, even in the midstroma.

In histological studies, strips of human corneas have been torn vertically and horizontally along the length of the sample through the centre. The corneal stroma along horizontal and vertical meridians shows a smooth interface at the centre, with no evidence of torn lamellae, and an irregular appearance towards the periphery, with increasing numbers of free ends of torn lamellae (Smolek et

al., 1990; Smolek, 1993). The upshot of this work was the discovery that the weakest cohesive strength is at the centre of the cornea, gradually increasing respectively, from inferior, superior, and lateral to strongest nasally at the periphery.

1.8.3 Collagen fibril orientation in human corneas.

In-depth studies of collagen fibril orientation using x-ray diffraction indicate two preferred directions of collagen in the central cornea along horizontal and vertical meridians. This is more pronounced in the posterior of the stroma (Meek et al., 1987; Daxer and Fratzl, 1997). In addition, Newton and Meek (1998a) and Boote et al. (2003) have revealed that the density of collagen fibrils increases from the centre towards the periphery. Recently, the separation of contributions of preferential aligned fibrils and total isotropic fibrils enabled Aghamohammadzadeh et al. (2004) to map collagen fibril orientation, and its relative distributions across the cornea, limbus, and sclera. In their study, strong preferences of collagen fibril orientation were shown at different points in the normal human cornea. The study suggested that the total in the human cornea increase in X-ray scatter from cornea that is seen through the limbus into the adjacent 2 mm of sclera is a result of the increasing thickness from cornea towards sclera. Another study revealed approximately 30% of collagen fibrils throughout the stromal depth tended to lie within a 45^{o} sector of both the superior-inferior and nasal-temporal meridians (Boote et al., 2005). This suggests that the collagen fibrils are populated equally in both directions at the centre of

the cornea, and the isotropic fibrils might be distributed equally to support corneal elastic along both meridians in order to withstand intraocular pressure.

1.8.4 Swelling pressure.

Swelling pressure depends mainly on an osmotic effect that results from the Donnan equilibrium. The cornea maintains its shape and thickness by balancing intra-ocular pressure with a transverse swelling pressure created by the mutual repulsion of stromal matrix fixed charges at physiologic hydration that result from the presence of collagen, salts and protoglycans (Hodson 1997).

1.8.5 Internal pressure.

In most eyes, the tension of intraocular pressure (IOP) on the tunic wall will not be equal in all directions. This is because (1) the eye is not spherical; (2) the radius of curvature of the cornea is less than that of the sclera; and (3) the tunic of the eye is unequal in thickness.

When the IOP rises, for example due to glaucoma, the cornea becomes very slightly stretched and flatter, but above 50mmHg the cornea is very inextensible and the distensibility falls as the IOP is raised (Gloster et al., 1957). This indicates that the cornea has certain rigidity and the greatest dimensional changes occur below the normal IOP. Jue and Maurice (1986) have found that

the human corneal stroma is responsible for the inextensible character of the anterior eye.

1.9 Misshapen cornea.

The human cornea, like any connective tissue, is predisposed to several dystrophies. The most frequent diseases that markedly affect the biomechanical stability of the cornea are keratoconus, keratoglobus, and pellucid marginal degeneration. There is considerable overlap between their clinical features and differentiation may be made on the basis of the stromal thinning. In pellucid marginal degeneration, stroma thinning is located mostly in the inferio-peripheral cornea, and is generalised in keratoglobus as shown in figure 1.4. However, in keratoconus the thinning is paracentral and occurs most commonly below the horizontal meridian.

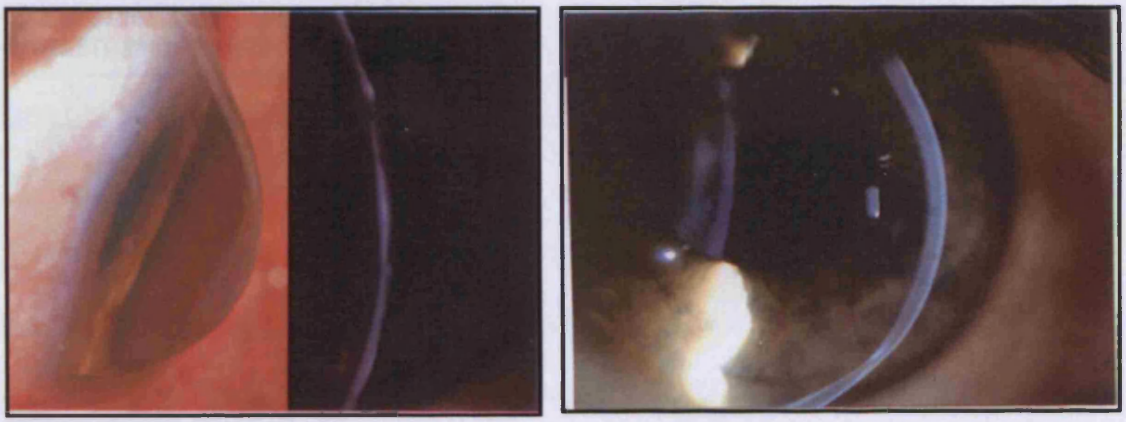

Figure 1.4: *Showing protrusion and thinning of the human cornea. (Left) Keratoglobus (Courtesy of Boruchff, 2001). (Right) Bilateral crescent- shaped inferior corneal thinning of pellucid marginal degeneration (Courtesy of Kanski, 1997).*

1.10 Aims of thesis.

The purpose of this work is to investigate the clinical and structural basis of topographic alterations in the cornea's shape due to keratoconus. Using a range of different methods investigations were conducted on patients with clinically diagnosed keratoconus, on postoperative human keratoconus corneas, and on two animal models of corneal disease with similarities to keratoconus.

First, keratoconus is discussed demographically and geographically because the influence of ethnicity on the incidence rate and severity of the disease in the world's population is of clear importance. Next, the incidence rate, onset age, severity of disease and associated signs and symptoms of keratoconus patients in a Saudi Arabian population is examined. Then moving on to investigate the relationship between different rigid contact lens designs and the severity of keratoconus in Saudi Arabian patients and the relationship between optimum lens back optic zone radius (BOZR) and keratometric readings.

Surgeons often use the topographical map in clinics to size the trephination for the treatment of keratoconus by penetrating keratoplasty. However, it is not known whether or not the clinical assessment is able to identify the full extent of the defect in the keratoconic cornea. Using scanning electron microscopy I next investigated disruptions to Bowman's layer at the central region of the cone and at more peripheral regions of the cornea. This will help to clarify the extent of Bowman's layer abnormalities and decide whether the steepest area on the

topographical map covers the full extent of the defect in the cornea or only the apical area of the cone.

Animal models are useful for the study of disease processes underlying a number of pathological human conditions. While there currently exists no mouse model for keratoconus, the availability of mice with some phenotypes resembling keratoconus corneas may shed light on the pathogenesis of the disease. In order to facilitate an understanding of factors associated with the biomechanical instability of misshapen versus normal corneas, transmission electron microscopy (TEM) was conducted to evaluate ultrastructural changes of the SPARC-deficient mouse that is predisposed to corneal shape change.

A high angle x-ray diffraction study was also carried out on the SPARC-deficient mouse, as well as another strain of mice that is predisposed to corneal ectasia (the JKC mouse) to investigate the spatial orientation of collagen fibrils across the entire corneal stroma. This was done to test the hypothesis that corneal thinning and ectasia might be due to misalignment of collagen fibrils and slippage of collagen lamellae from their attachment to other lamellae. This might help to validate the mouse as an animal model for corneal ultrastructural studies and understand the possible link between shape changes and extracellular matrix architecture.

Keratoconus

2.1 Description.

Hall (1963) indicates that keratoconus, the most common ectatic disorder of the cornea, was first described by Mauchart in 1748 and two decades later by Taylor. Duke-Elder (1965) cited that the first differentiation of keratoconus from other ectatic conditions was by Nottingham (1854) during practical observations of the conical cornea.

There are two types of keratoconus: posterior and anterior. Posterior keratoconus is a rare condition in which the posterior corneal surface has a conical protrusion into the anterior stroma which is a result of the absence of stromal tissue. It is non-progressive and does not affect visual acuity to any great extent. This thesis is concerned with anterior keratoconus only.

Anterior keratoconus, (hereafter, referred to as keratoconus) or conical cornea is a noninflammatory progressive ectatic and thinning disease process of the cornea (figure 2.1). The manifest behaviour of the disease is characterised by central corneal stromal thinning, distorted corneal curvature, apical stromal scarring, and anterior protrusion. These features impair vision due to the development of irregular myopic astigmatism.

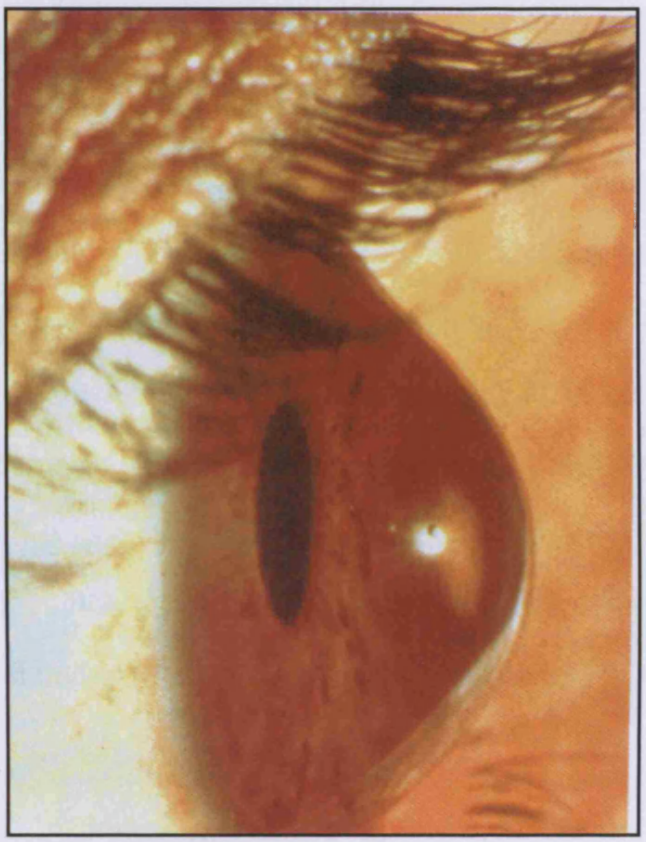

Figure 2.1: *Human keratoconus as a result of central or paracentral thinning.* ***Source****: (Boruchoff, 2001).*

Although most cases seen clinically are bilateral, the disease is usually more severe in one eye than the other (Zadnik et al., 2002). Unilateral cases have been reported, although the apparently unaffected eye assumes a very mild keratoconic form. Kennedy et al. (1986) reported that keratoconus was bilateral in 59% and unilateral in 41% of cases.

There are many conflicting views and lines of evidence concerning whether or not keratoconus expresses any sex-linkage. While some authors believe that it

affects both sexes equally (Reardon and Lowther, 1973), Woodward (1984) reported a greater prevalence among females in cases reported in the literature before 1955. Still, others believe a male predominance (Karseras and Ruben, 1976; Korb et al. 1982; Lim and Vogt, 2002). The disease becomes manifest around puberty in most cases, and the most common mean age of onset occurs at around age 16 (Krachmer et al. 1984; Ridley, 1956), although new cases have been claimed to occur as early as two years (Bennett, 1986). The progression is slow, taking up to five to six years to develop, thereafter remaining stationary for many years. In others, there is rapid progression over one or two years, followed by a long quiescent period (Duke-Elder, 1965).

2.2 Incidence and severity.

An estimation of the frequency of keratoconus varies widely depending upon the source. Although the disease occurs in all races (Rabinowitz, 1998), there appears to be a geographical influence on prevalence rate for the disease. As a result, prevalence of the disease varies between 50 and 230 cases per 100,000 in the general population (Krachmer et al., 1984; Kennedy et al., 1986). Whereas a low incidence of the disease is apparent in Japan, Taiwan, and Singapore (Khoo 1989; Chen et al., 2001), Mediterranean and Middle Eastern areas appear to demonstrate high incidence and an increased manifestation (Totan et al., 2001; Tabbara, 1999). The ethnic and geographical distribution of keratoconus will be covered in chapter three, part one.

2.3 Clinical characteristics.

2.3.1 Signs and symptoms.

The first symptom of keratoconus is a deterioration of vision which usually appears in one eye only as a result of regular or irregular myopic astigmatism. Glare, ghost image, monocular diplopia, photophobia, and frequent changes of glasses are usually first reported by patients (Edrington et al., 1995). The period between the onset of disease and the first clinical signs or symptoms is very difficult to detect. In the early stage, myopic astigmatism and a scissors motion can be detected using retinoscopy, a circular shadow can be seen through ophthalmoscopy, and irregular or distorted mires accompanied by an increase in corneal steepness can also be seen using keratometry (Robinowitz, 1998).

In moderate to advanced stages, one or more of the following signs may be detectable by biomicroscope slit-lamp examination of the cornea: stromal thinning, conical protrusion, apical stromal scarring, Fleischer's ring, and Vogt's striae (Edrington et al., 1995; Zadnik et al., 1996). Fleischer's ring is a yellow-brown to olive-green pigment forming an incomplete annulus seen at the base of the cone as a result of haemosiderin (iron) deposition in basal epithelial cells created by corneal stretching in the advanced stage of keratoconus as shown in figure 2.2A. Vogt's striae are fine vertical lines, which represent folds in the posterior stroma and Descemet's layer and disappear transiently on gentle pressure (figure 2.2B).

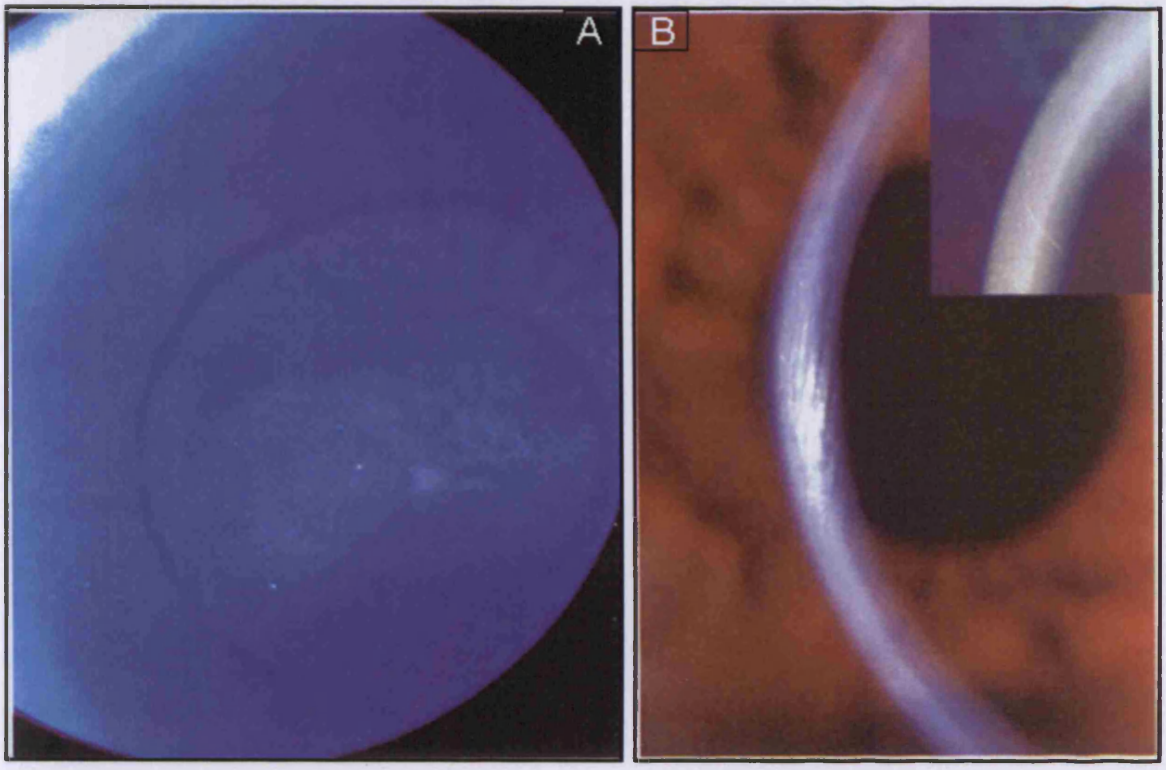

Figure 2.2 *Fleischer's ring:* (**A**) *epithelial iron deposits at base of cone best seen under cobalt blue light and* (**B**) *Vogt's striae: vertical lines in the posterior stroma seen by slit-lamp which disappear when pressing on the cornea.* ***Source****: (Boruchoff, 2001).*

Further clinical signs include Munson's sign and Rizzuti's sign (Maguire and Meyer, 1988). These two signs are useful confirmative external indicators associated with the disease. Munson's sign is a V-shaped angulation of the lower eyelid in terms of the upper lid rising when the patient looks downwards (see figure 2.3). Rizzuti's sign is a triangular focused beam seen near the nasal limbus, formed by lateral illumination of the cornea in cases with severe keratoconus.

Figure 2.3: *Munson's sign: bulging of the lower eyelid when patient looking downward.* ***Source****: (Boruchoff, 2001).*

One more clinical sign seen in the advanced stage is acute or hydrops keratoconus, characterised by a massive influx of aqueous humour into the stroma as a result of a tear in Descemet's membrane and endothelium (figure 2.4). The cornea then becomes densely edematous, leading to a severe reduction in visual acuity. Within 6 weeks, any endothelial damage has usually healed by enlargement of nearby cells and the stretching of these endothelial cells to cover the breaks. Tuft et al. (1994) assessed clinical factors associated with the development of corneal hydrops in keratoconus patients and found that hydrops were more common in younger males and in subjects with severe

allergic eye disease. Further, corneal hydrops is frequently seen in cases of Down's syndrome (Bron et al., 1978).

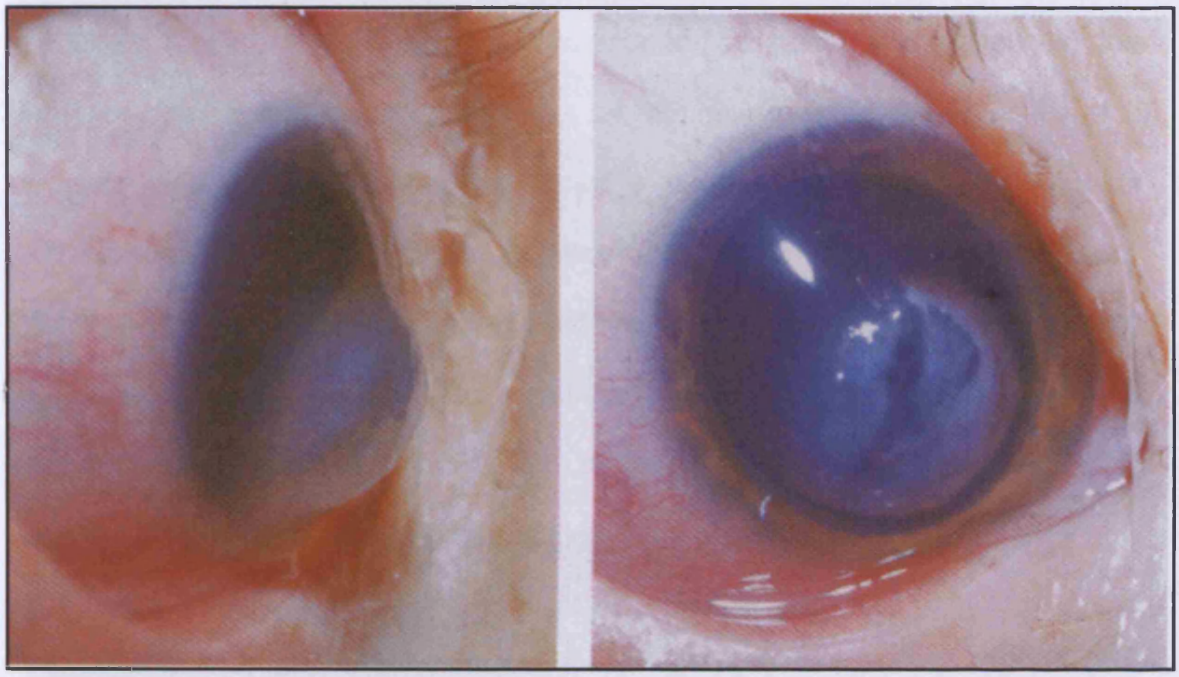

Figure 2.4: *Sudden development of corneal edema (left) secondary to rupture of Descemet's membrane (right).* ***Source****: (Boruchoff, 2001).*

2.3.2 Corneal topography.

Corneal topography is becoming an invaluable clinical tool because it provides information about corneal curvature which has direct relevance to optical elements of the cornea beyond the central 3 mm measured by the keratometer. However, the detection and identification of the very early stage of keratoconus and the ability to distinguish it from other disorders is still difficult.

As reported by Wilson (1991), prior to the introduction of the videokeratoscope, the detection of early keratoconus was one of the main reasons for using Amsler's Placido disc. It was used to monitor progressive alterations in the anterior corneal surface in keratoconus by monitoring the uniformity mires of a Placido disc. In 1984, Klyce introduced a new computer-based analysis of keratoscope images that produced three-dimensional wire models of corneal surface distortion. This technique offered the opportunity to evaluate the patterns of power distribution seen in the earliest stages of keratoconus. It also offered the opportunity for earlier diagnosis and better understanding of the degree of corneal irregularity compatible with a given level of visual function.

Maguire and Bourne (1989) used this procedure to detect the presence of keratoconus in patients without slit lamp or keratometry based evidence of keratoconus. They reported that corneal topography analysis systems were useful in the detection and description of corneal irregularity in the early stages, but only if used by an expert examiner. With the development of computer-assisted videokeratoscopes in the mid 1980s, it became apparent that some corneas have the topographic features of mild keratoconus in the absence of other clinical signs (Maguire and Lowery, 1991; Harrison and Maguire, 1995). Rabinowitz and McDonnell (1989) developed algorithms for the detection of keratoconus that are available on some corneal topographers and made the following observations:

- Power differences are noted between the superior and inferior paracentral corneal regions in keratoconus and are measurable as the I-S value.
- Central corneal power is higher in keratoconus than normal eyes.
- There is a difference in the progression of corneal steepening in the two eyes of a keratoconus patient.

This approach permits a positive identification of early suspected keratoconus, if the central corneal power is greater than 47.2 D or if the I-S value is greater than 1.4 D. It also generates a positive result for clinical keratoconus if the central corneal power is greater than 48.7 D or the I-S value is greater than 1.9 D. A study was designed to evaluate the topography of a large series of keratoconus patients using computer-assisted topographic analysis. This work indicated the technique had many potential applications for the study of keratoconus (Wilson et al. 1991). Other work using the same procedure at two to three-month intervals for a two-year period on patients with keratoconus in one eye, showed no evidence of keratoconus in the contralateral eye (Maguire and Lowry 1991). These findings pointed to the use of effective topography-assisted systems in documenting subclinical cone progression. Further, they may be a useful tool in the study of the true incidence and natural progression of subclinical keratoconus.

Maeda and colleagues (1994) developed an automated system to differentiate clinical keratoconus from other corneal topographies using videokeratography.

They concluded that this system could be used to distinguish clinical keratoconus from other corneal topographies. In addition, this quantitative classification method might also aid in refining the clinical interpretation of topographic maps. Finally, Dastjerdi and Hashemi (1998) utilised videokeratographs to map three groups of patients (the first group were known keratoconus, the second group were suspected, and the third group were normal). Using the highest rate of steeping as a sole index compared with six other measures, and utilising a discriminate analysis technique for a period of one year, their study showed high power and efficacy in differentiating the first two groups of keratoconus from normal eyes (94.9% accuracy). The above literature indicated that the authors used the highest reading (greatest power) on the topographic maps as an index for the point of maximum steepness (peak of cone) on the surface of the cornea to assess the existence of keratoconus and its position. In other words the colour-coded contour map of corneal powers conveys topographic information using colour association and pattern recognition. Normal powers were shown as green, very low powers were shown as cool or blue colours, and high powers were shown as warm or red colours (Klyce, 1984; Maguire et al, 1987).

In summary, the topography is designed to map the extent of astigmatism on the surface of cornea, and to classify the stages of keratoconus and monitor its progression.

2.3.3 Corneal thickness.

Undoubtedly, central corneal thickness decreases in keratoconic corneas. As regards the biomechanical properties of the cornea, scientists view the stroma as primarily responsible for most of the biomechanical stability of the cornea. In terms of keratoconus, the thinking is that the apical corneal stroma becomes weak due to thinning tissue. In advanced cases, the tissue begins to bulge and consequently changes the shape of the cornea.

The progress of disease is associated with central corneal thinning and with an increase in central corneal curvature (Insler and Cooper, 1986). In attempts to measure the central and peripheral corneal thickness of 20 keratoconus eyes using ultrasound pachymetry Gromacki and Barr (1994) found that the average central corneal thickness for keratoconus corneas was 0.52 mm compared to 0.56 mm for normal corneas. Furthermore, there was no difference in peripheral corneal thickness between keratoconus and normal corneas. However, ultrasound pachymetry is only capable of revealing average readings of central corneal thickness (Wheeler et al. 1992), it does not allow the identification of the thinnest corneal site. Consequently, central corneal thickness and apical central thickness were measured using Orbscan II and ultrasonic pachymetry in one eye of 72 normal subjects and 64 eyes of 36 keratoconus patients (Gherghel et al., 2003). The study showed that the Orbscan II provided good agreement with ultrasonic pachymetry for normal eyes. In keratoconic eyes, however, Orbscan II measurements were significantly lower than those obtained by ultrasonic

pachymetry. Using the Paradigm ultrasound biomicroscope, Avitabile and coworkers (2004) sought to classify the stages of keratoconus based on corneal thickness of 60 eyes, and to measure central and peripheral corneal thickness at different stages. They found that central corneal thickness values ranged between 0.278–0.592 mm, whereas corneal peripheral thickness values lay in the 0.475–0.992 mm range.

2.4 Stages of disease.

Understanding the progression of a disease plays a very important role in helping practitioners provide the best option for treatment and help for keratoconus patients. Consequently, many studies have attempted to categorise the disease according to its severity. According to Ihme et al. (1983), Amsler graded the disease into four different stages. The first two stages are rarely diagnosed and are characterised by depression and angulation of the horizontal axis of the placido disc image. The next two stages are categorised on the basis of slit-lamp findings. Stage three is characterised by the existence of cone apex thinning, a visible corneal nerve, and Vogt's striae. Finally, stage four is characterised by the presence of Fleischer's ring, apical scarring, and Munson's sign.

Based on the clinical appearance of cone shape and size, keratoconus is classified as:

1. A bow-tie cone, located superotemporal and superonasal and appearing at a very early stage of disease (Owens and Watters, 1996).

2. A round or nipple-shaped cone (smaller than 5 mm), the peak of which is located near the optical axis and often inferonasal to it, and rarely extends into the corneal periphery (Perry et al., 1980).
3. An oval or sagging cone (greater than 6 mm), which is less common and similar to the nipple cone, but is larger and more oval with an apex that is decentred inferotemporally (Perry et al., 1980).
4. A global cone, the largest cone, occupying around 75% of the corneal area (Caroline et al., 1978).

Fowler et al. (1988) classified keratoconus into three stages on the basis of keratometry reading.

- Mild: keratometer readings less than 48 D.
- Moderate: keratometer readings between 48 and 54 D.
- Advanced: keratometer readings more than 54 D.

This classification system has been adopted in the clinical aspects of this thesis.

2.5 Ultrastructural alterations in keratoconus.

The study of corneal structural changes as a result of keratoconus using various laboratory tools such as light microscopy, confocal microscopy and scanning and transmission electron microscopy have provided valuable information (Teng, 1963, Radner et al., 1998b, Sherwin et al., 2002). However, to date, the pathogenesis of the disease remains unknown.

In the early stage of keratoconus, the basal epithelial cells appear irregular, and as the disease progresses they become elongated and spindle-shaped at the base of the cone (Tusbota et al.,1995), with larger irregularly spaced wing cell nuclei (Hollingsworth et al., 2005b). Another change appearing in the epithelium is an accumulation of iron particles seen within the subepithelial basement membrane and between basal epithelial cells in areas corresponding to Fleischer's ring (Gass, 1964).

When Bowman's layer is involved, some authors have suggested that it becomes very thin or is ruptured in several sites at the apical lesion of the central cornea (Sawaguchi et al., 1998). Scroggs and Proia (1992) have noted discontinuities in Bowman's layer, and sometimes distortions in the stroma beneath these defects. Kenney et al. (1997) have seen gaps in Bowman's layer, and also observed fibrotic regions where the epithelium is in direct contact with the stroma.

Transmission electron microscopy (TEM) studies of keratoconus tissue have revealed that the thickness of collagen lamellae themselves is unaltered, but the number of lamellae appears to be less than in normal tissue (Takahashi et al., 1990). As counted by Pouliquen et al., (1970) the number of lamellae at the cone of the keratoconic stroma was 80-140, compared to 300 in normal corneal stroma. The lamellae that remain are often formed into Z-shaped folds (Fullwood et al., 1992). An x-ray diffraction study comparing normal and keratoconus human corneas revealed no difference in collagen interfibrillar spacing, but a

7.5% reduction in intermolecular spacing (Fullwood et al., 1992). The fibrillar diameters were normal (Pouliquen, 1987).

Using scanning electron microscopy (SEM) Sawaguchi and co-workers (1998) have investigated the stromal collagen fibrils in keratoconus corneas and observed loosely-packed, randomly-oriented, and distorted collagen fibrils in some keratoconus corneal stromas, which may reflect reduced collagen density. Radner et al (1998b) reported that the arrangement of collagen lamellae of the stromal keratoconus cornea at the apical region differs from those of the para-apical regions and normal cornea (figure 2.5).

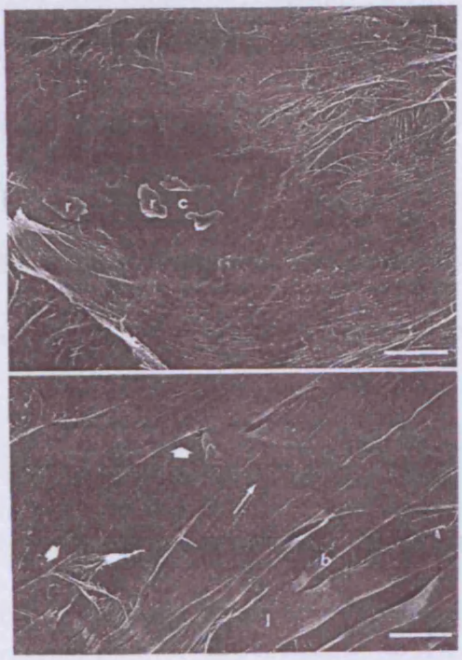

Figure 2.5: *SEM micrograph of the apex of a keratoconus cornea. Collagen fibrillar changes at the apex in C (above) and lamellae split into branches in B (below).* ***Source****: Ophthalmic Res. (Radner et al. 1998).*

Using x-ray diffraction, Daxer and Fratzl (1997) found the orthogonal arrangement of fibrils at the apical lesion of the stromal cone had broken down, whereas outside the diseased region the arrangement was normal. Recently, Meek and his co-authors, (2005) mapped the collagen orientation and relative distribution of collagen fibrillar mass in the human keratoconus cornea and found that changes as an average of the whole corneal thickness were more widespread.

Recently, a confocal microscope study revealed bands varying in width in keratoconus corneas which ran mainly in a vertical direction, and corresponded with the steepest sim-K axis of the corneal topographic map in the posterior stroma (Hollingsworth and Efron, 2005a). Conversely, the authors reported that in the anterior stroma, bands appeared thinner and varied in their orientation. The study indicated that bands corresponded with Vogt's striae, and suggested that they represented collagen lamellae under stress rather than folds.

It has been suggested that keratoconus corneas contain an abnormal form of keratan sulphate proteoglycan (Funderburgh, 1989). Subsequently, abnormal proteoglycans were reported to accumulate in keratoconus lamellae in a study carried out by Sawaguchi (1991). In addition, Fullwood and Meek (1990) found that proteoglycans of the keratoconus stroma were arranged parallel to the collagen fibrils, unlike the normal tissue arrangement, where most proteoglycans are arranged crosswise to the fibril. These abnormal parallel arrangements of

proteoglycans were found only in some regions of keratoconus corneas. It was suspected that the enzymatic degradation of keratan sulphate proteoglycans may alter interfibrillar cohesion and lead to an alteration of the arrangement of collagen at the fibrillar (Funderburgh et al., 1990) and lamellar level (Scott, 1988). The viscolastic properties representing proteoglycan-collagen interactions were found to be abnormal in keratoconus (Wollensak, 1990).

Descemet's membrane and the endothelium are infrequently affected in early keratoconus. However, in advanced stages the potential ruptures in Descemet's membrane are usually repaired by an extension of flattened endothelial cells (Krachmer et al., 1984). The alterations found in keratoconus endothelial cells are likely to be a secondary event occurring due to mechanical stresses (Sturbaum and Peiffer, 1993).

2.5.1 Biochemical changes.

To-date, biochemical studies have revealed a decrease in three different enzyme inhibitors in keratoconus corneas: the alpha 1- proteinase inhibitor, the alpha 2-macro-globulin inhibitor, and tissue inhibitor of matrix metalloproteinases (TIMP-1) (Sawaguchi et al., 1990; Zhou et al., 1998). In addition, increased activities of enzymes were measured that can degrade various extracellular matrix components within keratoconus corneas (Brown et al., 1993; Smith and Easty, 2000; Maruyama et al., 2001). This inhibitor-enzyme imbalance is thought to play

a role in stromal thinning and Bowman's layer / basement membranes ruptures (Kenney and Brown, 2003).

Immunohistochemical staining performed by Sherwin et al. (2002) revealed elevated levels of the enzymes cathepsin B and G within keratocytes of keratoconic corneas. Similarly, Kenney and her colleagues (2005) studied 25 normal and 32 keratoconic corneas, using semi-quantitative reverse transcription-polymerase chain reaction and southern blot analysis to analyse the mRNAs, and immunohistochemistry and/or Western blot analysis to assess protein, and catalase activity. The study confirmed an increase in catalase mRNA level, enzyme activity, cathepsin V/ L2, B and G, and abnormal protein distribution, and a decrease in TIMP-1 mRNA and protein. The authors concluded that the decrease in TIMP-1 and increase in cathepsein V/ L2 may play a role in matrix degradation in keratoconus. Also, their findings support the theory that keratoconus corneas undergo oxidative stress and tissue degradation.

Another immunohistochemistry study of 33 normal and 34 keratoconus corneas demonstrated that keratoconus corneas showed a greater accumulation of mitochondrial DNA damage than the normal corneas (Atilano et al., 2005). This study indicated that increased oxidative stress and altered integrity of mtDNA may be related to each other and may be important in keratoconus pathogenesis.

2.6 Current hypotheses for the pathogenesis of keratoconus.

Although extensive studies have been carried out to find the causes of keratoconus, it remains unknown. From the reviewed literature, various hypotheses have been proposed, but no single theory fully explains the clinical findings. The proposed hypotheses suggest that alterations in the corneal tissue occur in either the epithelium and its basement membrane, or stroma, in early stages.

Evidence from histopathological studies led Teng (1963) to suggest that the earliest alterations appear in the basal cells of the epithelial layer. Unspecific enzymes are released and cause fibrillation of Bowman's layer and stromal collagen degradation. According to Teng's analysis, keratoconus is a disease of the ectodermal layer not the mesenchymal layer of the cornea. Kim et al. (1998) and Wilson, (2000) supported this postulation and demonstrated that the loss of anterior stromal keratocytes is probably due to chronic repetitive removal of the corneal epithelium, leading to stimulated stromal apoptotic cell death. It had previously been demonstrated that keratocytes from keratoconus corneas have a four-fold greater number of IL-1 receptors than keratocytes from normal corneas (Fabre et al., 1991). As a result, Wilson et al. (1996) and Bron and Rabinowitz (1996) suggested that the higher expression of interleukin 1 receptors, acting through a paracrine pathway, may interrupt keratocyte activity and turnover, causing a loss of keratocytes through apoptosis and a decrease in stromal mass

over time. This hypothesis assumes that keratoconus appears consequent to eye rubbing, contact lens wear and atopy.

Conversely, Kenney et al. (1997) postulate that there is probably a factor in the stroma that stimulates the epithelium, which then feeds back down to the stroma, causing apoptosis and cytotoxic byproducts to be released. This would explain why the reappearance of keratoconus following keratoplasty is very rare, even though the host limbal cells supply the graft epithelium. Recently, Sherwin et al. (2002) studied morphological changes in peripheral keratoconic corneas using confocal microscopy. These corneas exhibited discrete incursion of fine cellular processes into Bowman's layer. These fine cellular processes originated from keratocytes even though there are no keratocytes in normal Bowman's layer.

2.7 Biomechanics and rigidity in keratoconus.

Biomechanical studies have revealed that the interlacing between lamellae plays an important role in determining the cohesive and tensile strength of the cornea (Smolek 1990; Smolek 1993; Muller et al., 2001). Accordingly, Smolek and Beekhuis (1997) confirmed that the position of the keratoconus cone is usually at the weakest area between the central and inferior periphery of the corneal stroma. Radner and his colleagues (1998b) also showed that the interlacing of the lamellae decreases or is even absent at the apex of the keratoconus corneal stroma. This will affect the biomechanical properties of the cornea and lead to a further progression of keratoconus.

According to Polack (1976), collagen lamellae in keratoconus are released from their attachment to other lamellae or to Bowman's layer and slide, resulting in a thinning of the cornea without collagenolysis. Meek and his associates (2005) have also indicated that keratoconus may be due to unravelling of the anterior stromal lamellae or Bowman's lamellae without loss of tissue mass, but by sliding of collagen fibrils and lamellae over each other. They suggested that it occurs as a result of incomplete normal lock of corneal and limbal lamellae during childhood.

Many authors have concluded that there is a correlation between the low ocular rigidity and the distensibility of the cornea in keratoconus (Davies and Ruben, 1975; Andreassen et al., 1980; Edmund, 1988). On the other hand, Foster and Yamamoto (1978) found no significant difference between the ocular rigidities of keratoconic and normal corneas.

In an attempt to determine the biomechanical properties of the cornea and their relationship to intraocular pressure, Luce (2005) measured corneal hysteresis in normal and keratoconus corneas, Fuch's dystrophy corneas, and before and after laser assisted in situ keratomileusis (LASIK). They achieved this using an ocular response analyzer (ORA). The study showed an average of 9.6 mmHg and 8.1 mmHg in normal and keratoconic populations respectively. Further, the results indicated that corneas having LASIK, corneas with keratoconus, and corneas with Fuch's dystrophy demonstrate a general decrease in corneal

hysteresis compared to corneas from normal eyes. This means that in all cases of keratoconus, the cornea becomes unusually thin at the centre and is thus weakened due to reduced stiffness and elasticity. Consequently, the cornea becomes unable to support or withstand the intraocular pressure, the effect of which causes it to bulge forward in the shape of a conical protrusion.

The apex of the cone constantly coincides with the thinnest part of the cornea (Hall, 1963). Strips of cornea from healthy subjects and from those with keratoconus were biomechanically compared, and it was concluded that the reduced strength of keratoconus corneas is partly the result of reduced thickness, reduced stiffness, and associated reduced capacity for relative energy absorption (Andreassen et al., 1980). The authors here, suggest that the decreased mechanical resistance plays a role in the protrusion of the keratoconus cornea.

2.8 Associated diseases.

A review of the literature to-date reveals that the causes of keratoconus are unclear. The associations between keratoconus and other diseases are variable and there is no specific disease proven to indicate the existence of keratoconus. Different studies have combined keratoconus with other ocular or rare systemic disorders, or biomechanical instabilities or mechanical abuses. In contrast, the most common presentation of keratoconus is as an isolated sporadic condition with no other associated disorders.

2.8.1 Atopy and other allergic conditions.

An atopic disease is a genetically determined disorder in which there is an increased tendency to attain certain conditions, such as bronchial asthma, hay fever, and atopic dermatitis. The condition is triggered by a regain antibody (immunoglobulin E) which sensitises the skin and other tissues. When combined with the corresponding antigen, it is responsible for the liberation of histamine and other mediators which cause atopic symptoms.

Many authors have noted the co-existence of keratoconus with atopic diseases. Raised serum levels of immunoglobulin E have been reported in 47% to 52% of keratoconus patients (Rahi et al., 1977; Kemp and Lewis, 1982). Rahi et al. (1977) and Gasset et al. (1978) found atopic disease in 35% of keratoconus patients compared with 12% of normal patients. Further, Zadnik et al. (1996) reported that 34.6 per cent of patients had some form of atopy; with 13% and 10.9% suffering from asthma or with a history of atopic dermatitis, respectively. Maguire and Meyer, (1988) reported that the commonest type of allergic disease linked with keratoconus is hay fever, followed by asthma and eczema.

2.8.2 Associated ocular and systemic conditions.

Several ocular abnormalities documented to occur concurrently with keratoconus are retinitis pigmentosa, congenital cataract, aniridia, microcornea, corneal degeneration, ectopia, lenticonus, persistent papillary membrane, and blue sclera. Although most associations between connective tissue conditions and

keratoconus appear to be epidemiologically insignificant, a few reports suggest that some cases of keratoconus may be a manifestation of a systemic disease of collagen metabolism. Rabinowitz (1998) summarised most systemic syndromes previously reported. These included Ehlers-Danlos, Mitral valve prolapse, Osteogenesis Imperfecta and Marfan's syndromes.

On the other hand, some common diseases have been reported to have a high association with keratoconus. Down's syndrome, for example, has been reported as having a 0.5% to 15% association with keratoconus and Leber's congenital amaurosis has been found in up to 30% of keratoconus patients older than 15 years (as cited by Rabinowitz, 1998). These two disorders are attributed to a high incidence of eye rubbing, but Elder (1994) disputes this hypothesis and suggests that the association with keratoconus may be due to a genetic factor rather than eye rubbing. Ridley (1961) was the first to draw attention to the possibility that eye rubbing might contribute to the development of keratoconus. Five years later, (1966) the same author reported a 70% incidence of eye rubbing in his studied sample. In southern climates, keratoconus is often more prevalent, especially in those countries where there is a high incidence of vernal catarrh (Theophanides, 1980). Many authors have concluded that the stimulus for eye rubbing is an atopic or bioallergic disorder, like hay fever, vernal catarrh, eczema and belpharitis. Thus, eye rubbing is now thought to be secondary to allergy rather than being the primary cause of keratoconus (Bawazeer et al., 2000).

It has been suggested that the long-term wear of both soft and hard contact lenses may trigger the onset of keratoconus in patients who are predisposed to it, or may be associated with the development of keratoconus. Gassest et al. (1978) and Macsai et al. (1990) sought to clarify the role of contact lenses in the development of the disease. These two studies reported that the same proportion, 26.5% of 162 and 398 patients, respectively, developed keratoconus when wearing hard contact lenses.

Recently, a study investigated the effects of contact lenses on corneal thickness and curvature (Yeniad et al., 2003). The authors concluded that both soft and rigid gas-permeable contact lenses cause corneal thickening and flattening in the first month, and corneal thinning and steepening with the progress of time. These alterations due to lenses may negatively influence corneal physiology, thereby leading to keratoconus.

The apical clearance and annular bearing of rigid contact lens fitting may increase curvature or ectasia in corneas with keratoconus (McMonnies, 2004; McMonnies, 2005). These authors presented a hypothesis that the mid peripheral cornea that corresponds with the annular bearing of apical clearance fitting will resist an increasing force of intraocular pressure, thereby causing the central cornea to distend forward. The second hypothesis is that the central cornea that coincides with the apical bearing of fitting will lead to chronic epithelial trauma that may cause stromal thinning. It is therefore not clear

whether the contact lens contributes to the onset of keratoconus or promotes progression of the ectasia.

2.9 Genetics and keratoconus.

Although attention has been given to keratoconus as a hereditary disease, whether genetic factors play a role in its pathogenesis remains unclear. However, some clinical studies have pointed to a genetic influence in the development of keratoconus. One study reported a positive family history in 6%-10% of patients with keratoconus (Tretter et al., 1995) and another study found a strong familial history in 23.5% of patients with keratoconus in New Zealand, exceeding previously reported figures (Owen and Gamble, 2003).

Regarding the modes of hereditary transmission of keratoconus, the majority of studies have documented autosomal dominant and minor recessive hereditary transmission patterns with variable expression (Rabinowitz et al., 1990; Sallum and Erwenne, 1996). Rabinowitz (1998) also indicated that the literature has made mention of monozygotic and dizygotic twins. As a result of rapid development in molecular and statistical methods, one study reported in a single, large family the linkage between keratoconus and chromosome 21 (Rabinowitz and coworkers, 1999). An abnormality in chromosome 13 has also been associated with keratoconus (Heaven et al., 2000). Further, one study reported that the locus for keratoconus and cataract are linked to the long arm of chromosome 15 (Hughes et al., 2003). Heon et al (2002) identified that there are mutations in the VSX1 homeobox gene for two distinct inherited corneal

dystrophies; posterior polymorphous dystrophy and keratoconus. Recently, Rabinowitz et al (2005) found that the suppression of transcripts for Aquaporin 5 provides clear evidence of a molecular defect identified in keratoconus.

2.10 Optical correction and management.

Although keratoconus is a noninflammatory disorder, it is a particularly problematic disease for both the patient and practitioner for several reasons. First, there is no ideal technique to tackle keratoconus immediately without transplantation. Also the development of the disease is difficult to anticipate, vision is not stable with spectacles, and fitting contact lenses is a complex task which is not free from complications that result from long-term lens use (Mackie, 1993). Patients face big challenges with contact lenses, such as intolerance to hard contact lenses, the daily complexity of the contact lens regimen, and chronic conjunctival diseases related to long-term use of contact lenses. Moreover, the transplantation is not free from complications (i.e. a high degree of residual astigmatism, graft rejection, and reoccurrence of keratoconus).

2.10.1 Glasses.

Commonly, myopia and simple astigmatism develop in the very early stages of keratoconus, and many patients begin spectacle wear before signs of the disease are evident. The milder forms of keratoconus often can be satisfactorily corrected with spectacles, and this is the treatment of choice for as long as it

provides acceptable visual acuity. However, as the disease progresses, patients experience unstable vision, anisometropia, inadequate visual acuity, distortion, and/or poor visual acuity with glasses.

2.10.2 Contact lenses.

Rigid gas permeable (RGP) contact lenses are usually resorted to when the visual acuity with spectacles drops to an unacceptable level. Rigid contact lenses neutralise the induced corneal irregularity, and visual acuity usually improves markedly. Regardless of the complications associated with rigid contact lens wear, it has advantages over spectacles. It provides good acuity for irregular corneas (i.e. keratoconus, trauma, and subsequent to refractive surgery), a wider field of view, and better refractive anisoconia.

Apart from surgery, RGP contact lenses are considered the mainstay of therapy in this disorder and represent the treatment of choice in 90% of patients (Buxton, 1978). Simddy et al. (1988) refitted more than 70% of patients presenting for surgical consideration of penetrating keratoplasty for keratoconus and successfully maintained patients in contact lens wear. Belin et al. (1988) also refitted 88% of keratoconus cases who were referred for surgical arrangements due to contact lens failure. It was thought that rigid contact lenses had some therapeutic effect in that they halted or at least retarded the progression of the cone (Kemmetmuller, 1975; Mandell, 1997), but this has been disputed (Theophanides, 1980).

Usually the stage of the disease and the specific type of cone presentation play an important role in selecting lens design, and in successful contact lens fitting. Therefore, as the disease progresses, more complex RGP contact lenses are used. These lenses include spherical lenses, bicurve, tricurve, multi-curve spherical lenses, and aspheric lenses. Despite the development in rigid contact lens design and materials over the past three decades, the Soper cone, McGuire, and Rose-K keratoconic lenses systems have been the mainstays of conical correction for keratoconic patients (Norman, 2000).

Further special lenses are used in fitting keratoconus patients who cannot adapt to RGP lenses. If a keratoconus patient is intolerant of rigid lenses, the use of a rigid lens fitted over a soft lens is sometimes a viable alternative. The concept refers to a piggyback fitting that was first advocated by Westerhout (1973). Initially, the patient is fitted with a large diameter soft lens with proper centration and movement. Keratometry readings of the front surface of the soft lens in situ are taken, and then the rigid lens is fitted on the top of the soft lens. The theoretical advantage of this method of correction is that it enables an advanced case of keratoconus to be optically well corrected with added comfort.

The Softperm lens is a hybrid lens of a RGP of 6 mm optical portion centrally surrounded by a soft, hydrophilic skirt lens of 14.3 mm diameter. The lens fits over the cone and provides excellent vision because the larger diameter soft skirt provides good centration on displaced apices, as well as comfort. It helps in fitting early keratoconic patients who cannot adapt to RGP lenses, but edema, neovascularisation of the peripheral cornea, and insignificant movement are the

main disadvantages and regular and careful follow up is required (Maguen et al., 1991).

2.10.2.1 Fitting techniques for RGP lenses.

Generally, the shape and cone apex have been used to classify cones into three distinct groups which can be used as the basis for choosing a fitting philosophy (Woodward, 1997). Keratoconus is commonly managed by various RGP lens designs, and each design has its origin in one of the three essential fitting techniques. These three widely-debated fittings are steep apical clearance, flat apical bearing, and divided support (see figure 2.6).

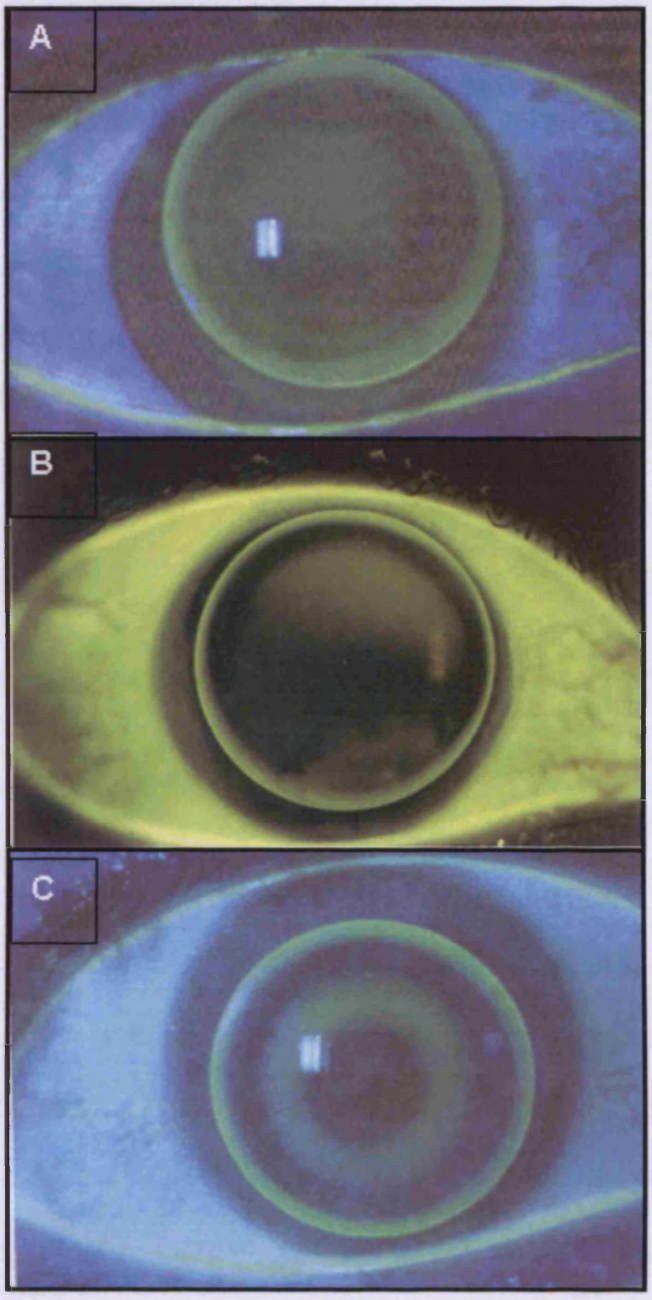

Figure 2.6: *Steep apical alignment fitting (**A**), flat apical alignment fitting (**B**), and three point touch alignment fitting (**C**). Sources: Contact Lens & Anterior Eye J. (Pullum, 2003) and (Bennett and Weissman, 2005).*

Principally, in steep apical clearance fitting, lens support is directed onto the paracentral cornea, and away from the apex of the cornea. This technique has several advantages, for example, apical scaring, corneal oedema and punctate staining can be avoided, but several disadvantages can also result from this technique, such as reduced visual acuity, flare, poor tear exchange, and more negative power (Mandell, 1997; Woodward, 1997). Further, this method is only suitable for the small nipple cone, and not for the advanced stage (Gundle, 1996).

In the flat apical bearing fitting method, lens support and bearing are directly on the apex of the cornea, resulting in better visual acuity and less negative power and this is easy to achieve (Ham, 1986). However, corneal abrasions and apical scarring are the main disadvantages (Korb et al., 1982).

Finally, divided support or three-point-touch rigid lens fitting is currently the most frequently used approach. The three-point-touch refers to the support provided for the lens by an area of central bearing (2-3 mm in diameter) and two other areas of bearing at the corneal mid-periphery. Lens weight is therefore distributed over the cornea, and eliminates most disadvantages of both flat apical bearing and steep apical clearance. Further, it is useful for large cone and advanced stages of keratoconus (Leung, 1999). An initial trial lens BOZR should be selected based on average keratometric readings or steepest meridian as a

starting point, then changed up and down until the best fitting is obtained (for further details see chapter three, part two).

2.10.3 Surgical options.

The last treatment option for keratoconus patients is surgery. Currently, various surgical approaches are available. However, penetrating keratoplasty (PKP) represents the best and most successful surgical option for patients who cannot tolerate contact lenses or have significantly lost visual acuity with contact lenses. In this method, the central affected area of the cornea is removed, and replaced by the full thickness of a normal donor cornea. Trephines between 7.5 and 8.5 mm are usually used, but Fleischer's ring can be used as the limit of the conical cornea. A study which investigated the results of 100 post-PKP keratoconus patients between 1968 and 1986 showed a 93% rate of success, and 81% had visual acuity 20/40 or better (Sharif and Casey, 1991). Moreover, complications after PKP are rare. These include rejection, post-operative astigmatism, a fixed dilated pupil, and recurrence of keratoconus (Kremer et al., 1995; Tuft and Buckley, 1995).

An alternative surgery for keratoconus patients is a partial corneal transplant named epikeratoplasty. This technique involves partial removal of the cornea which is replaced by the donor cornea which has been frozen and shaped to patient requirements in a cryo-lathe. This technique is suitable for contact lens intolerant patients in whom scarring has not yet occurred (Dietze and Durrie,

1988). Phototherapeutic keratectomy (PTK) with an excimer laser has been used with some success to remove anterior stromal scarring, and in order to smooth the tip of the cone, and improve contact lens tolerance (Ward et al., 1995). Intrastromal corneal rings (Intacs) used to change the shape of the cornea in eyes with low myopia has been used limitedly in keratoconus patients to reduce the corneal steepening and astigmatism (Colin et al., 2000). This technique is based on reshaping the cornea by inserting ring segments into stromal lamellae to flatten the central cornea (Burris et al., 1991). Finally, another therapeutic method used recently is based on collagen cross-linking by combined riboflavin and ultraviolet-A treatment, and this has been claimed to be of significant use in stopping the progression of keratoconus (Wollensak et al., 2003).

3.1 An epidemiologic study of the keratoconus profile in a Saudi Arabian population

3.1.1 Introduction.

Most previous epidemiologic studies of keratoconus vary widely in their findings due to the rarity of disease, and the different criteria and tools used in its diagnoses. This has led to several studies reporting the overall incidence rate of keratoconus as between 1.4 and 600 cases per year per 100,000 (Ihalanainen, 1986; Kennedy et al., 1986; Crews et al., 1994; Zadnik et al., 1996; Barr et al., 1999; Totan et al., 2001).

The onset of keratoconus appears characteristically at puberty (the mean age of onset is 16 years) and progresses over a period of 7 to 20 years (Ridley, 1956; Krachmer, 1984). But Hall (1963) and Bennett (1986) reported that the onset of keratoconus can occur at ages as young as 6 years. These reports have mainly considered Caucasian populations, with recent studies suggesting an influence of ethnic origin on the incidence rate and age at onset. For example, a study by Pearson et al. (2000) on Asian and Caucasian populations living in the UK disclosed an incidence rate of 19.6 and 4.5 cases per 100,000, respectively. Similarly, Georgiou et al. (2004) studied British Asian and Caucasian populations and reported incidence rates of 25 and 3.3 cases per 100,000, respectively.

Previous studies on keratoconus in Saudi Arabia are very limited. One study investigated indications for corneal transplantation at the King Khaled Eye Specialist Hospital over a twenty years period (1983 – 2002) and found that the annual number of corneal transplants performed for keratoconus increased from approximately 30 to 170 per year, accounting for over 40% of all grafts (Al-Towerki et al., 2004). This apparent sharp increase in keratoconus incidence, however, was attributed to the recent increases in the Saudi Arabian population, and the expansion of modern ophthalmic services.

The influence of ethnic origin on the incidence rate and severity of keratoconic disease has been recently suggested to be of significant importance. Reports on keratoconus in Saudi Arabia are very limited, therefore, the first half of this chapter presents a prospective study that assesses the incidence rate, onset age, as well as the severity of keratoconus disease and associated signs and symptoms of new patients with keratoconus attending the Department of Ophthalmology of Asir Central Hospital (ACH), Saudi Arabia.

3.1.2 Background.

Saudi Arabia is an extensive country; with an area of about 2,331,000 km^2, it comprises about 80% of the Arabian Peninsula and is physically divided into six parts from west to east. The western coastal plain is located along the Red sea coast. The highlands, the belts of mountains which extend from north to south parallel to the coastal plain, gradually increase in width and height towards the south. The highest peaks and widths of mountains are located in the Asir Province (the highest is 3248 metres located in Asir Province). Asir

province (where the study was undertaken) is located in the south-west of Saudi Arabia, and Abha is the capital city of Asir Province shown by the yellow triangle in figure 3.1.1. In the northern area of the kingdom is the northern steppe land which is used for pasture by nomadic herders. In the centre of the country, is the Najed Plateau in which the capital, Riyadh City is located. Finally, deserts extend from north to south and stretch to the Arab Gulf which contains all the major oil fields in the kingdom (Ministry of Planning, 1985). Generally, Saudi Arabia has a dry climate; it is hot in summer and cool in winter in the northern and central areas. Higher humidity occurs on the coasts, and the mountainous areas in the west have a mild climate (Ministry of Planning, 2000). The common population is distributed in the western and central regions (about 77.3% of the total population) (Ministry of Planning, 1999). Asir Province represents more than 25% of the Kingdom's population living in thousands of villages and few small urban centres in these highlands (Ministry of Planning, 1985).

Figure 3.1.1: Map of Saudi Arabia. It shows different characteristics of topographic relief and demographic distribution of population in Saudi Arabia. As indicated by yellow triangle, Asir region is located in the south-west and Abha is the capital city of Province. Website: *www.worldatlas.com/webimage/countrys/asia/lgcolor/sacolor.*

The current health services system, as it is in other parts of the world, is divided into government (public) sector and private sector. In the public sector, the state's plans aim to provide full-scale health care to all Saudi citizens free

of charge (Yamani, 2000). The health care responsibilities in Saudi Arabia are undertaken by several governmental agencies supervised by Ministry of Health (Yamani, 2000). The medical facilities that are provided by Ministry of Health in Saudi Arabia include the following: 135 general hospitals, 1,737 primary health care centres and 47 specialised hospitals (Al-Shahrani, 2003). The health care system process that follows Ministry of Health is to examine patients in primary health care centres and then refer them to general / tertiary hospitals. Medical cases that can not be treated in general / tertiary hospitals are referred to specialist hospitals by their general practitioners (Al-Saati, 2000). Further, there are 39 high sophisticated hospitals in the central and western regions run by other governmental agencies, which provide medical services to their staff but also receive the complicated cases from hospitals that follow Ministry of Health (Al-Shaharani, 2003). Specialist keratoconus contact lens services in Saudi Arabia are limited. They are only available in the sophisticated hospitals that are located in Riyadh city such as King Khaled Eye Specialist Hospital, National Guard Hospital and King Faisal Hospital and Research Centre. To the best of my knowledge, only two Ministry of Health referral hospitals have specialist contact lens clinics, Asir Central Hospital in Asir region and the Eye Hospital in Jeddah.

3.1.3 Materials and Methods.

3.1.3.1 Clinical Methods.

All patients attending the Department of Ophthalmology, Asir Central Hospital, Saudi Arabia, for one year (May 2001 – April 2002) who were suspected of

having keratoconus were recruited. Further, patients newly diagnosed with keratoconus, but attending the Department of Ophthalmology in other tertiary hospitals in Asir province, were referred directly to the screening clinics in Asir Central Hospital for further management. In the Ophthalmology Department, of Asir Central Hospital cases were first seen by consultants and then referred directly to the screening clinic to conduct the study requirements and continue patient management. Thereby, cases could be seen by more professionals to confirm the diagnosis of keratoconus, especially in the subtle or early stages of the disease. Screening for each patient was achieved at a single session lasting approximately 45 minutes. The clinical assessment routine for each patient included the following:

- **Case history.**

Data were gathered concerning age at the time of presentation, self-reported patient age at time of incidence (age at the time of first vision complaint), sex, symptoms (blurred and decreased vision, monocular diplopia, photophobia, headache, glare, ghosting of images and frequent Rx changes), history of ocular disease (tearing, rubbing, redness, allergy and vernal keratoconjunctivitis) and any active treatment, systemic disease (especially atopic diseases), medication, family history, and occupation.

- **Snellen visual acuity**

The principal measurements of visual acuity (VA) were carried out: monocular unaided VA, habitual VA, and optimal VA (with the best manifest correction). A high contrast Snellen VA chart viewed from six metres was used. The

Snellen chart was moved close to the patient when it was not possible to discriminate between chart letters. Finally, luminance of the chart was maintained at 80 cd / m^2, and the room was kept illuminated.

- **Keratometry measurement.**

Javal Schiotz (Shin/Nipon Japan 2190) keratometry was used to acquire the central corneal curvature. This unit has a range of between 30 D (11.20 mm) and 60 D (5.60 mm). Auxiliary lenses (+1.25 D or a +2.25 D) over the aperture of the instrument were used to extend the usual range when necessary (Zadnik et al., 1998). Consequently, the keratometric reading extended over the usual range by 8.25 D or 16 D. Finally, the mire quality of the keratometer was graded according to the amount of distortion from 1 (clear) to 4 (very distorted).

- **Refraction.**

Objective measurement (Streak Retinoscopy) provides a sensitive assessment for detecting and confirming the diagnosis of early keratoconus. It was used to determine the initial refractive error. Further, careful objective over-refraction and subjective refraction after each contact lens fitting was performed.

- **Slit-lamp Biomicroscopy examination.**

Complete examinations were performed to detect any abnormalities or anomalies of the eyelids, eyelashes, conjunctiva, tear layer, anterior chamber, and iris, using a Haag-Streit slit lamp microscope. In addition, the presence or

absence of biomicroscopic signs of keratoconus, such as apical thinning, Fleischer's ring, Vogt's striae and scars or any other abnormality, were observed.

- **Fundus examination.**

Direct ophthalmoscopy or an indirect Biomicroscopy were used to inspect the lens, vitreous, and retina. Examination of retinal vessels, retinal periphery, macular area, and optic nerve head, was carried out. None of the patients included in the study had any abnormalities, apart from keratoconus.

- **Intraocular pressure and anterior chamber angle.**

Intraocular pressure (IOP) assessment was undertaken using a C.T 80 Topcon computerised non-contact Tonometer, and recorded as the average of at least two IOP measurements for each patient. Hence, the IOPs in the population study were within the normal limit. The Van Herick procedure was used to estimate the anterior chamber angle depth. The ethical approval process for clinical research for this study was achieved in agreement with the regulations of the Asir Central Hospital as indicated in Appendix 3.

3.1.4 Subjects.

Consecutive screenings were conducted for patients referred to the Ophthalmology Department, Asir Central Hospital for the first time for further management. One hundred and twenty-five patients (240 eyes) were recruited, comprising 51 males and 74 females, with a mean age of 18.45 ± 3.9 years (standard deviation) at the time of screening. Patients' age ranged

from 8 – 28 years. The keratoconic eye diagnosis was made on the basis of changes in the best corrected VA, familial keratoconus, an irregular surface evidenced by distorted corneal curvature, keratometry, scissoring of the Retinoscopic reflex, or irregularity in the red reflex with direct ophthalmoscopy. Clinical signs were at least one of the following biomicroscope characteristics: central corneal stromal thinning, apical stromal scarring, Vogt's striate, Fleischer's ring, and Munson's sign. Unusual cases for which the diagnosis of keratoconus could not be established with confidence were excluded from the study. Patients with atopic diseases were referred to the appropriate medical practitioners for further management. Patients with vernal keratoconjunctivitis (VKC), and allergy were treated by ophthalmologists in the department.

3.1.5 Statistics.

After completion of the data coding, the information was entered into the computer using SPSS 12 for analysis. In this study, descriptive statistics and analytical methods were used to describe the data collected from all keratoconus epidemiology variables. Multiple response analysis was used to describe the atopic ocular history (allergy, rubbing, VKC, tearing and redness) since the patient may have had one or more of the symptoms. Cross tabulation was used to detect VA measurements in right and left eye independently in each stage of keratoconus on the basis of average keratometric reading groups. In addition, VA measurements were categorised into three groups, then cross tabulation was used to observe VA responses in each stage of the disease. Pearson's correlation coefficient and scatter plots

were used to correlate VA measurements and the progress of keratoconus in right and left eye, independently.

3.1.6 Results.

3.1. 6.1 Incidence Rate.

The incidence rate was calculated using the area population of 654,163 for those aged between 5 and 29 in Asir Province, Saudi Arabia (Ministry of Planning, 2001). This was selected because the disease usually develops within this age range, and because the study's age range was also of this order (8 - 28 years). With this calculation, the keratoconus incidence rate was 20 cases per 100,000 (1 per 5,000) in Asir province.

3.1.6.2 Age of diagnosis / Age of onset.

The mean age at the time of the survey was 17.7 ±3.6 years for males, whose ages ranged between 8 to 24 years, and 19.0 ±3.8 years for females, whose ages ranged between 12 and 28 year (figure 3.1.2). The mean age of the self-reported disease onset among males was a 13.9 ±3.2 year, ranging between 6 and 21 years, 14.6 ±2.6 years among females, ranging between 8 and 22 years.

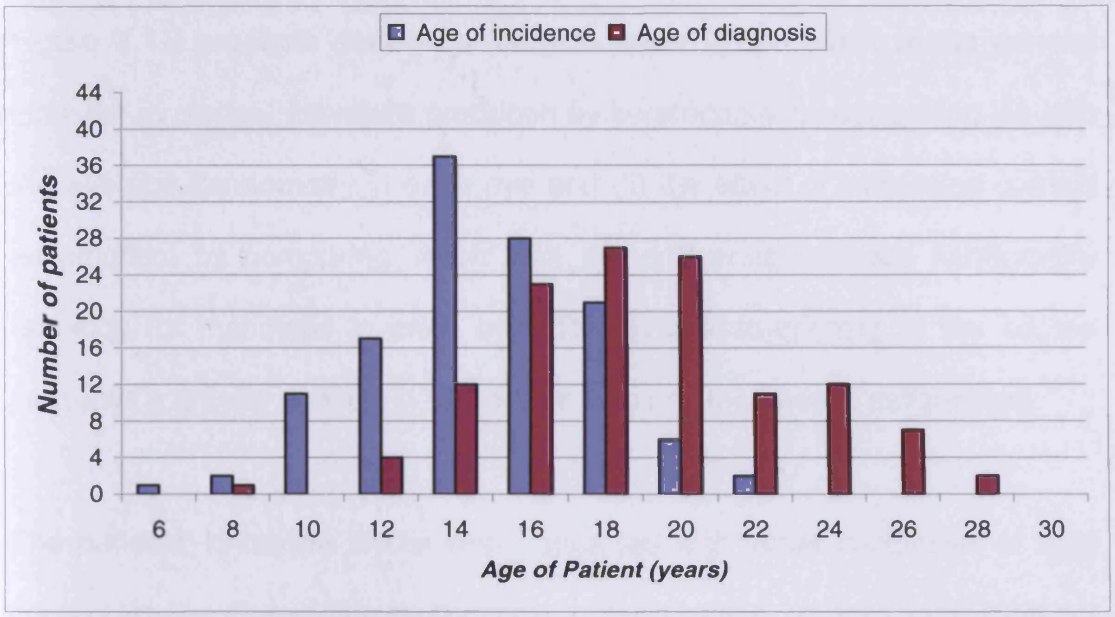

Figure 3.1.2: *Age distribution of patients enrolled in this study at the time of self-reported incidence and ophthalmological diagnosis.*

3.1.6.3 Visual Acuity.

Analysis of the VA measurements indicated that uncorrected vision decreased with increasing severity of the disease (disease severity was classified on the basis of average keratometry readings as shown in table 3.1.2). As the degree of corneal astigmatism and curvature increased, vision decreased, as expected. However, VA values were variable even for patients at the same stage of disease.

Uncorrected vision	Average K-reading		
	Up to – 48 D	> 48.25 – 54 D	> 54.0 D
Up to 6/24	57	21	2
> 6/24 up to 6/60	34	68	18
> 6/60	3	13	24
Overall	94	102	44

Table 3.1.1: *Vision varies with severity of keratoconus, but is influenced by the degree of astigmatism and myopia.*

Figure 3.1.3 presents data graphically to show (i) the effect of the general increase in corneal curvature produced by keratoconus by comparing VA with the average keratometry in each eye and (ii) the effect of increasing corneal astigmatism by comparing vision with the difference between keratometry readings for meridians in each eye. The overall steepening of the cornea produces a greater change in VA, rather than any increase in astigmatism.

The patients' refractive errors were corrected with either spectacles or rigid contact lenses. Depending on the stage of the disease, VA was improvable for 108 eyes with spectacles, while 132 eyes were corrected with different types of rigid contact lens. The distributions of best rigid contact lenses, VA results and spectacle-corrected VA results are shown in table 3.1.1. For spectacles wearers 33.3% of eyes achieved 6/6 or better, but 100% of eyes achieved 6/12 or better. For rigid contact lens wearers, 93% of eyes achieved 6/6 or better, and 97% had 6/12 or better.

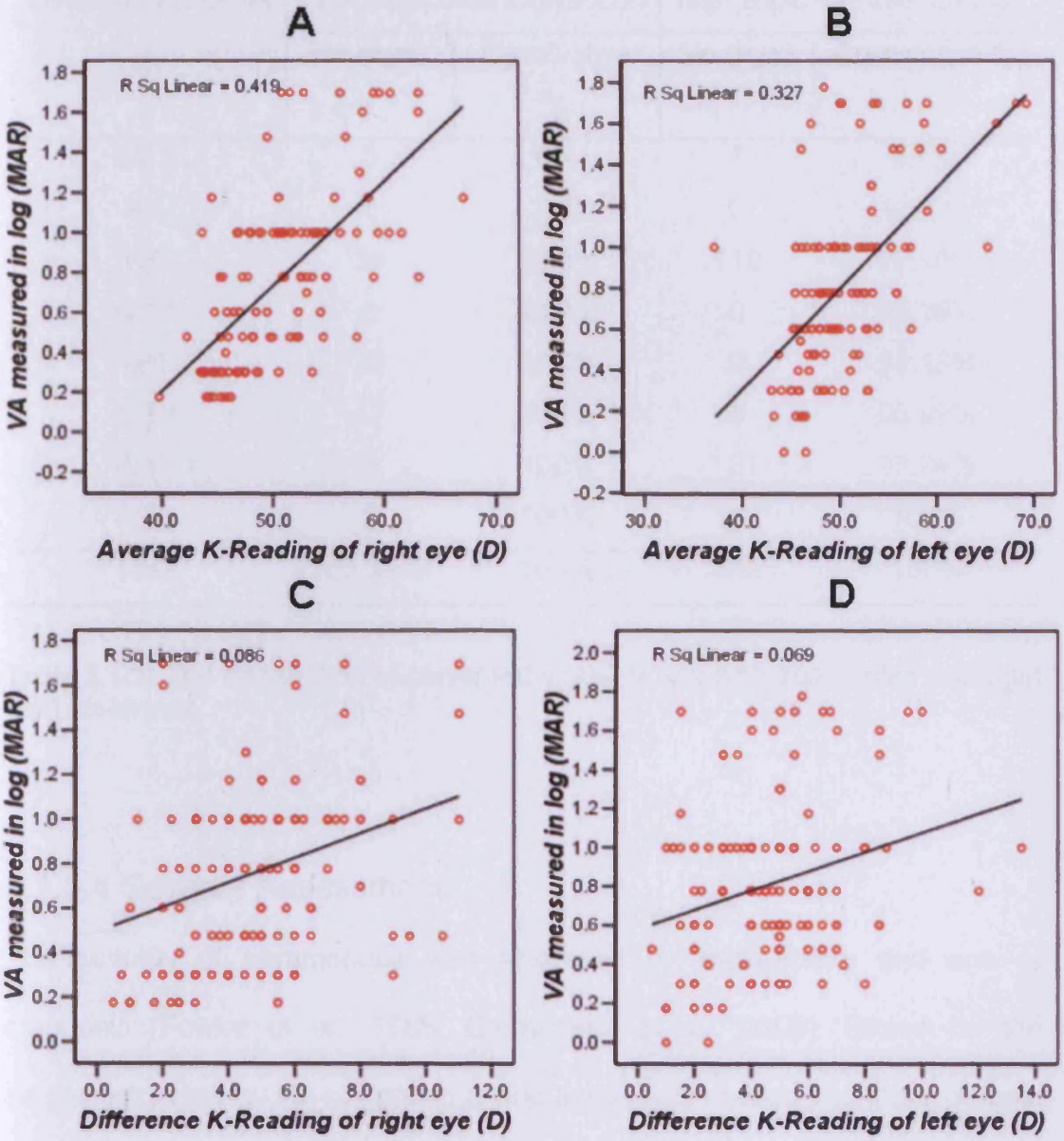

Figure 3.1.3: *Scatter plot illustrating visual acuity against keratometry measurements: (A) & (B) VA decreases with increasing corneal curvature (R^2 =0.42 and 0.33) for right and left eye respectively. (C) & (D) VA decreases with increasing corneal astigmatism, although with only a weak relationship: right eye (R^2 = 0.09) left eye (R^2 = 0.07).*

Visual Acuity Level	With Spectacle Correction		With Rigid Contact Lenses	
	No (eye)	Cumulative %	No (eye)	Cumulative %
6/4.5	0	0%	7	5.3%
6/5	0	0%	6	9.85%
6/6	36	33.3%	110	93.18%
6/7.5	8	40.7%	0	93.18%
6/9	22	61.1%	0	93.18%
6/12	42	100%	5	96.97%
6/15	0	100%	3	99.24%
6/18	0	100%	1	100%
Total	108 eyes	100%	132	100%

Table 3.1.2: The distribution of corrected visual acuity with spectacles and rigid contact lenses.

3.1.6.4 Severity Assessment.

The severity of keratoconus was assessed by keratometry and age at diagnosis (Fowler et al., 1988; Carmichael et al., 2003). Based on the keratometry results, the keratoconus population was divided into three groups: Early, (keratometer reading ≤ 48 D), Moderate, (keratometer reading between 48 – 54 D), and Advanced, (keratometer reading > 54 D). Figure 3.1.4 illustrates the mean age of patients in each keratometry group, suggesting that an earlier age of diagnosis of the disease affects keratoconus severity.

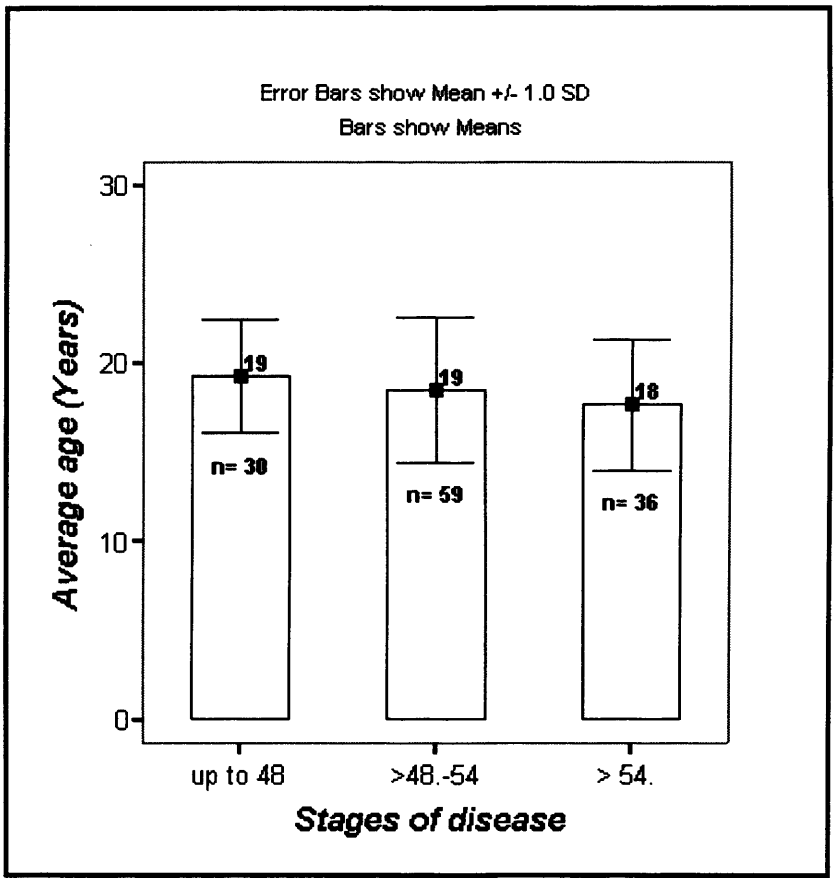

Figure 3.1.4: *Age at the time of ophthalmological diagnosis for each keratometry group. Error bars show means (± 1.0 SD).*

3.1.6.5 Associated signs and symptoms.

All patients were asked general questions concerning ocular history with the worst eye used to investigate the relationship between the ocular history and the severity of the disease and the concomitance with atopic ocular disease.

Regarding atopic dermatitis diseases, twenty patients of 125 (16%) had eczema, asthma and vitiligo. Another 20 patients of 125 (16%) had a positive family history of keratoconus. There was no evidence of Tapeto-retinal

degeneration or Reiger's anomaly. Further, there was no associated incidence of systemic disease, such as Down's, Marfan's or Ehlers-Danlos syndromes.

Seventy patients of 125 (56%) had a positive ocular history, and each of the seventy reported one or more of the five keratoconus-associated factors: eye rubbing, ocular allergy, tearing, ocular redness or VKC (figure 3.1.5). Five patients between the ages of 6 and 12 years reported all five symptoms and three of these also had a family history of keratoconus.

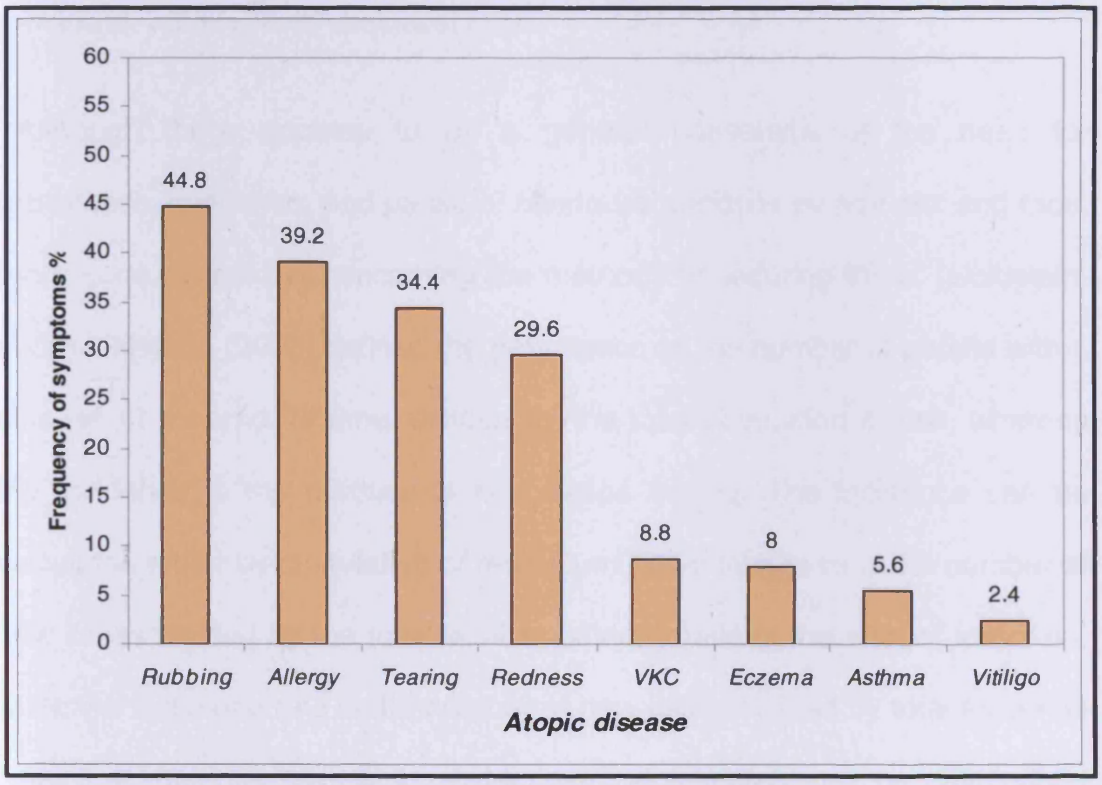

Figure 3.1.5: *Percentage of patients with ocular signs and symptoms accompanying keratoconus.*

3.1.7 Discussion.

The epidemiology of any disease varies widely from one part of the world to the other due to geographic, demographical, racial, climatic and environmental characteristics. Hence, the ability to describe the incidence rate of a disease is important for predicting current and future clinical needs, and in establishing the disease characteristics in a particular population. This study found the incidence rate of keratoconus for Asir Province in Saudi Arabia to be 20 per 100,000 of the population based on new patients referred to the provincial, tertiary-level specialist clinic.

"Although there appears to be a general consensus of the need for prevalence, incidence, and cause-of blindness statistics by age sex and race, there is no consensus concerning the methods of securing them" (Goldstein, 1980). Johnson (2003) defined the prevalence as the number of people with a disease at a particular time, divided by the total population at risk, whereas the incidence is the number of new cases arising. The incidence can be calculated either by cumulative or rate. Cumulative incidence is the number of new cases divided by the total number of individuals at the start of follow-up, while the incidence rate is the number of new cases divided by total follow-up time. The methods utilised in epidemiological research may be categorised into two main types: experimental and observational studies and each generates sub-types of study. The observational study has three types of study, cross-sectional, case-control and cohort (longitudinal) studies, each of which has advantages and disadvantages. For example, the cross-sectional observational cohort study that is used here has a selection bias in that

patients selected for inclusion into a study may not be representative of the population to which the results will be applied (Petrie and Sabin, 2001). In the current study there are limitations and drawbacks. For example, all of the primarily health care and general hospitals did not have a professional eye clinic and practitioners in these health services are not qualified to diagnose the cause of the vision loss. Moreover, these hospitals are far away from each other geographically leading to considerable logistical problems.

Although the author is convinced that the results of hospital-based surveys can not provide accurate information on the prevalence of eye disease in the community, there is no specific method can overcome this matter at the present time. Therefore, the author found some advantages that may at least help to estimate the approximate incidence of the disease in Asir Province. Subjects presented for medical evaluation through referral from screening programmes or because of noticeable changes to their vision or because of other symptoms associated with the condition such as VKC. Age of incidence is usually within school age (education until 18 years is compulsory). The vision screening test for students is usually taken regularly through primary to high school, the whole area is covered with school and health services and any suspected or diagnoses case of keratoconus or other abnormal disease should be referred to the only specialised hospital in the area in order to take further management. Therefore a high proportion of keratoconic cases would be expected to be picked up. Some asymptomatic cases arising after school-leaving age may not be picked up. The vast majority of students are following their education in the universities after high school and are more aware of any

types of vision loss. The whole number in the targeted age (5-29 years) of the population in this area is known, so the incidence in the 'at-risk' population can be calculated. Further, some published studies have used the same method, and this encouraged the author to use it (Pearson et al., 2000; Saini et al., 2004; Georgiou et al., 2004).

So, although the current study has shortcomings because it is clearly did not reflect the real picture of disease incidence in the population, it gave some indications about the characteristics of the keratoconus population in Saudi Arabia especially in Asir region.

The present findings of an incidence rate of 20 per 100,000 compares with 1 per 100,000 in the UK (Duke-Elder and Leigh, 1965), 2 per 100,000 in Minnesota, USA (Kennedy et al. 1986), 2.2 per 100,000 in Finland (Ihalainen, 1986), 2.5 per 100,000 in Holland (Woodward, 1984), and 50 per 100,000 in New Zealand (Sabiston, 1978). These variations suggest an ethnic or environmental influence.

The incidence of keratoconus in our cohort of patients is comparable to that of 20-25 per 100,000 in British Asian populations living in the UK (Pearson et al., 2000; Georgiou et al., 2004). A genetic factor underlying this higher incidence was suggested by the authors of the UK studies comparing the incidence between Caucasian and Asian populations. Both Asian and Caucasian groups have similar environmental influences, and the higher number of consanguine marriages among Muslims, especially first-cousin marriages among Pakistani people, was proposed as a possible cause of the increased genetic

concentration of keratoconus. A similar genetic factor may also have contributed to the present study's findings because a positive family history was found.

Previous reported rates of a positive family history of keratoconus in Caucasian populations are 6% (Zadnik et al. 1996), 8.8% (Swann and Waldron, 1986) and 23.5% (Owens and Gamble, 2003). This compared with 16% (20 cases) of patients in the current study. For one family reported here, comprising seven brothers and sisters, four had keratoconus in at least one eye. Moreover, anecdotal evidence from keratoconus patients referred to King Khaled Eye Specialist Hospital indicates that more referrals are from the Asir province compared to other provinces of Saudi Arabia. This suggests that a genetic factor might be involved in the aetiology, since communities living in this area are relatively isolated geographically from the rest of country and any inherited defects will therefore be exacerbated.

Environmental or geographical factors may also have contributed to the incidence rate and severity of keratoconus. Asir Province is a mountainous region, and the majority of the keratoconus patients (95%) were distributed among the high mountain peaks at an altitude of 3000 metres on average. People living at this altitude are likely to have a greater exposure to ultraviolet radiation from the intense sun given that ultraviolet radiation increases with altitude by approximately 10% for every 1000 meters of elevation (Marin et al., 2005). Ultraviolet radiation has been linked to keratoconus previously because it is considered to be a source of reactive oxygen species in the cornea. Kenney and Brown (2003) have put forward a cascade hypothesis which

states that keratoconic corneas have underlying defects (e.g. defective enzymes in lipid peroxidation and/or nitric oxide) in their ability to process the accumulated reactive oxygen species in the cornea and as a consequence undergo oxidative damage. This oxidative damage can lead to a series of cellular and extracellular events such as apoptosis, altered signaling pathways, increased enzyme activities, and fibrosis. Based on this, Kenney and Brown (2003) suggested that ultraviolet radiation might contribute to the pathogenesis of keratoconus.

Another report suggests that keratoconus corneas do not process reactive oxygen species in a normal manner, and that this may play an important role in the pathogenesis of the disease (Lim and Vogt, 2002). The occurrence rate of keratoconus in Hawkes Bay, New Zealand, was one in two thousand of the population and was found to be equally present in both Maoris and Europeans (Sabiston, 1978). The effect of ultraviolet radiation has been proposed to explain the higher incidence rate for keratoconus in New Zealand, which has a Caucasian population similar to the UK, but because the ozone layer is thinner, a greater ultraviolet background. The study by Owens and Gamble (2003) proposes this as a possible explanation for the increased incidence of keratoconus. However, this could not be proved since it was not possible to robustly assess the actual ultraviolet dosage in individuals. Thus, the effect of ultraviolet on the eye requires further study before it can be determined as a risk factor in the development of keratoconus in patients from Asir Province, Saudi Arabia.

Another possible environmental factor that might contribute to the cascade hypothesis for keratoconus development is the lower oxygen pressure at high altitudes as would be the case in Asir Province. Thus, hypoxia may also partially contribute to the cause or the observed rapid progress of keratoconus disease. The cornea is an avascular tissue and needs oxygen from the atmosphere. In hypoxia, corneal physiological changes will trigger a change in glycogen metabolism. The anaerobic metabolism provides less energy than aerobic metabolism, so glycogen stores in the epithelium are reduced (Klyce and Beuerman, 1988).

Genetic and environmental factors may both have an influence on the severity of keratoconus in Asir Province. This can be seen in the earlier age of presentation recorded in the current study (18.5 years), in comparison to other studies. Approximately three quarters of patients examined here (74.4%) presented before the age of 20 years, whereas in the Collaborative Longitudinal Evaluation of Keratoconus (CLEK) study in USA only 4% presented at the same age (Zadnik et al. 1996). Similarly, several other investigators in a Caucasian population have reported a fairly high age at the time of study (mean, 27 years) suggesting a later disease onset (Kennedy et al., 1986; Pearson et al., 2000; Georgiou et al., 2004; Lim and Vogt., 2002; Owens and Watters, 1996). This contrasts with the results of other authors (Saini et al. 2004; Pearson et al., 2000; Georgiou et al., 2004) who found a mean presentation age for Asian patients of 20.2, 21.5 and 22.5 years respectively. The mean age of self-reported disease-onset in this study was 14.3, ranging between 6 and 22 years, compared with 16 years mean onset in

the general population (Krachmer et al., 1984). Although females out-numbered males, there was no significant difference in onset age between males and females.

The increased severity of keratoconus in subjects reported here is also revealed in the classification of disease severity by keratometry readings. Based on average keratometric values, 94 eyes (39.2%) were in the 'Early stage', 102 eyes (42.5%), in the 'Moderate stage', and 44 eyes (18.3%) 'Advanced stage'. However, 37 eyes in the advanced stage (84%) belonged to subjects who were twenty years or under, more than the 67% reported by Saini and associates (2004). Another report investigated all patients with keratoconus and vernal keratoconjunctivitis who underwent penetrating keratoplasty at King Khaled Eye Specialist Hospital between 1986 and 1996. Here, researchers alluded to a higher level of disease severity in Saudi Arabian keratoconus patients, as judged by an early mean age of patients at the time of surgery (18.7 years) (Mahmood et al., 2000). Further, the average age of patients in the advanced stage was 18 ±1 years. Thus, data in this study indicate a rapid progress of the disease and suggest that the severe stage is reached at a younger age in Middle Eastern countries.

This study shows that VA decreases as corneal curvature and astigmatism increase (figure 3.1.4). However, the correlations are not strong because of the variable influence from the amount, regularity and obliqueness of the astigmatism, the level of progressive myopia, the scar type, morphology of the cone and extent of any atopic disease. This indicates that the VA of a

keratoconus patient does not present an accurate picture of the progress of the disease. Clinically this is seen when a keratoconic patient presents with an equal bilateral stage of the disease, but the VA in each eye is different.

Vision correction was possible in the patients investigated here with either spectacles or rigid contact lenses. The contact lenses generally provided the best means of improving VA, with 93% of eyes achieving 6/6 or better. In contrast, only 33.3% of spectacle wearers achieved 6/6. This difference highlights the benefit of fitting rigid contact lenses, since they are better able to overcome corneal astigmatism using the tear lens. It suggests that contact lenses should be fitted earlier in order to provide the optimal visual correction, as well as providing a therapeutic benefit for the cornea by supporting the cone.

Atopic diseases (e.g. asthma and atopic dermatitis), have been suggested as aetiological components of keratoconus, but this study did not find a strong pattern of association. Only 16% of patients included here reported any form of atopy. This compares with the average 35% reported by Gasset et al (1978) and Rahi et al (1977). Similarly, this study had only 7 cases (5.6%) of asthma, and 10 cases (10.4%) of eczema or vitiligo, compared with 13% (asthma) and 10.9% (dermatitis) reported by Zadnik et al (1996). These findings suggest that atopy alone does not predispose to keratoconus, but rather that atopic patients develop keratoconus due to eye rubbing (Bawazeer et al., 2000). The interaction between allergy and rubbing has been reported previously (McMonnies, 2003). Karseras and Ruben (1976) elicited a history of eye rubbing in 66 per cent of their keratoconus patients, while Weed and

McGhee (1998) reported 48% of keratoconus patients rubbed their eyes. In the current study, 49 (39.2%) and 56 (44.8%) patients complained of allergy and rubbing, respectively. In addition, 23 cases of 36 patients (63.8%) in the Advanced stage, 32 cases of 59 patients (54%) in the Moderate stage, and 15 cases of 30 patients (50%) in the early stage complained of both allergy and rubbing.

The question that arose from this work is how could the research into incidence have been done better? After the ethical approval process and with consent from parents of students for preliminary screening, the study could be carried out at randomly selected schools from different regions of Asir Province or from the whole country. The study would focus on ages between 10-yrs and 18-yrs because this is the critical age for keratoconus incidence, and would use a suitable form mainly including the history of ocular or systemic problems, age and sex. Using a Snellen chart to measure VA in a suitable room in the school and portable Ophthalmoscopy, Retinoscopy and keratometry it would be possible to carry out the study. Students with abnormal vision could be referred to hospital for further management. By this way the incidence of keratoconus could be estimated by calculating the ratio of keratoconus cases to the total number of examined students.

It might also be possible to collaborate with other practitioners in the same field in other hospitals to organised multi-centre trials in Saudi Arabia for keratoconus population database similar to the CLEK study in the United States (Szczotka et al., 2001).

In conclusion, this study has found an early onset and increased severity in patients with keratoconus in the Asir Province of Saudi Arabia. This might be related to a combination of genetic and/or environmental factors. Clinically, contact lens correction should be considered early in treatment to maximise visual performance.

The author understands that the funding of keratoconus screening is not a priority for health care services compared to other diseases for which early detection may prevent blindness. This is because the detection of early keratoconus cannot stop or prevent the progress of disease. Further, the onset of keratoconus is accompanied by symptoms and it is likely that, sooner or later, a subject with the condition will present to the medical services.

3.2 An investigation of different rigid contact lens fitting in a keratoconic population

3.2.1 Introduction.

As mentioned, the biomechanical properties of the human cornea play a very important role in its shape, resistance, optical function, and transparency. In keratoconus, it is likely that the biomechanical instability of the central cornea leads to axial protrusion caused by progressive thinning and steepening. As the central cornea thins, the curvature also steepens, and the patient will experience a decrease in vision. The best treatment for keratoconus depends on the development of the corneal cone and how this affects refractive error.

Initially, in the mild stage of the disease, only a small amount of refractive error is produced and either a contact lens or spectacles are suitable. However, as the disease progresses, the rigid contact lens becomes the principal form of correction (Krachmer et al., 1984). Rigid contact lenses are much better than spectacles in several respects:

1) The lens can provide a spherical anterior refracting surface, while also correcting any irregular astigmatism by creating a tear lens in the space between the correcting rigid lens and the astigmatic cornea. This has the effect of

correcting the corneal astigmatism produced by the keratoconus (Kame and Kennedy, 1987).

2) There is no interference in refractive correction in different fields of gaze, as there can be with spectacles.

3) Any prismatic or anisoconic effects from an anisometropic spectacle correction can be avoided.

Once all contact lens options have been exhausted, surgery must be considered to obtain adequate vision. Surgical procedures include simple lamellar keratoplasty, epikeratoplasty, and penetrating keratoplasty (Davis, 1997; Mandell, 1997). Rigid contact lenses are sometimes still needed after corneal transplantation to obtain maximum visual acuity by correcting any oblique astigmatism using the tear lens (Mannis and Zadnik, 1989).

There are a number of different keratoconic lens designs used for keratoconus fitting. These lenses include spherical, elliptical and cone lens designs. For example, Soper cone, Rose K, McGuire lens, Persecon K, Piggyback, Softperm, Keratosoft and Scleral contact lens designs. However, most of these lens designs are not available in Saudi Arabia. The use of Piggyback, Keratosoft, and scleral lens designs is not considered appropriate because of the hot and dry weather conditions. Softperm and Piggyback lenses have disadvantages, such as corneal oedema, neovascularisation, insufficient movement, high cost for

patients and difficulty in handling (Lawless et al., 1989; Maguen et al., 1992). These reduce their common use.

The initial selection of a rigid contact lens is dependent on the location, morphology and progress of the corneal cone, and on the lens design. There is no single method for successful rigid lens fitting for the keratoconic eye. However, several studies have been undertaken that consider the initial lens selection according to keratometric readings. Edrington et al. (1996) used a tricurve lens design with a constant diameter (8.6 mm) and fitted patients according to the average keratometric reading. This small diameter has the effect that, if the lens back optic zone radius (BOZR) is selected on the average keratometric reading, the lens will rest on top of the cone and produce a flat fit appearance in the early stage of disease. To obtain an optimum fit, a BOZR must be chosen that is steeper than the average reading of flat and steep meridians. In the moderate and advanced stage of disease the initial lens selection was found to be closer to the optimum base curve fitting as the corneal cone develops. In general, the BOZR chosen was approximately 1 D steeper than the average keratometric reading.

The Soper cone is a bicurve design consisting of 10 lenses, designated by the letters A to J. There are three groups for a given diameter/optic zone diameter relationship. The first group (4 lenses of 7.4 mm diameter, 6 mm BOZD) is designed for mild keratoconus or K-readings of less than 48 D in either corneal

meridian. The second group (3 lenses of 8.5 mm diameter, 7 mm BOZD) is for moderate keratoconus or K-readings of 48 D - 54 D in either corneal meridian. The third group (3 lenses of 9.5 mm, 8 mm BOZD) is for advanced stage or K-readings of 54 D or greater (Burger, 1993). Burger reported that the major disadvantage of this lens is the constant peripheral edge lift design which may be too steep for some keratoconus patients.

The Rose K lens is a multicurve design available in base curves of 4.75 to 8.0 mm and total diameters of 7.9 to 10.2 mm, although the 8.7 mm diameter typically is used. Betts et al. (2002) examined the visual performance and comfort of the Rose K lens on keratoconus patients using an 8.7 mm diameter and base curves ranging from 5.1 – 7.6 mm in 0.1 mm increments. The initial BOZR lens selection was 1.38 D (0.2 mm) steeper than the average keratometry reading. The study indicated that an improvement in vision and comfort could be achieved for more advanced keratoconus with the Rose K lens.

Recently, Lee and Kim (2004) evaluated clinical outcomes and fitting characteristics with a multicurve lens for keratoconus. They used a constant diameter (8.8 mm) and base curves ranging from 5.0 to 7.6 mm. The initial lens was selected according to the average keratometric readings of flat and steep meridians. This study concluded that the steep and average meridian readings were better correlated with the BOZR than the flat meridian reading. They

suggested that the average or steep keratometric readings could be used as a guideline to select the first choice BOZR of the diagnostic lens.

In terms of a continuous curve design (Percon), the initial lens selection of BOZR should be flatter than the flattest keratometric reading by 0.5 D (Gasson and Morris, 2003). However, the same authors also state that there is no consensus concerning the initial BOZR selection.

Due to the unpredictable nature of keratoconus progression, a range of different rigid contact lens designs must be available in the contact lens clinic. Each keratoconus lens has unique characteristics, and no single lens can provide an ideal fitting for every patient. Eye care professionals should have appropriate expectations for the relationship between various lens designs and keratoconus severity when selecting the initial lens design and BOZR, in order to improve the speed of lens fitting. Therefore, several lens designs that were available in the clinic were used in this study to investigate the relationship between rigid contact lens design and the severity of keratoconus in Saudi Arabian keratoconus patients. The aim was to assess the relationship between optimum lens BOZR choice and keratometric readings.

The specifications for the lenses used in this study are given in Appendix (1).

3.2.3 Methods.

3.2.3.1 Study design.

The study followed a prospective, observational, survey based design over a one-year period. Consent from the subjects or his/her parent was obtained before the details of an examination were assessed. Ethical approval for the study was obtained from the Hospital Medical Director and the Head of Ophthalmology Department of the Asir Central Hospital (appendix 3).

3.2.3.2 Rigid contact lens materials and designs.

Six different lens designs were used: McGuire Regular and Steep (Multicurve), Tricurve, Percon (aspheric), Metro^2 and Softperm, which were all available in the clinic. All designs were made of Fluoroperm 30 Dk material (fluorosilicon acrylate) to achieve a thin lens design. They were supplied by Cantor and Nissel Limited, Brackley, Northamptonshire, UK. The McGuire Steep lens was designed by Thomas White especially for Saudi Arabian keratoconus patients with the severe form of the disease.

3.2.3.3 Subjects.

Seventy subjects, comprising 14 males and 56 females with mean age of 19.5 ± 5 years, and ranging between 11 and 28 years, were recruited from a consecutive series of 125 patients attending the Department of Ophthalmology, Asir Central Hospital, Saudi Arabia. Each subject was clinically assessed prior to

any contact lens fitting. Since keratoconus progresses at different rates in each eye of an individual patient, the subjects' eyes were also individually classified according to the severity of keratoconus in each eye (mild: ≤ 48 D; moderate: 48 D – 54 D; severe: > 54 D), and to the mode of keratoconus correction.

3.2.3.4 Contact lens fitting.

Comprehensive clinical information for each keratoconic patient was collected at a single session for all patients. A clinical assessment procedure was performed similar to that explained in section 3.1.4. During the session, a comprehensive case history was completed. Monocular and binocular, near and distant VA was taken, using Snellen high contrast letters at 80 cd / m^2 luminance. Javal-Schiotz keratometry (Shin/Nipon Japan 2190) was used to measure the central corneal curvature. This instrument has a measurement range of 30 D (11.20 mm) to 60 D (5.60 mm). Auxiliary lenses (+1.25 D or +2.25 D) over the aperture of the instrument were used to extend the measurement range when necessary. Objective and subjective refraction was achieved.

Indications for fitting a contact lens were dependent on the severity of disease, inadequate VA with spectacles, anisometropia, anisoconia, and willingness of the patient to wear a rigid contact lens. The initial lens design selection was based on the average keratometric reading of both meridians (stages of the disease) and cone morphology. In mild keratoconus, Percon or tricurve designs were employed with initial lens diameters 9.5 or 9 mm. Subjects with moderate

keratoconus and oval or sagging cones were initially fitted with a tricurve lens of 9 mm diameter. In moderate nipple or round cone cases the initial lens fittings were performed with the tricurve-9 mm diameter or multicurve (McGuire Regular or Steep) designs of 8.6 mm diameter. In advanced keratoconus, patients with sagging oval or globus shaped cones were fit with multicurve lens designs.

The initial trial lens was inserted and allowed to settle for approximately 20 minutes. For each patient, one drop of Benoxinate (Oxybuprocaine hydrochloride 0.4%) was instilled into the eye prior to the insertion of the lens to reduce sensation of the cornea and excessive tearing. This allowed blinking to normalise and tearing to subside before the fluorescein pattern was evaluated. To evaluate the lens-cornea fitting relationship, a fluorescein strip (Fluorescein sodium BP 1%) was wetted with an ophthalmic irrigating solution of normal saline. The strip was gently applied against the superior sclera with the patient viewing inferiorly. The patient was then asked to gently blink for several seconds. A Haag-Streit slit-lamp microscope, with the illumination adjusted using a cobalt blue filter, was used to evaluate the fluorescein pattern of the lens on the cornea. The lens BOZR was increased or decreased to accomplish a "light feather touch" on the centre of the cornea (more details see section 2.10.2.1). The radii of the peripheral curves were also adjusted to allow interchange of tears, and to achieve adequate edge lift, where necessary. A rigid contact lens with the required specifications was ordered. After the ordered lenses arrived in the clinic, subjects were scheduled for dispensing visits. If the lens gave acceptable fit,

vision and comfort, the subject was scheduled for follow-up in two weeks. If the fit, vision and comfort were still acceptable after two weeks of wear, the subject was scheduled for a regular follow-up of two months. If the first ordered lens was not acceptable, the lens was reordered with the appropriate changes.

The majority of eyes were fitted with a three-point touch (divided support) technique. Apical bearing and apical clearance techniques were used when the former technique was not applicable. In addition to the fluorescein appearance evaluation, lens centration and lens movement with normal blinking and with eye movement was noted. Finally, best VA and over-refraction for minimum power were taken into account. Following a successful fitting, the lenses were not changed until the 4-month follow-up appointment.

The study followed the regulations of the Saudi Arabian Health Service and Asir Central Hospital. Comprehensive information about the nature of the routine examinations was provided to the patients in advance.

3.2.4 Statistics.

The statistical software package SPSS 12 (SPSS Inc, USA) was used for data analysis. Correlation analysis was used to describe the relationship between the different lens designs and keratometric readings in relation to the stages of the disease. General linear model repeated measures analysis was used to compare different lens BOZR choices and different lens keratometric readings. When

comparing the mean differences between the optimum lens BOZR readings and the flat, steep and average keratometric readings for each lens type, a Bonferroni adjustment for multiple comparisons was used to correct for a 5% type I error.

3.2.5 Results.

Of the 240 eyes (115 binocular, 10 monocular), 108 eyes were corrected by spectacles, and 132 by rigid contact lenses. Six eyes fitted with Metro^2 (4) or Softperm lens (2) designs, but these have been excluded from the analysis due to their small number. The distributions of the different lens designs in each stage are shown in Table 3.2.1.

Disease Severity	**Lens Design**				
	McGuire S	McGuire R	Tricurve	Percon	**Total**
	No %	No %	No %	No %	No %
Mild	**6** (4.76)	**3** (2.38)	**20** (15.87)	**7** (5.55)	**36** (28.6%)
Moderate	**23** (18.25)	**17** (13.49)	**22** (17.46)	**4** (3.17)	**66** (52.4%)
Severe	**10** (7.94)	**7** (5.55)	**7** (5.55)	**0** (0)	**24** (19%)
Overall	**39** (30.95%)	**27** (21.42%)	**49** (38.88%)	**11** (8.73%)	**126** (100%)

Table 3.2.1: *Distributions of lenses in each disease stage. Bold numbers represent eyes fitted with lens, with percentage of total rigid lens fits in brackets. (Mild: K< 48 D; Moderate: K = 48 – 54 D; Severe: K > 54 D).*

Keratometry Reading (D)	Lens Design			
	McGuire Steep	McGuire Regular	Tricurve	Percon
Flat	50.43 ± 4.8	50.24 ± 4.9	47.39 ± 3.6	45.11 ± 2.0
Steep	55.24 ± 4.6	55.84 ± 5.4	52.10 ± 3.6	50.18 ± 2.8
Average	52.84 ± 4.6	53.04 ± 5.0	49.74 ± 3.5	47.65 ± 1.9
BOZR	52.77 ± 3.5	54.33 ± 4.4	50.17± 3.0	45.79 ± 1.5

Table 3.2.2: *Average keratometric readings, and average BOZR lens choice.*

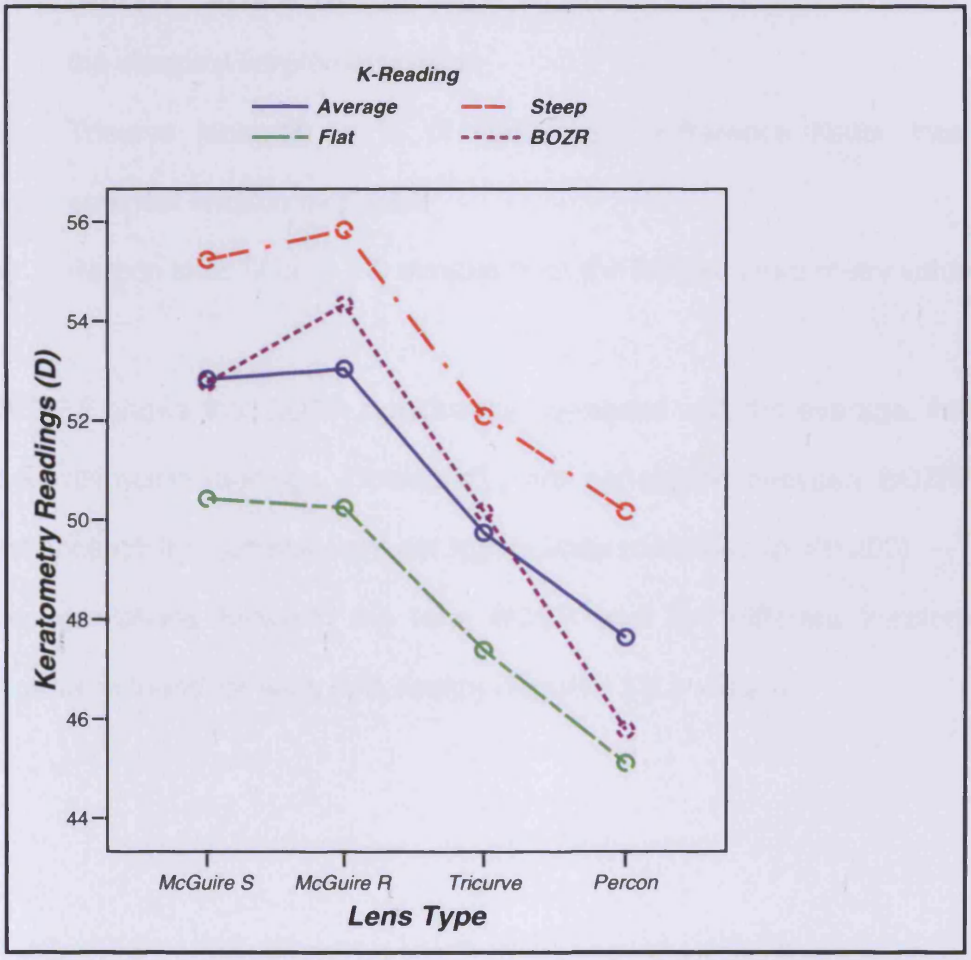

Figure 3.2.1: *Illustrates general linear model repeated measures of various keratometric readings and their relationship with the best BOZR choice for each lens design.*

By comparing the average BOZR fitted for each lens design with the mean of flat, average and steep keratometry readings for patients fitted with that lens, it is possible to establish the optimum keratometry parameter for selection of lens BOZR. From Table 3.2.2 and Figure 3.2.1 the following recommendations can then be made:

(i) McGuire Steep lens: fit on average keratometry value.

(ii) McGuire Regular lens: fit on ¼ of keratometry difference flatter than the steepest keratometry value.

(iii) Tricurve lens: fit on ⅓ of keratometry difference flatter than the steepest keratometry value.

(iv) Percon lens: fit on 0.7 D steeper than the flattest keratometry value.

Figure 3.2.2 shows that BOZR significantly correlates with the average, flat and steep keratometric readings. Conversely, the correlation between BOZR and corneal eccentricity readings were not significantly correlated ($p = 0.203$).
Similar correlations between the lens BOZR and the different keratometric readings were found for each lens design (Figures 3.2.3 – 3.2.6).

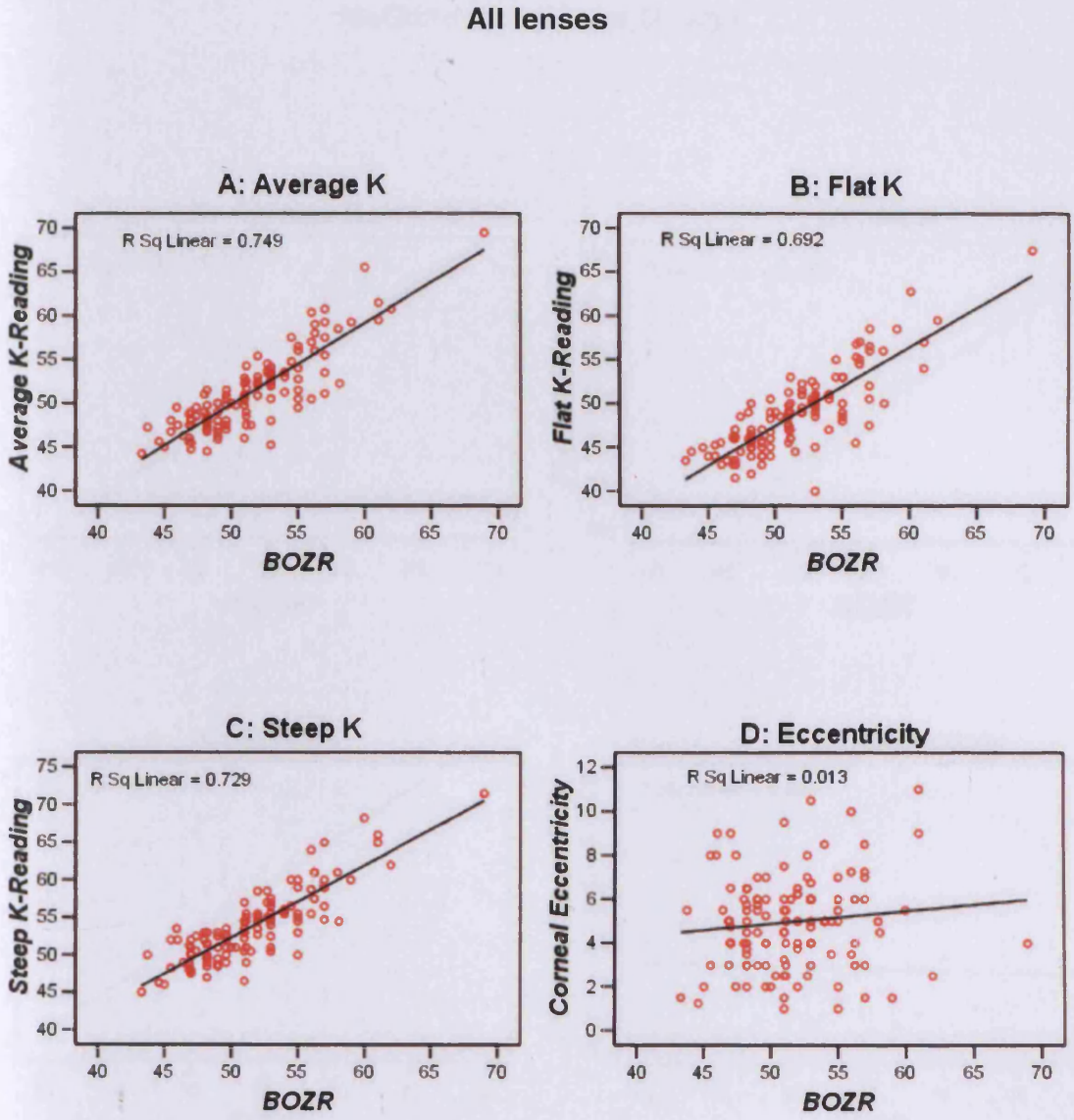

Figure 3.2.2: *Scatter plot correlations between keratometric readings and lens BOZR for all lens designs.* (**A**) *Correlation between average keratometry reading and lens BOZR* (R^2 *= 0.75),* (**B**) *Correlation between flat reading and lens BOZR* (R^2 *= 0.7),* (**C**) *Correlation between steep reading and lens BOZR* (R^2 *= 0.73),* (**D**) *Correlation between corneal eccentricity and lens BOZR* (R^2 *= 0.013).* (**A** – **C**) *showed significant correlations with BOZR but* (**D**) *showed no significant correlation.*

McGuire Steep Lens Design

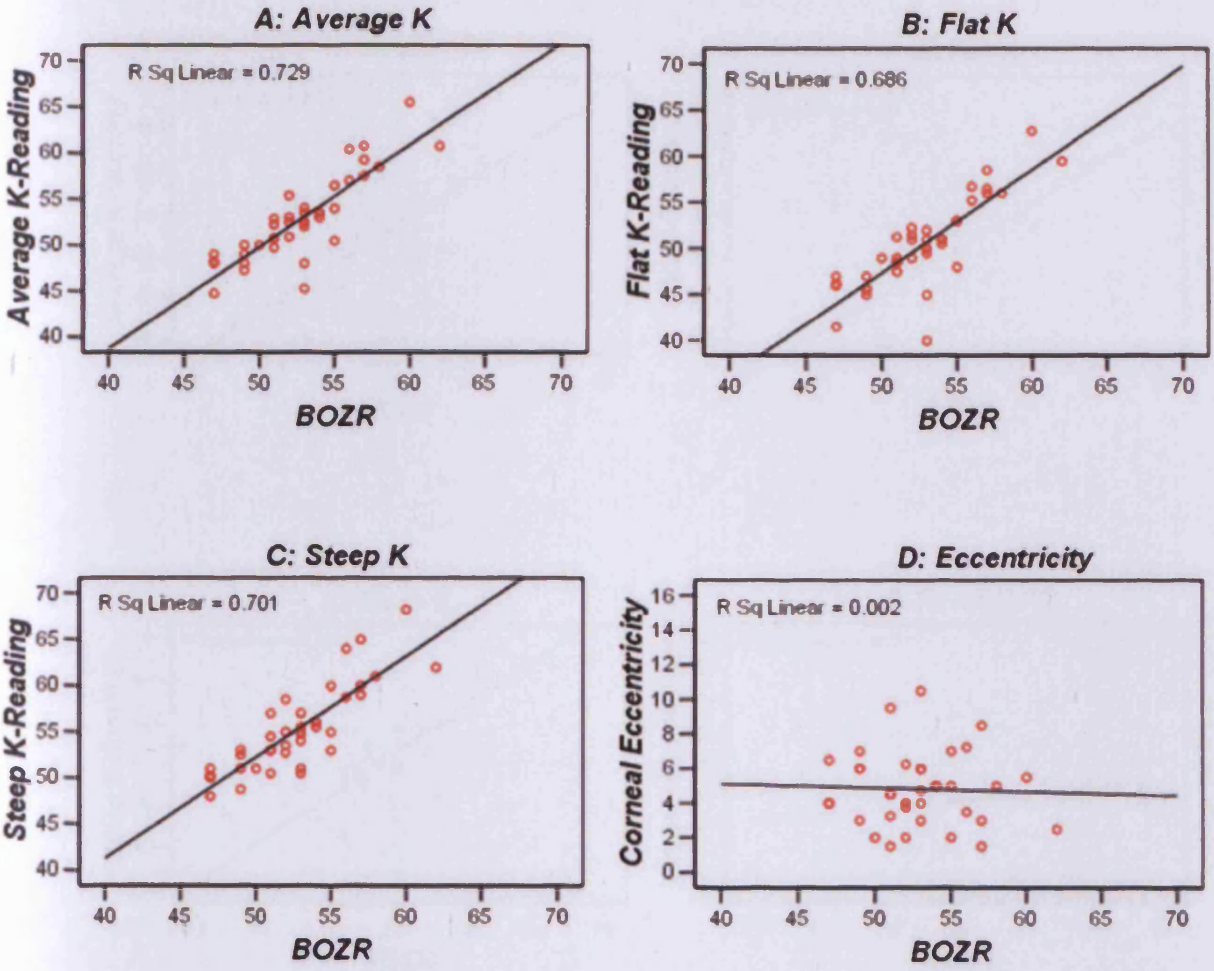

Figure 3.2.3: *Scatter plot correlations between lens BOZR and keratometric readings for the McGuire Steep lens design.* (**A**) *Correlation between average keratometric reading and BOZR (R^2 = 0.73)*, (**B**) *Correlation between flat reading and BOZR (R^2 = 0.69)*, (**C**) *Correlation between steep reading and BOZR (R^2 = 0.70)*, (**D**) *Correlation between corneal eccentricity and BOZR (R^2 = 0.002)*. (**A** – **C**) Showed significant correlations with BOZR but (**D**) *showed no significant correlation.*

McGuire Regular lens Design

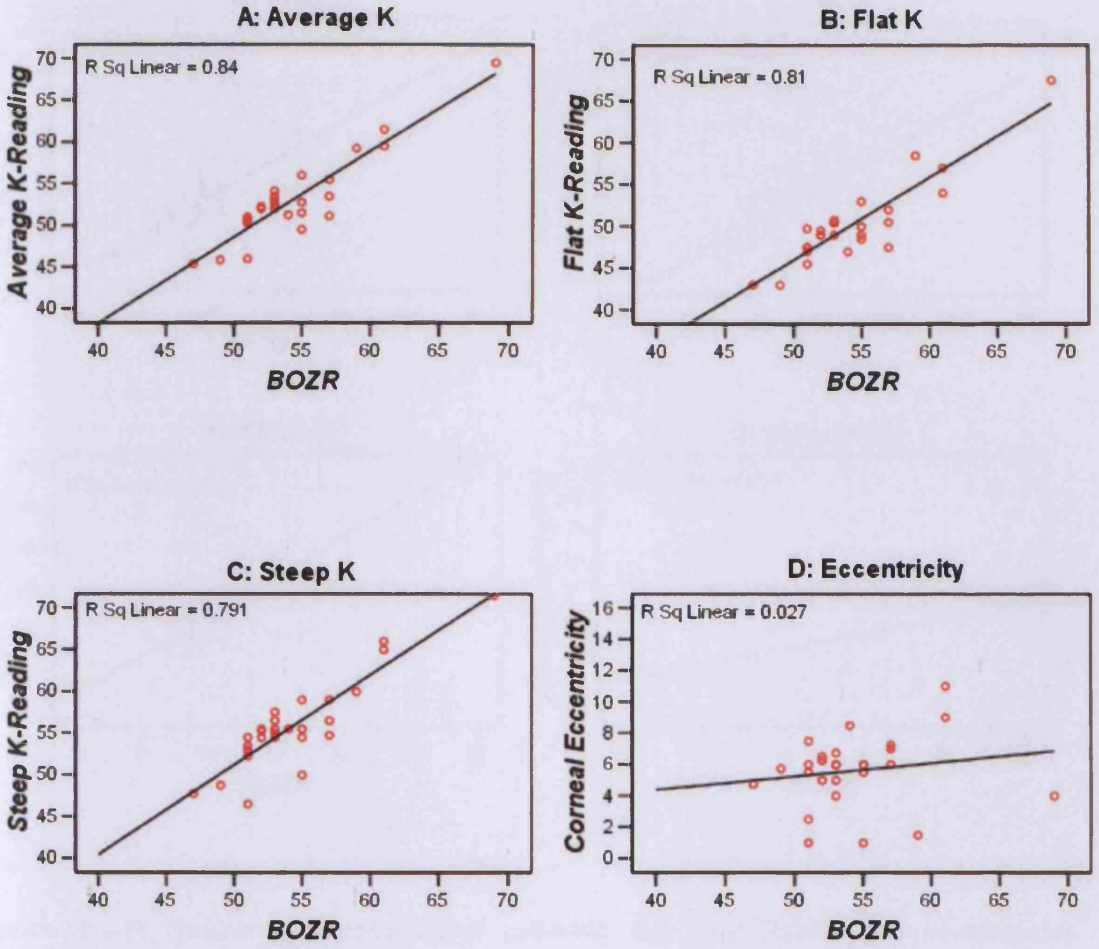

Figure 3.2.4: *Scatter plot correlations between the lens BOZR and keratometric readings for the McGuire Regular lens design.* (**A**) *Correlation between average keratometric reading and BOZR* (R^2 *= 0.84),* (**B**) *Correlation between flat reading and BOZR* (R^2 *= 0.81),* (**C**) *Correlation between steep reading and BOZR* (R^2 *= 0.79),* (**D**) *Correlation between corneal eccentricity and BOZR* (R^2 *= 0.027).* (**A** – **C**) *Showed significant correlations with BOZR, but* (**D**) *showed no significant correlation.*

Tricurve Lens Design

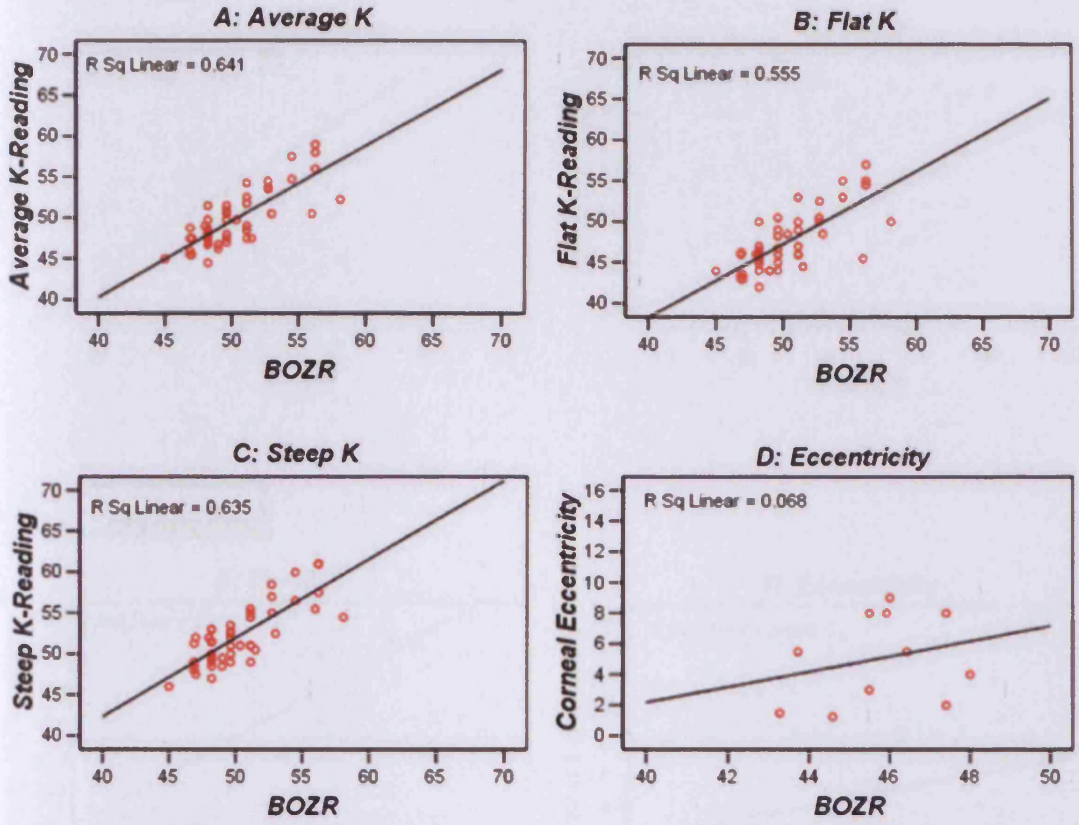

Figure 2.2.5: *Scatter plot correlations between the lens BOZR and keratometric readings for the Tricurve lens design.* (**A**) *Correlation between average keratometric reading and BOZR* (R^2 = 0.64), (**B**) *Correlation between flat reading and BOZR* (R^2 = 0.56), (**C**) *Correlation between steep reading and BOZR* (R^2 = 0.64), (**D**) *Correlation between corneal eccentricity and BOZR* (R^2 = 0.068). (**A** – **C**) *Showed significant correlations with BOZR, but* (**D**) *showed no significant correlation.*

Percon Lens Design

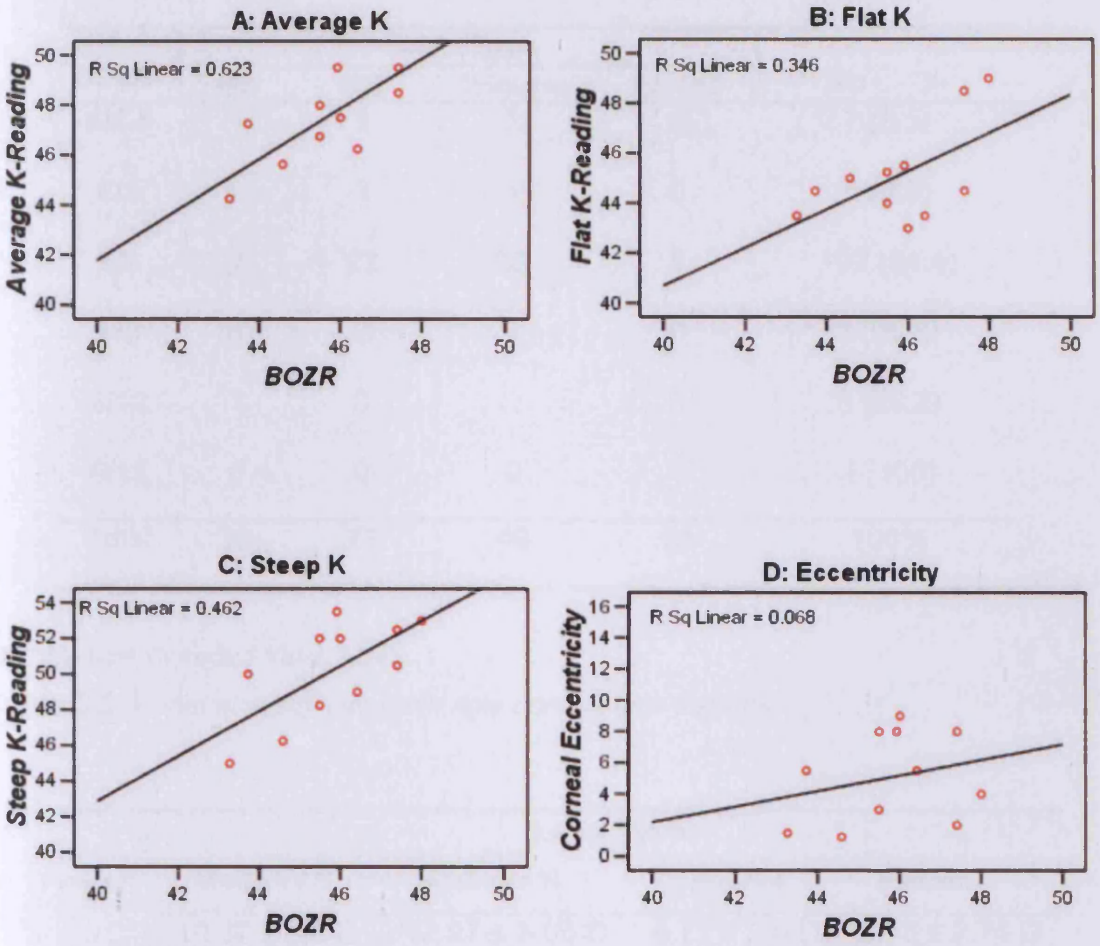

Figure 3.2.6: *Scatter plot correlations between the lens BOZR and keratometric readings for the Percon lens design,* (**A**) Correlation between average keratometric reading and *BOZR (R^2 = 0.62),* (**B**) *Correlation between flat reading and BOZR (R^2 = 0.35),* (**C**) *Correlation between steep reading and BOZR (R^2 = 0.46),* (**D**) *Correlation between corneal eccentricity and BOZR (R^2 = 0.07).* (**A – C**) *Showed significant correlations with BOZR, but* (**D**) *showed no significant correlation.*

Of the 126 eyes fitted with a contact lens, 122 (97%) achieved 6/9 or better, while the other four (3%) achieved acceptable vision at 6/12 - 6/18 (Table 3.2.3).

BCVA	Lens Type				No %
	MS	MR	Tricurve	Percon	
6/4.5	1	1	3	2	7 (5.5)
6/5	2	2	1	0	5 (9.5)
6/6	35	22	42	8	107 (94.4)
6/9	0	2	1	0	3 (96.8)
6/12	1	0	2	0	3 (99.2)
6/18	0	0	0	1	1 (100)
Total	**39**	**27**	**49**	**11**	**100%**

BCVA: Best Corrected Visual Acuity.

Table 3.2.3: *Visual acuity with each rigid contact lens designs.*

Power	Lens Type			
	McGuire S	McGuire R	Tricurve	Percon
	10.37 ± 3.0 D	12.27 ± 3.85 D	6.77 ± 3.0 D	3.73 ± 2.74 D

Table 3.2.4: *Average lens power required for each rigid contact lens.*

A large variation in lens power was noted, with the Multicurve (McGuire Regular and Steep) lenses requiring the highest average power. This reflects the fact that these lenses were more useful for severe keratoconus with steep corneas (table 3.2.4).

3.2.6 Discussion.

Recreating the smooth optical surface of the cornea by using a rigid contact lens is considered the best method for vision rehabilitation in keratoconus. This study supports the affirmation that most keratoconus patients can be managed with glasses or rigid contact lenses rather than transplantation (Fowler and Chambers, 1988; Crews et al., 1994). Of the 240 eyes examined, 45% benefited from wearing spectacles, 55% benefited from using a rigid contact lens (no cornea underwent transplantation during the period of study). Visual acuity of 6/6 or better was maintained in 94.4% of eyes fitted in this study, which is better than earlier reports where only 87% of patients achieved acuities of 6/9 or better with a rigid contact lens (Fowler et al., 1988; Lim and Vogt, 2002).

The question that arises is that if rigid contact lens wear is the best method for vision correction in keratoconus, can the best lens design also be predicted? This study found that the continuous design (Percon) was best suited to early stages of the disease probably because of the larger optical zone diameter, and larger overall diameter of the lens, which allowed the lens to 'bridge' across the cornea over the keratoconus zone. In contrast, the tricurve and multicurve lens designs were able to fit all stages of the disease. This reflects their wider BOZR and reduced lens diameter. Similar results were found by Betts et al. (2002) who reported that 72% of patients were fitted successfully with a multicurve (Rose K) lens, and Lee and Kim (2004) who fitted 83% of patients with a multicurve lens. Earlier, Lim and Vogt (2002) reported that 96% of patients could be fitted with

spherical, elliptical or cone lens designs. In this study, the three types of multicurve and tricurve lenses were able to fit 91% (114 eyes) of eyes spread over all stages of keratoconus. These results suggest that tricurve and multicurve lens designs are the optimum choice for fitting all stages of keratoconus.

Each keratoconus lens has unique characteristics, and practitioners should be aware of each lens type's appropriateness for the different stages of keratoconus when selecting the BOZR of the initial lens. The current study revealed that the BOZR of tricurve and multicurve lens designs fitted variably between average and steep keratometry readings, while aspheric (Percon) lens design fitted slightly steeper than the flatter keratometry reading. Henry (2000) assessed tetracurve and pentacurve lens designs and found that the best choice for lens BOZR was slightly steeper (i.e. approximately ¼ to ⅓ of the difference between K readings) than the flatter keratometric reading and as the disease progresses the BOZR should be equal to optical zone and the overall diameter should be decreased. This is because in the early stage of the disease, when the patient is wearing a continuous curve, the curvature of the cornea is moulded and converted from an aspherical to a spherical shape. However, with tricurve and tetracurve lenses, the weight of the lens on the cornea will be distributed and the pressure of the lens on the surface of the cornea will be less (Riviera and Polse 1991). The BOZR selected for Tricurve and McGuire Regular and Steep lens types in our study displayed agreement with the study achieved by Edrigton et al. (1996) who revealed that the mean BOZR was steeper than the average

keratometry readings. However, the current study was contrasted compared to that reported by Henry (2000), possibly the difference is due to the type of fitting technique. Precon lens design showed similarity with Henry's philosophy in the early stage, and contrasted with Gasson and Morris (2003) who proposed that the initial BOZR selected for the Percon design of 9.4 mm, in the early stage, should be flatter than the flattest keratometric reading by 0.5 D. In this study the average Percon BOZR was 0.7 D steeper than the flattest keratometric reading. The relationship between lens BOZR and average keratometric readings for all lenses showed the highest correlation. This finding was similar to that of Lee and Kim (2003), who suggested using the average readings of both meridians as a guideline to select the BOZR of the initial trial lens.

However, the conclusions from the study are limited by the survey based design that was used. While the results give an indication that the tricurve and multicurve lens designs were applicable and appropriate for all stages of the disease, further investigation is needed to determine which type of lens design best suits cones of different shapes and severity. Using the results from this study as a guide, an intervention design could be produced, in which a subject is fitted with each lens in turn, in a random order, to assess optimum lens fit. Alternatively, a series of patients who consecutively attend the contact lens clinic could be randomly fitted with just one lens. The number of lens designs should be reduced from six to three (McGuire Steep, McGuire Regular and tricurve) with each subject better classified for keratoconus severity. The important feature for

fitting appears to be the shape and location of the cone. Therefore, an improved clinical assessment is necessary using automated keratoscopy and corneal thickness measurements to assist in defining the keratoconus type. This will allow improved analysis of lens / patients interactions leading to refined clinical conclusions.

In conclusion, although keratoconus affects each cornea in a different way, and prediction of the performance of a lens is not easy, practitioners should take into account the shape, position and stage of the cone when selecting a lens diameter and design. From this study, the tricurve lens design, with a 9.0 mm diameter, is the best option among the lenses available to use at first, regardless of the stage of disease. Regular and Steep McGuire lens designs are a suitable second option. In the advanced stage, the multicurve McGuire Steep lens design may be more effective than the McGuire Regular (multicurve) and Tricurve designs. The Percon design is suitable only for some cases in the very early stages of the disease. The initial BOZR for the tricurve lens design, of 9.0 mm diameter, may be based on average keratometric readings. For the multicurve lens design of 8.6 mm diameter, lens selection should be based on the steepest keratometric reading in the early stage, but in moderate and advanced stages it may be selected on the average keratometric reading. For the Percon continuous curve design, it may be based on the flattest reading or slightly steeper than the flattest meridian in the early stages of the disease.

Microscopical study of Bowman's layer in keratoconic human cornea

4.1 Introduction.

Examination of the central keratoconic zone using conventional SEM reported altered collagen organisation and thinning at the apex of the stromal cone, but in the para-apical cone there was no evidence to suggest any difference in collagen organisation from that found in the normal cornea (Radner et al., 1998b). Keratoconus was found to have gross tissue breaks in its anterior surface in what was assumed to be Bowman's layer at the apex of cone using scanning electron microscopy (SEM) (Sawaguchi et al., 1998). Ultrastructurally, however, Sawaguchi's paper provided poor resolution of the fibrillar or lamellar nature of the breaks that did not allow Bowman's layer (or its absence) to be properly identified. Neither is it known whether or not ruptures in the corneal surface of Bowman's layer coincide with the highest peak of the cone and the highest reading of the topographical map. Reported studies on the human keratoconic cornea outside the defect of the cone zone are few, although one study using a confocal laser scanning microscope suggested more localised disruption of Bowman's layer than that observed within the central cone (Sherwin et al., 2002) and Meek and associates (2005) have used X-ray diffraction to identify structural

matrix changes outside the cone region. At present, little is known of the 3-dimensional corneal surface structure in the corneal paracentral zone (4 to 7-8 mm) beyond the apical zone (defined here as the central 4 mm).

Corneal topography used together with other methods of clinical assessment can help the surgeon to select the appropriate graft size, especially in keratoconus because the area of the cornea affected by irregular astigmatism can be identified and encompassed by a sufficiently large trephine. However, it is not known whether or not the clinical assessment is able to identify the full extent of the defect in the keratoconic cornea. This study aimed to investigate keratoconus in the human corneal Bowman's layer at the apical zone (4 mm) and para-apical zone (an annulus of between 4 to 7-8 mm diameters). This was achieved using SEM, and where possible data was compared to topographic findings. This will help to clarify whether the steepest area on the topographical map covers the full extent of the defect in the cornea or only the apical area of the cone.

4.2 Methods and Materials.

4.2.1 Clinical characteristics.

Seven keratoconus corneas were obtained post-operatively from seven patients who had undergone penetrating keratoplasty (PKP) (table 4.1). Two graft buttons were from Kyoto Prefectural University of Medicine, Kyoto, Japan, one from the Great Wall Hospital, Beijing, China, two were from Moorfields Eye Hospital, London, and two were from Manchester Eye Hospital, UK. One normal donor

cornea with endothelial cell counts too low to be used for surgery was obtained from the Bristol Eye Bank, UK. All of the graft buttons were oriented superiorly by a suture at 12 o'clock at the time of surgery, and all keratoconus buttons were immersed in fixative (glutaraldehyde 2.5%) and shipped to Cardiff University. The normal cornea was maintained in cultural media and on arrival immersed in glutaraldehyde 2.5%.

The clinical characteristics of the patients with keratoconus, including sex, age at surgery, disease stage, and ocular manifestations of the disease, graft diameter and type of examination are summarised in table 4.1. Except for patient 3, all patients had a corneal scar, and patients 1 and 3 had a history of hydrops. Patient 5 had a history of hay fever. Patients 1, 6 and 7 had no history of hard contact lens use whereas patients 2, 4 and 5 had a history of hard contact lens use. Graft diameter varied between 7.5 mm and 8 mm for all graft buttons of patients. The normal button size was 6.5 mm from a 60 year old donor. Tissue was provided with local ethical approval.

Patient No./ Sex	Age	Eye	BCVA	Lens history	Stage	Clinical features	Graft diameter	Other data	Source	Topography	SEM	ESEM	SM
1/ M	40 Y	R	6/60 with G	N/A	Advanced	Scar	7.5 mm	Acute hydrops	Kyoto	Yes	Yes	No	No
2/ M	39 Y	R	6/9 with C.L	Yes	Advanced	Scar	7.5 mm	No	Moorfields	Yes	Yes	No	No
3/ F	42 Y	L	6/12 with C.L	Yes	Advanced	N/A	8.0 mm	Post hydrops	Manchester	Yes	Yes	No	No
4/ F	41 Y	L	HM with C.L	Yes	Advanced	Scar	8.0 mm	Vogt's striae	Kyoto	No	Yes	No	No
5/ M	17 Y	R	6/36 with C.L	Yes	Advanced	Scar	7.5 mm	Hay fever	Bejing	No	Yes	No	No
6/ M	26 Y	L	6/60 with G	N/A	Advanced	Scar	8.0 mm	No	Manchester	No	No	Yes	Yes
7/ M	26 Y	R	6/60 with G	N/A	Advanced	Scar	7.5 mm	No	Moorfields	No	No	Yes	Yes

Table 4.1: *Clinical features of patients with keratoconus disease, the type of examinations and source of corneas. Scanning electron microscopy (SEM), environmental electron microscopy (ESEM) and stereoscopic microscopy (SM).*

4.2.2 Preparation of specimen.

Each cornea was processed for imaging by either environmental scanning electron microscopy (ESEM) or conventional scanning electron microscopy (SEM). On excision corneas were immediately placed in 2.5% glutaraldehyde chemical fixative in 0.1M phosphate-buffered saline (PBS) and transported to the laboratory in Cardiff. On receipt corneas were transferred to PBS buffer for two ten minute washes to remove fixative, and then rinsed several times by distilled water to remove the buffer. Corneas were then placed in a solution of 10% NaOH for 5 days (on rotator) to remove most of the cellular elements, basal lamina, and other interfibrillar components of the matrix. Images of some buttons were then captured using a stereoscopic microscope (Nikon M250E) connected to a digital camera. For ESEM, two buttons were rinsed and stored in distilled water and then taken by me to the Cavendish Laboratory, Cambridge University, UK, where I attempted the first detailed investigation of keratoconus using a Philips XL30 environmental scanning electron microscope.

4.2.3 Conventional SEM.

After 5 days in NaOH corneal buttons were rinsed with distilled water several times and then immersed in 1% tannic acid solution overnight. After this, the sample was again immersed in distilled water for several hours. The cornea was then post-fixed in 1.0% aqueous osmium tetroxide for 2 hours. Specimen preparation was conducted at room temperature on a rotator in the fume cupboard.

Corneas were then dehydrated in a series of graded concentrations of ethanol ranging from 50%, 70%, 85%, 95%, and 100% for 20 minutes at each stage and once more in 100% ethanol overnight. Next, the specimen was incubated in a 1:1 mixture of hexamethyl disilazane (HMDS) and 100% ethanol for 30 minutes. The sample was then immersed three times in 100% hexamethyl disilazane for 30 minutes each. The cornea was placed in a desiccator in an incubator in the fume cupboard at room temperature for three days to allow solution evaporation. Finally, the cornea was mounted on an aluminum stub with adhesive carbon discs, and coated with gold in a Polaron SEM sputter coating system. The sample was transferred to a high vacuum SEM (Philips XL 20) fitted with computerised imaging facilities displaying 3-dimenstional images.

4.2.4 Environmental SEM.

Wet, fixed corneas were placed on an aluminium microscope stub. Several drops of distilled water at room temperature were placed around the sample inside the microscope chamber, (Philips/FEI XL30 ESEM FEG microscope), which was cooled on the microscope stage to a temperature of 2°C. At this temperature, the vapour pressure of water is 5 Torr. The chamber was pumped down to a pressure of ~6 Torr. During this process, water droplets at room temperature evaporated first, and minimal evaporation occurred to the sample. To replace the gas in the chamber with distilled water vapour, the chamber was flooded with water vapour to a pressure of ~10 Torr and then pumped down again to ~6 Torr. This procedure was repeated 5 times so that the pressure was slowly lowered to

~5 Torr. The pressure was carefully controlled by increasing or decreasing the pressure in steps of 0.1 Torr by monitoring the sample to avoid the possibility of water condensing or evaporating, and thus maintaining the hydration state of the sample. The microscope, in Professor Athene Donald's laboratory in Cambridge University, was fitted with computerised imaging facilities and images were captured with a digital camera. Details about this technique can be found in Donald, (2003).

4.3 Results.

4.3.1 SEM observations.

Normal subject.

At low magnification SEM images of the normal cornea indicate the anterior corneal surface covered with a series of small ridges (figure 4.1). Possibly these ridges are linked to the anterior corneal mosaic that may be induced at the surface of the normal cornea by massage through lids and is seen in the epithelium layer by fluorescein (Bron, 1997), or might be artefacts of the preparation process. At higher magnifications, a honeycomb-like fibrillar structure can be seen in (figure 4.2). This is the typical morphologic appearance of Bowman's layer on SEM as evidenced by the work of Komai and Ushiki (1990).

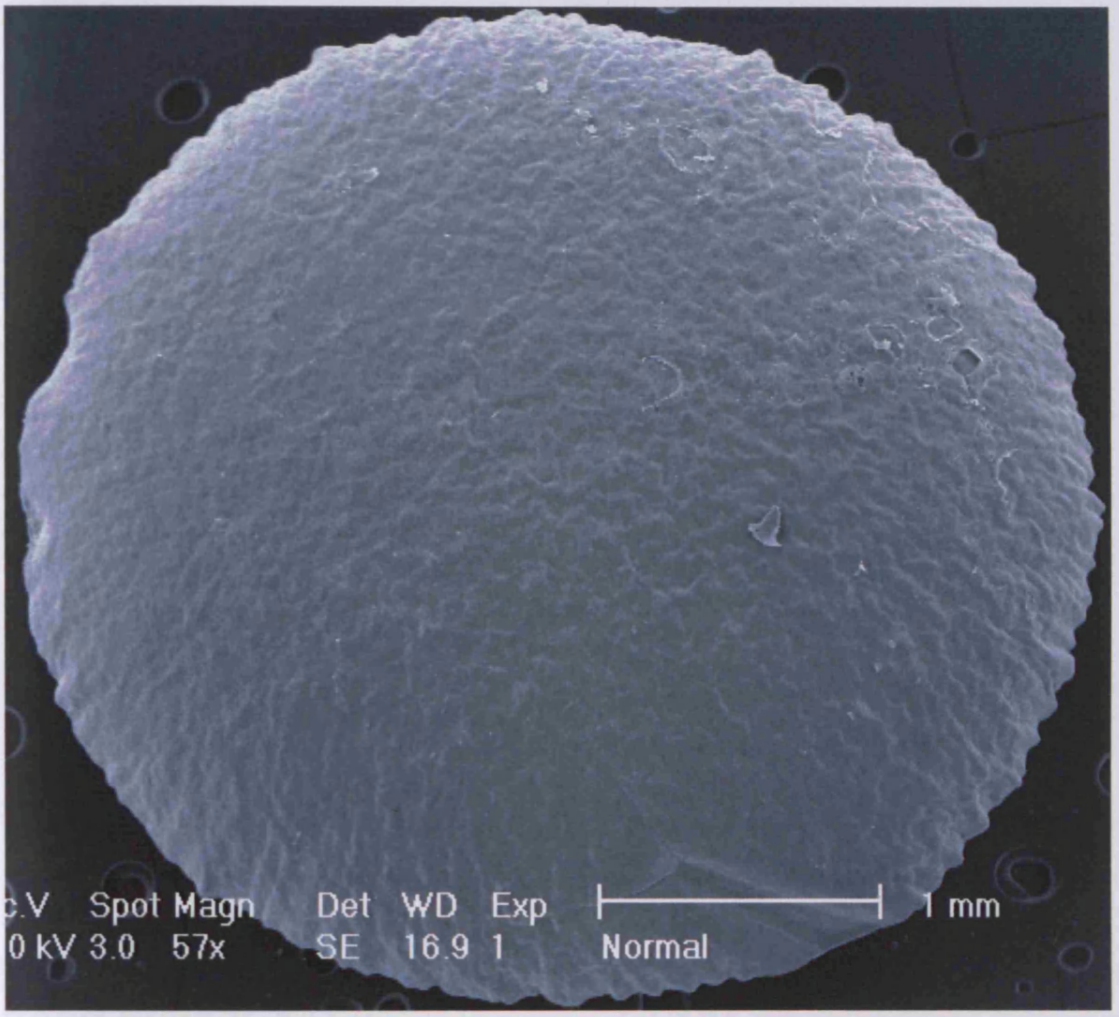

Figure 4.1: *Normal subject SEM micrograph showing the anterior surface of normal Bowman's layer. The diameter here is about 4 mm in diameter as a result of tissue shrinkage by chemical fixation and dehydration. Shrinkage of tissue is a normal preparative artefact of SEM (Sawaguchi et al. 1998). Scale Bar 1 mm.*

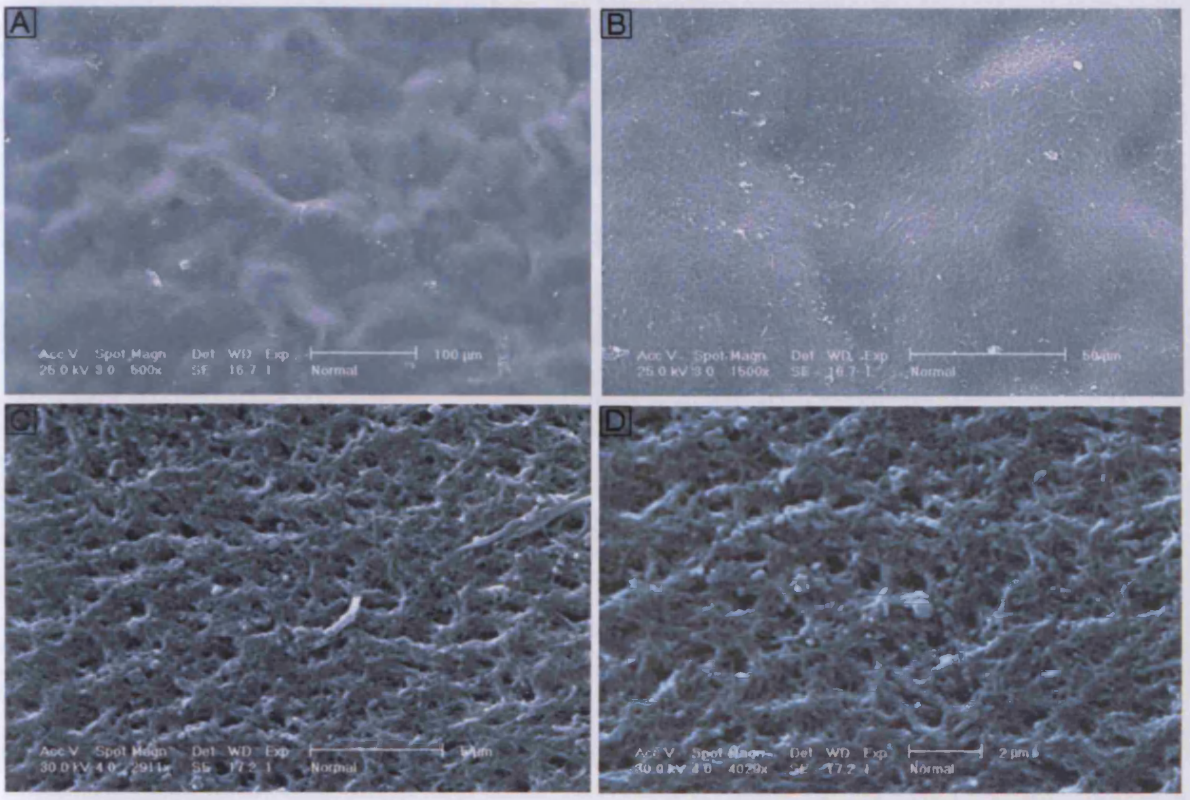

Figure 4.2: *Normal subject SEM micrographs show the anterior surface of Bowman's layer of normal cornea at increasing magnifications. Normal polygonal ridges pattern of the anterior surface at moderate magnifications* (**A** *and* **B**) and *normal honeycomb like-porous structures at high magnifications* (**C** *and* **D**). *The images in* **C** *and* **D** *are typical of the high magnification morphological appearance of the anterior aspect of Bowman's layer regardless of location across the cornea. Scale bar in* (**A** *is 100μm*), (**B** *is 50 μm*), (**C** *is 5 μm*) *and* (**D** *is 2μm*).

Patient 1

Patient 1 had a history of Descemet's membrane rupture which led to acute hydrops and subsequent central corneal scarring. The clinical photograph and relative videokeratography image are shown in figure 4.3.

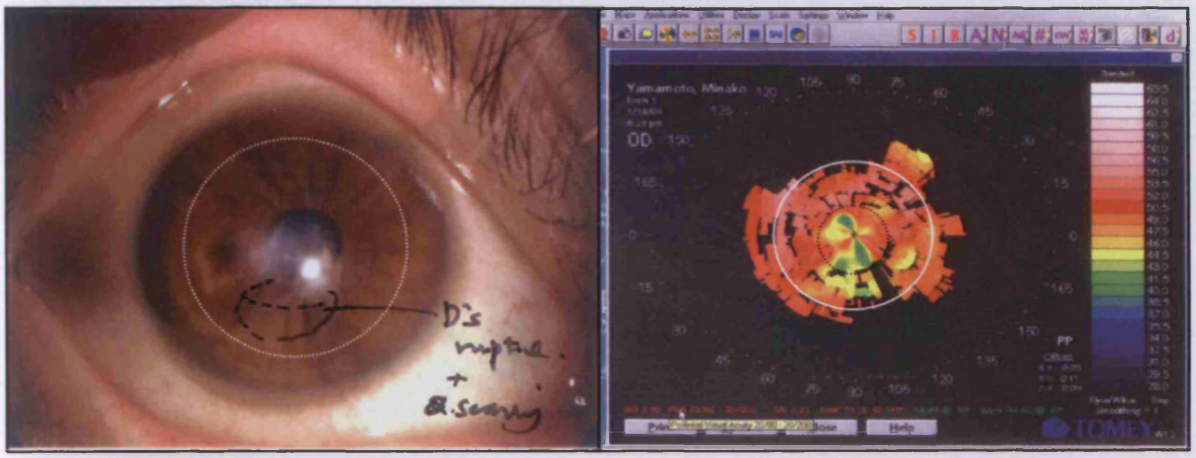

Figure 4.3: *Clinical photograph and corresponding videokeratography image of keratoconus in the right eye of patient 1. The surgeon reported scarring and rupture of Descemet's membrane at the inferior-temporal portion of the cornea in the excised corneal button of 7.5 mm in diameter as marked by the white circular. The videokeratographic map shows a flat surface (green) in the centre (circular dots) and seventh (circular line) zones inferiorly. Descemet's membrane rupture had caused acute hydrops, swelling of the cornea and subsequent oedematous scarring resulting in thinning and flattening of the cornea in the ruptured area (green area).*

The corneal button that was excised is indicated by a white circle, 7.5 mm in diameter. The lesion appeared more severe in the inferior-temporal portion of the cornea from the visual axis. Compared to the clinical photograph, the videokeratographic map showed a very flat area (green and yellow) at the centre which extended to the inferior-temporal zone of the cornea exceeding the first

central zone (3 mm) as a result of post-acute hydrops. However, beyond the central zone, the topography omitted part of the defect area inferiorly.

The SEM image of the anterior surface of Bowman's layer of patient 1 at low magnification is shown in (figure 4.4). This image clearly reveals a normal anterior corneal surface in the upper portion of the button and its edges, with a severe vertical lesion centrally and inferiorly. Comparison with figure 4.3 indicates that the topographic map does not delineate the actual limits of the lesion area on the cornea.

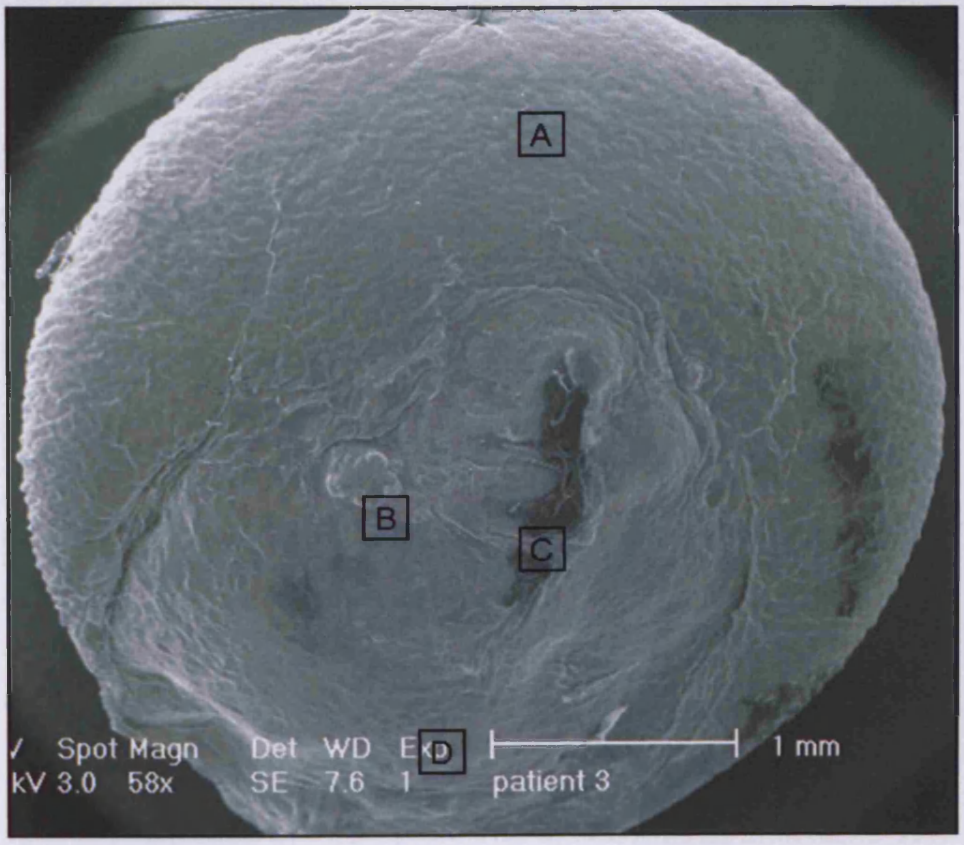

Figure 4.4: *SEM image of the right eye of patient1 showing the graft button that is represented in the topography in figure 4.3. Regions* **A** *to* **D** *are shown at higher magnification in figure 4.5. Scale bar is 1 mm.*

More detailed high magnification SEM micrographs of the anterior surface of corneal button from patient 1 were taken to illustrate the surface structure at the different sites indicated on figure 4.4. These sites are shown in figure 4.5. A site (**A**) outside the central affected area reveals a honeycomb-like porous structure typical of normal Bowman's layer. The appearance of the immediate sub-epithelial zone, however, is altered at the para-apical cone in the central zone (**B**). Here fibril bundles are elongated and lamellar-like and cleave apart in multiple bifurcations. Centrally, most of the apex area of the cone exhibits a severe lesion (figure 4.5 (**C**) and (**D**)). Despite the severe defect at the central cone, fibrils still show the anterior-posterior interweaving. The take-home message here is that while a normal, intact Bowman's layer is indicated outside the central affected area (figure 4.5A), near the apex there are clearly breaks in Bowman's layer, because the tissue imaged at this point has a lamellar structure more akin to anterior stromal lamellae than the classic appearance of Bowman's layer as seen in figure 4.2.

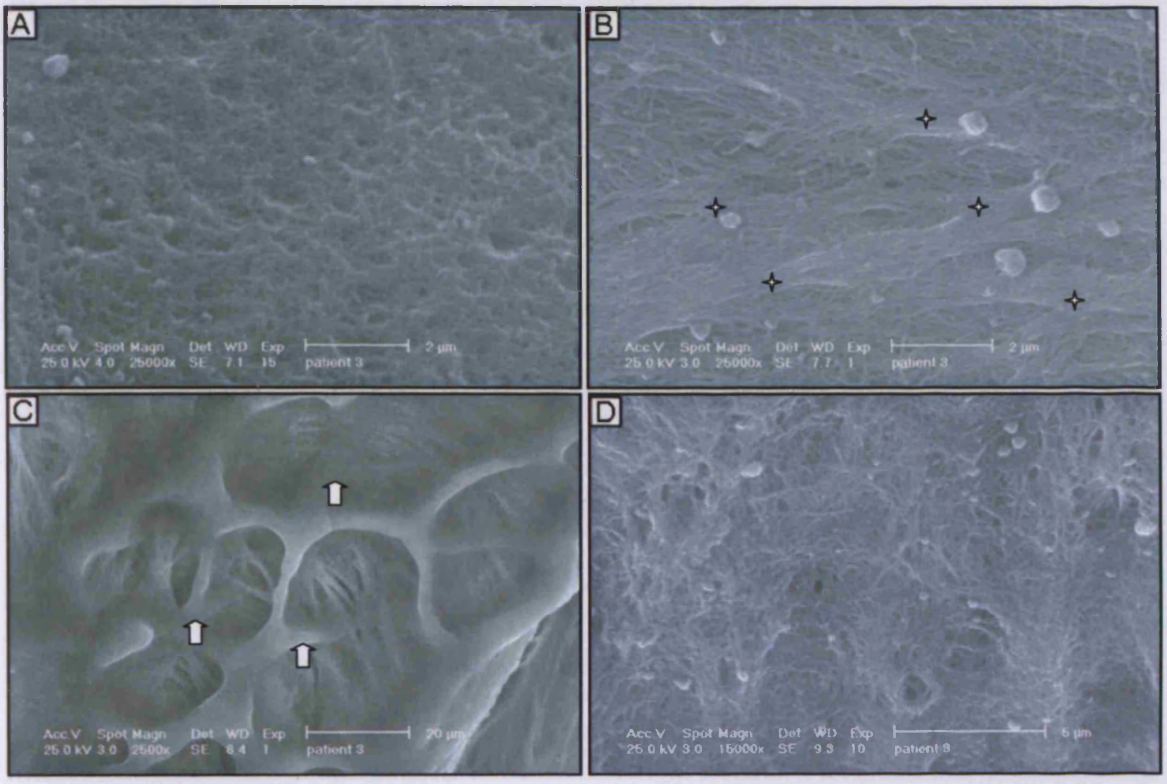

Figure 4.5: *Patient 1 SEM micrographs show the normal and abnormal appearance of the anterior corneal surface at different sites in the graft button as indicated in figure 4.4. Superiorly a normal honeycomb like-porous structure is visible at the periphery beyond the central zone* (**A**). *Centrally temporal to the apex of the cone, the tissue shows an abnormal lamellar-like ultrastructure appearance stars* (**B**); *within the ruptured area at high magnification unusual tissue morphology is seen arrows* (**C**). What appear to be *early Bowman's layer changes are located beyond the central zone inferiorly* (**D**). *Scale bars in (***A** *and* **B** *are 2µm),*

Patient 2

A clinical photograph and relative anterior float of the topographic map of the right eye of patient 2 indicated that the severity of the disease is clearly concentrated at the inferior-temporal zone at the centre of the cornea, and has spread to occupy most of the inferior and the central zone of the corneal button that was excised as indicted by white circle, 7.5 mm in diameter (figure 4.6). Possibly long term use of a hard contact lens has contributed to this widespread scarring. As can be seen in figure 4.6 the topographic map is divided to 4 circular zones, zones 3, 5, 7 and 9. The topographic map shows the apex of the cone located in the middle of the fifth zone inferiorly from the centre. In this case, it seems that the anterior float of the topographic map accurately corresponds to the clinical photography.

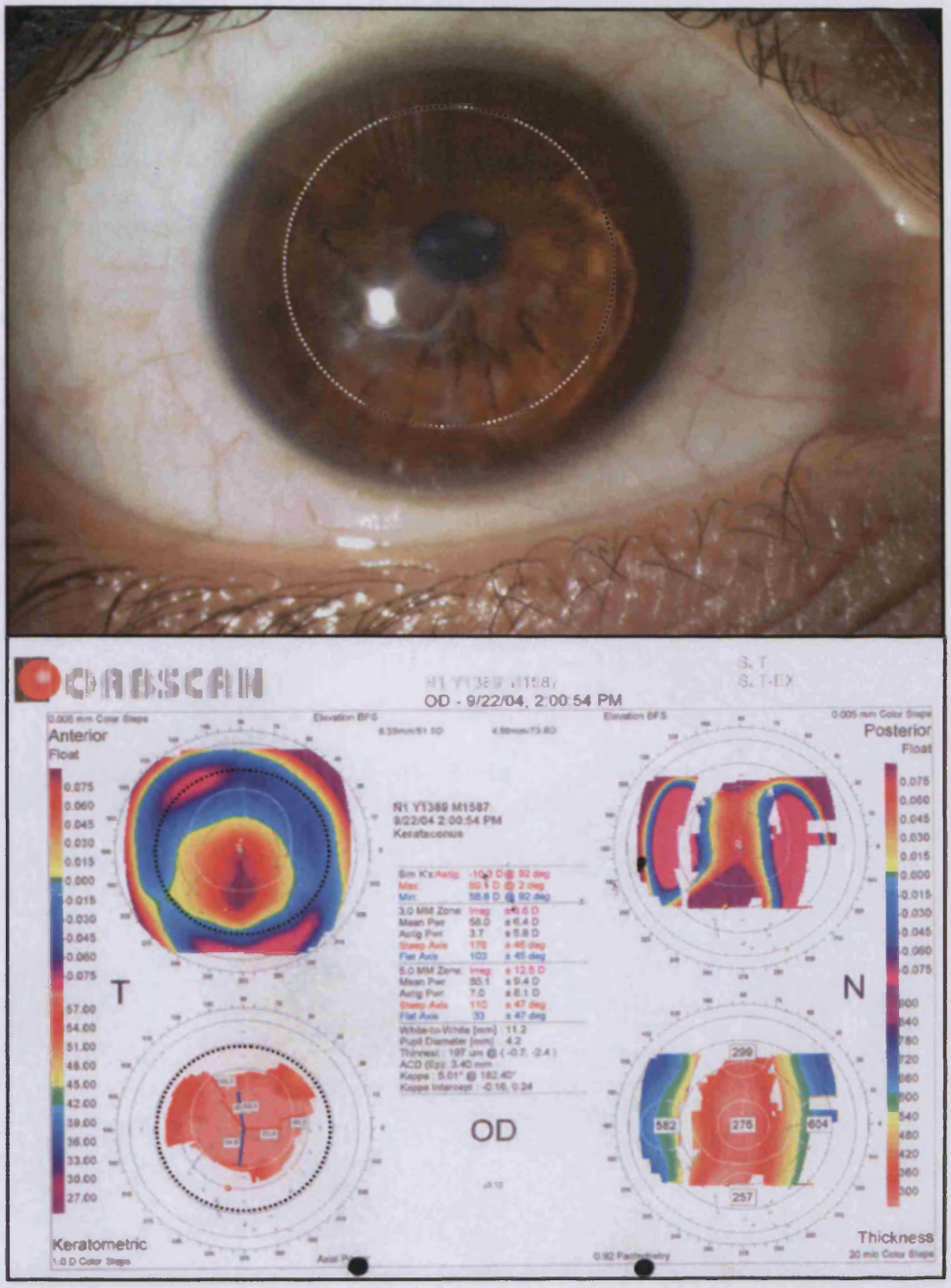

Figure 4.6: *Clinical photograph and relative anterior float topographic map of keratoconus of the right eye of patient 2. Disease scar is located centrally, spreading into the inferior temporal portion of the cornea including the first three zones inferiorly as indicated by the circular line. The anterior float of the topographic map seems to correspond to the clinical photography.*

The 7.5 mm diameter graft button of patient 2 (figure 4.7) has experienced some distortion and excessive artefactural wrinkling during processing, possibly exacerbated because the suture included a fairly large area of tissue. It appears, however, that the spread of the disease as indicated by surface abnormalities extends to the excised edge of the button inferiorly, whereas the topographic map did not show the lesion beyond the seventh zone.

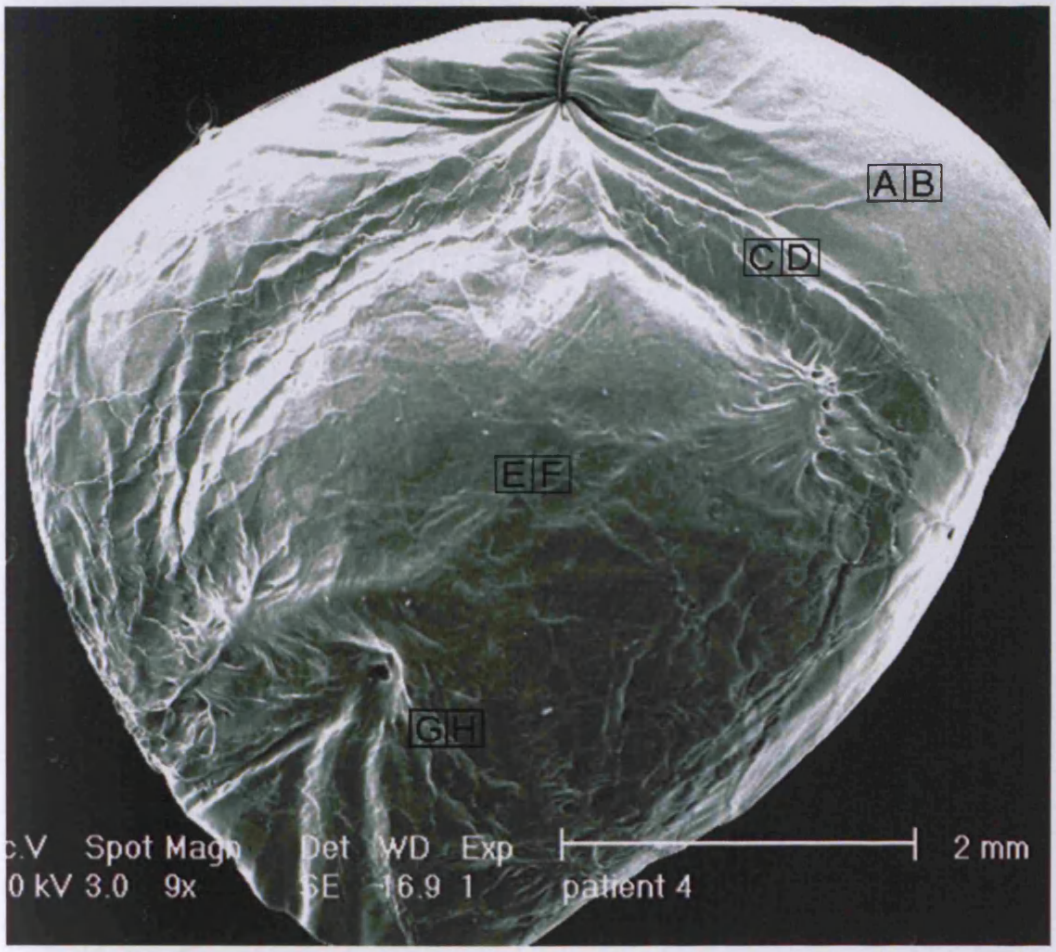

Figure 4.7: *SEM shows the 7.5 mm diameter graft button of the right eye of patient 2. The central and the most of the inferior portion seem to be involved and exceed the seventh zone that indicated in the topographic map inferiorly. Regions A to H are shown at higher magnifications in figure 4.8. Scale bar is 2 mm*

At higher magnifications (figure 4.8A - H) spatial alterations were seen in the anterior surface of the exposed corneal stroma of patient 2. The sites of these observations are indicated in figure 4.7. SEM micrographs **A** and **B** display the normal appearance of Bowman's layer at the superior-nasal portion of the button. Micrographs **C** and **D** illustrate dispersed and ruptured collagen fibrils that are subsequently elongated and coalesce together. Interestingly, micrograph **E** shows very wide, combined bundles of exposed fibrillar lamellae of the anterior stroma and holes at the central zone and micrograph **F** an elongated collagen lamellar structure. In the seventh zone inferiorly, micrographs **G** and **H** show irregularly-shaped stromal defects with irregularly and loosely-arranged collagen fibrils.

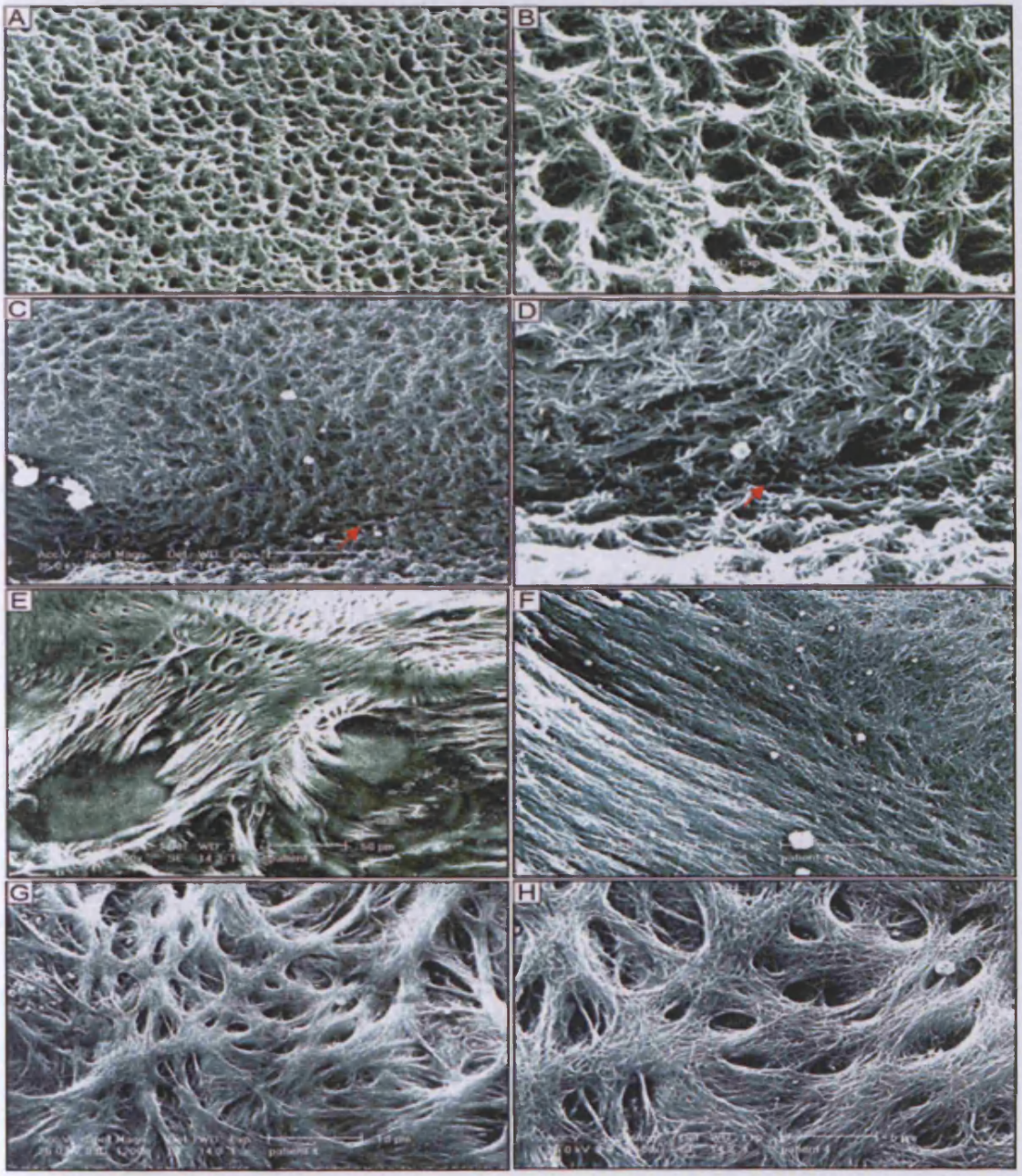

Figure 4.8: *Patient 2 SEM micrographs depict the anterior tissue structure at each position indicated in figure 4.7. Normal appearance of Bowman's layer* (**A** *and* **B**), red *arrows indicate early changes and breaks in* (**C** *and* **D**), *stromal fibrillar defect at the apex of the cone* (**E** *and* **F**), *and depostion and altered Bowman's architecture beyond the central zone inferiorly* (**G** *and* **H**). *Scale bars in* (**A**, **C**, **F** *and* **H** *are 5 µm*), *in* (**B** *and* **D** *are 2 µm*), *in* (**E** *is 50 µm*) *and in* (**G** *is 10 µm*).

Patient 3.

The anterior float of the topographic map of the left eye of this patient indicated that the disease was in its moderate stage and had spread from the central to the inferior-temporal portion of the cornea, covering the central, fifth, and part of the seventh zones as shown in (figure 4.9). However, clinically, the patient was in the advanced stage of the disease. The patient had likely recovered from the invasion of hydrops a long time ago which is why the topographical analysis showed the moderate stage of the disease.

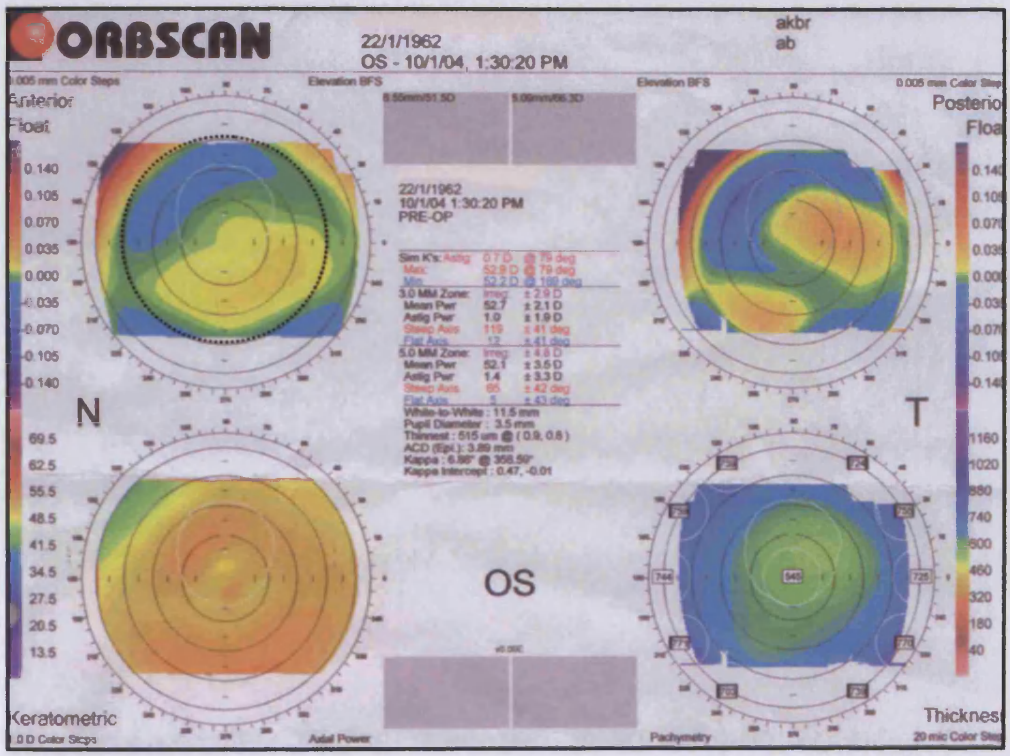

Figure 4.9: *Patient 3 a topographical map of keratoconus in left eye. The anterior float of topography indicated that the lesion located to inferior-temporal portion of the cornea and the position of the cone seems to be in the fifth zone inferior temporal zone.*

SEM of the whole graft button of patient 3 is shown in figure 4.10. At low magnification, erosions and irregular folds were observed radiating from the centre of the cone to the periphery.

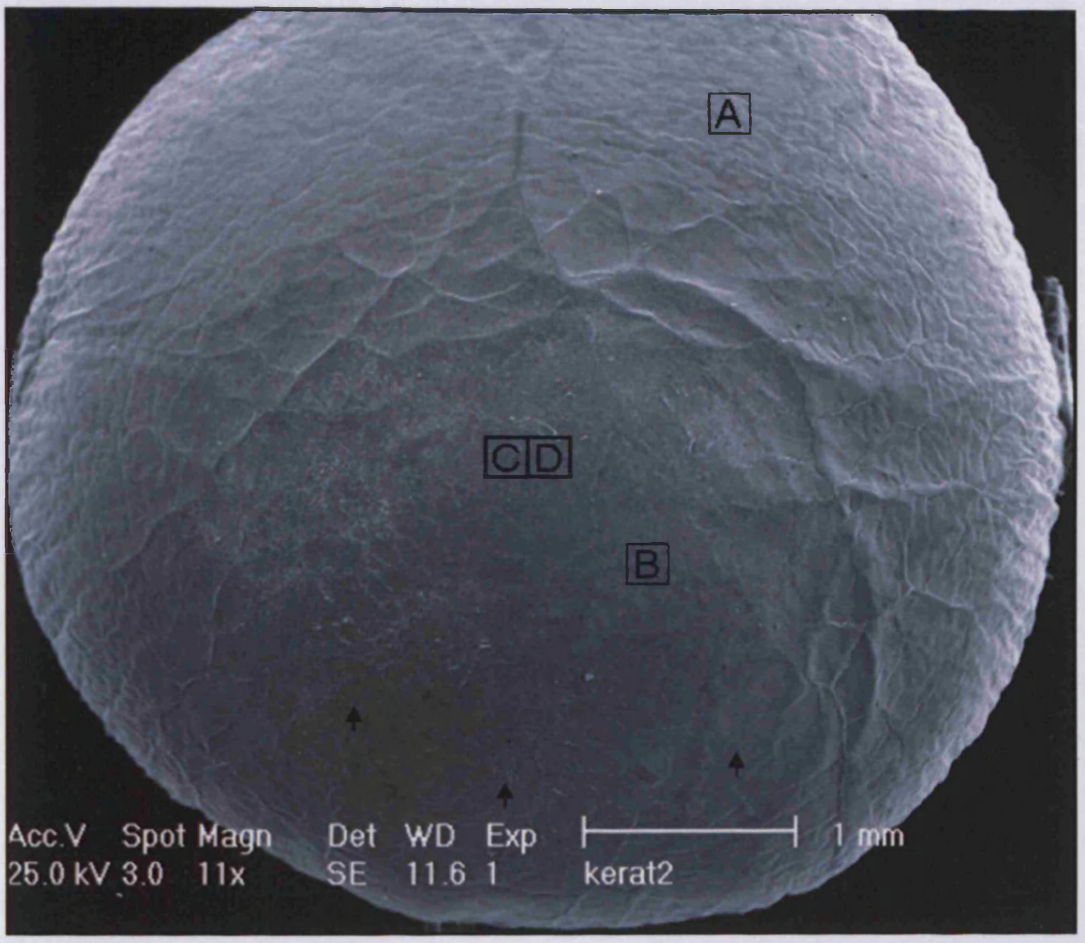

Figure 4.10: *SEM shows the 8 mm diameter graft button of a left keratoconus eye of patient 3. The appearance of Bowman's layer is normal at the periphery* (**A**) *Clinically the disease has spread only to the inferior portion of the cornea beyond the central zone* (**B** *and short arrows*). *Regions* **A** *to* **D** *indicate sites from which more detailed SEM data shown in figure 4.11 was obtained. Scale bar is 1 mm.*

Although this patient was in the advanced stage of keratoconus, changes in the regular appearance of Bowman's layer are not severe. The normal appearance of a honeycomb like-porous structure is seen at most of the periphery as shown in micrograph **A** of figure 4.11. In micrograph **B**, many small pits, amorphous or globular material, and possibly residue cellular material due to the incomplete digestion of keratocytes by NaOH are seen on the surface of Bowman's layer around the cone. However, at the centre of the cone apex **C** and **D**, breaks are indicated because the typical Bowman's layer is missing.

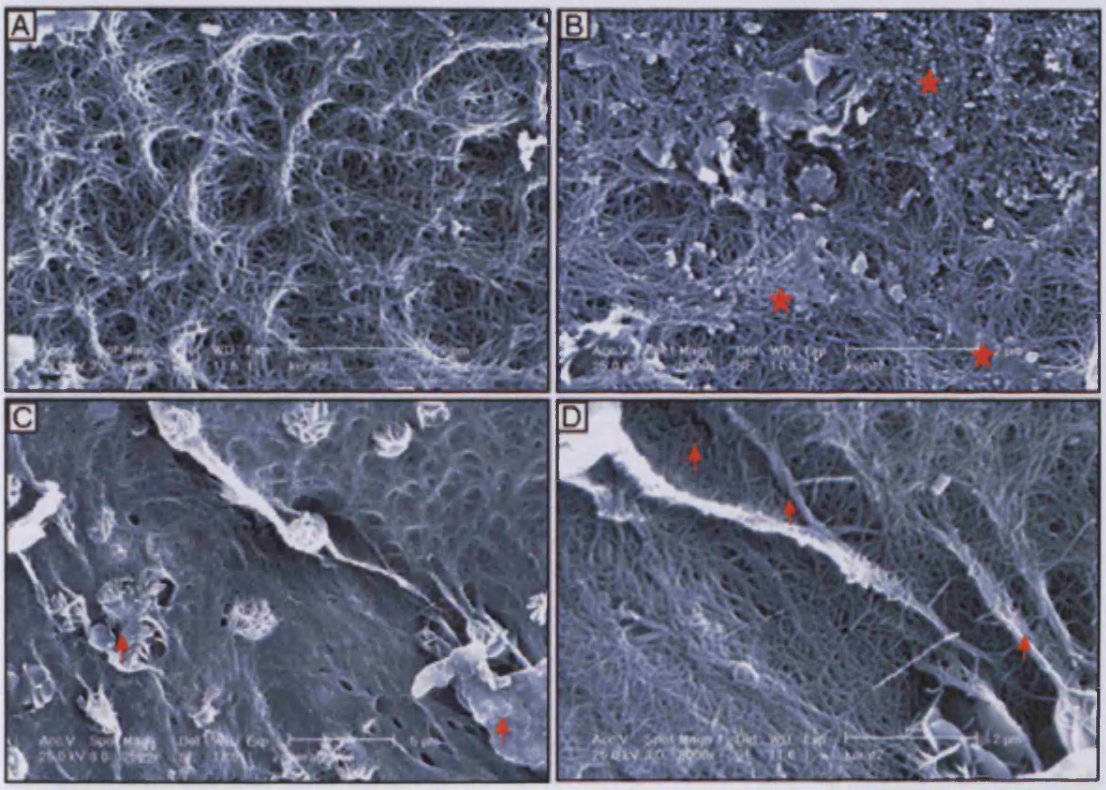

Figure 4.11: *Patient 3 SEM shows normal and abnormal appearance of Bowman's layer. Normal Bowman's layer at the periphery is shown in figure 4.10 (**A**); pits and deposits within Bowman's layer are illustrated in (**B**) (stars), possible residue of keratocytes, ruptures and abnormal conglutinated fibrillar material within Bowman's layer appear in* (**C** *and* **D**) (red *arrows*). *Scale bars in* (**A**, **B** *and* **D** *are 2μm) and in* (**C** *is 5μm*).

Patient 4.

An SEM image of the left cornea from patient 4 is shown in figure 4.12. The micrograph depicts the anterior surface of Bowman's layer with 8 mm diameter graft tissue. Similar to most previous patients, the anterior surface of Bowman's layer at the periphery appears smooth and normal. In contrast, the defect area is visible inside the centre of the cornea. Irregular fissures are seen at the apex of the cone radiating obliquely towards the periphery.

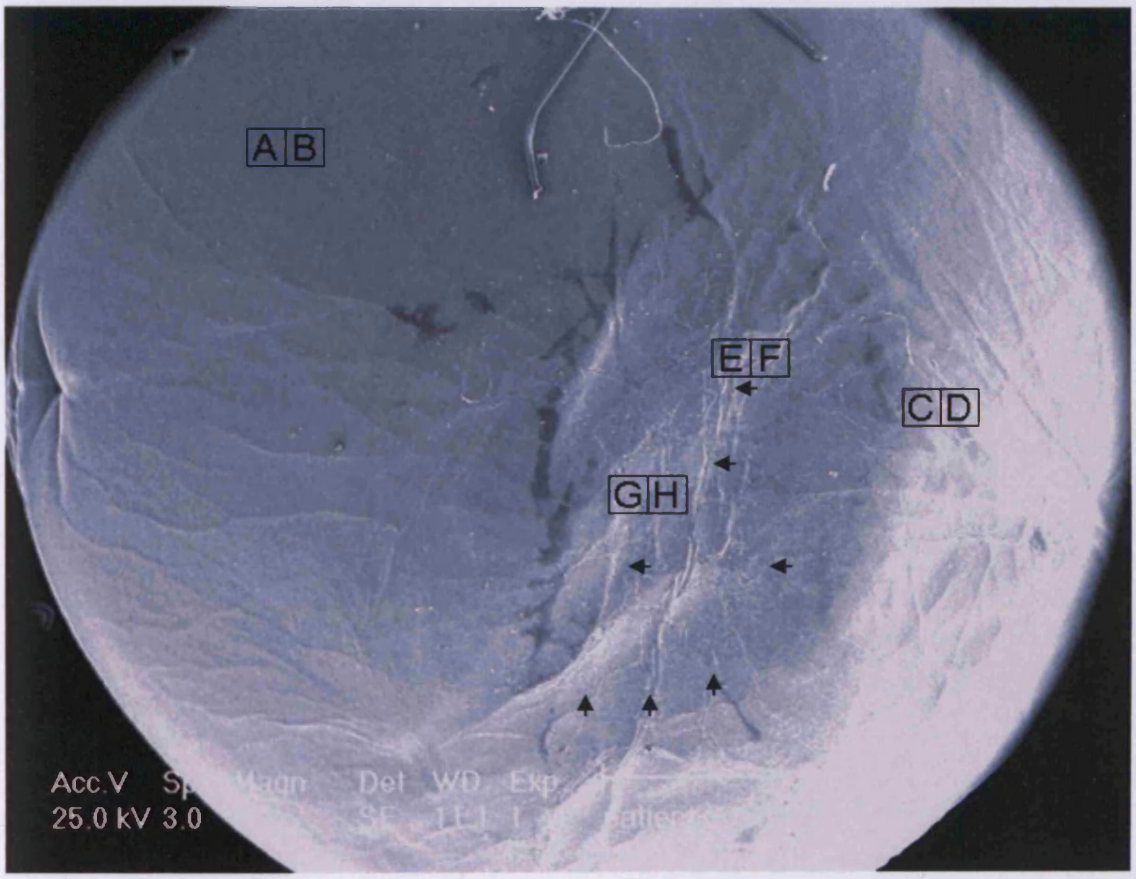

Figure 4.12: *SEM illustrates an 8 mm diameter graft size of a keratoconic left eye of patient 4. Oblique fissures in the temporal region of the central zone (arrows)* resemble Vogt's striae. **A – H** *indicate sites from which more detailed SEM data shown in figure 4.13 was obtained. Scale bar is 2 mm.*

At higher magnification (figure 4.13A – H) SEM revealed alterations in the anterior surface of Bowman's layer at multiple sites as shown in (figure 4.12). Similar to previous patients, micrographs **A** and **B** in (figure 4.13) show the normal appearance of Bowman's layer under low and high magnifications. Micrographs **C** and **D** show the irregular shape of Bowman's layer beyond the central zone temporally. At higher magnification, (figure 4.13 **E** and **F)** sedimentation of materials and degraded fissures at the temporal portion of the central zone were observed. Micrographs **G** and **H** display clearly the exposed anterior surface of the stroma demonstrating that the Bowman's layer is substantially reduced or absent at the apex of the cone.

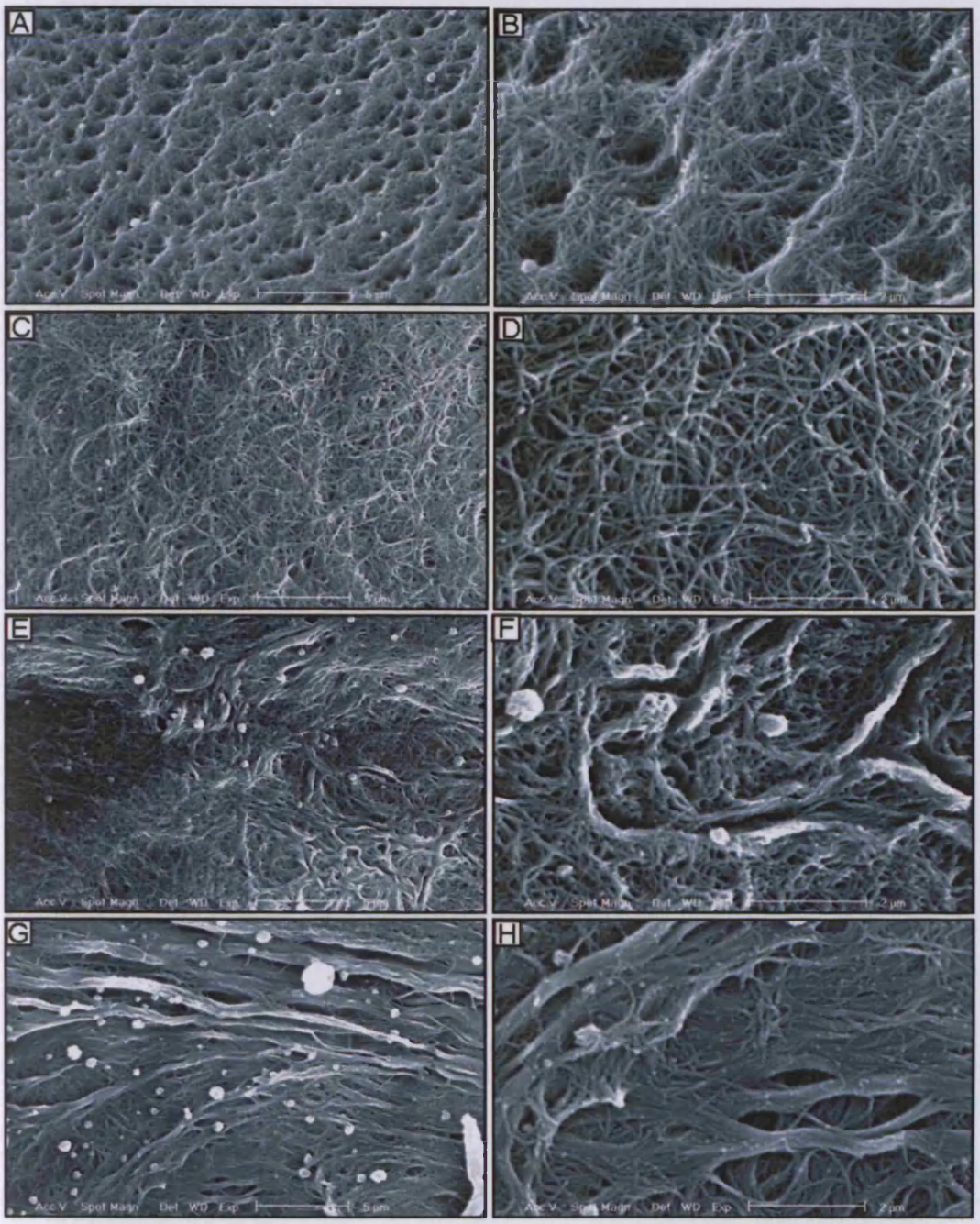

Figure 4.13: *SEM micrographs present magnified images of sites (**A** –**H**) in figure 4.12. The anterior surface of Bowman's layer at the periphery is normal in appearance (**A** and **B**), but somewhat more loosely packed in (**C** and **D**). Micrographs (**E** - **H**) show wide and narrow stromal lamellae are exposed at the apex of the cone. Scale bars in* (**A, C, E** *and* **G** *are 5µm*) *and in* (**B**, **D**, **F** *and* **H** *are 2µm*).

Patient 5.

Figure 4.14 shows SEM of graft tissue from the right cornea of patient 5. Although this patient is diagnosed clinically in the advanced stage of keratoconus, most of the anterior corneal surface appears not to be greatly distorted. The lesion spreads from the apex of the cone towards the inferior-nasal portion of the cornea beyond the central zone.

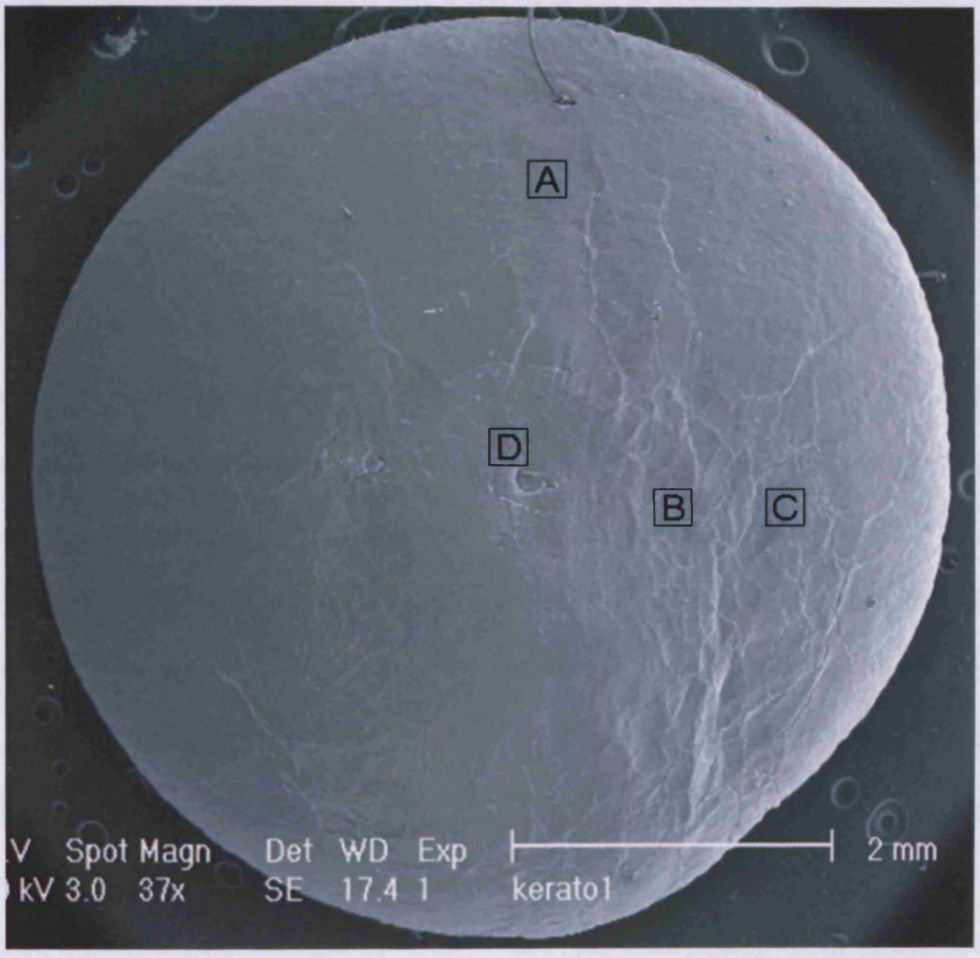

Figure 4.14: *SEM micrograph of a 7.5 mm diameter graft button of patient 5. It shows the anterior surface of Bowman's layer from a right keratoconic eye. The cone is located slightly towards the inferior-temporal portion of the cornea in the central zone. Regions A to D are shown at higher magnifications in figure 4.15. Scale bar is 2 mm.*

Micrographs **A** - **D** in (figure 4.15) disclose normal and abnormal sites on the anterior surface of the tissue at different areas indicated in figure 4.14. Micrograph **A** depicts the normal appearance of Bowman's layer at higher magnifications at the periphery of the cornea. The anterior corneal surface seen in micrograph **B** at the nasal side of the cone region displays a clear lamellar arrangement. Changes and elongated collagen fibrous materials in Bowman's layer are seen beyond the central zone as shown in micrograph **C**. Exposed thin sheets of the anterior surface of stromal defects within Bowman's layer are indicated in micrograph **D** at the apex of the cone.

The SEM investigation showed that even though the study used the standard, published procedures for specimen's preparation, the unavoidable chemical fixation and dehydration caused shrinkage of the corneal buttons, so that the dimension after processing was approximately reduced by 2 mm in each corneal button. This problem led me to attempt to use ESEM in order to overcome it, but as will be seen with only limited success because of significant reduction in resolution. So despite the fact that SEM studies unavoidably fixed tissue it provides very good morphology enabling clear distinctions to be made between Bowman's layer and anterior stromal tissue.

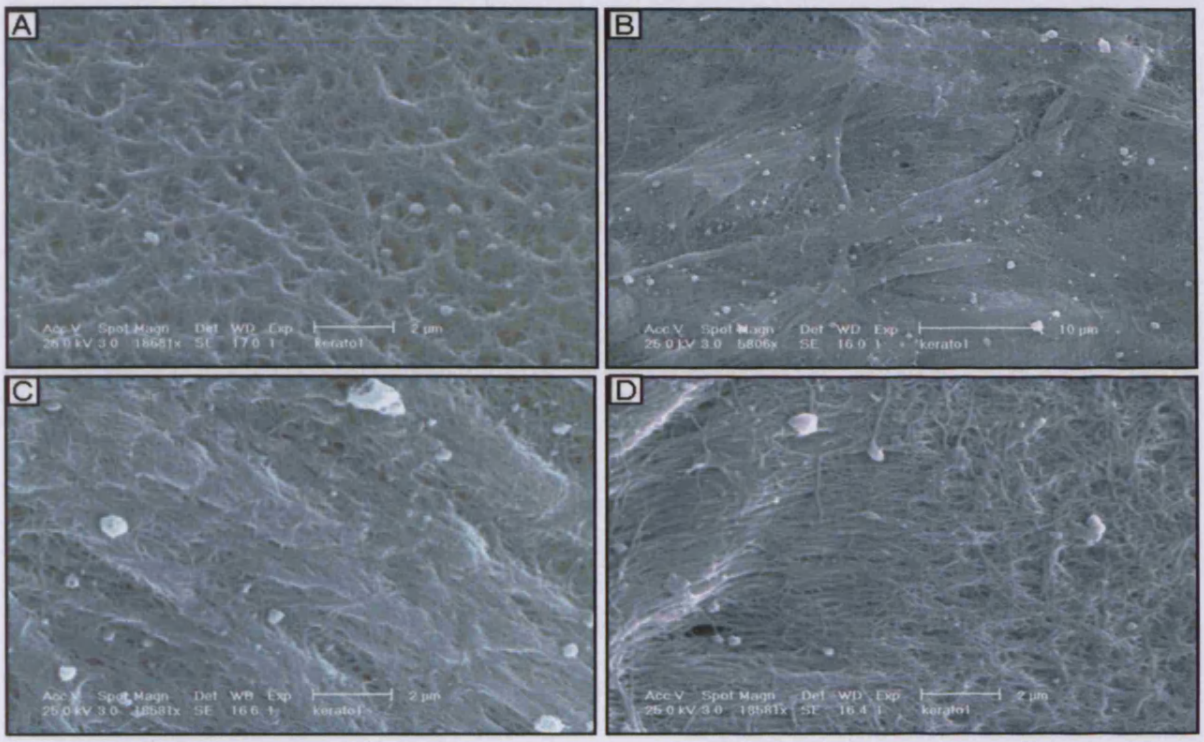

Figure 4.15: *SEM shows anterior changes for different positions in Bowman's layer labelled in figure 4.13. Normal appearances of Bowman's layer in the periphery (**A**), exposed stromal lamellae within Bowman's layer at the apex of the cone (**B**), and alteration of stromal lamellae near the cone (**C**). Interestingly, changes in collagen fibrils within Bowman's layer are seen at the periphery (**D**), where the micrograph indicates a transition between lamellar structure (to the left of the image) and Bowman's appearance (to the right). Scale bars in (**A**, **C** and **D** are 2μm and in **B** is 10μm).*

4.3.2 Stereo and ESEM observations:

In an attempt to study the anterior cornea in its hydrated state, and avoid the requirements to dehydrate the cornea for placement in the vacuum chamber of the SEM environmental (ESEM) a recent development of the conventional SEM technique was used. Its main advantage over SEM is that a gaseous environment can be maintained around the sample inside the chamber whilst imaging is carried out, instead of the sample having to be held in a high vacuum as it is for SEM. Therefore, hydrated samples can be imaged in their native state without significant preparation (Donald, 2003). Several images from two patients' keratoconus buttons were captured and are presented here.

Patient 6.

The deepithelialised anterior corneal surface from patient 6 imaged using a stereo microscope and ESEM are shown in figure 4.16A. As was the case for conventional SEM the epithelial cells had been removed by NaOH digestion, therefore, the anterior corneal surface is exposed. Many small tips, erosion at the centre, scar and irregular folds radiating from the centre to the periphery were seen in figure 4.16 B – E, however the resolution obtainable by ESEM was considerably less than with conventional SEM.

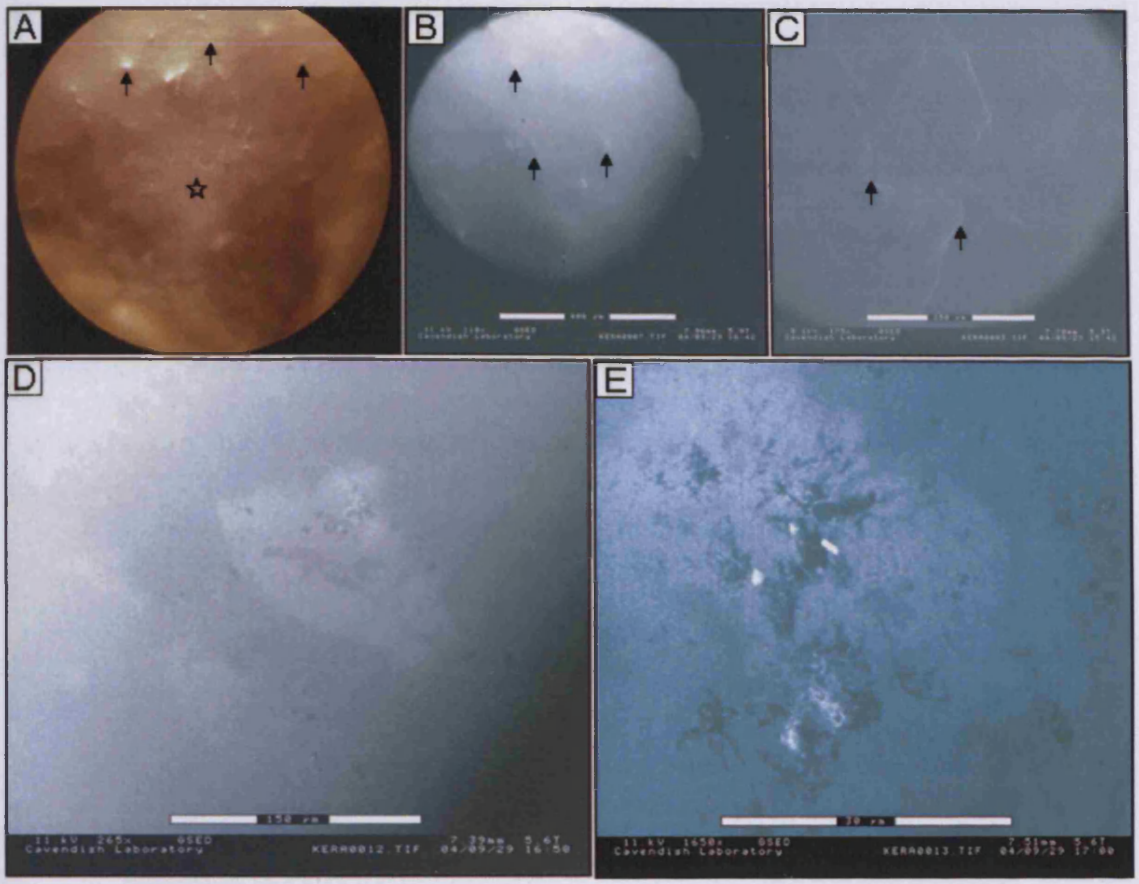

Figure 4.16: *Images from stereo (**A**) and environmental scanning microscopes (**B – E**) from patient 6. Erosion (as indicated by open star) at the central cornea in (**A**), unknown small tips and radial folds are seen under the stereoscopic microscope at the surface of Bowman's layer (arrows) (**A**). These observations are seen also with ESEM at low magnifications (**B** and **C**), and the same erosion and scar are seen at high and low magnifications in (**D** and **E**). Scale bars in* (**B**, **C**, **D** *and* **E** *are 400μm, 250μm, 150μm and 30μm respectively*).

Patient 7.

A stereoscopic image of a button from patient 7 after epithelial cells had been removed to expose the anterior corneal surface shows branched furrows radiating from the apex of the cone and extending to the periphery (figure 4.17A). The surface of the unaffected area at the periphery appears smooth on ESEM (figure 4.17B). Tips at the apex of the cone where the branches start, and at the periphery, are shown at low and high magnifications in figure 4.17 C and D.

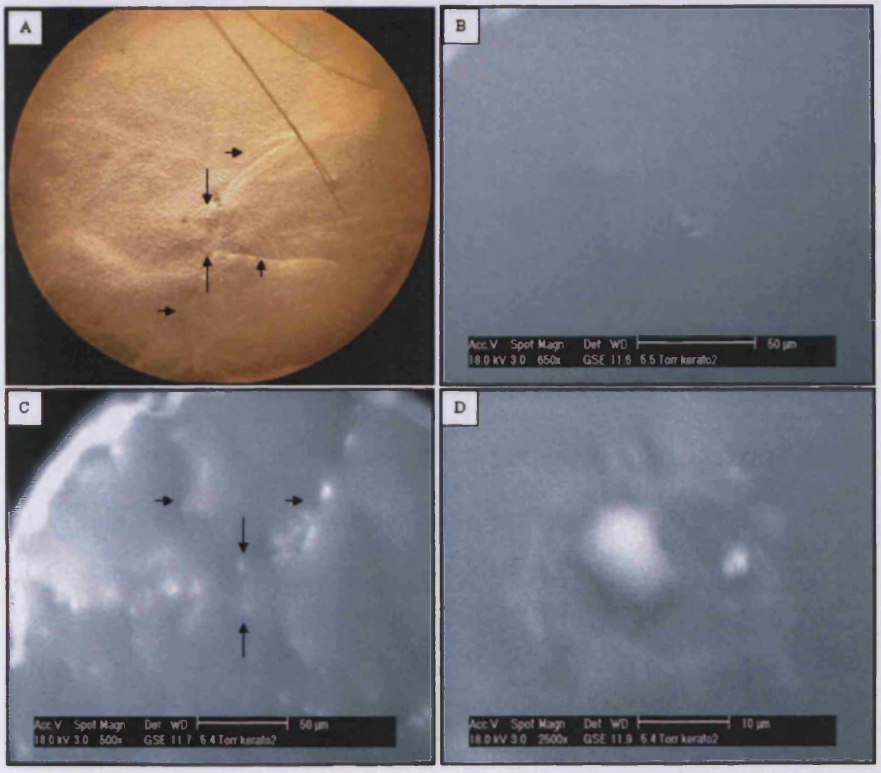

Figure 4.17: *Images from stereo* (**A**) *and environmental scanning microscopes* (**B – D**) *from patient 7. the smooth surface of the normal area at periphery of the cornea is shown in* (**B**).*The apex of cone at the inferior-temporal from the centre as indicated by (long arrows) in* (**A** *and* **C**). *Branch furrows are indicated by (short arrows) in* (**A** *and* **C**) *and tips at low and high magnifications* (**C** - **D**). *Scale bars in* (**B** *and* **C** *are 50μm and in* **D** *is 10μm*)

Taken together, SEM revealed that in all five buttons examined here, keratoconus had spread to the inferior-temporal portion of the cornea, whether the disease was in the right or left eye. The superior portion for all patients, on the other hand was still normal. Centrally, severe defects in Bowman's layer and the superficial stroma were noted in all patients and were imaged much better than has been achieved before (Sawaguchi et al., 1998). Also, at the periphery, irregular changes and ruptures beyond the central zone were seen in all patients, while, interestingly, the apparent severity of the breaks in Bowman's layer did not necessary mesh with the severity of the topographic change. Severe degradation of the stromal layer proximal to the anterior surface was observed only with patients exposed to acute hydrops.

Topographic maps from the first three patients were not sufficiently sensitive to accurately define defect areas of keratoconus, nor did they provide extensive structural detail when compared with data from SEM.

Stereomicroscopy and ESEM show fissures, erosion, random fold, tips and thin vertical lines at the affected areas on the exposed Bowman's layer for the last two patients. However, accurate details were not possible from these microscopes. Despite the potential advantage of this microscope, the achievable resolution of the image of the hydrated corneal sample was less than with conventional SEM, making it difficult to produce accurate details on the surface of the sample at either low or high magnifications.

4.6 Discussion.

The majority of topographic systems in clinical use today are based on the principle of reflection (e.g. videokeratoscopes) that measures the slope of the corneal surface, or based on the principle of projection (e.g. slit-lamp photography) that measures corneal shape relative to elevation. Although, topography is able to quantify the anterior and posterior shape and extent of the cone, its capability to cover the whole lesion area of keratoconus is limited.

In terms of severe keratoconus, most cones have an oval shape in the topographic map, however, outside the affected areas, topography may depict a relatively normal appearance. Moreover, in some cases with very high astigmatism it is beyond the capability of systems to produce topographic maps. The highest point on the map usually represents the apex of the cone, and contours lie closest together in the inferior region where the cornea is steepest due to the small curvature below the apex of the cone. In contrast, contours lie widest superiorly where the cornea is flattest (Rabinowitz and McDonnell, 1989; Wilson et al., 1991). Although, surgeons may use topography as well as information from other instruments (e.g. slit-lamp, callipers and microscopy in theatre) to determine the size of trephination in keratoconus, they also consider the possibility of the disease having spread to the periphery, its likely reoccurrence due to small and central trephination, and the risk of rejection of a donor cornea implant due to large trephination too close to the limbus.

This study has shown that breaks in Bowman's layer occur frequently in keratoconus corneas, but to differing extents. Breaks in Bowman's layer are identified because the anterior surface resembles a lamellar corneal structure rather than a Bowman's meshwork. This work has shown that the defect area typically exceeds the fifth and seventh zones of the topographic map inferiorly.

Despite the importance of accurately delineating the defect area in keratoconus, surgeons may prefer to use standard trephination of 7 to 8 mm. This approach would reduce the probability of rejection of the donor cornea or the occurrence of post-operative astigmatism (both more serious consequences than possible reoccurrence of the disease) if the lesion area exceeds the trephination. It should also be noted that map scales differ between commercial topographic systems. Nevertheless, although the small number of topographic maps used in this study were obtained from cases exhibiting only advanced stages of the disease, and regardless of the differences between systems, the study has provided some evidence to suggest that topography alone is unable to reflect the actual defect area in keratoconus.

A honeycomb pattern of collagen fibrils in Bowman's layer has been reported in normal human cornea (Komai and Ushiki, 1991). Similarly, in this study the furthest areas from the apical zone of the anterior surface of the cornea in all keratoconus patients showed a honeycomb-like meshwork typical of the SEM

images shown by Komai and Ushiki (1991). However, changes in anterior corneal morphology were discovered in the damaged regions.

Patients with a history of hydrops illustrated more severe defects in both Bowman's layer and superficial stromal layers. The finding of gross tissue breaks in the anterior corneal surface in keratoconus is in agreement with a previous report relating to the central part of the keratoconic cornea, but the image presented here show much more structural detail than detail those displayed by Sawaguchi et al. (1998).

At the periphery beyond the central zone, all patients investigated in the present study using SEM had ruptures in Bowman's layer with varying degrees of change exposing the morphologically distinct stromal tissue below. This study, in investigating areas peripheral to the central cone, supports the findings of Sherwin et al (2002) who used a confocal laser scanning microscope and found discrete incursion of fine cellular processes originated from keratocytes into Bowman's layer. Interestingly, these authors also noted that processes originating from keratocytes were observed in conjunction with a defined indentation from the basal epithelium. Furthermore, the present finding of structural matrix changes in the corneal periphery in keratoconus is in line with the findings of Hayes (2005) who used high-angle X-ray diffraction to map the orientation of collagen fibrils in the stromal of 13 keratoconus patients, and found that the orientation of collagen fibrils at the periphery were altered in patients with

advanced stage of keratoconus. To the best of my knowledge, the present study is the first to use high magnification SEM to investigate surface zones beyond the central region and show ruptures at the periphery.

Ruptured areas at the apical cone of Bowman's layer in keratoconus have been reported to be filled with epithelium and a hypertrophic collagenous proliferation derived from the anterior stroma (Teng, 1963; Kaas-Hansen, 1993; Sawaguchi et al., 1998). Teng (1963) suggested that the primary lesion occurs in the basal epithelium due to secretion of proteolytic enzymes from dying basal epithelial cells. These enzymes, such as Cathepsin B and G, have been found with increased levels in keratoconic corneas compared to normal corneas (Zhou et al., 1998, Kenney, 2005), and appear to cause fragmentation of the basement membrane and fibrillation or ruptures of Bowman's layer. In addition to the above stated evidence of keratocyte degeneration and hypertrophic collagenous proliferation in Bowman's layer, it has been documented that keratocytes in keratoconic corneas have a fourfold greater number of membrane receptors for the inflammatory cytokine interleukin 1 compared to normal corneas (Fabre, 1991). Frequent erosion of epithelial cells may result in the release of mediators that stimulate the release of interleukin 1 from keratocytes, causing a loss of keratocytes through apoptosis and a decrease in stromal mass over time (Wilson et al., 1996). It has been documented, also, that abnormal proteoglycan molecules and keratocytes occupy pores in Bowman's layer in the keratoconic cornea (Sawaguchi et al., 1991). This might explain the degeneration keratocytes

and other fragmentations passing throughout ruptured areas and occurring in the anterior surface of Bowman's layer.

Recent histological examination of Bowman's layer in the keratoconic cornea revealed progress of keratoconus at the bilayer lamella at the periphery of the cone, which appeared to contain keratocytic nuclei and other components near the apical scar (Hollingsworth et al., 2005b). The present study revealed the bifurcation of fibrils in the anterior stroma exposed by a damaged Bowman's layer in patients three and four.

Radner et al., (1998) investigated the corneal stroma in keratoconus and reported that the arrangement of collagen lamellae in the apical region differed from that in the para-apical regions in that the collagen fibrils formed uniform layers and clear collagen borders could not be differentiated. In their study, the splitting of lamellae in the anterior-posterior and lateral directions totally was absent at the centre and only partially present at the periphery. Evidence from X-ray diffraction has confirmed that the organisation of stromal lamellae in severe keratoconus at the apex of the cone dramatically alters (Daxer, 1997, Meek et al., 2005). Recently, Meek et al. (2005) proposed that lamellar slippage might cause weakness in the central cornea in keratoconus. As is shown here (figure 4.13 E – H for example), it might be the case that some lamellae branch in the anterior stroma and are perhaps unravelling.

The discovery of a suitable instrument to investigate human keratoconus in the native state is the hope of both clinicians and scientists. ESEM has an advantage in that if water is used as the gas in the sample chamber, a correct balance between chamber pressure and sample temperature makes it possible to maintain samples in a hydrated state (Donald, 2003). Further, there is no need to coat samples with a conductive material to prevent charge build up. This technique is, therefore, suitable for the study of materials that are naturally wet, such as biological specimens, complex fluids (colloidal suspensions), foodstuffs and mixtures of solvents (e.g. water and oil). However, the study here did not produce overall satisfactory results, but achieved reasonable results at low magnification. Overall, this study found it impossible to obtain high resolution images of corneas at high magnification, even though the microscope does have the ability to reach high resolution capability. It is likely that the operating conditions in the specimen chamber were not optimal for cornea, but conceivably this could be remedied by more extensive investigation.

In keratoconus long-term use of a rigid contact lens with an apical touch fitting may increase the risk of scarring as reported by Korb (1982). The clinical histories reported that patients in this study had used a rigid contact lens for a long time. The morphology of keratoconus from SEM suggests that the erosion and scarring might be compounded by long-term rigid contact lens wearing. When the patient is in an advanced stage of the disease, tortuous folds emerging from the apex of the cone may reflect fissures in both Bowman's and stromal

layers and represent an early sign of the risk of acute hydrops. Band patterning, proposed to represent collagen lamellae under stress, has been reported recently using a confocal microscope, and it has been suggested that these correspond to Vogt's striae in severe disease (Hollingsworth, and Efron, 2005a). Similarly in this study, very faint vertical lines like hairs were noted during the examination in the ESEM of patient 7 on either side of the apical scar that appear like reflected furrows within bands. The study also identified the presence of many small tips seen distributed across the corneal buttons by stereomicroscopy and ESEM. Conclusive interpretation of these features was not possible although they were most likely to have been ruptures in the anterior surface of Bowman's layer. Thus, the application of the ESEM in the study of human cornea presents several challenges as limitations have been revealed, and here it provides acceptable information at low, but not at higher magnification. The lower resolution of ESEM at high magnification is likely due to the existence of water in the chamber of microscope. A more intensive effort to optimise chamber conditions could possibly improve this, however.

In conclusion, from the three cases in which preoperative topographic data were available it was found that topographical features alone failed to indicate the full extent of the progress of keratoconus towards the corneal periphery. Moreover, in addition to profound changes seen in the central zone of the cornea that presumably contribute to the apex of the cone, tissue changes and ruptures in Bowman's layer were found too at the corneal periphery. A clear link between the

severity of the disease clinically and the extent of the Bowman's breaks was not apparent here, suggesting perhaps that events deeper in the stroma have a significant influence on the tissue changes seen in keratoconus.

5.1 A study of structural changes in mice with misshapen cornea

5.1.2 Introduction.

Researchers attempting to investigate the pathogenesis of keratoconus have encountered difficulty ascertaining the onset of the disease because patients do not usually complain about any sign or symptom at an early stage. Thus, it is difficult to understand the pathogenesis and progress of the disease, and to distinguish the very early stage of keratoconus from other disorders. In recent years, researchers have attempted to study the abnormal structure of the misshapen cornea genetically and biophysically in different strains of mice that have abnormally shaped corneas that in some ways resemble keratoconus. Two such strains are called SKC and JKC, which have been proposed as useful models in the study of the underlying structural defects that might cause a cornea to take on an abnormal topography (Tachibana et al., 2002a; Tachibana et al., 2002b; Quantock et al., 2003). Studies of the JKC mouse strain will be discussed in the second part of this chapter. First, this study will describe an evaluation of structural abnormalities in mice deficient in the protein SPARC (secreted protein acidic and rich in cysteine) that often display a distended cornea with a possible keratoconic-like shape as discovered by Gilmour et al. (1998). Also, because the

previous chapter concluded that changes within the stroma itself undoubtedly have a bearing on the severity of keratoconus (and because rodents do not have a true Bowman's layer in the same way as humans do (Quantock et al. 2005)) I will move on from a study of surface morphology to a study of the stromal interior.

It is known that collagen fibrils in the corneal stroma play a very important role in the biomechanical stability and shape of the tissue and a number of detailed studies had been achieved on the corneal stroma in keratoconus. The internal fine structure of corneal stroma in the SPARC-deficient mouse has not been investigated. Therefore, light and transmission electron microscopic studies were carried out to evaluate the internal fine structures of the corneal stroma in these mice to shed some light on the factors that may contribute to biomechanical instability in the misshapen cornea.

5.1.2 Background.

Secreted protein, acidic and rich in cysteine (SPARC), also known as osteonectin or basement membrane-40 (BM-40), is a collagen-binding glycoprotein that belongs to the matricellular category of proteins. It associates with the extracellular matrix and appears to act as a modulator of cell- extracellular matrix (ECM) interaction, but currently with no defined structural function (Bornstein and Sage, 2002). SPARC is secreted by many cells, such as fibroblasts,

endothelium, osteoblasts, and platelets (Stenner et al, 1986; Kasugai et al, 1991), but does not contribute structurally to the extracellular matrix. Rather, it regulates the production of several proteins of the extracellular matrix (Bradshaw and Sage, 2001).

The extracellular matrix is composed of structural proteins, proteoglycans, growth factors, and matricellular proteins, such as thrombospondins 1 and 2, osteopontin, tenascin-c, and SPARC. The initial description of SPARC protein by Termine and colleagues (1981) presented it as a major non-collagenous constituent of bovine and human bone. Then Sage et al. (1981 and 1984) described it as a protein secreted by proliferating cells in vitro while Otsuka and associates (1984) referred to it as a protein produced by cultured fibroblasts. Mason et al. (1986) were the first to isolate the complementary deoxyribonucleic acid (cDNA) from a library of mouse embryonal carcinoma cells differentiated in culture with retinoic acid and cyclic adenosine monophosphate (cAMP).

SPARC has considerable functional diversity. It clearly plays an important role in remodelling tissue, and contributes prominently in morphogenesis, development, injury and repair. With thrombospondins 1 and 2, tenascins C and X, and osteopontin, SPARC is the prototype of the matricellular class of secreted glycoproteins that are structurally dissimilar, regulate interactions between cells and their extracellular matrix (Lane and Sage, 1994; Bornstein, 1995). SPARC is shown to inhibit the cell cycle, disrupt cell adhesion, inactivate cellular responses

to certain growth factors, regulate the production of extracellular matrix, and promote a rounded cell shape (Lane and Sage, 1994). Motamed and Sage (1998) have shown that the counter-adhesive and antiproliferative properties of SPARC appear to proceed through separate signalling pathways. Moreover, as can be seen in figure 5.1.1, the early development of cataracts in SPARC-null mice establishes that the gene is essential to the maintenance of lens transparency (Gilmour et al. 1998; Norose et al. 1998). These SPARC deficient mice also possess misshapen corneas, as can be seen in histologic section in figure 5.1.1.

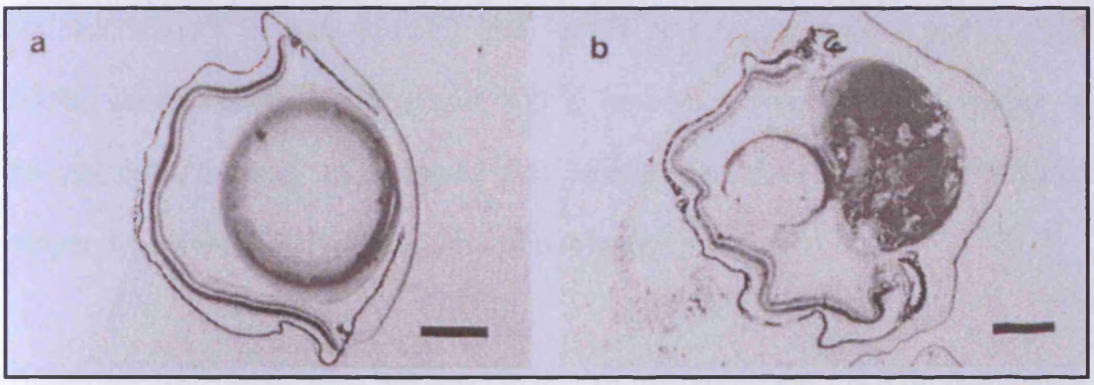

Figure 5.1.1: *Sagittal sections through whole mouse eye (**a**) wild type (**b**) SPARC-deficient showing misshapen cornea and lens pathology in SPARC mutant. **Source**: The EMBO Journal (Gilmour et al., 1998).*

Rhee et al. (2003) showed that SPARC mRNA and protein are present in non-glaucomatous human trabecular meshwork and cultured human trabecular meshwork cells. Thus, because of its effect on matrix metalloproteinases, SPARC may play a role in the regulation of intraocular pressure.

SPARC is expressed widely during embryogenesis (Sage et al., 1989), and Brekken and Sage (2001) have found that its production accompanies the induction of collagen type I. Iruela-Arispe et al. (1996) concluded that the production of collagen type I appears to be requisite for the association of SPARC with embryonic extracellular matrix in the mouse. Francki et al. (1999) investigated the function of SPARC in the regulation of collagen type I and transforming growth factor-β1 (TGF-β1) in mesangial cell cultures from wild-type and deficient mice. They found that SPARC-deficient cells exhibited a significant diminution of both collagen type I and TGF-β1, but after treatment of these cells with recombinant human SPARC, the levels of collagen type I and TGF-β1 SPARC were restored to 70% and 100%, respectively, of those produced by wild-type cells. Further, they showed that SPARC exhibits some of its effects on collagen type I via a TGF-β1-dependent pathway.

SPARC deficient mice have reduced levels of collagen type I in skin (Bradshaw et al., 2003), and coetaneous wounds close faster compared to those in wild type mice (Bradshaw et al., 2002). The absence of SPARC also influences the foreign body reaction to implanted biomaterials, resulting in a decreased capsular thickness in SPARC deficient dermis (Puolakkainen et al., 2003).

Several studies have previously reported the role of SPARC protein in the cornea. A study of normal and wounded cat corneas using a immunohistochemical polyclonal rabbit anti-murine SPARC antibody showed

weak immunoreaction from the SPARC protein in the cytoplasm of epithelial and endothelial cells. However, SPARC was not seen in the keratocytes of either normal or wounded corneas (Latvala et al., 1996). In contrast, Mishima and co-authors (1998) reported that SPARC, as well as appearing in epithelial cells, was also detected around keratocytes adjacent to the wound. These authors suggested that the difference between their study and others was due to the deep damage in the stroma in their study. Immunohistochemical staining of mouse corneal stroma with antisera to SPARC seven days post-wounding was performed by Berryhill et al (2003) who confirmed the presence of accumulated SPARC in the regions undergoing repair. The above cited studies suggest that SPARC plays a certain role in wound healing. In an in-depth study of the extracellular matrix, Abe et al (2004) revealed that adding an epidermal growth factor (EGF) to the conditioned medium of corneal epithelial cells leads to a markedly reduced amount of SPARC. They suggested that the cytokines and growth factors modulate cell-matrix interactions in corneal healing, possibly by regulating the production of SPARC synthesis.

The ultrastructure of the SPARC-deficient cornea was studied here to ascertain whether any abnormalities in the ultrastructure of the corneal extracellular matrix could be identified that might lead to the corneal ectasia that has been seen in tissue sections of null eyes.

5.1.3 Methodology and materials.

5.1.3.1 Specimen preparation.

With the help of Dr. Robert Young and Dr. Mike Wride and in line with ethical regulations, four SPARC-deficient mice and three wild-type mice were killed by cervical dislocation, and their eyes enucleated using a Zeiss Stemi-binocular dissecting microscope. All mice were in the 6-11 month age range. Corneas were dissected using fine-point Vannas Bowspring scissors, a scalpel fitted with a No.11 blade and fine forceps. Some of the corneas of SPARC-deficient mice had developed a lens cataract. Corneas were fixed by immersion in 2.5% glutaraldehyde in 0.1M phosphate buffered saline (PBS) (pH 7.3) overnight. The next day they were washed three times with 0.1M PBS for 10 minutes, followed by secondary fixation in 2% osmium tetroxide (O_SO_4) in distilled water for two hours. Cupromeronic blue (USBiological, C8210, USA) was included in the fixative to enhance the contrast and visibility of the corneal proteoglycans (Scott and Haigh, 1985). Therefore, some of the specimens were fixed in 2.5% glutaraldehyde in 25mM sodium acetate buffer (pH 5.7) containing 0.05% cupromeronic blue, 0.3M $MgCl_2$, overnight. The following day, samples were washed three times for 15 minutes in a mixture of 25mM sodium acetate buffer, and 0.3M $MgCl_2$. After this, samples were immersed three times for 5 minutes each in 0.5% aqueous sodium tungstate, and then, washed in 0.5% sodium tungstate in 50% ethanol. Each solution was changed three times, with a 5 minute interval between each change of solution.

Specimens were dehydrated in a graded ethanol series, 50%, 70%, 85% and 95% each for 20 minutes followed by, 100% three times for 15 minutes on each occasion. Next, each cornea was cut into two halves and immersed in propylene oxide for 45 minutes. The specimens were then transferred to a mixture of propylene oxide and Epon resin (epoxy resin 24.0g, hardener DDSA 16.0G, hardener MNA 10.0g, and accelerator BDMA 1.50g). After 3 hours, the tops of the vials were removed for propylene oxide evaporation. After this, samples were placed in 100% fresh resin overnight to allow impregnation of resin into tissues. Tissue preparation was done at room temperature on a rotator in the fume cupboard, with constant agitation to facilitate penetration of the resin. Specimens were placed in labelled moulds and polymerised in pure Epon resin at 60° C for 48 hours.

Once hardened, the block was trimmed using a razor blade to expose the sample, and to form a pyramidal cutting face. A glass knife was made using an LKB 7800 knife marker, and a tape trough was attached to the knife using wax to hold the water onto which the cut sections could float. Sections, approximately 70-90 nm thick for examination in the TEM and 1µm thick for investigation using the light microscope, were cut with glass or diamond knives on a Reichert-Jung ultramicrotome. Sections were stretched in the water trough with chloroform vapour and then collected onto 300 square mesh copper 3.05 mm grids. Grids were then dried in a Petri dish prior to staining.

Staining solutions were made then cleared of aggregates by centrifugation at 14,000 r/pm for 5 minutes and Millipore filtration before use. The staining was achieved for TEM using two methods. First, some of the grids were stained at 50° C for 40 minutes by floating on droplets of freshly dispensed 2.0% uranyl acetate, and then washed in distilled water 3 times. These grids were further floated on freshly prepared 2.0% lead citrate at 50° C for 40 minutes and then washed again with distilled water 3 times. After this, the grids were dried ready for transmission electron microscopy examination. Second, the remaining grids were stained at 50°C for 40 minutes by floating on droplets of 1.0% phosphotungstic acid (PTA). The same method was applied as previously described excluding lead citrate.

All semithin sections of SPARC corneas were stained with toluidine blue for examination by light microscopy.

Stained, ultrathin sections of corneas were examined using JEOL 1010 (JEOL Ltd., Akishima, Japan) transmission electron microscope at 80KV. Electron-optical images from the anterior, mid and posterior regions of the corneal stroma were taken at various magnifications, ranging between x15,000 and x40,000, and captured on a Kodak MegaPlus, Model 1.4/digital camera, which digitises images in a 512X512 pixels raster in 256 grey levels.

Semithin sections were examined using the (Leica DMR A2) digital light microscope. Images were taken at 20x, 40x and 63x magnifications and captured by the Leica DC 500 digital camera which is linked to digital image processing and analysis software for professional microscopes (Leica Q win V3).

Using image analysis software (analysis 3.0; soft imaging system GmbH, Germany), numerous mathematical filters and morphological functions were applied to calculate collagen fibril diameters in each image at different sites in the corneal stroma according to the following steps:

Acquisition of images: The image was obtained and displayed onto a monitor via a digital camera.

Contrast equalisation: This function enhances and modifies the contrast of the original images of the grey values.

Image filtration: This filter calculates the arithmetic mean of the pixel and the 8 surrounding neighbours in order to suppress the artificial noise.

Binary image: The analysis program transfer the detected grey values and converted them into a binary image. A binary image has 2 grey levels. Therefore, all pixels lying within the threshold were considered to be corresponded to the foreground or to a particle. All other pixels corresponding to the background, and were ordinarily displayed in black. The shading correction function was used if the image has a non-constant background caused by inhomogeneous illumination.

Morphological filters: This function was used to erase (decreasing the size) or dilate (expensing the size) the object. Therefore, attached objects will be separated and objects with small holes will be filled, and irregular margins of objects will be smoothed.

Fibril measurement: The measurement of fibrils diameter was achieved by setting the analysis software to analyse all binary objects within specific threshold values, e.g. a value between 20-50 nm. This range was classified, giving that objects with similar diameter have specific colour. Objects falling outside the range of values were not coloured and required further analysis. The measurements of fibril size; minimum, maximum and average diameter were displayed in an Excel program. Here, minimum diameter was used because in some sections the fibril outline appears to be a little oval because of fibrils that cross the plane of the section not totally at right angles to the section. In this case the minimum diameter represents the true fibril diameter. From a total of 7 corneas 21 images were obtained; anterior, mid, and posterior from the central cornea (Connon et al., 2000). The current study presented here three representative images from different regions of one control and one SPARC-deficient cornea.

5.1.4 Results.

5.1.4.1 Light microscope observations.

Illustrative light micrographs of control and SPARC-deficient mice corneas show the outermost epithelial layer stroma, Descemet's membrane, and the innermost endothelial layers of the cornea (figure 5.1.2). In places, the SPARC-deficient cornea was thinner than the control corneal section. Moreover, in sections of normal mouse cornea the stroma revealed regular undulations of collagen lamellae, and keratocytes were distributed parallel within lamellae. However, in SPARC-deficient corneas the collagen lamellae had a disrupted, interwoven appearance in the anterior two-thirds of the corneal stroma. At this level Descemet's membrane and endothelial layer did not appear to differ from the normal appearance of control cornea and there was no other distinct abnormality.

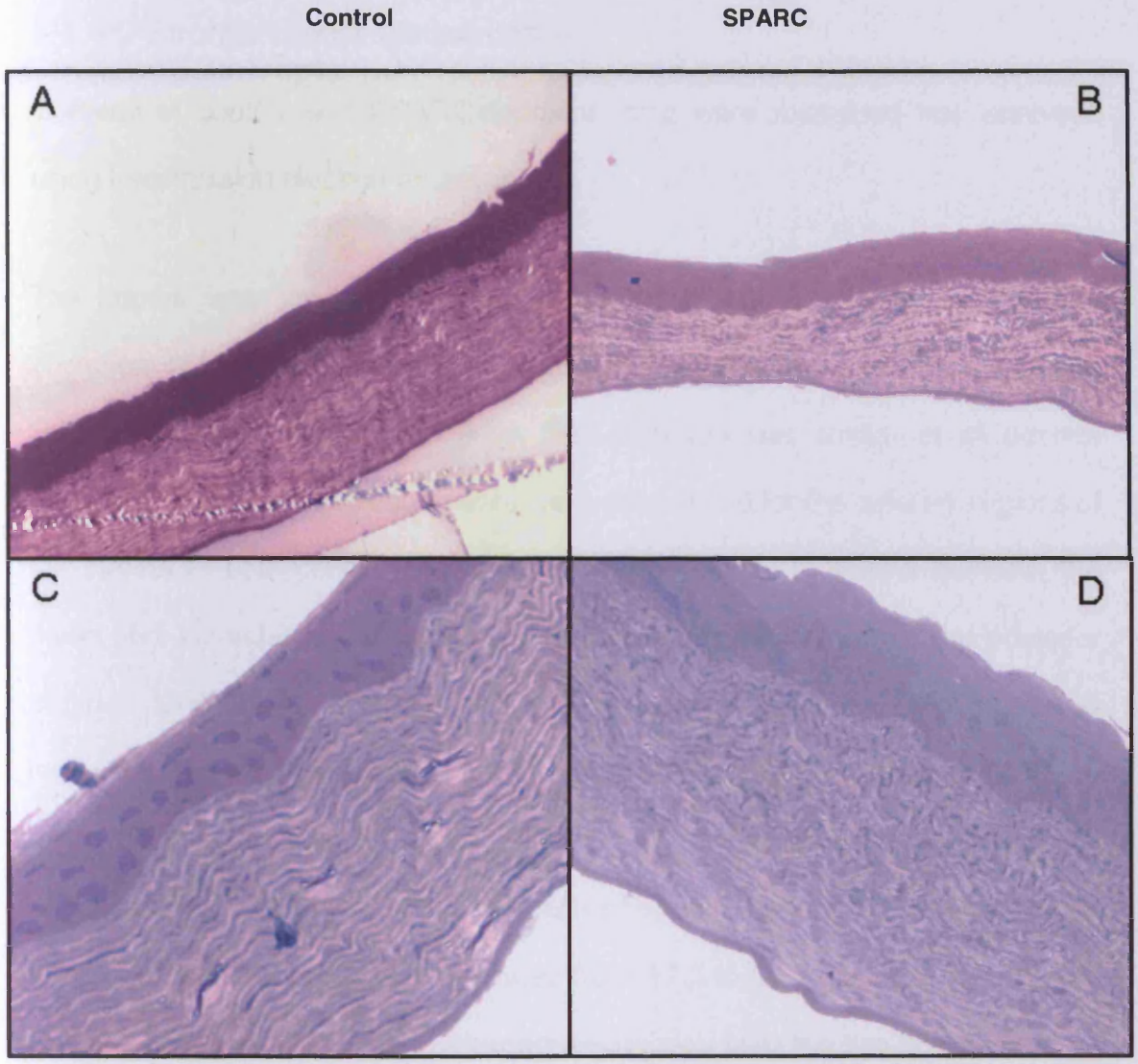

Figure 5.1.2: *Light microscopy of 1 um thick section showing the normal and SPARC-deficient corneas. Normal cornea of wild type mice* (**A**); *Thin cornea of SPARC mice* (**B**); *Regular interwoven normal corneal stroma of wild type mice* (**C**) *and disrupted two-third anterior section of the corneal stroma of SPARC mice* (**D**). **A** *and* **B** *are X20* **C** *and* **D** *X63.*

5.1.4.2 Stromal matrix ultrastructure.

Corneas of control and SPARC-deficient mice were examined and analysed using transmission electron microscopy.

The stroma was divided into three regions for analysis: anterior, mid and posterior. In SPARC-deficient and control corneas the structure of the collagen fibrils themselves with their uniform fibril contours was similar at all stromal depths. Normal fibrillar arrangements were determined for the different regions of the stroma of both control and SPARC-deficient mice. In control corneas, the mean fibril diameter gradually increased from the anterior towards the posterior stroma. Similarly, in SPARC-deficient corneas, the mean fibril diameter increased, but was the same in the mid and posterior stroma (table 5.1.1). The mean diameter of collagen fibrils of SPARC-deficient corneas taken from all regions was greater than the fibril diameter of control corneas, 29.9 ± 3.9 nm and 28.2 ± 3.2 nm, respectively, and ranged from 17.2 to 50.8 and 21.8 to 41.9 nm, respectively. According to the Kolmogorov-Smirnov test, the two groups (control and SPARC-deficient) are not normally distributed ($p < .05$). Also, Levene's test indicates that the variances of the groups are not equal ($p < .05$). As the assumptions of the independent samples T-test are not passed, the nonparametric alternative Mann-Whitney test is used. This indicates that the mean diameter of the two groups is significantly different ($p< 0.001$) with the control group having a lower score (figure 5.1.4).

With regard to collagen fibrillar arrangement fibrils in the SPARC-deficient cornea appeared much less tightly packed together in the anterior and mid stroma, and far more dispersed in the posterior stroma (figure 5.1.3).

Control SPARC

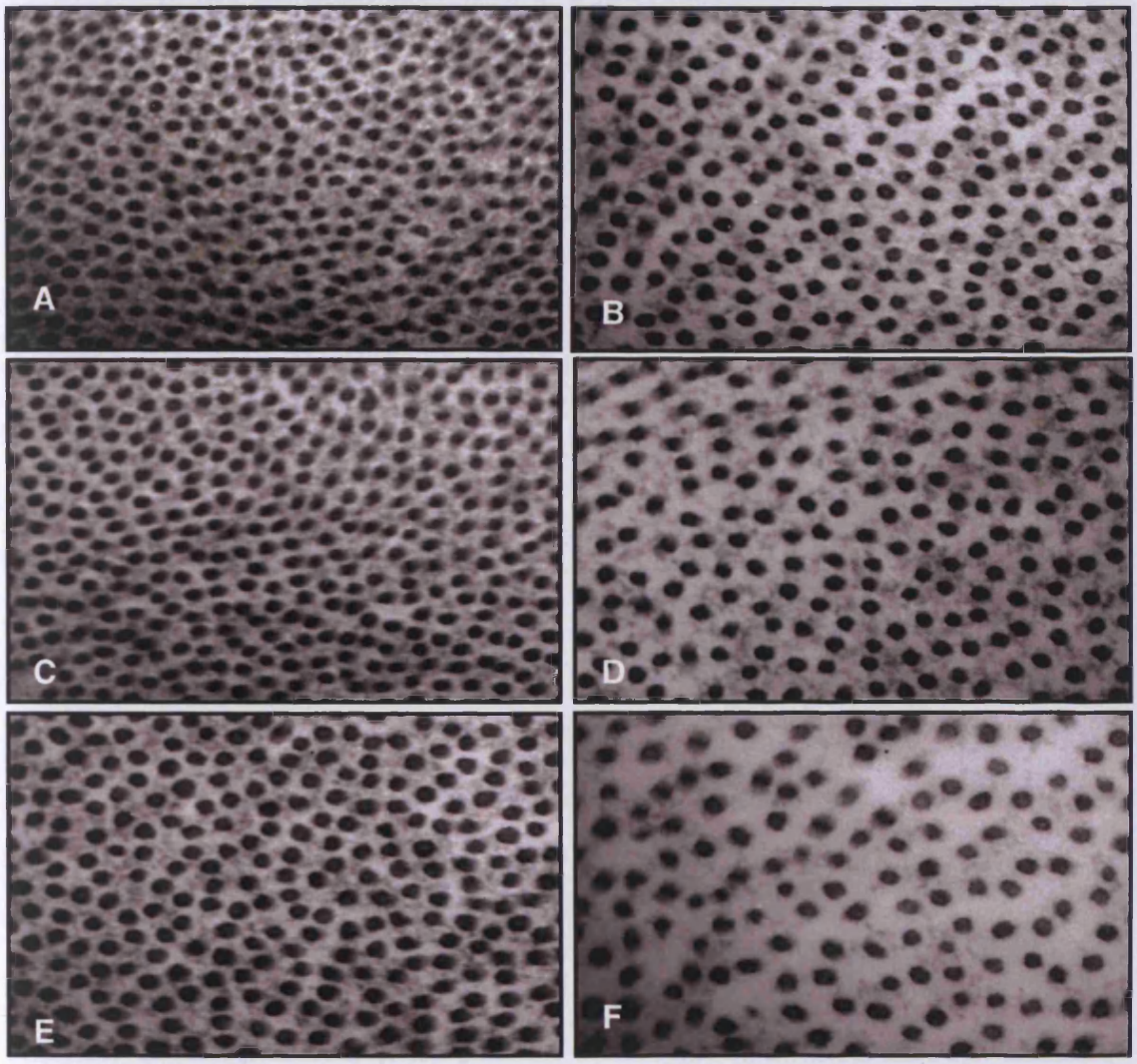

Figure 5.1.3: *TEM of SPARC control and SPARC-deficient mice corneas.* (**A**, **B**) *anterior,* (**C**, **D**) *mid and* (**E**, **F**) *posterior stroma. (***B**, **D**, *and* **F***) illustrate the decrease in fibril number density in SPARC deficient mice, which is more severe in the posterior stroma. Magnification is 40K throughout.*

Stromal site	Control 1 nm SP 129	Experimental 1 nm $Sp^{-/-}$ 129Sv/Ev
Anterior	25.0 ± 5.4	26.0 ± 4.6
Mid	27.7 ±3.5	32.0 ± 6.4
Posterior	32.0 ± 2.9	32.0 ± 6.9

Table 5.1.1: *The mean collagen fibril diameters of different regions of the stromal cornea.*

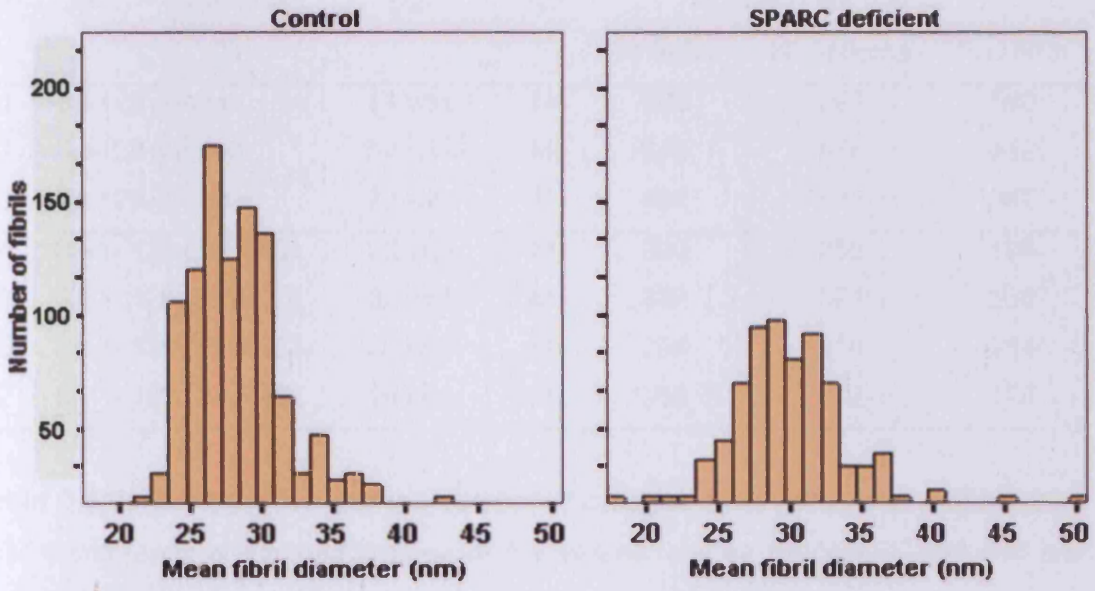

Figure 5.1.4: *Histogram of diameter distribution of collagen fibrils of control SPARC and SPARC-deficient mouse corneas. Mean fibril diameter within control SPARC was 28.2 ± 3.2 mm (left) and in SPARC-deficient corneas 29.9 ± 3.9 mm (right).*

To quantify the collagen fibril spacing the number of collagen fibrils were counted in 40 X 1μm^2 regions. From this, the number density of collagen fibrils was seen to be lower in SPARC-deficient corneas than control mice corneas. A sharp decrease in collagen fibril number density was observed across the thickness of the stroma. This was less prominent between the anterior and mid-stroma but particularly evident in the posterior stroma.

No	Mouse type/ strain	Age	sex	Fibril number (per μm^2)		
				Anterior	Mid-stroma	Posterior
1	Sp-129 control	54 wks	M	528	598	560
2	Sp-129 control	54 wks	M	610	558	412
3	Sp-129 control	22 wks	F	434	424	340
4	Sp-1- 129 (SPARC)	22 wks	M	332	258	198
5	Sp-1- 129 (SPARC)	22 wks	M	382	372	236
6	Sp-1- 129 (SPARC)	22 wks	M	294	310	284
7	Sp-1- 129 (SPARC)	16 wks	M	258	272	108

Table 5.1.2: *The age, sex and the number of collagen fibrils per* μm^2 *measured from TEM micrographs at different regions of the stromal cornea for SPARC-deficient and wild-type of mice.*

5.1.4.3 Proteoglycan morphology.

The nature and distribution of proteoglycans within the corneal stroma of SPARC-deficient and control corneas were examined stained with cupromeronic blue using the critical electrolyte concentration method. No apparent difference in the proteoglycan filament arrangement was noted, with the filaments oriented

crosswise to the collagen fibrils in both cases (figure 5.1.5). However, the proteoglycan filaments of SPARC-deficient mouse cornea seem to be slightly enlarged in size, although the relevance of this is not clear.

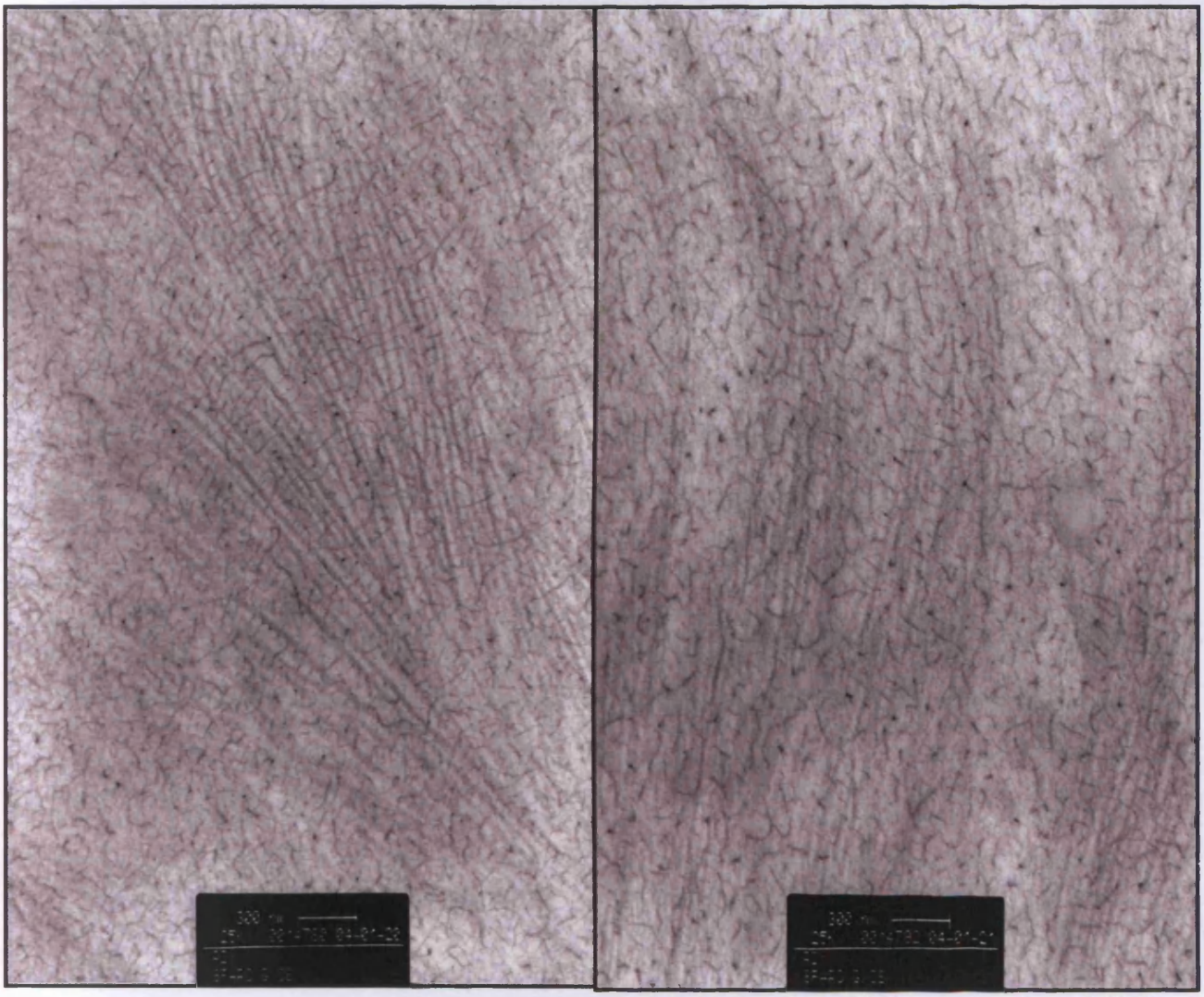

Figure 5.1.5: *TEM micrographs of corneal proteoglycan arrangement in SPARC control (left) and SPARC-deficient mice (right). Proteoglycan arrangements show no difference between the two groups x25K.*

5.1.5 Discussion.

The normal shape of the corneal stroma is predominantly dependent on the biomechanical stability bestowed by the lamellar arrangement of collagen fibrils, with the assembly and final properties of the fibrillar collagen matrix significantly influenced by the molecular heterogeneity of corneal collagen fibrils. In cornea, fibrils are hybrids of collagen type I and collagen type V (Birk et al., 1990). Increased proportions of collagen type V molecules in the predominantly collagen I fibril regulates the lateral growth of the fibril and leads to thinner fibrils, and consequently likely changes in the overall corneal biomechanics (Rada et al., 1996). The interaction with collagen of the proteoglycans decorin and lumican were found to inhibit the rate of collagen fibrillogenesis (Rada et al., 1993). Chakravarti et al. (2000) reported that the lumican-deficient corneal stroma displayed a 40% reduction in stromal thickness. The current study found that SPARC-deficient mice corneas were also thinner than those of the control group, but not to the extent that the lumican-null cornea is.

The diameter of collagen fibrils in the normal corneal stroma of the mouse, as measured by electron microscopy, has been reported to range between 25 and 33 nm (Haustein, 1983). In humans one study has reported it at between 17.9 to 33.4 nm with a 26 nm average (Quantock et al 1993). Chakravarti et al. (1998) found thicker collagen fibril in the lumican-null corneal mice 47 ± 1.4 nm compared to normal wild type mice. Characteristically, the diameters of collagen fibrils of the control groups in our study were in agreement with the previously

cited studies but with a wider average diameter 28.2 ± 3.2 with a range from 21.8 to 41.9 nm.

Abnormal fibril diameters with a wide range have been reported in humans for macular corneal dystrophy as well as a number of other diseases such as Hurler syndrome, and Scheie syndrome (Quantock et al., 1997; Huang et al., 1996; Quantock et al., 1993). In Hurler and Scheie's syndromes, collagen fibril diameters have been reported as thicker than normal with a wide range of sizes (Huang et al., 1996; Quantock et al., 1993). In macular corneal dystrophy pockets of thicker fibril diameters ranging from 20 to 58 nm have been reported (Quantock et al., 1997). In human keratoconus, Akhtar and associates, (unpublished) report the fibril diameter to be reduced in size compared to the normal human cornea and to range from 20 to 24 nm. In our study, there were variations among the study corneas. SPARC-deficient mice corneas revealed a thicker fibril diameter with a wider range (the mean collagen fibril diameter in SPARC-deficient corneas was 29.9 ± 3.9 nm and ranged from 20 to 50 nm).

The question remains as to what might be the biological mechanisms behind the structural matrix changes in the corneas of SPARC–deficient mice. Perhaps SPARC protein acts to modify the surface of collagen fibrils early in development to promote the aggregation and/or stability of the fibrils in the extracellular matrix through cross-linking. Also, absence of SPARC protein might prevent the collagen fibrils from progressing beyond an early developmental stage, either

because of a lack of protein interaction at the fibril surface, or, incomplete cross-link formation that acts to stabilise collagen complexes (Bradshaw et al., 2003).

Keratan sulphate is present on three proteins in the cornea, lumican, keratocan and mimecan (Funderburgh et al., 1993). In the human keratoconus cornea the proteoglycan arrangement is reported to alter and run parallel with collagen fibrils in some affected areas (Fullwood et al., 1990). It has also been reported that keratan sulphate expression decreases in keratoconus (Funderburgh et al., 1990), but that keratocan is overexpressed and may alter collagen fibrillogenesis and lead to the development of keratoconus (Wentz-Hunter et al., 2001). Studies on gene targeted mouse models of proteoglycan deficiencies have shown that lumican and keratocan play critical roles in the regulation of fibril diameter during post natal development, and any alteration in keratan sulphate may lead to reduced fibril diameter and organisation (Chakravarti et al., 1998). However, the proteoglaycan arrangement in SPARC-null corneas appears normal on electron microscopic histochemistry, so a proteoglycan-related pathologic mechanism seems unlikely to be the direct overriding cause of matrix disruption in SPARC deficiencies.

Because of the reduced collagen fibril number density seen in EM sections of SPARC-deficient corneas it is clear that SPARC tissue is slightly swollen. This implies some changes, either in the endothelial pump action or the swelling pressure or both. In the latter case, these could be proteoglycan changes not

detected with cupromeronic blue which need a biochemical investigation. Also, changes in the chloride-binding might lead to SPARC-deficient tissue swelling (Hodson 1997).

Collagen fibrils provide mechanical strength for corneal curvature maintenance and consequently correct refractive error. Corneal mechanical properties are maintained by uniform orientation and distribution of collagen fibrils. A reduction or alteration in collagen fibrils will lead to reduced tensile strength and consequently the development of a misshapen cornea may occur. Eming et al. (1999) found lower tensile strength in SPARC mouse skin compared to control mouse skin. I have no data on the tensile strength of SPARC-deficient corneas, but this is an area that should probably be investigated in the future.

SPARC null-mice revealed a decrease in the collagen content at adult ages and an increase in the relative levels of type VI collagen in the skin (Bradshaw et al., 2003). Data on the low fibril number density in SPARC-null corneas presented in this chapter show that in SPARC null-mice, the content fibrillar collagen of the corneal stroma is reduced in whole regions of the stroma, but that this is particularly severe in the posterior region of the stroma. Rawe et al (1994) found that the collagen fibrils in scarred rabbit cornea are restored with the progress of age, and matrix architecture approximates that of the control cornea after 9 months. Given that collagen type VI forms networks in the corneal stroma it might play a role in the control of stromal architecture. Thus, a study of possible

increased type VI collagen levels in the corneas of SPARC-null mice is warranted.

Brekken and Sage (2001) reported that the production of SPARC accompanies the induction of collagen type I. Iruela-Arispe and co-authors (1996) found that the association of SPARC with embryonic extracellular matrix is required for collagen type I production. Therefore, Bradshaw and co-workers (2003) suggested that SPARC acts to control collagen accumulation in the skin through regulation of collagen deposition into the Extracellular matrix, rather than through regulation of transcription of collagen type I mRNA. This is because at an early age no difference between wild type and SPARC-deficient mice has been found.

Numerous studies have shown that collagen synthesis and deposition are regulated by transforming growth factor–ß1 (TGF ßI), synthesised by keratocytes (Reed et al., 1994; Grande et al., 1997; Abe et al., 2004). A study reported that SPARC–null cells displayed diminished expression of collagen type I and TGF-ß1 (Francki et al., 1999). However, adding recombinant human SPARC to SPARC-null cells restored collagen type 1 mRNA to 70% and TGF-ß1 mRNA to 100% in wild type mice. Poncelet and Schnaper (1998) suggested that SPARC activates the TGF-ß1 which induces the production of collagen type I.

The results of this series of experiments indicate that SPARC protein influences the production of collagen fibrils in the mouse cornea. The absence of SPARC

protein revealed a wide spacing of the collagen fibrils that might lead to biomechanical instability and subsequently cause structural weakening and an altered shape of the SPARC-null mouse cornea.

5.2 An x-ray diffraction study of collagen fibril orientation in mice with misshapen corneas

5.2.1 Introduction.

The collagen fibril orientation of the corneal stroma plays an important role in the maintenance of biomechanical stability and corneal transparency. Several studies have investigated collagen fibril orientation in the human corneal stroma. Using low-angle X-ray scattering, Meek et al. (1987) found two preferred directions of orientation in the centre of the human corneal stroma: inferior-superior and medial-lateral. These preferred directions were more pronounced posteriorly. Also, collagen fibrils in some radial directions at the edge of the cornea were found to run circumferentially. Newton and Meek (1998a; 1998b) later found a complete circum-corneal annulus of collagen fibrils at the limbus in the human cornea.

In a study using X-ray diffraction by Boote et al. (2003), the collagen fibrils in the central cornea were more closely packed than in the peripheral cornea, and it

was judged that this is probably necessary for biomechanical stability and to maintain corneal strength, and hence curvature, in a region of reduced tissue thickness. In an attempt to map both collagen fibril orientation throughout the full thickness of the cornea, as well as the relative fibril mass distribution in normal human corneas Aghamohammadzadeh and his associates (2004) used high angle synchrotron X-ray scattering, and reported an orthogonal orientation of collagen fibrils in vertical and horizontal directions and a circular disposition of fibrils at the limbus. Boote et al. (2004) conducted an investigation into the collagenous structure of the small primate (marmoset) cornea. Results revealed the circular disposition of collagen fibrils at the limbus similar to that in the normal human cornea. However, unlike orthogonal collagen fibrils in the human cornea, the fibrils' preferred organisation was mainly oriented towards a superior-inferior direction. Unlike the normal human cornea (and the primate cornea), the central cornea of mouse does not contain a significant amount of collagen preferentially aligned in an orthogonal manner (Quantock et al., 2003).

Regarding keratoconus, using high angle X-ray diffraction, Daxer and Fratzl (1997) reported that the orientation of collagen fibrils inside the lesion was altered dramatically, whereas outside the diseased region orientation was normal. Earlier in this thesis (chapter 4), however, I showed that surface matrix changes occurred outside the central lesion in keratoconus. Recently, Meek and his co-workers (2005) used synchrotron x-ray scattering across the entire human keratoconus cornea and found a changed collagen fibril orientation within the

stroma at the apex of the affected area and outside the affected area, too. As can be seen in figure 5.2.1, the map revealed an uneven distribution of collagen fibrillar mass and changes in stromal lamellae organisation compared to the normal cornea.

Polack (1976) postulated that the thinning of the human keratoconic cornea is due to releasing and slippage of lamellae from other lamellae without collagenolysis. Meek et al. (2005) suggested that the redistribution of collagen organisation is due to the lack of proper development of this cross-linking between lamellae during the development of stromal cornea.

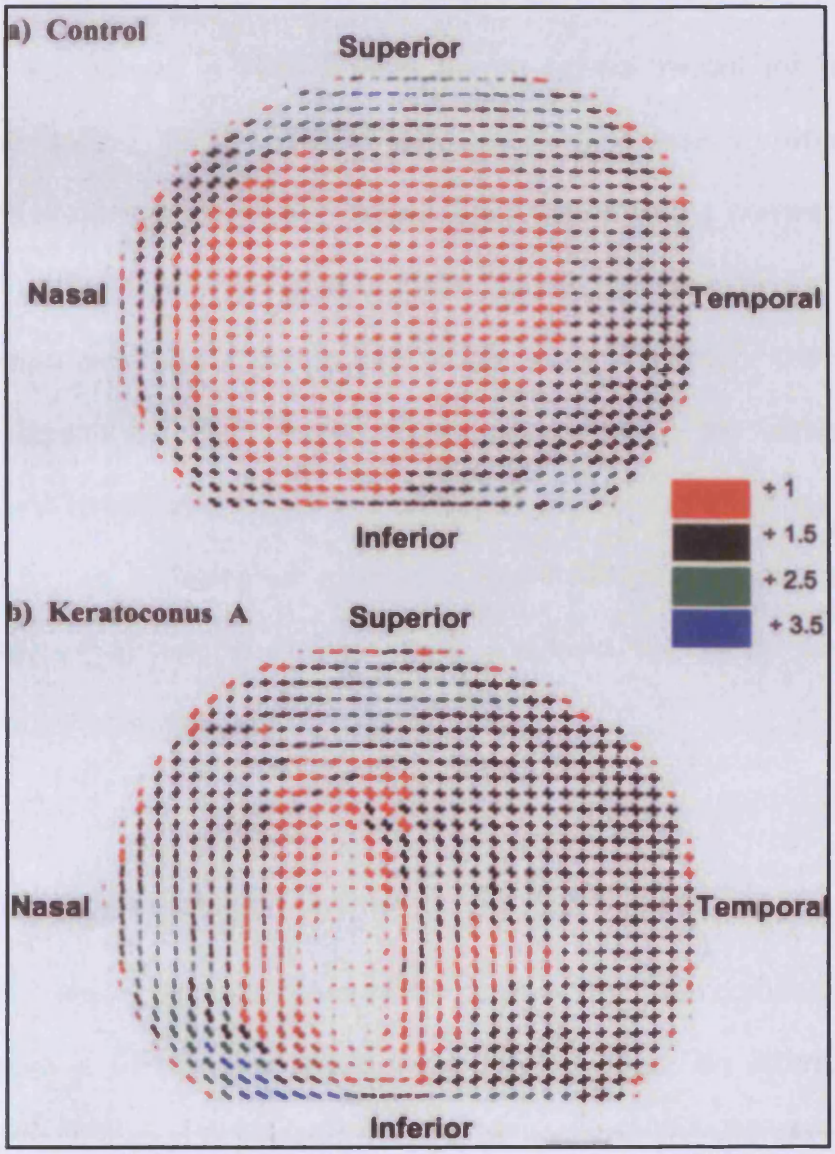

Figure 5.2.1: *The preferred collagen fibril orientation at a series of positions across (a) a normal human cornea and (b) a keratoconus cornea. Each polar plot (i.e. the cross-shaped symbols) represents the preferred alignment of collagen fibrils throughout the thickness of the cornea at that point in the cornea. The normal cornea revealed that collagen fibrils lie primarily in orthogonal directions, whilst the keratoconic cornea showed an altered fibrillar orientation predominantly at the centre of the cornea (i.e. the preponderance of "propeller-shaped" plots is lacking). In this representation the polar plots have to be scaled to be visible on a single montage because those at the edge are larger because the cornea is thicker here with more collagen. A colour-coded scale was chosen to indicate the scaled-down factors.* ***Source***: *IOVS (Meek et al. 2005).*

Clinically, the mouse is widely used as an animal model for human ocular disease. In chapter 5.1 the SPARC-deficient mice corneas showed variations in collagen fibril diameter and fibril spacing compared to the corneas of wild type mice and it was postulated that this might weaken the tissue and predispose it to ectatic shape changes. Utilising high angle x-ray diffraction, the current study aimed to investigate and map collagen orientation in the corneal stroma in SPARC mice to see whether or not abnormal collagen orientations may exist as they do in human keratoconus corneas. I also investigate the corneas of another strain of mice that tend to develop corneal ectasia, the Japanese Keratoconus (JKC) mouse (Tachibana et al., 2002b).

5.2.2 Principle of wide angle x-ray scattering.

Seventy per cent of the total mass of the corneal stroma is composed of collagen types I and V formed into heterotypic fibrils. When an intensive beam of monochromatic X-rays is passed through an isolated corneal stroma parallel to the visual axis, wide-angle X-ray patterns from the corneal stroma are formed because of the interference between the X-rays scattered by individual collagen molecules within the fibrils. X-ray scattering patterns are recorded and contain an equatorial arc on the detector that is formed by the lateral separation of these molecules. The X-ray patterns from a single lamella will form two equatorial diffraction maxima on either side of an axis on the X-ray detector given that all collagen fibrils are running semi-parallel with the axis of each lamella, and the

molecules that comprise fibrils are also running semi-parallel to the fibril axis shown in (figure 5.2.2).

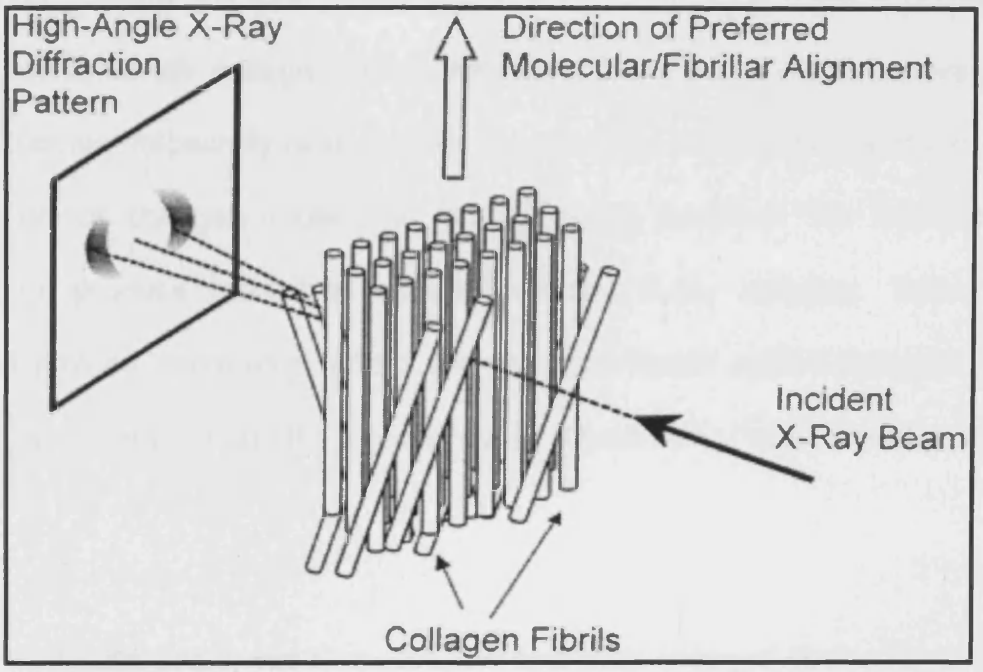

Figure 5.2.2: *Schematic diagram of the formation of a X-ray diffraction pattern from a single lamella of collagen fibrils, with most fibrils running in one direction. The reflections on the detector represent the collagen molecules that comprise the fibrils and run parallel with its axis.* ***Source****: (Quantock et al., 2003).*

In the instance of two isolated lamellae aligned at right angles with one another, the X-ray pattern will consist of two additional equatorial diffraction maxima the same distance from the centre of the X-ray patterns but at a right angle (90°) to each other. The upshot is that the identification of two diffraction maxima horizontally on the detector indicates that the majority of molecules are arranged in vertical orientation in this part of the cornea, and vice versa if the maxima are

vertical on the detector. Therefore, in the case of a stack of such lamellae with a completely isotropic radial distribution of fibrils, a circular intermolecular reflection of uniform intensity will form on the X-ray detector because there is no preferred orientation of fibrillar collagen molecules (and, therefore, fibrils). However, in the human cornea, especially over the first 7 mm of the central cornea, the preferred orientation of collagen molecules is orthogonal because the intermolecular reflections produce four-lobed maxima on the X-ray detector. These lobed maxima provide information about the fibril orientation within the plane of the cornea, averaged through the stromal depth (Meek et al. 1987; Daxer and Fratzl, 1997).

In this study, the focus was to investigate and map collagen fibril orientation and the relative distribution of collagen fibrils in SPARC-deficient and JKC mouse corneas and compare them with the normal mouse cornea to see if orientation changes might be responsible for the tendency towards a corneal shape change.

5.2.3 Methods and materials.

5.2.3.1 Specimens.

In total, six corneas of six male mice were used in this study. Corneas were obtained from one normal and two SPARC-deficient mice aged between 8 and 9 months, and one normal mouse aged 3.5 months, along with two JKC mice aged 6 months table (5.2.1).

No	Mouse type/ strain	Age	Sex
1	Sp-129 (control for SPARC corneas)	32 weeks	Male
2	KOR (control for JKC corneas)	14 weeks	Male
3	Sp-1-129 SPARC-deficient	36 weeks	Male
4	Sp-1-129 SPARC-deficient	36 weeks	Male
5	JKC	25 weeks	Male
6	JKC	23 weeks	Male

Table 5.2.1: *The mouse type, age and sex.*

Immediately after the mice had been killed, their eyes were enucleated and placed under a Zeiss Stemibinocular dissecting microscope. Using Vannas Bowspring scissor, Scalpel No.11 blade, and fine forceps, corneas including a small scleral rim were dissected. A 'V' was cut in the scleral rim as a marker to show the superior pole of the cornea which was then wrapped in Clingfilm to prevent dehydration with the mark clearly visible to show the anterior face of the cornea. Corneas were stored in dry ice at -80°C in the biophysics laboratory. The corneas of the JKC mice had been excised and then placed between Clingfilm and stored in dry ice by Prof. Tachibana in the Saitama Cancer Centre, Japan, and then sent on dry ice to the laboratory at Cardiff University. All samples were stored at -80° C until measurements were undertaken. The orientation of the JKC corneas was indicated on the plastic film.

5.2.3.2 Data acquisition.

Wide-angle synchrotron X-ray diffraction patterns for all experiments were obtained at the UK Synchrotron Radiation Source (Daresbury, UK), station 14.1. Each cornea was allowed to thaw between two sheets of Mylar and positioned

and fixed in a sample holder to ensure the beam passed through the anterior surface parallel to the cornea's optical axis. From 6 mice corneas, X-ray diffraction patterns were obtained using a focused monochromatic X-ray beam with a wavelength of 0.1488 nm and dimensions of 200 μm x 200 μm at the cornea. A lead backstop was carefully positioned immediately behind the specimen to block any undeviated X-ray beam. Starting from outside the left edge of the cornea and moving to the right edge of the central cornea across the horizontal meridians for the lower and then the upper zones, a series of x-ray exposures of 45 seconds length were collected, and x-ray patterns were recorded. A Newport stepper-motor interfaced with the beam shutters was used to move the cornea in the X-ray beam in between exposures that were recorded on a Quantum 4R charge-couple device (CCD) x-ray detector (ADSC, Poway, CA) placed 150 mm behind the cornea. Data collection was completed when the whole of the cornea had been mapped by 200 μm x 200 μm raster scans vertically and horizontally. Once recorded, all data were transferred to the Biophysics Department at the School of Optometry and Vision Sciences, Cardiff University for analysis.

5.2.3.3 Analysis.

Several parameters were used to analyse the distribution of normalised intensity profiles and maps of X-ray patterns as follows:

1. UNIX based image analysis software-Fit2dnew (ESRF, France);
2. Windows based graphics package-Optimas (Media Cybernetics, UK);
3. Windows based spreadsheet software, Excel (Microsoft, UK);
4. Windows based statistics package (Starsoft Statistica).

Image normalisation in x-ray fibre diffraction studies such as these is usually achieved using the average ion chamber reading. Normalisation in this way of data form mice cornea was not possible, however, because ion chamber readings were not successfully recorded. Therefore, normalisation was performed using the intensity of X-ray scatter from the Mylar window of the sample holder because the intermolecular spacing of Mylar is well defined and is lower than that of collagen, thus it produces a narrow band of X-ray scatter which occurs at a position well beyond X-ray scatter from corneal collagen.

Analysis begins with a wide angle X-ray scattering pattern (the example in figure 5.2.3A is an X-ray pattern from the edge of the cornea where the majority of collagen runs vertically) where the white circle represents the shadow of the backstop seen at the centre of the pattern, and two equally lobed maxima on either side correspond to X-ray scattering from collagen molecules. These two

lobed maxima indicated the spread of fibril axis orientations about the horizontal direction.

Although collagen molecules do not run in perfect alignment with the fibril axis, the tilt is small, therefore molecular orientation can be used as an indication of the fibril alignment. As a result, the Fit2dnew program was used to convert X-ray images usually captured in "IMG", to "TIF" format because "IMG" imaging generates files of excessive size for compatibility with the Optimas Software. Using an approach similar to that used by Daxer and Fratzl, (1997) and Newton and Meek (1998a), X-ray scatter distribution was divided into two components using Optimas and Excel programs: (i) isotropic (shaded area) scatter arising from collagen fibrils distributed evenly in all directions, and (ii) aligned (unshaded area) scatter arising from preferentially aligned fibrils (figure 5.2.3B).

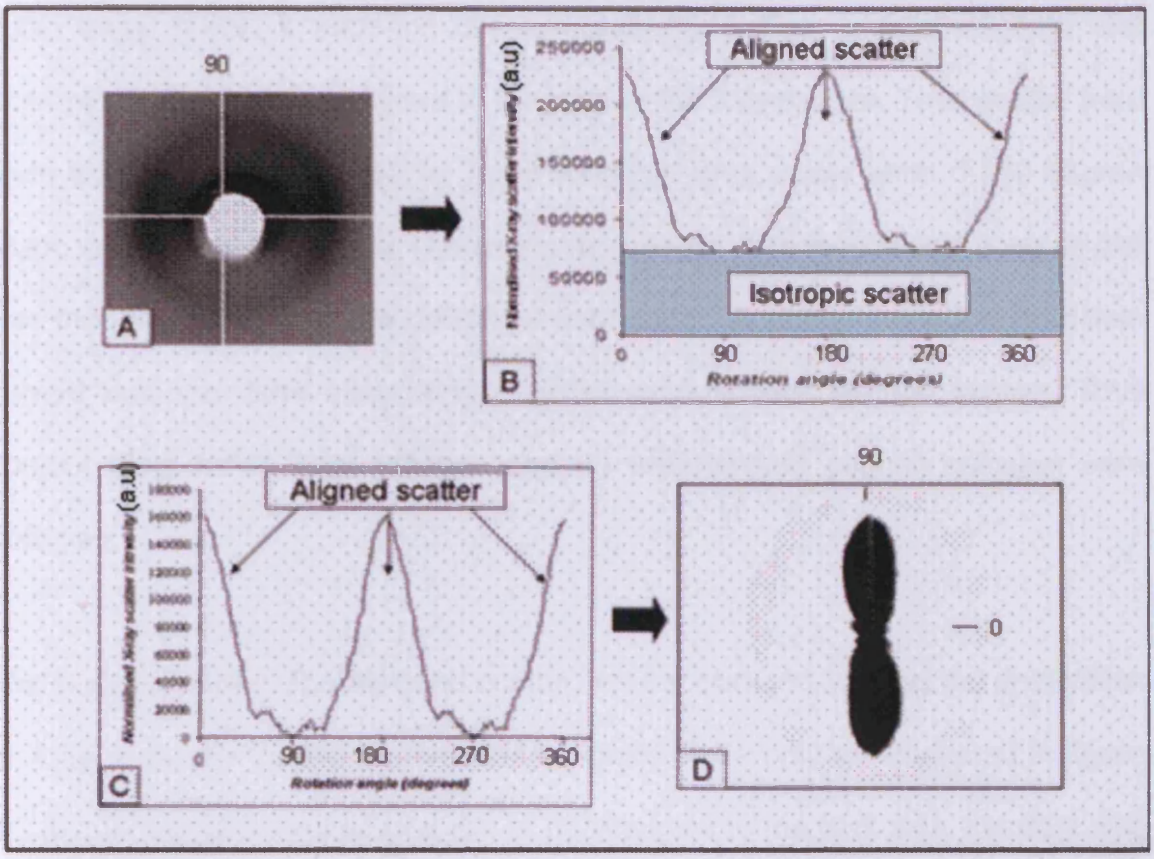

Figure 5.2.3: *Analysis steps of collagen alignment from wide angle X-ray scattering data. A typical wide angle X-ray scattering reflection from wild type SPARC cornea* (**A**). *To acquire the distribution of normalised X-ray scatter intensity around the intermolecular collagen reflection (shown in* **B**) *a series of concentric circumferential intensity distributions encompassing the width of the intermolecular reflection were taken anticlockwise starting from the 3 O'clock position. This distribution may be divided into two components; (i) isotropic scatter from collagen fibrils distributed equally in all directions, and (ii) scatter from preferentially aligned fibrils. Step* **B**-*to*-**C** *simply consists of a subtraction of isotropic scatter. The next step is the conversion of the X-ray scatter distribution* (**C**) *into polar coordinates* (**D**). *The radial extent of the polar plot* (**D**) *in any direction is proportional to the number of fibrils preferentially aligned in that direction. A 90° phase shift is imported to account for the fact that collagen fibrils scatter X-rays in a plane normal to their long axis.*

From these areas, it was possible to obtain the values of total, aligned, and isotropic scatter from each point in the path of the X-ray beam. Total scatter from each cornea was generated by integrating the area under each 0-360 degree graph of scattering intensity versus rotation angle. A colour-coded contour plot was then produced from the combined data series. A similar procedure was then carried out, this time integrating only for preferentially aligned scatter. Thus contour plots for (i) total collagen and (ii) preferentially aligned collagen were obtained.

The isotropic scatter (background scatter) was subtracted, leaving the distribution of X-ray intensity for the preferentially aligned fibrils only as illustrated in figure 5.2.3C. Because the reflections are at right angles to the fibril axis, the data was shifted by 90° to produce a new plot showing the relative mass of aligned collagen fibrils as a function of the actual angle at which they occur in the tissue. This was then converted into polar plot using Excel and Statistica software. By plotting this data as a 360° polar plot (figure 5.2.3D), the distance from the centre of the polar plot in any given direction is representative of the amount of fibrils preferentially oriented in that particular direction at that point in the tissue. The overall size of the plot is related to the total mass of the aligned collagen, whereas the asymmetry gives an indication of the preferential direction of collagen fibrils at that point. After this, the polar plot was assembled as a montage to display the preferred collagen orientation across the cornea. In

addition, maps of total, aligned, and the ratio of total to aligned collagen fibril distribution across the whole cornea were obtained using the Excel program.

5.2.4 Results.

5.2.4.1 SPARC-deficient corneas.

Maps of preferentially aligned collagen fibrils were produced for the entire cornea and limbus of a normal mouse by recording diffraction patterns at intervals of 0.2 mm (vertically and horizontally). Preferential collagen alignment at each point is indicated by a polar plot. Each plot in the map represents the distribution of preferentially aligned collagen fibrils at that point in the cornea. The sizes of the plots represent the amount of preferentially aligned collagen. This suggests that lower amounts of preferentially aligned collagen are seen over the first 0.6 mm of the central cornea, but that this increases towards the limbus through the periphery of the cornea (figure 5.2.4). Further, the shape of each plot also indicates the preferred meridian(s). Thus, at the central region of the normal mouse cornea, the map shows a preferred orientation of collagen fibrils along the vertical meridian. Thus, the preferred lamellar orientation in the central cornea of the mouse is along the superior-inferior directions.

In the X-ray diffraction plots presented here a partial circum-corneal annulus formed by a large amount of collagen fibrils running tangentially was discovered 1.2 mm from the centre of the cornea in each direction. The semi-annulus representing the limbus of the normal cornea is indicated by the red/brown plots

(marked "L" in figure 5.2.4) ranging between 0.2 -0.4 mm in width. The large sizes of the plots at the limbus suggest that the collagen fibrils are highly oriented here. Quantock et al. (2003) investigated the possibility of a limbal annulus of the cornea in the SKC mouse strain and suggested that the semi-annulus might exist in normal mouse based on vertical collagen directions at two edges of a single horizontal meridian, however, that study was very preliminary with the current data representing the first report of a limbal annulus in the mouse cornea.

The map of preferred collagen orientation in a SPARC-deficient mouse cornea is similar in appearance to the normal corneal montage showing collagen fibrils preferentially aligned along the vertical meridians and fibrils preferentially aligned tangentially at the limbus (figure 5.2.5A). The upper left quadrant, however, shows some distortion in the overall collagen arrangement.

Figure 5.2.5B shows the map of preferred fibrillar orientation in the second SPARC-deficient mouse cornea. This map reveals that the collagen fibrils tend to be preferentially aligned obliquely rather than vertically as they are in the normal mouse cornea, suggestive of rearrangement of the lamellar orientation across the centre of the cornea.

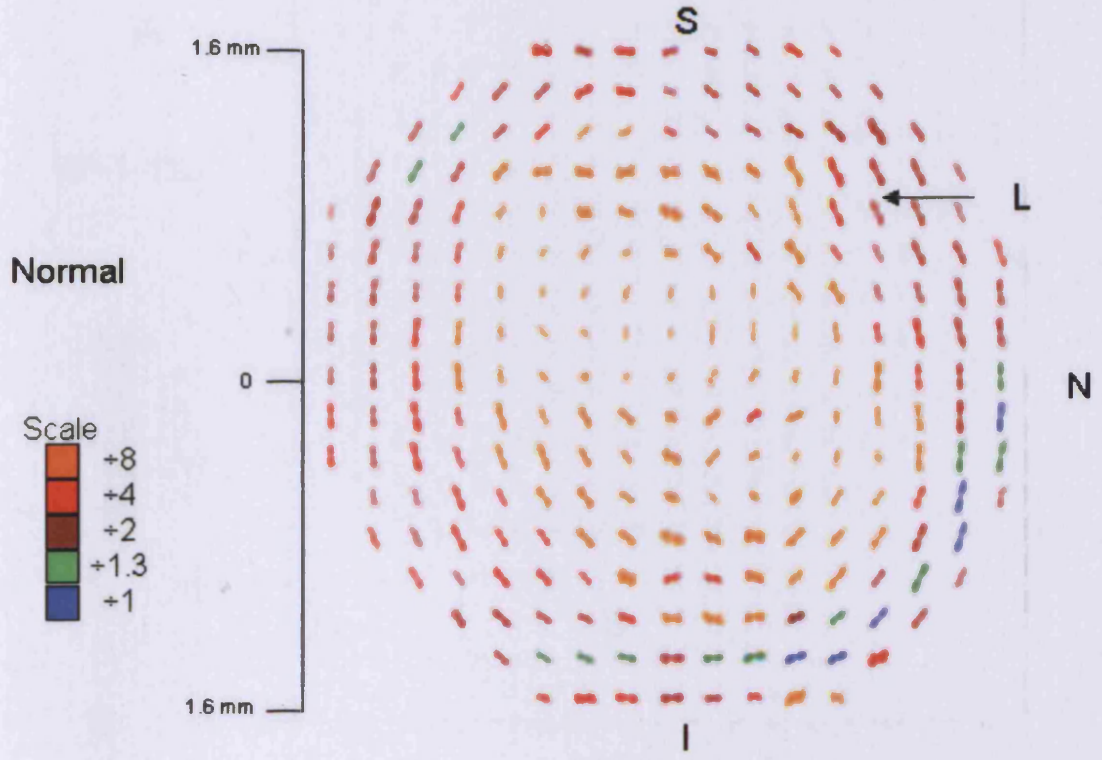

Figure 5.2.4: *Preferred collagen fibril orientation across right normal mouse cornea. Each polar plot represents the relative number of fibrils preferentially aligned in the direction at that point in the cornea. The polar plots are scaled-down to display unseen plots at the center as a result of various corneal thicknesses. The superior of cornea is indicated by* (**S**)*, nasal by* (**N**)*, inferior by* (**I**) *and the limbus by* (**L**)*. Green and blue plots are looked in the sclera. Scale is arbitrary with internal normalisation.*

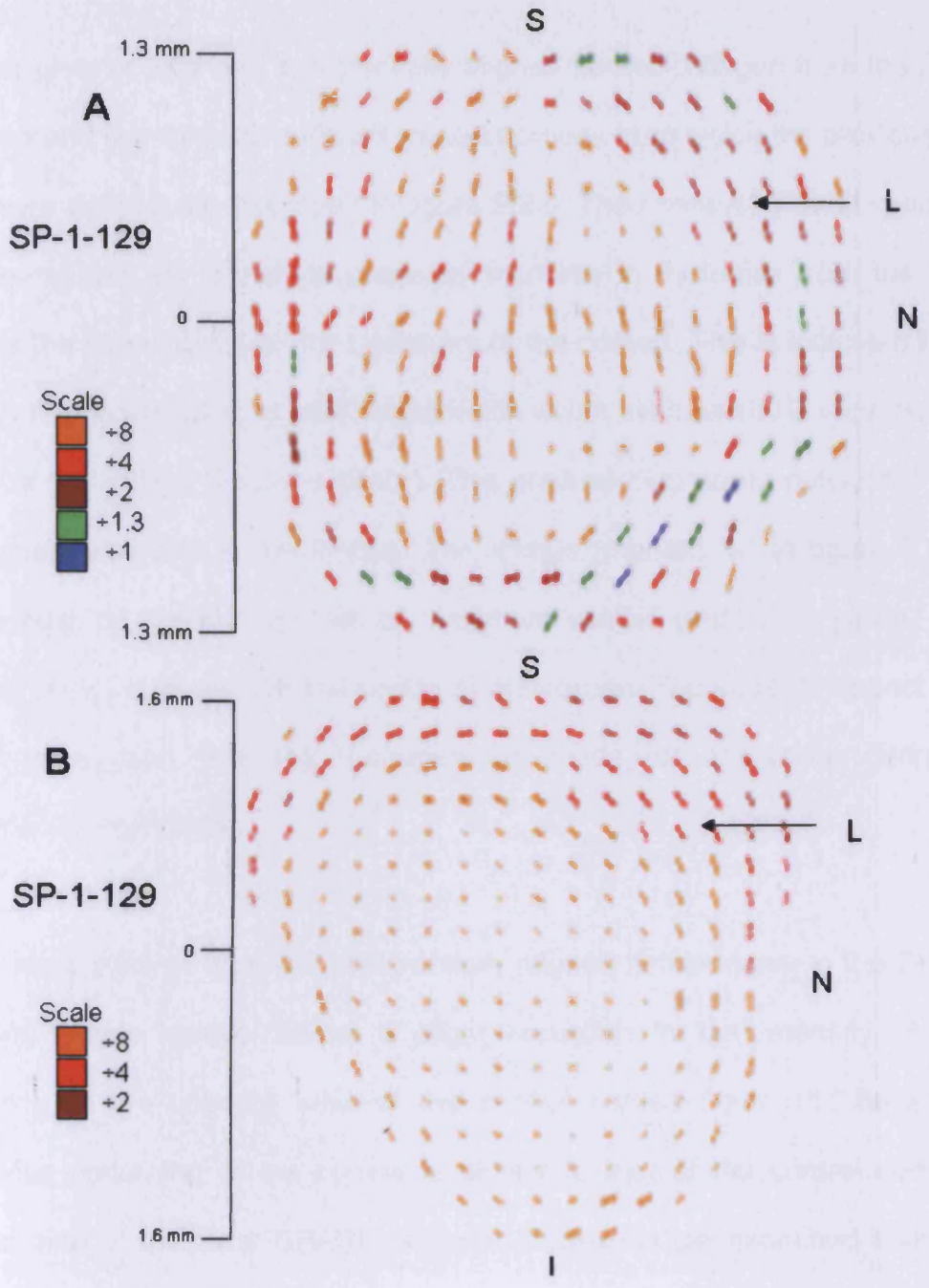

Figure 5.2.5: Preferred collagen fibril orientation across SPARC-deficient mice corneas. *(A),* and *(B).* Each polar plot represents the relative number of fibrils preferentially aligned in that direction at that point in the cornea. All corneas represent the right eye and *(L)* marks the position of the limbus. *Scale is arbitrary with internal normalisation.*

Contour plots of total and preferentially aligned fibrillar collagen from the normal wild type and two SPARC-deficient mouse corneas from which the previous polar plots were derived are displayed in figure 5.2.6. The corneas of most species so far investigated are known to gradually increase in thickness from the centre towards the limbus through the periphery of the cornea. This is indicated here in mice by the normal plots of total scattering in which the intensity is very low at the centre of the cornea (yellow contour). This gradually increases outward to reach the highest intensity at the limbus. The limbus (marked "L" in figure 5.2.6) is represented by a clear annulus of maximum scatter (red/brown plots), and a rhombic shape is formed at the centre of the cornea. The superior aspect of the cornea is marked with the V-shaped cut made for orientation during the extraction of the cornea.

The contour plots of total and preferentially aligned fibrillar mass in the SPARC-deficient mouse cornea reveal a slight reduction in the intensity of X-ray scattering at the superior area of the central cornea figure (5.2.6b and e). Otherwise patterning of the cornea is similar to that of the control cornea. A second map of the other SPARC-deficient mouse cornea examined shows the total scattering and the preferentially aligned collagen fibrils with clear thinning at the centre of the cornea. Due to a lower amount of collagen here, the intensity is scaled-down. Nevertheless, the superior limbus shows high intensity of X-ray scatter both total and aligned which is more likely to be tissue from sclera. In contrast, the total and aligned scatter of the limbus shows discontinuities and

weakness of the annulus. This might suggest that the limbus is stretched accidentally or it is vulnerable to disease.

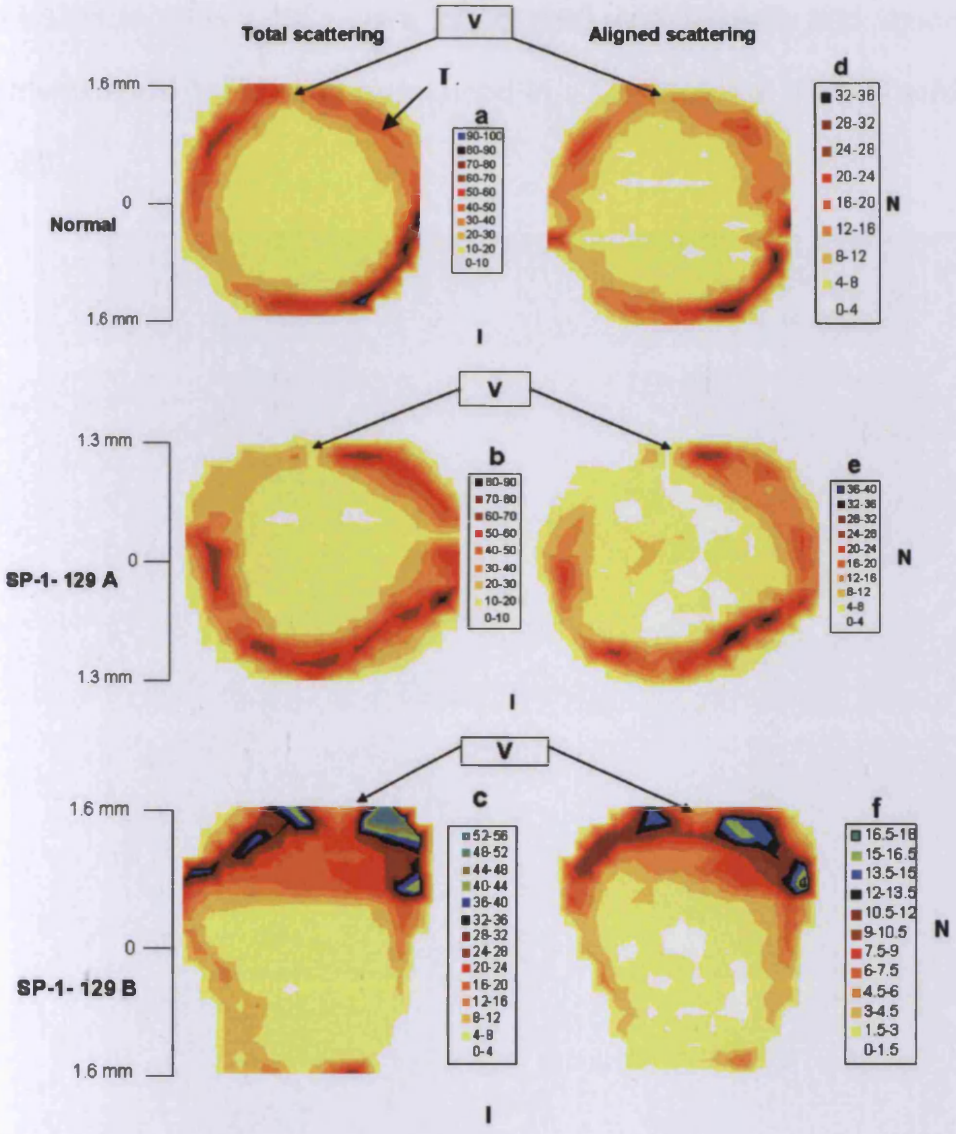

Figure 5.2.6: *Contour maps of X-ray scatter from right normal and SPARC-deficient mice corneas. (a), (b), and (c) are the total scattering and (d), (e), and (f) are aligned scattering. The superior is identified by the 'V-shaped' cut during of extraction corneas. The Inferior is identified by (I), the nasal identified by (N), and the limbus by (L). The high intensity at superior in (c) and (f) is more likely to be tissue from sclera. Scale is arbitrary with internal normalisation.*

5.2.4.2 JKC corneas.

In attempts to establish an animal model for human keratoconus, Japanese keratoconus mice (JKC) were discovered one decade ago among Mishima molosius mice (MSM) and maintained in a homozygous state (Tachibana et al., 2002b).

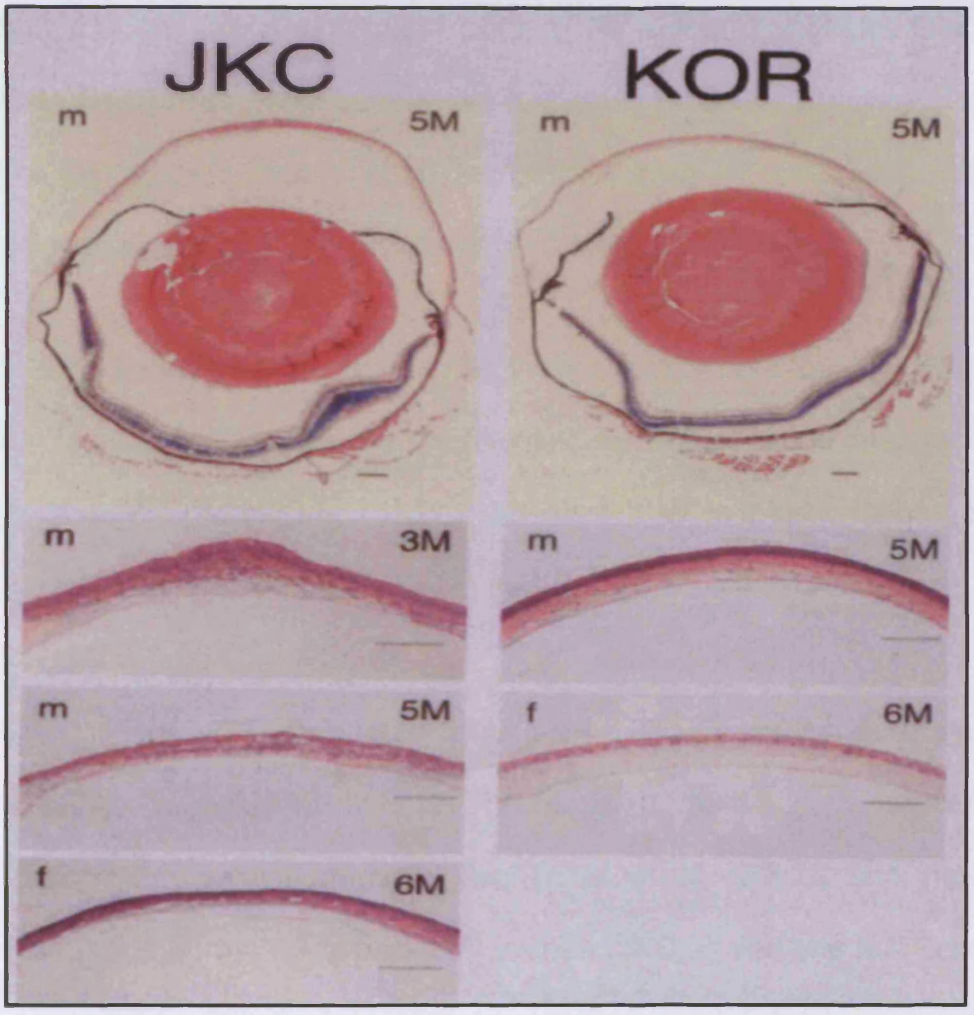

Figure 5.2.7: *Micrograph of KOR control and JKC mouse. Picture shows histological appearance of JKC and KOR at different ages for male and female.* ***Source****: Mammalian Genome J (Tachibana et al., 2002b).*

The hybrid mice were obtained by mating male JKC and female laboratory mice (BALB/c or C57BL/6L), backcrossed with parental JKC mice. The corneal phenotype of JKC strain mice resembled human keratoconus after 18 generations of inbreeding (Tachibana et al, 2002b). Although histological examination showed inflammatory changes (i.e. capillaries, infiltration and hematocytes), that are unlike human keratoconus, the authors suggested that the pathogenesis of JKC mice might be relevant to that of human keratoconus (figure 5.2.7), in that keratoscope images often documented irregular mires indicative of abnormal corneal topography (Tachibana et al., 2002b).

In this series of experiments on JKC tissue, I was not only able to map collagen orientation in mouse corneas that are predisposed to corneal shape changes (as was the case for the SPARC-null mice), but was able to obtain topographic images of the corneas first from my collaborator (Prof. Tachibana) in Japan

As evident from figure 5.2.8 the normal (KOR strain) mouse cornea investigated here has a regular topography. Also JKC corneas can either have normal or abnormal topography as reported by Tachibana et al (2002), and here I investigate JKC, one normally shaped JKC cornea (JKC 1) and one is a cornea with gross topographic alterations (JKC 2) as seen in figure 5.2.8.

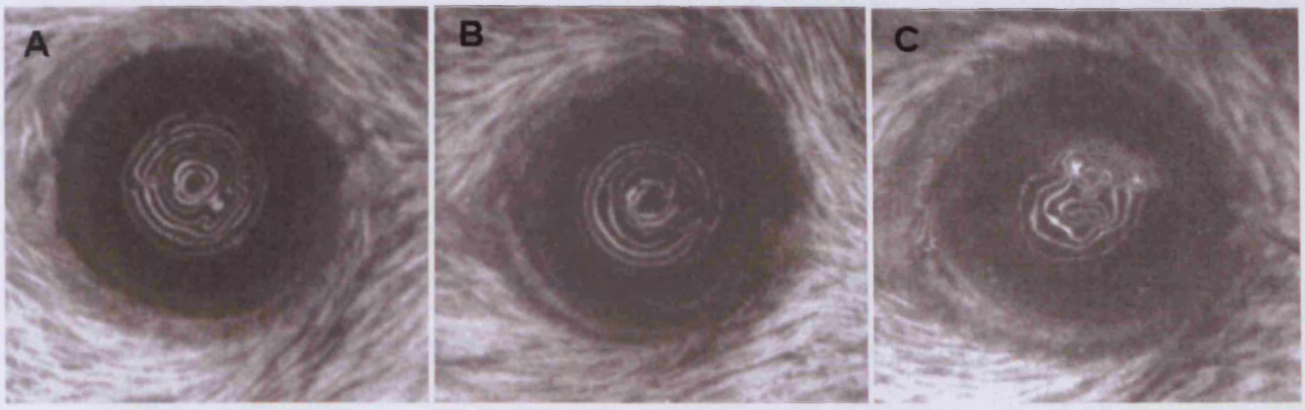

Figure 5.2.8: *Clinical keratoscopic images of the mouse cornea. Normal cornea (**A**), unaffected JKC1 cornea (**B**), and the superior-nasal affected cornea of JKC 2 (**C**). From Prof. Tachibana's laboratory.*

The map of preferentially aligned fibrillar collagen across only the left half of the normal KOR (Kariyama strain of Japanese wild mouse) cornea is presented here due to the accidental deformation of the other half during preparation. The polar plots of preferentially aligned collagen fibril differ very little from those in the normal mouse cornea in the SPARC investigation (figure 5.2.4), except for the fact that the sizes of the polar plots in the central region seem to be larger. The radial extent of each plot in any direction represents the number of preferentially aligned fibrils oriented in that direction. In the central region of the normal KOR cornea, the map reveals a preferred fibril orientation along the vertical meridians, along with an abundance of fibrils that run tangentially to the cornea comprising a non uniform circum-corneal annulus at the limbus.

On the other hand, the map of preferentially aligned fibrils in the JKC 1 cornea (figure 5.2.10) shows that it was relatively unaffected as regards collagen fibril orientation. Also, as can be seen in figure 5.2.8B corneal topography is approximately normal. However, ultrastructurally we do see somewhat smaller polar plots at the centre of the cornea that suggest less aligned collagen (these extend to the superior-temporal margin of the cornea (intermittent light line)). Moreover, the orientation of collagen fibrils, particularly at the inferior-nasal region of the central cornea (intermittent dark line) is manifestly different. The peripheral cornea and limbus did not reveal any difference from a normal cornea.

The map of the affected cornea of the JKC **2** mouse shown in figure 5.2.10 shows preferentially aligned fibrils with no detectable changes in collagen orientation, however, smaller polar plots point to thinning at the cornea's centre. In general, outside the defective area, the periphery of the cornea is similar to that of the normal cornea. These data reasonably corresponded with the clinical images of irregular mires at the superior-nasal cornea in (figure 5.2.8C). The image mires were distorted in the central region but more severely at the superior-nasal from the cornea's centre.

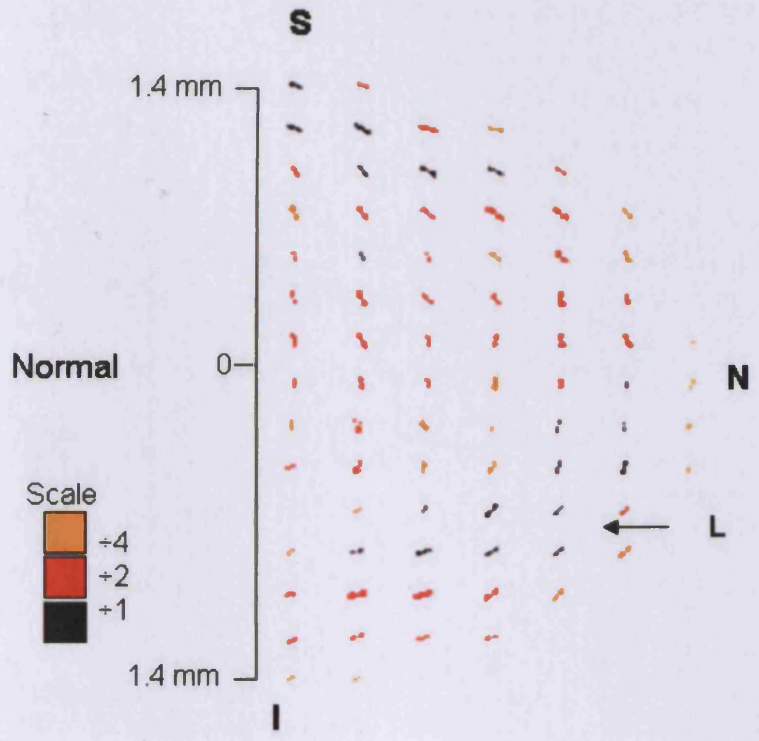

Figure 5.2.9: *Preferred collagen fibril orientation across a normal KOR mouse cornea of the right eye. Each polar plot represents the relative number of fibrils preferentially aligned in that direction at that point in the cornea. The limbus is marked by (L), Superior (S), nasal (N), and inferior (I). Scale is arbitrary with internal normalisation.*

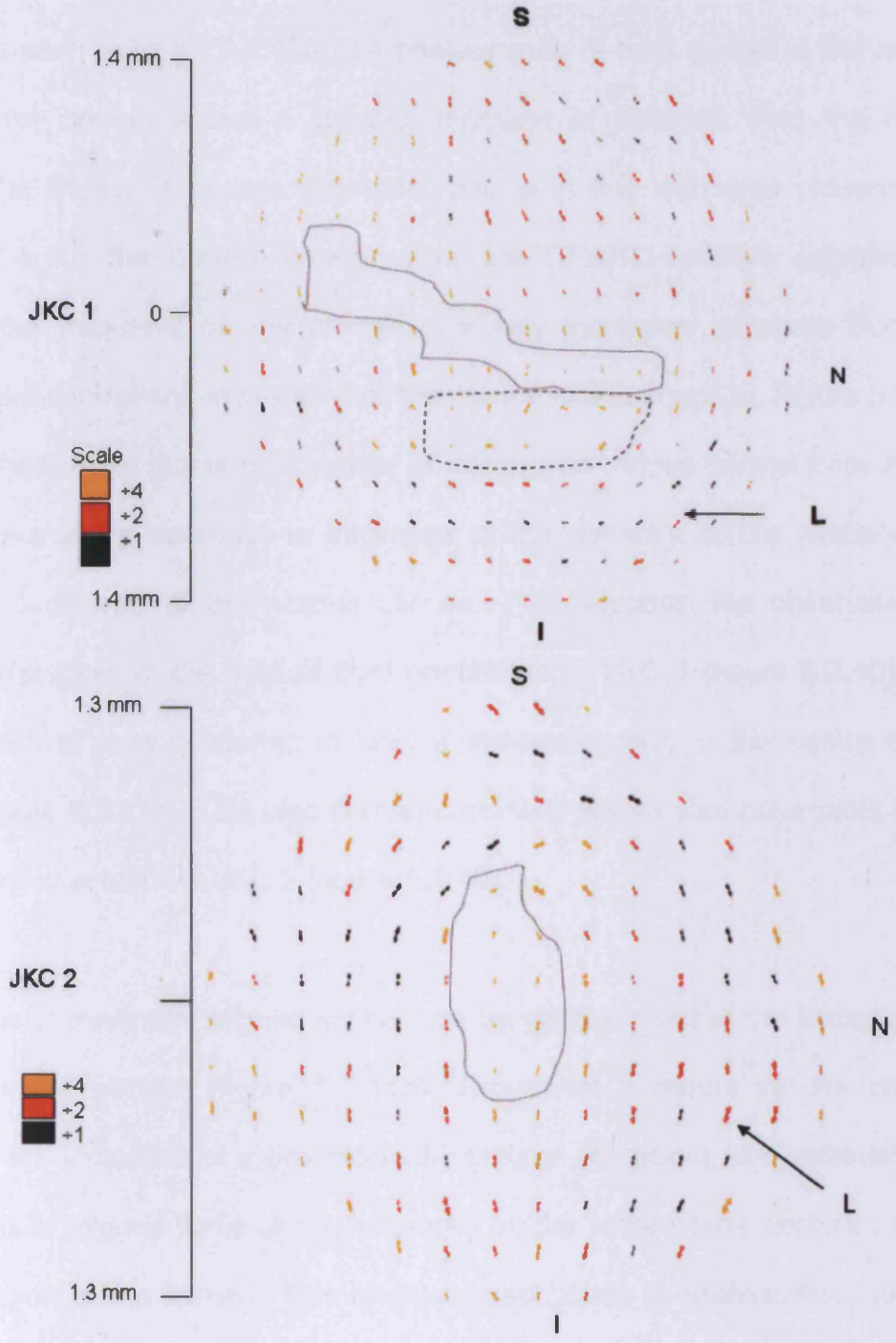

Figure 5.2.10: *Preferred collagen fibril orientation across right eye of JKC 1 and JKC 2 corneas. Each polar plot represents the relative number of fibrils preferentially aligned in that direction at that point in the cornea. The limbus is marked by (L), Superior (S), nasal (N), and inferior (I). Scale is arbitrary with internal normalisation.*

As can be seen in figure 5.2.11a, the contour map of total scatter in the normal KOR mouse cornea shows a gradual increase in collagen from the centre towards the limbus. This was expected, and is in line with data presented in figure 5.2.4 for the normal cornea from the SPARC-deficient experiments, because the thickness of any cornea gradually increases outwards from the centre of the cornea and indicates that the mouse is no exception. Figure 5.2.11b displays the contour plot of total scatter of misshapen mouse cornea from JKC 1. There was a sharp decrease in thickness at the cornea's centre (white/yellow contours) compared to the normal cornea. This supports the observation of smaller polar plots in the map of fibril orientation of JKC 1 (figure 5.2.10). The contour map of total scattering in JKC 2 shows thinning at the centre of the cornea (figure 5.2.11c). This also corresponds with the smaller polar plots in the map of fibril orientation in JKC 2 (figure 5.2.10).

An annulus of maximum aligned scatter can be clearly noted at the limbus in the normal mouse cornea (figure 5.2.11d). Brown/red contours at the corneal periphery are indicative of a proportionally greater alignment, and relatively low proportions of aligned fibrils are represented by the white/yellow contours at the central region of the cornea. This analysis also points to preferentially aligned fibrils at the central defect area of misshapen corneas of JKC 1 and 2. The thinnest region in the defect area is circumscribed by thick discontinuities, a non-uniform annulus of the limbus, and appears more rhombic in shape.

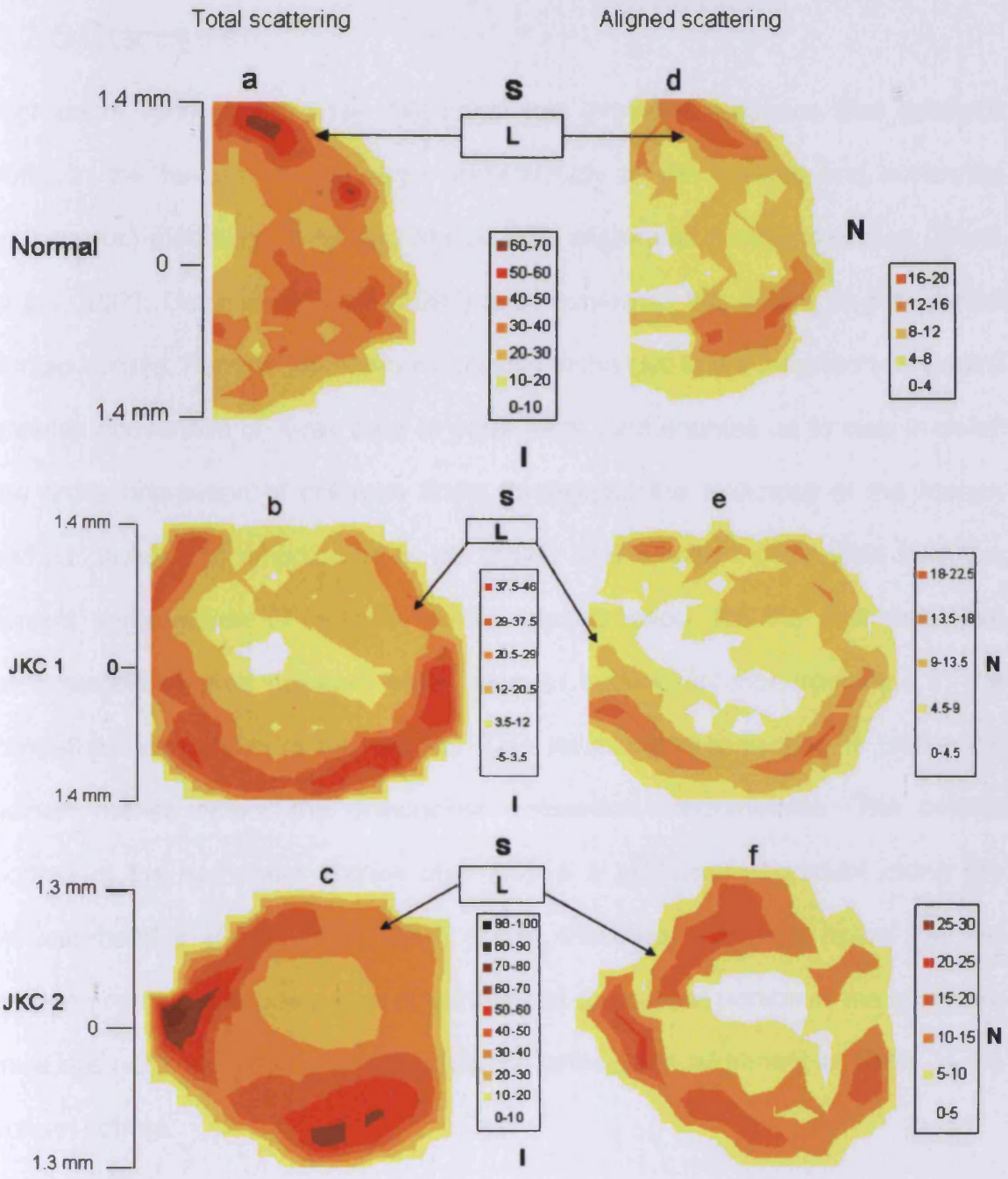

Figure 5.2.11: *Contour maps of X-ray scattering from normal KOR and JKC mice corneas. Total scattering intensity is shown in a, b, and c. Aligned scattering intensity is shown in d, e, and f. Scale is arbitrary with internal normalisation.*

5.2.5 Discussion.

High-angle synchrotron X-ray diffraction has provided evidence that collagen fibrils in the human cornea align preferentially in the vertical and horizontal (orthogonal) meridians, over and above their alignment in other meridian (Meek et al., 1987). Daxer and Fratzl (1997) later confirmed this finding in the normal human cornea. Recent developments of this technique in our laboratory in Cardiff enables conversion of X-ray data to polar plots, and enables us to map in detail the gross orientation of collagen fibrils throughout the thickness of the human cornea (Aghamohammadzadeh et al., 2004). The resultant polar plots from the current investigation of normal mouse cornea show for the first time that preferentially aligned collagen fibrils exist in superior-inferior meridians in the central corneal region in the mouse. This structural organisation is unlike the human cornea where the orthogonal orientation predominates. The central portion of the marmoset cornea also shows a preferred alignment along the vertical meridian (Boote et al., 2004). Thus, this study's findings reveal that the collagen content and orientation of lamellae at the central portion of the cornea in mice are not consistent with the preferred orthogonal alignment of fibrils in the human cornea.

Meek et al. (1987) showed that the orthogonally preferred fibril organisation of the human cornea is more pronounced in the posterior stroma. From data here I cannot tell whether the preferred fibril arrangement in mouse cornea is from the anterior or posterior part of the stroma, but have shown that, although some

collagen fibrils undoubtedly cross at right angle as indicated by Haustein (1983) the majority runs vertically.

Towards the corneal periphery, the data presented here show a commonality with human data (Newton and Meek, 1998a; Meek and Newton, 1999). A non-uniform annulus of collagen fibrils around the corneal circumference corresponds to the limbus and forms a rhombic shape similar to that in the marmoset (Boote et al., 2004). It is suggested that the aim of an annulus of highly ordered fibrils is to provide reinforcement to withstand the increased tension at the limbus (Maurice, 1969).

The proposed propensity of SPARC-deficient corneas to become abnormally shaped suggests a role for SPARC in altered corneal structure, and in chapter 5.1 I indicated that perhaps a low fibril number density contributes to this. The question remains as to what is the collagen fibril orientation in SPARC-null mice, and might this have affected on corneal shape.

Daxer and Fratzl (1997) reported that collagen fibrils at the central cone in keratoconus were rearranged obliquely (60 and 120 degrees) instead in the vertical and horizontal directions as seen in normal corneas. Similarly, some polar plots at the centre of SPARC-deficient cornea **B** are arranged obliquely (figure 5.2.5B). The contour map of preferentially aligned collagen fibrils in figure 5.2.6f shows less intensity at the cornea's centre due to thinning, and this

coincides with the altered plots in figure 5.2.5B. It is possible therefore, that collagen misalignment in the SPARC-null cornea **B**, accompanied by a lower collagen fibril number density, might lead to a misshapen cornea. Lack of any detailed topographic data on the specific SPARC-deficient corneas makes the link between collagen misalignment and topographic changes speculative, however, the development of new techniques to investigate the topography of the mouse cornea that are currently under development in our laboratory hold promise for future studies of the relationship between stromal organisation and topographic changes in SPARC-null mice.

Regarding possible mechanisms of corneal topography change, however, the present study would point out that transforming growth factor-ß1 synthesised by keratocytes regulates collagen synthesis and deposition (Abe et al., 2004), and that the absence of SPARC cells leads to a diminishment of collagen type I and TGF- ß1 (Francki, 1999). It could be the case, therefore, that the SPARC protein has an influence on TGF- ß1 to induce the production of collagen type I (Poncelet, 1998), thus leading to corneal slippage and ectasia.

In JKC mice, I was better able to compare corneal shape with stromal ultrastructure because topographic data was available. Although, keratoscopic images showed mires distortion only in JKC 2 (figure 5.2.8c), contour maps of both JKC mice 1 and 2 corneas (figure 5.2.10) showed thinning with collagen fibril redistribution. This was consistent with the lower intensity at the same sites

of preferentially aligned fibrils seen in figures 5.2.11e and f. Recently, Meek et al (2005) mapped the human keratoconus cornea and showed similar thinning and redistribution of collagen fibril at the area of defect. It is possible that corneal ectasia in JKC mice occurs as a result of a genetic mutation or existence of genes that suppress the corneal topographic change because backcrossing of JKC with BAL/c mice did not revealed any sign of keratoconus-like changes, whereas backcrossing JKC with C57BLB/6L mice did revealed keratoconus-like changes (Tachibana et al., 2002b).

Although the misshapen JKC cornea experiences inflammation (keratitis), several events similar to those noted in human keratoconus are observed. It was also suggested that mutation of cathepsin J or R on mouse chromosome 13 may cause keratitis and a misshapen corneas in JKC mice (Tachibana et al., 2002b). Similarly, Heaven et al (2000) reported that an abnormality of chromosome 13 has been associated with human keratoconus. Cathepsin B and G within keratocytes of human keratoconus were found at high levels compared to the normal cornea (Sherwin et al., 2002).

Linkage between keratoconus and chromosome 21 has also been reported (Zadnik et al., 1984). There are clinical distinctions between misshapen JKC corneas and human keratoconus corneas. These include the thickness of the cornea at its centre in the very early stage of the disease, vascular infiltration, and inflammation. In human keratoconus, patients may be exposed to

inflammation at the time the disease attacks because vascular infiltration in the keratoconus patient with a mutation of the VSX1 gene has been reported (Heon, 2002).

In conclusion, this is the first study that maps the collagen fibril orientation of the mouse cornea. Structurally, it has been shown that a preferred orthogonal arrangement of aligned collagen fibrils that is seen in the human cornea is not a feature of the mice corneas; rather, the corneal collagen fibrils of mice are arranged mainly in vertical meridians. The work has also, for the first time, demonstrated the presence of a limbal annulus of circumferential collagen fibrils at the edge of the cornea in the mouse. Further, the study has shed light on collagen fibril orientation in misshapen mice corneas and while no current mouse model for keratoconus exists, the data suggest that structural abnormalities in the stromal fibrillar matrix might accompany topographic changes.

Concluding Remarks.

The overarching aim of this thesis was to investigate the progressive disease of keratoconus, and seek representative animal models with keratoconus-like changes for further study of possible disease processes and structure-function relationships. It was decided to incorporate a wide range of techniques, from clinical epidemiological studies through clinical management issues, to structural biophysics studies of the human keratoconus condition to give an overall appreciation of the disease on a number of levels. Subsequently, biophysical investigations of mouse strains that had demonstrated a propensity for corneal shape changes were investigated.

Epidemiological data gathered here (Chapter 3.1) shows that the influence of ethnic origin on the incidence rate and severity of keratoconus is significantly higher than in Caucasian populations. Furthermore, the study revealed that the deterioration of keratoconus to the severe stage at an earlier age in Asir Province, Saudi Arabia was obviously faster than in Caucasians. Whether this is due to genetic or environmental factors is not absolutely clear, but I contend that a combination of the two is likely. This information will have clear implications for health planning in Saudi Arabia, to improve the earlier detection and management of this condition.

From a clinical management standpoint, the selection of lens design and back optic zone radius to reshape the cornea and correct the refractive error in keratoconic patients are big challenges for practitioners and patients alike. This is particularly true because anticipating the development of the disease is difficult. This thesis (Chapter 3.2) has shown the importance of using different types of rigid contact lens designs in the clinic. Moreover, it is suggested that the selection of the Tricurve lens design with 9 mm diameter is the best option to use at first, irrespective the disease stage. The Regular and Steep McGuire lens designs represent the second options with the multicurve McGuire Steep lens design best for the advanced stage of the disease rather than Regular McGuire or Tricurve lens designs, at least in patients in the Saudi Arabia population.

With a high sensitivity to detect shape anomalies in the cornea, topographical systems can provide useful information about the corneal surface irregularities. These techniques however, failed to detect fully the extent of the progress of keratoconus over the cornea to include peripheral regions. Using scanning electron microscopy to investigate the anterior corneal surface after chemical removal of corneal epithelial cells and epithelial basement membrane has allowed me to study the extent of the disruption of Bowman's layer (Chapter 4). This proved that ruptures were found at the apical cone, but that the severity of the rupture does not correlate with disease severity clinically. Also surface breaks were found beyond the central apex in more peripheral areas within the optical zone (8 mm). This was especially true in advanced stages of the disease.

Utilising environmental scanning electron microscopy did not yield many informative results on the human cornea due to limited resolution. I feel however, as though this approach warrants further study to optimize the machine's settings to improve resolution in studies of human cornea so that a more hydrated tissue can be studied.

There is currently no animal model for keratoconus. However, to study possible links between corneal instability and stromal matrix architecture, the corneas of SPARC-null and JKC mice strains were investigated by light and transmission electron microscopes and high angle X-ray diffraction (Chapter 5). A sharp decrease in collagen fibril number density that was less prominent between the anterior and mid-stroma, but particularly evident in the posterior stroma in SPARC-null might, causes wide spacing of the collagen fibril and subsequently might lead to weakening of cornea and altered shape. However, this is unlike keratoconus in human cornea where collagen spacing is normal (Fullwood et al., 1992).

Applying wide-angle X-ray diffraction (Chapter 5.2) to the corneas of SPARC deficient and JKC mice strains to clarify the organisation of collagen fibril in the corneal stromas provided some useful information. Here, I demonstrated for the first time that an orthogonal preferred alignment of collagen fibrils that is seen in the human cornea is not a feature of the normal mouse cornea. Rather collagen fibrils of mice are arranged mainly in vertical directions in the cornea. There is,

however, an annulus of collagen fibrils at the limbus in mice as there is with humans. Knowledge such as this is crucial if the mouse cornea is to be used for research and related to the human situation. This approach also illustrated that the arrangement and distribution of collagen mass was altered at the centre of corneas in the majority of both SPARC deficient and JKC mice corneas. The results from the SPARC deficient mice support a hypothesis proposed by Polack (1976) and Meek et al. (2005) that corneal thinning and ectasia of cornea could occur as a result of collagen lamellae slippage.

Appendix 1

1.1 Specifications of different lenses designs

1.1.1 McGuire lenses specifications.

1. The overall size was 8.6 mm.
2. The optic zone diameter was 6 mm.
3. For McGuire Steep, from most central to most peripheral, the curves were flatter than the BOZR by 0.5 mm (3 D), 1.2 mm (7 D), 2 mm (12 D) and 3.2 mm (19 D), respectively.
4. For McGuire Regular, from most central to most peripheral, the curves were flatter than the BOZR by 0.5 mm (3 D), 1.5 mm (9 D), 3 mm (17 D) and 5 mm (27 D), respectively, i.e. the McGuire Regular BOZR differences are larger than McGuire steep base curve radii differences.
5. The three inner curves had a width of 0.3 mm and the peripheral curve was 0.4 mm wide.
6. The base curve range was 6.75 mm (50 D) – 4.52 mm (71 D).
7. The axial edge left (AEL) was constant (0.105 mm).
8. The power was variable, as the lens steepened the power increase.

Table 1 McGuire Steep Multicurve rigid contact lens.

BOZR mm (D)	Total diameter / BOZD (mm)	Power (D)	1st peripheral Curve radius/ Width D (mm)	2nd Peripheral Curve radius/ Width D (mm)	3rd peripheral Curve radius/ Width D (mm)	4th Peripheral Curve radius/ Width D (mm)
6.75 (50.0)	8.6 / 6.0	- 9.00	47.0 / 0.30	43.0 / 0.30	38.0 / 0.30	31.0 / 0.4
6.62 (51.0)	8.6 / 6.0	- 10.0	48.0 / 0.30	44.0 / 0.30	39.0 / 0.30	32.0 / 0.4
6.49 (52.0)	8.6 / 6.0	- 10.0	49.0 / 0.30	45.0 / 0.30	40.0 / 0.30	33.0 / 0.4
6.37 (53.0)	8.6 / 6.0	- 11.0	50.0 / 0.30	46.0 / 0.30	41.0 / 0.30	34.0 / 0.4
6.25 (54.0)	8.6 / 6.0	- 11.0	51.0 / 0.30	47.0 / 0.30	42.0 / 0.30	35.0 / 0.4
6.14 (55.0)	8.6 / 6.0	- 12.0	52.0 / 0.30	48.0 / 0.30	43.0 / 0.30	36.0 / 0.4
6.03 (56.0)	8.6 / 6.0	- 13.0	53.0 / 0.30	49.0 / 0.30	44.0 / 0.30	37.0 / 0.4
5.92 (57.0)	8.6 / 6.0	- 14.0	54.0 / 0.30	50.0 / 0.30	45.0 / 0.30	38.0 / 0.4
5.82 (58.0)	8.6 / 6.0	- 15.0	55.0 / 0.30	51.0 / 0.30	46.0 / 0.30	39.0 / 0.4
5.73 (59.0)	8.6 / 6.0	- 15.0	56.0 / 0.30	52.0 / 0.30	47.0 / 0.30	40.0 / 0.4
5.63 (60.0)	8.6 / 6.0	- 15.0	57.0 / 0.30	53.0 / 0.30	48.0 / 0.30	41.0 / 0.4
5.54 (61.0)	8.6 / 6.0	- 16.0	58.0 / 0.30	54.0 / 0.30	49.0 / 0.30	42.0 / 0.4
5.44 (62.0)	8.6 / 6.0	- 17.0	59.0 / 0.30	55.0 / 0.30	50.0 / 0.30	43.0 / 0.4
5.35 (63.0)	8.6 / 6.0	- 18.0	60.0 / 0.30	56.0 / 0.30	51.0 / 0.30	44.0 / 0.4
5.26 (64.0)	8.6 / 6.0	- 18.0	61.0 / 0.30	57.0 / 0.30	52.0 / 0.30	45.0 / 0.4
5.17 (65.0)	8.6 / 6.0	- 19.0	62.0 / 0.30	58.0 / 0.30	53.0 / 0.30	46.0 / 0.4
5.07 (66.0)	8.6 / 6.0	- 20.0	63.0 / 0.30	59.0 / 0.30	54.0 / 0.30	47.0 / 0.4
4.98 (67.0)	8.6 / 6.0	- 21.0	64.0 / 0.30	60.0 / 0.30	55.0 / 0.30	48.0 / 0.4
4.70 (69.0)	8.6 / 6.0	- 21.0	66.0 / 0.30	62.0 / 0.30	57.0 / 0.30	50.0 / 0.4
4.52 (71.0)	8.6 / 6.0	- 22.0	68.0 / 0.30	64.0 / 0.30	59.0 / 0.30	52.0 / 0.4

Table 2 McGuire Regular Multicurve rigid contact lens.

BOZR mm (D)	Total diameter / BOZD (mm)	Power (D)	1st Peripheral Curve radius/ Width (mm)	2nd Peripheral Curve radius/ Width (mm)	3rd Peripheral Curve radius/ Width (mm)	4th Peripheral Curve radius/ Width (mm)
6.75 (50.0)	8.6 / 6.0	- 9.00	47.0 / 0.30	41.0 / 0.30	33.0 / 0.30	23.0 / 0.4
6.62 (51.0)	8.6 / 6.0	- 10.0	48.0 / 0.30	42.0 / 0.30	34.0 / 0.30	24.0 / 0.4
6.49 (52.0)	8.6 / 6.0	- 10.0	49.0 / 0.30	43.0 / 0.30	35.0 / 0.30	25.0 / 0.4
6.37 (53.0)	8.6 / 6.0	- 11.0	50.0 / 0.30	44.0 / 0.30	36.0 / 0.30	26.0 / 0.4
6.25 (54.0)	8.6 / 6.0	- 11.0	51.0 / 0.30	45.0 / 0.30	37.0 / 0.30	27.0 / 0.4
6.14 (55.0)	8.6 / 6.0	- 12.0	52.0 / 0.30	46.0 / 0.30	38.0 / 0.30	28.0 / 0.4
6.03 (56.0)	8.6 / 6.0	- 13.0	53.0 / 0.30	47.0 / 0.30	39.0 / 0.30	29.0 / 0.4
5.92 (57.0)	8.6 / 6.0	- 14.0	54.0 / 0.30	48.0 / 0.30	40.0 / 0.30	30.0 / 0.4
5.82 (58.0)	8.6 / 6.0	- 15.0	55.0 / 0.30	49.0 / 0.30	41.0 / 0.30	31.0 / 0.4
5.72 (59.0)	8.6 / 6.0	- 15.0	56.0 / 0.30	50.0 / 0.30	42.0 / 0.30	32.0 / 0.4
5.63 (60.0)	8.6 / 6.0	- 15.0	57.0 / 0.30	51.0 / 0.30	43.0 / 0.30	33.0 / 0.4
5.54 (61.0)	8.6 / 6.0	- 16.0	58.0 / 0.30	52.0 / 0.30	44.0 / 0.30	44.0 / 0.4
5.44 (62.0)	8.6 / 6.0	- 17.0	59.0 / 0.30	53.0 / 0.30	45.0 / 0.30	35.0 / 0.4
5.35 (63.0)	8.6 / 6.0	- 18.0	60.0 / 0.30	54.0 / 0.30	46.0 / 0.30	36.0 / 0.4
5.26 (64.0)	8.6 / 6.0	- 18.0	61.0 / 0.30	55.0 / 0.30	47.0 / 0.30	37.0 / 0.4
5.17 (65.0)	8.6 / 6.0	- 19.0	62.0 / 0.30	56.0 / 0.30	48.0 / 0.30	38.0 / 0.4
5.07 (66.0)	8.6 / 6.0	- 20.0	63.0 / 0.30	57.0 / 0.30	49.0 / 0.30	39.0 / 0.4
4.98 (67.0)	8.6 / 6.0	- 21.0	64.0 / 0.30	58.0 / 0.30	50.0 / 0.30	40.0 / 0.4
4.70 (69.0)	8.6 / 6.0	- 21.0	66.0 / 0.30	60.0 / 0.30	52.0 / 0.30	42.0 / 0.4
4.52 (71.0)	8.6 / 6.0	- 22.0	68.0 / 0.30	62.0 / 0.30	54.0 / 0.30	44.0 / 0.4

1.1.2 Tricurve lens specifications.

1. The overall size of lens was 9 mm.
2. The optic zone diameter was 7.5 mm.
3. The second base curve radius was 2 mm (12 D) flatter than the central base curve radius with a width of 0.2 mm.

4. The third base curve radius was constant 10.5 mm (57 D) with a width of 0.2 mm. However, the changes were in the central and second base curve radii, which were stepped-down by 0.2 mm increments.
5. The base curve radius range was 7.2 mm (46.87 D) – 5.4 mm (60.78 D).
6. The axial edge left was 0.1 mm.
7. The power was constant - 5 D

Table 3 Tricurve rigid contact lens.

BOZR mm (D)	Total diameter / BOZD (mm)	Power (D)	Second Peripheral Curve radius / Width (mm)	Third Peripheral Curve radius / Width (mm)
7.20 (46.87)	9.00 / 6.50	- 5.00	9.20 / 0.20	10.50 / 0.20
7.00 (48.25)	9.00 / 6.50	- 5.00	9.00 / 0.20	10.50 / 0.20
6.80 (49.62)	9.00 / 6.50	- 5.00	8.80 / 0.20	10.50 / 0.20
6.60 (51.12)	9.00 / 6.50	- 5.00	8.60 / 0.20	10.50 / 0.20
6.40 (52.75)	9.00 / 6.50	- 5.00	8.40 / 0.20	10.50 / 0.20
6.20 (54.43)	9.00 / 6.50	- 5.00	8.20 / 0.20	10.50 / 0.20
6.00 (50.62)	9.00 / 6.50	- 5.00	8.00 / 0.20	10.50 / 0.20
5.80 (58.19)	9.00 / 6.50	- 5.00	7.80 / 0.20	10.50 / 0.20
5.60 (60.39)	9.00 / 6.50	- 5.00	7.60 / 0.20	10.50 / 0.20
5.40 (60.78)	9.00 / 6.50	- 5.00	7.40 / 0.20	10.50 / 0.20

1.1.3 Percon lens specifications.

1. The overall size was 9.4 mm.
2. The optic zone diameter was 7.5 mm with a central thickness of 0.03 mm.
3. The power was constant - 5 D.

4. The base curve range was 7.05 mm (47.87 D) – 8.17 mm (41.25 D), with a 0.07 mm (0.5 D) interval.
5. The axial edge lift was 0.12 mm.

Table 4 Percon rigid contact lens.

BOZR mm (D)	Total diameter / BOZD (mm)	Power (D)
7.05 (47.87)	9.40 / 7.20	- 5.00
7.12 (47.37)	9.40 / 7.20	- 5.00
7.20 (46.87)	9.40 / 7.20	- 5.00
7.27 (46.37)	9.40 / 7.20	- 5.00
7.35 (45.87)	9.40 / 7.20	- 5.00
7.42 (45.50)	9.40 / 7.20	- 5.00
7.50 (45.00)	9.40 / 7.20	- 5.00
7.57 (44.50)	9.40 / 7.20	- 5.00
7.65 (44.12)	9.40 / 7.20	- 5.00
7.72 (43.75)	9.40 / 7.20	- 5.00
7.80 (43.25)	9.40 / 7.20	- 5.00
7.87 (42.87)	9.40 / 7.20	- 5.00
7.95 (42.50)	9.40 / 7.20	- 5.00
8.02 (42.12)	9.40 / 7.20	- 5.00
8.10 (41.62)	9.40 / 7.20	- 5.00
8.17 (41.25)	9.40 / 7.20	- 5.00

Appendix 2

Form of ocular studies in keratoconus

Patient's Name:		Ref. No.	Date:	
Age: years	Sex:	M □ / F □	Occupation:	

Case History

History of the disease:				
Age of incidence:		Age of screening:		
Ocular history:	Rubbing □	Trauma □	Redness □	Allergy □
Ocular disease:				
Systemic disease:				
Ophthalmic correction history:				
VA:	OD:	With □	Without □	
	OS:	With □	Without □	
Keratometry:	OD:	@	@	Mires quality:
	OS:	@	@	Mires quality:

Slit Lamp Examination

Lids Lashes:		Conjunctiva:		
Cornea:	Oedema □	Striae □	Fleisher's ring □	
	Scarring □	Munson's sign □	Other signs	
Eye Signs:	Unilateral □		Bilateral □	
Tear film quality:		OD:	OS:	
Anterior chamber angle assessment:		OD:	OS:	
Stage of Keratoconus		OD:	OS:	

Ophthalmoscopy finding (Media and Fundi)

Refraction:	**Retinoscopy reflex:**	**VA:**	**Tonometry:**
OD:	OD:	OD:	OD:
OS:	OS:	OS:	OS:

Contact Lens Fitting

Fitting type:	Divided support □	Steep □	Flat □
Lens type:	OD:	OS:	
BOZD.	OD:	OS:	
Power:	OD:	OS:	
Over-refraction:	OD:	OS:	
VA:	OD:	OS:	
Contact lens fitting assessment:			
Movement:	OD:	OS:	
Coverage:	OD:	OS:	
Fluorescein pattern:	OD:	OS:	

Appendix 3

الـــرقـــم :
التـــاريخ :
المشـفـوعـات :
07 Dhulhajj 1426H
(January 7, 2006) الموضوع :

وزارة الصحة
Ministry of Health

المملكة العربية السعودية
وزارة الصـحة
المديرية العامة للشئون الصحية بمنطقة عسير
مستشفى عسير المركزى

CERTIFICATION

This is to certify that study has been carried out by **MR.ABDULLAH ASSIRI** on keratoconus patients between May 2001 and April 2002 with the agreement of the ethical regulations of the Aseer Central Hospital.

DR. ABDULLAH THABIT
Director & Consultant of Ophthalmology Dept.
Aseer Central Hospital
P. O. Box 34, Abha
Kingdom of Saudi Arabia

DR. ALI MANA
Medical Director

Publications and Presentations.

1. A. A. M. Assiri A, M. A. Wride A, F. C. Mansergh B, V. E. Walker B, R. D. Young A, M.J. Evans B, and A. J. Quantock. Corneal stromal ultrastructure in mice with Sparc-null mutation. ARVO 2003, Florida. Poster.
2. Assiri A. A. Structural Changes in Human Corneas with Keratoconus. Speaking of Sciences, 2004, Cardiff. Presentation.
3. A.A. Assiri, B.I. Yousuf, A.J. Quantock, P.J. Murphy. An epidemiologic study of keratoconus in a Saudi Arabia population. 2nd SERI-ARVO 2005, Singapore. Poster.
4. Assiri A A, Yousuf B I, Quantock A J, and Murphy P J (2005) Incidence and severity of keratoconus in Asir Province, Saudi Arabia. *Br J Ophthalmol* 89 (11): 1403-1406.
5. Assiri A A, Yousuf B I, Quantock A J, and Murphy P J (2005) Rigid contact lens fitting in a Saudi Arabian keratoconic population. Br J Ophthlamol; submitted
6. Assiri A, Yousuf B, Woodhouse MJ, Quantock AJ, Murphy PJ. Ultrasound biometry in the diagnosis of amblyopia in keratoconus. CLAE 2005; in press.

References.

Abe K, Hibino T, Mishima H, and Shimomura Y (2004) The cytokine regulation of SPARC production by rabbit corneal epithelial cells and fibroblasts in vitro. *Cornea* 23: 172-179.

Aghamohammadzadeh H, Newton RH, and Meek KM (2004) X-ray scattering used to map the preferred collagen orientation in the human cornea and limbus. *Structure (Camb)* 12 (2): 249-256.

Akhtar S, Bron A, Salvi S, Hawksworth N, Tuft S, and Meek K (2004) Ultrastructural features and Quantative analysis of proteoglycans and collagen fibrils in keratoconus corneal stroma. *Eurpean Association for Vision and Eye Research*. Belgium: EVER organisation.

Al-Saati, A (2000) *Principles of Hospital administration and their implementation in the Kingdom of Saudi Arabia*. Riyadh: King Fahad National Library.

Al-Shahrani A (2003) *The professionmal practice of social work in hospital settings in Saudi Arabia*. PhD thesis, Cardiff University.

Al-Towerki A, El-Sayed G, Al-Rajhi A, and Wagoner M (2004) Changing indications for corneal transplantation at the King Khaled Eye Specialist Hospital (1983-2002). *Cornea* 23 (6): 584-588.

Andreassen T, Simonsen AH, and Oxlund H (1980) Biomechanical properties of keratoconus and normal corneas. *Exp Eye Res* 31 (4): 435-441.

Asbar for studies, Research and Information (1999) *Health in a century*. Riyadh: King Fahad National Library.

Atilano SR, Coskun P, Chwa M, Jordan N, Reddy V, Le K, Wallace DC, and Kenney MC (2005) Accumulation of mitochondrial DNA damage in keratoconus corneas. *Investigative Ophthalmology & Visual Science* 46 (4): 1256-1263.

Avitabile T, Franco L, Ortisi E, Castiglione F, Pulvirenti M, Torrisi B, Castiglione F, and Reibaldi A (2004) Keratoconus staging: a computer-assisted ultrabiomicroscopic method compared with videokeratographic analysis. *Cornea* 23 (7): 655-660.

Bairaktaris G, Lewis D, Fullwood NJ, Nieduszynski IA, Marcyniuk B, Quantock AJ, and Ridgway AE (1998) An ultrastructural investigation into proteoglycan distribution in human corneas. *Cornea* 17 (4): 396-402.

Barr JT, Schechtman K, Fink B, Pierce G, Pensyl C, Zadnik K, Gordon M, and the CLEK study Group (1999) Corneal scarring in the collaborative longitudinal evalution of keratoconus (CLEK) study. Baseline prevalence and repeatability of detection. *Cornea* 18: 34-46.

Bawazeer AM, Hodge WG, and Lorimer B (2000) Atopy and keratoconus: a multivariate analysis. *Br J Ophthalmol* 84 (8): 834-836.

elin MW, Fowler WC, and Chambers W A (1988) Keratoconus. Evaluation of recent trends in the surgical and nonsurgical correction of keratoconus. *Ophthalmology* 95 (3): 335-339.

ennett E, and Weissman B (2005) *Clinical contact lens practice.* Philadelphia: Lippincott Willliams and Wilkins.

ennett S (1986) Keratoconus. In: Bennett, S G, M ed. *Rigid gas-permeable contact lenses.* New York: Professional press books, pp. 297- 344.

ergmanson J (2001) Light and electron microscopy. In: Efron, N ed. *The cornea: its examination in contact lens practice.* Vol. 4. Manchester: Butterworth Heinemann, pp. 137-177.

ergmanson JP, Sheldon TM, and Goosey JD (1999) Fuchs' endothelial dystrophy: a fresh look at an aging disease. *Ophthalmic Physiol Opt* 19 (3): 210-222.

erryhill B, Kane B, Stramer B, Fini E, and Hassell J (2003) Increased SPARC accumulation during corneal repair. *Exp Eye Res* 77: 85-92.

etts AM, Mitchell GL, and Zadnik K (2002) Visual performance and comfort with the Rose K lens for keratoconus. *Optom Vis Sci* 79 (8): 493-501.

irk DE, Fitch JM, Babiarz JP, Doane KJ, and Linsenmayer TF (1990) Collagen fibrillogenesis in vitro: interaction of types I and V collagen regulates fibril diameter. *J Cell Sci* 95 (Pt 4): 649-657.

lochberger TC, Vergnes JP, Hempel J, and Hassell JR (1992) cDNA to chick lumican (corneal keratan sulfate proteoglycan) reveals homology to the small interstitial proteoglycan gene family and expression in muscle and intestine. *J Biol Chem* 267 (1): 347-352.

oote C, Dennis S, Huang Y, Quantock A, and Meek K (2005) Lamellar orientation in human cornea in relation to mechanical properties. *J Struct Biol* 149 (1): 1-6.

oote C, Dennis S, and Meek K (2004) Spatial mapping of collagen fibril organisation in primate cornea-an X-ray diffraction investigation. *J Struct Biol* 146 (3): 359-367.

oote C, Dennis S, Newton R, Puri H, and Meek K (2003) Collagen fibrils appear more closely packed in the prepupillary cornea: optical and biomechanical implications. *Investigative Ophthalmology & Visual Science* 44 (7): 2941-2948.

orcherding S, Blacik L, Sittig R, Bizzel U, Breen M, and Weinstein H (1975) Proteoglycans and collagen fibre organization in human corneo-scleral tissue. *Exp Eye Res* 21: 59-70.

ornstein P (1995) Diversity of function is inherent in matricellular proteins: an appraisal of thrombospondin 1. *J Cell Biol* 130: 503-506.

ornstein P, and Sage E (2002) Matricellular proteins: Extracellular modulators of cell function. *Curr Opin Cell Biol* 14: 608-616.

oruchoff S (2001) *Anterior segment disease: a diagnostic color atlas.* Boston, USA: Butterworth-Heinemann.

Belin MW, Fowler WC, and Chambers W A (1988) Keratoconus. Evaluation of recent trends in the surgical and nonsurgical correction of keratoconus. *Ophthalmology* 95 (3): 335-339.

Bennett E, and Weissman B (2005) *Clinical contact lens practice.* Philadelphia: Lippincott Willliams and Wilkins.

Bennett S (1986) Keratoconus. In: Bennett, S G, M ed. *Rigid gas-permeable contact lenses.* New York: Professional press books, pp. 297- 344.

Bergmanson J (2001) Light and electron microscopy. In: Efron, N ed. *The cornea: its examination in contact lens practice.* Vol. 4. Manchester: Butterworth Heinemann, pp. 137-177.

Bergmanson JP, Sheldon TM, and Goosey JD (1999) Fuchs' endothelial dystrophy: a fresh look at an aging disease. *Ophthalmic Physiol Opt* 19 (3): 210-222.

Berryhill B, Kane B, Stramer B, Fini E, and Hassell J (2003) Increased SPARC accumulation during corneal repair. *Exp Eye Res* 77: 85-92.

Betts AM, Mitchell GL, and Zadnik K (2002) Visual performance and comfort with the Rose K lens for keratoconus. *Optom Vis Sci* 79 (8): 493-501.

Birk DE, Fitch JM, Babiarz JP, Doane KJ, and Linsenmayer TF (1990) Collagen fibrillogenesis in vitro: interaction of types I and V collagen regulates fibril diameter. *J Cell Sci* 95 (Pt 4): 649-657.

Blochberger TC, Vergnes JP, Hempel J, and Hassell JR (1992) cDNA to chick lumican (corneal keratan sulfate proteoglycan) reveals homology to the small interstitial proteoglycan gene family and expression in muscle and intestine. *J Biol Chem* 267 (1): 347-352.

Boote C, Dennis S, Huang Y, Quantock A, and Meek K (2005) Lamellar orientation in human cornea in relation to mechanical properties. *J Struct Biol* 149 (1): 1-6.

Boote C, Dennis S, and Meek K (2004) Spatial mapping of collagen fibril organisation in primate cornea-an X-ray diffraction investigation. *J Struct Biol* 146 (3): 359-367.

Boote C, Dennis S, Newton R, Puri H, and Meek K (2003) Collagen fibrils appear more closely packed in the prepupillary cornea: optical and biomechanical implications. *Investigative Ophthalmology & Visual Science* 44 (7): 2941-2948.

Borcherding S, Blacik L, Sittig R, Bizzel U, Breen M, and Weinstein H (1975) Proteoglycans and collagen fibre organization in human corneo-scleral tissue. *Exp Eye Res* 21: 59-70.

Bornstein P (1995) Diversity of function is inherent in matricellular proteins: an appraisal of thrombospondin 1. *J Cell Biol* 130: 503-506.

Bornstein P, and Sage E (2002) Matricellular proteins: Extracellular modulators of cell function. *Curr Opin Cell Biol* 14: 608-616.

Boruchoff S (2001) *Anterior segment disease: a diagnostic color atlas.* Boston, USA: Butterworth-Heinemann.

Bradshaw D, and Sage H (2001) SPARC, a matricellular protein that functions in cellular differentiation and tissue response to injury. *J Clin Invest* 107: 1049-1054.

Bradshaw D, Puolakkainen P, Dasgupta J, Davidson M, Wight N, and Sage H (2003) SPARC-null mice display abnormalities in the dermis characterized by decreased collagen fibril diameter and reduced tensile strength. *J Invest Dermatol* 120 (6): 949-955.

Bradshaw D, Reed J, and Sage H (2002) SPARC-null mice exhibit accelerated cutaneous wound closure. *J Histochem Cytochem* 50 (1): 1-10.

Brekken A, and Sage H (2001) SPARC, a matricellular protein: at the crossroads of cell-matrix communication. *Matrix Biol* 19: 816-827.

Bron A (1997) The cornea and sclera. In: Bron, A, Tripathi, R., and Tripathi, B eds. *Wolff's anatomy of the eye and orbit.* (Eighth edition), Chapter seven. London: *Chapman and Hall.*

Bron A, Tripathi R, Harding J, and Crabbe M (1978) Stromal loss in keratoconus. *Trans Ophthal Soc UK* 98: 393-396.

Bron A, and Rabinowitz Y (1996) Corneal dystrophies and keratoconus. *Curr Opin Ophthalmol* 7 (4): 71-82.

Brown D, Chwa M, Opbroek A, and Kenney C (1993) Keratoconus corneas: increased gelatinolytic activity appears after modification of inhibitors. *Current Eye Res* 12 (6): 571-581.

Bukusoglu C, and Zieske D (1988) Characterisation of a monoclonal antibody that specifically binds basal epithelial cells in the limbal epithelium. *Investigative Ophthalmology & Visual Science* (sup) 29: 192.

Burger D (1993) Contact lens alternatives for keratoconus: An overview. *Spectrum* March: 49-55.

Burgeson R E (1988) New collagens, new concepts. *Ann Rev Cell Biol* 4: 551-577.

Burris TE, Ayer CT, Evensen DA, and Davenport JM (1991) Effects of intrastromal corneal ring size and thickness on corneal flattening in human eyes. *Refract Corneal Surg* 7 (1): 46-50.

Carmichael R, Ben-Simon J, and Chopamba-Kamba A (2003) Keratoconus associated with limbal vernal keratoconjunctivitis in african patients. *S Afr Optom* 62 (2): 47-54.

Caroline P, McGuire JR, and Doughman D J (1978) Preliminary report on a new contact lens design for keratoconus. *Contact intraoc Lens Med J* 4: 69-73.

Chakravarati S, Magnuson T, Lass J, Jepsen K, and LaMantia C (1998) Lumican regulates collagen fibril assembly: Skin fragility and corneal opacity in the absence of lumican. *J Cell Biology* 141 (5): 1277-1286.

Chakravarati S, Petroll W, Hassell J, Jester J, Lass J, Paul J, and Birk D (2000) Corneal opacity in lumican-null mice: Defects in collagen fibril structure and packing in the posterior stroma. *Investigative Ophthalmology & Visual Science* 41: 3365-3373.

Chen WL, Hu FR, and Wang IJ (2001) Changing indications for penetrating keratoplasty in Taiwan from 1987 to 1999. *Cornea* 20 (2): 141-144.

Colin J, Cochener B, Savary G, and Malet F (2000) Correcting keratoconus with intracorneal rings. *J Cataract Refract Surg* 26 (8): 1117-1122.

Connon C (2000) *The changes in ultrastructure and transparency in chemically or physically altered rabbit cornea.* PhD Thesis, The Open University.

Connon C J. Meek, K M. Newton, R H. Kenney, M C. Alba, S A. and Karageozian, H (2000) Hyaluronidase treatment, collagen fibril packing, and normal transparency in rabbit corneas. *J Refract Surg* 16 (4): 448-455.

Corpuz LM, Funderburgh JL, Funderburgh ML, Bottomley GS, Prakash S, and Conrad GW (1996) Molecular cloning and tissue distribution of keratocan. Bovine corneal keratan sulfate proteoglycan 37A. *J Biol Chem* 271 (16): 9759-9763.

Crews J, Driebi T, and Stern A (1994) The clinical management of keratoconus: a 6 year retrospective study. *CIAO J* 20: 194-197.

Dastjerdi M, and Hashemi H (1998) A Quantitative corneal topography index for detection of keratoconus. *J Ref surg* 14: 427-436.

Davies P, and Ruben M (1975) The Paretic pupil: its incidence and aetilogy after keratoplasty for keratoconus. *Br J Ophthalmol* 59: 223-228.

Davis J (1997) Keratoconus: Current understanding of diagnosis and management. *Clin Eye Vis Care* 9: 13-22.

Daxer A, and Fratzl P (1997) Collagen fibril orientation in the human corneal stroma and its implication in keratoconus. *Investigative Ophthalmology & Visual Science* 38 (1): 121-129.

Dietze TR, and Durrie DS (1988) Indications and treatment of keratoconus using epikeratophakia. *Ophthalmology* 95 (2): 236-246.

Donald AM (2003) The use of environmental scanning electron microscopy for imaging wet and insulating materials. *Nat Mater* 2 (8): 511-516.

Donaldson D (1966) A new instrument for the measurement of corneal thickness. *Arch Ophthalmol* 76 (1): 25-31.

Duke-Elder S, and Leigh G (1965) Diseases of the outer eye. *System of Ophthalmology.* Vol. VIII. London,UK: Kimton, pp. 964.

Edmund C (1988) Corneal tissue mass in normal and keratoconic eyes. In vivo estimation based on area of horizontal optical sections. *Acta Ophthalmol (Copenh)* 66 (3): 305-308.

Edrington TB, Barr JT, Zadnik K, Davis LJ, Gundel RE, Libassi DP, McMahon TT, and Gordon MO (1996) Standardized rigid contact lens fitting protocol for keratoconus. *Optom Vis Sci* 73 (6): 369-375.

Edrington T B, Zadnik K, and Barr JT (1995) Keratoconus. *Optom Clin* 4 (3): 65-73.

Elder M (1994) Leber congenital amaruosis and its association with keratoconus and keratoglobus. *J Peditra Ophthalmol Strabismus.* 31: 38-40.

Eming A, Whitsitt S, He L, Krieg T, Morgan J, and Davidson M (1996) Partical-mediated gene transfer of PDGF isoforms promotes wound repair. *J Invest Dermatol* 112: 297-302.

Fabre EJ, Bureau J, Pouliquen Y, and Lorans G (1991) Binding sites for human interleukin 1 alpha, gamma interferon and tumor necrosis factor on cultured fibroblasts of normal cornea and keratoconus. *Curr Eye Res* 10 (7): 585-592.

Foster CS, and Yamamoto GK (1978) Ocular rigidity in keratoconus. *Am J Ophthalmol* 86 (6): 802-806.

Fowler WC, Belin MW, and Chambers WA (1988) Contact lenses in the visual correction of keratoconus. *CIAO J* 14 (4): 203-206.

Francki A, Bradshaw AD, Bassuk JA, Howe CC, Couser WG, and Sage EH (1999) SPARC regulates the expression of collagen type I and transforming growth factor beta-1 in mesangial cells. *J Biol Chem* 274 (45): 32145-32152.

Fullwood NJ, Meek KM, Malik NS, and Tuft SJ (1990) A comparison of proteoglycan arrangement in normal and keratoconus human corneas. *Biochem Soc Trans* 18 (5): 961-962.

Fullwood NJ. Tuft SJ, Malik NS, Meek KM, Ridgway AE, and Harrison RJ (1992) Synchrotron x-ray diffraction studies of keratoconus corneal stroma. *Investigative Ophthalmology & Visual Science* 33 (5): 1734-1741.

Funderburgh JL, Corpuz LM, Roth MR, Funderburgh ML, Tasheva ES, and Conrad GW (1997) Mimecan, the 25-kDa corneal keratan sulfate proteoglycan, is a product of the gene producing osteoglycin. *J Biol Chem* 272 (44): 28089-28095.

Funderburgh JL, Funderburgh ML, Brown SJ, Vergnes JP, HassellJR, Mann M, and Conrad GW (1993) Sequence and structural implications of a bovine corneal keratan sulfate proteoglycan core protein. Protein 37B represents bovine lumican and proteins 37A and 25 are unique. *J Biol Chem* 268 (16): 11874-11880.

Funderburgh JL, Funderburgh ML, Rodrigues MM, Krachmer JH, and Conrad GW (1990) Altered antigenicity of keratan sulfate proteoglycan in selected corneal diseases. *Investigative Ophthalmology & Visual Science* 31 (3): 419-428.

Funderburgh JL, Hevelone N , Roth MR, Funderburgh ML, Rodrigues MR, Nirankari VS, and Conrad GW (1998) Decorin and biglycan of normal and pathologic human corneas. *Investigative Ophthalmology & Visual Science* 39 (10): 1957-1964.

Funderburgh JL, Panjwani N, Conrad GW, and Baum J (1989) Altered keratan sulfate epitopes in keratoconus. *Investigative Ophthalmology & Visual Science* 30 (10): 2278-2281.

Gass JD (1964) The Iron Lines Of The Superficial Cornea. *Arch Ophthalmol* 71: 348-358.

Gasset AR, Houde WL, and Garcia-Bengochea M (1978) Hard contact lens wear as an environmental risk in keratoconus. *Am J Ophthalmol* 85 (3): 339-341.

Gasson A, and Morris J (2003) *The contact lens manual: a practical guide to fitting.* 3rd edition ed. London: Butterwarth Heinemann.

Georgiou T, Funnell L, Cassels-Brown A, and O'connor R (2004) Influence of ethnic origin on the incidence of keratoconus and associated atopic disease in Asian and white patients. *Eye* 18: 379-383.

Gherghel D, Hosking S, Mantry S, Banerjee S, Naroo S, and Shah S (2003) Corneal pachymetry in normal and keratoconic eye: Orbescan II versus ultrasound. *J Cataract Refract Surg* 30: 1272-1277.

Gilmour D, Lyon G, Carlton M, Sanes J, Cunningham J, Anderson J, Hogan B, Evans M, and Colledge W (1998) Mice deficient for the secreted glycoprotein SPARC/ oseteonectin/ BM-40 develop normally but show severe age-onset cataract formation and disruption of the lens. *EMBO J* 17: 1860-1870.

Gloster J, Perkins ES, and Pommier M L (1957) Extensibility of strips of sclera and cornea. *Br J Ophthalmol* 41 (2): 103-110.

Goldstein H (1980) The reported demography and cause of blindness throughout the world. *Adv. Ophthalmol.* 40: 1-99.

Grande JP, Melder DC, and Zinsmeister AR (1997) Modulation of collagen gene expression by cytokines: stimulatory effect of transforming growth factor beta-1, with divergent effects of epidermal growth factor and tumor necrosis factor-alpha on collagen type I and collagen type IV. *J Lab Clin Med* 130 (5): 476-486.

Gromacki SJ, and Barr JT (1994) Central and peripheral corneal thickness in keratoconus and normal patient groups. *Optom Vis Sci* 71 (7): 437-441.

Gundel RE, Libassi DP, Zadnik K, Barr JT, Davis L, McMahon TT, Edrington TB, and Gordon MO (1996) Feasibility of fitting contact lenses with apical clearance in keratoconus. *Optom Vis Sci* 73 (12): 729-732.

Hall KG (1963) A Comprehensive Study of Keratoconus. *Br J Physiol Opt* 20: 215-256.

Ham M (1986) Another perspective on keratoconus contact lens fitting. *J Am Optom Assoc* 53: 199-205.

Hamada R (1974) *Aspect ultrastructural des cellules et du tissu conjonctif corneen normal.* In Bron, A. Tripathi, R. and Tripathi, B (1997) *Wolff's anatomy of the eye and orbit.* 8th Ed. Chapman and Hall, UK.

Harrison DA, and Maguire LJ (1995) Biomicroscopic evidence of keratoconus with an apex power of 45.5 diopters by videokeratoscopy. *Am J Ophthalmol* 119 (3): 366-367.

Hassell R, Kimura H, and Hascall C (1986) Proteoglycan core protein families. *Annual Review of Biochemistry* 55: 18843-18846.

Haustein J (1983) On the ultrastructure of the developing and adult mouse corneal stroma. *Anat Embryol (Berl)* 168 (2): 291-305.

Hayashi J, Osawa T, and Tohyama K (2002) comparative observations on corneas, with special reference to Bowman's layer and Descemet's membrane in mammals and amphibians. *J. Morphology* 254: 247 258.

Hayes S (2005) *The structural organisation of collagen in the corneas of primates and other mammals and the stromal changes associated with the disease keratoconus.* PhD Thesis, Cardiff University.

Heaven CJ, Lalloo F, and McHale E (2000) Keratoconus associated with chromosome 13 ring abnormality. *Br J Ophthalmol* 84 (9): 1079.

Henry A (2000) Keratoconus. In: Bennett ES, H V, ed. *Clinical manual of contact lenses.* Philadelphia: Lippincott Williams and Wilkins, 2000, pp. 493-530.

Heon EA, Kopp KK, Rootman D, Vincent AL, Billingsley G, Priston M, Dorval KM, Chow RL, McInnes RR, Heathcote G, Westall C, Sutphin JE, Semina E, Bremner R, and Stone E M (2002) VSX1: a gene for posterior polymorphous dystrophy and keratoconus. *Hum Mol Genet* 11 (9): 1029-1036.

Hodson S (1997) Corneal stromal swelling. *Progress in retinal and eye research* 16: 99-116.

Hogan M, Alvarado J, and Weddell J (1971) *The cornea.* In Bron, A. Tripathi, R. and Tripathi, B (1997) *Wolff's anatomy of the eye and orbit.* 8th ed. Chapman and Hall, UK.

Hollingsworth JG, and Efron N (2005a) Observations of banding patterns (Vogt striae) in keratoconus: a confocal microscopy study. *Cornea* 24 (2): 162-166.

Hollingsworth JG, Bonshek RE, and Efron N (2005b) Correlation of the appearance of the keratoconic cornea in vivo by confocal microscopy and in vitro by light microscopy. *Cornea* 24 (4): 397-405.

Huang YA, Meek K, Vellodi A, and McDonald B (1996) Ultrastructural study of the cornea in a bone marrow transplanted Hurler syndrome patient. *Exp Eye Res* 62: 377-387.

Hughes A, Dash D, Jackson J, Frazer D, and Silverstri G (2003) Familial keratoconus with cataract: Linkage to the long arm of chromosome 15 and exclusion of candidate genes. *Investigative Ophthalmology & Visual Science* 44 (12): 5063-5066.

Ihalainen A (1986) Clinical epidemiological features of keratoconus:genetic and external factors in the pathogenesis of the disease. *Acta Ophthaloml* 178 (suppl): 5-64.

Ihme A, Krieg T, Muller RK, and Wollensak J (1983) Biochemical investigation of cells from keratoconus and normal cornea. *Exp Eye Res* 36 (5): 625-631.

Insler M, and Cooper HD (1986) New correlation in keratoconus using pachymetric and keratometric analysis. *CIAO J* 12: 101-105.

Iruela-Arispe LV, Wu H, Jaenisch R, and Sage H (1996) Type I collagen-deficient mov-13 mice do not retain SPARC in the extracellular matrix: implications for fibroblast function. *Dev Dyn* 207: 171-183.

Johnson D, Bourne W, and Campbell R (1982) The ultrastructure of Descemet's membrane:1. changes with age in normal corneas. *Arch Ophthalmol* 100: 1942-1947.

Jue B, and Maurice DM (1986) The mechanical properties of the rabbit and human cornea. *J Biomech* 19 (10): 847-853.

Kadler KE, Holmes DF, Trotter JA, and Chapman JA (1996) Collagen fibril formation. *Biochem J* 316 (Pt 1): 1-11.

Kaas-Hansen M (1993) The histopathological changes of keratoconus. *Acta Ophthalmol (Copenh)* 71 (3): 411-414.

Kame R, and Kennedy J (1987) Corneal contour change with 3M fluoropolymer lenses. *Contact Lens Spectrum* 2: 53-59.

Kanski J (1997) *Clinical Ophthalmology*. 3rd ed. Oxford: Butterworth-Heinemann.

Karseras G, and Ruben M (1976) Aetiology of keratoconus. *Br J Ophthalmol* 60: 522-525.

Kasugai S, Todescan, R. Nagata, T. Yoa, K. Butler, W. and Sodek, J (1991) Expression of bone matrix proteins associated with mineralised tissue formation by adult rat bone marrow cells in vitro: inductive effects of dexamethasone on the osteoblastic phenotype. *J Cell Physiol* 147: 111-117.

Kemmetmuller H (1975) Contact lenses as an atopic aid in case of keratoconus. *Contact and Int. Lens Med J* 1: 163-168.

Kemp EG, and Lewis CJ (1982) Immunoglobulin patterns in keratoconus with particular reference to total and specific IgE levels. *Br J Ophthalmol* 66 (11): 717-720.

Kennedy RH, Bourne WM, and Dyer JA (1986) A 48-year clinical and epidemiologic study of keratoconus. *Am J Ophthalmol* 101 (3): 267-273.

Kenney C, and Brown D (2003) The cascade hypothesis of keratoconus. *Contact Lens and Anterior Eye* 26: 139-146.

Kenney MC, Chwa M, Atilano SR, Tran A, Carballo M, Saghizadeh M, Vasiliou V, Adachi W, and Brown DJ (2005) Increased levels of catalase and cathepsin V/L2 but decreased TIMP-1 in keratoconus corneas: evidence that oxidative stress plays a role in this disorder. *Investigative Ophthalmology & Visual Science* 46 (3): 823-832.

Kenney MC, Nesburn AB, Burgeson RE, Butkowski RJ, and Ljubimov AV (1997) Abnormalities of the extracellular matrix in keratoconus corneas. *Cornea* 16 (3): 345-351.

Khoo CY (1989) Corneal blindness in Singapore and its prevention. *Ann Acad Med Singapore* 18 (2): 123-130.

Kim WJ, Shah S, and Wilson SE (1998) Differences in keratocyte apoptosis following transepithelial and laser-scrape photorefractive keratectomy in rabbits. *J Refract Surg* 14 (5): 526-533.

Klyce D, and Beuerman W (1988) Structure and function of cornea. In: Kaufman HE, B, McDonald MB, et al., eds. ed. *The cornea.* New York: Churchill Livingstone, pp. 3-54.

Klyce S (1984) Computer-assisted corneal topography: high resolution graphic presentation and analysis of keratoscopy. *Investigative Ophthalmology & Visual Science* 25: 1426-1435.

Koch M, Foley JE, Hahn R, Zhou P, Burgeson RE, Gerecke DR, and Gordon MK (2001) Alpha 1 (XX) collagen, a new member of the collagen subfamily, fibril-associated collagens with interrupted triple helices. *Journal of Biological Chemistry* 276: 23120-23126.

Komai Y, and Ushiki T (1991) The three-dimensional organization of collagen fibrils in the human cornea and sclera. *Investigative Ophthalmology & Visual Science* 32 (8): 2244-2258.

Korb DR, Finnemore VM, and Herman JP (1982) Apical changes and scarring in keratoconus as related to contact lens fitting techniques. *J Am Optom Asso* 53 (3): 199-205.

Krachmer JH, Feder RS, and Belin MW (1984) Keratoconus and related non-inflammatory corneal thinning disorders. *Surv Ophthalmol* 28 (4): 293-322.

Kremer I, Eagle RC, Rapuano CJ, and Laibson PR (1995) Histologic evidence of recurrent keratoconus seven years after keratoplasty. *Am J Ophthalmol* 119 (4): 511-512.

Kruse FE (1994) Stem cells and corneal epithelial regeneration. *Eye* 8 (Pt 2): 170-183.

Kuwabara T (1978) Current concepts in anatomy and histology of the cornea. *Contact and Intraoc. Lens Med J* 4: 101.

Lane T, and Sage H (1994) The biology of SPARC, a protein that modulates cell-matrix interactions. *FASEB J* 8: 163-173.

Latvala T, Poulakkainen P, Vesaluoma M, and Tervo T (1996) Distribution of SPARC protein (osteonectin) in normal and feline cornea. *Exp Eye Res* 63: 579-584.

Lawless M, Coster DJ, Phillips AJ, and Loane M (1989) Keratoconus: diagnosis and management. *Aust N Z J Ophthalmol* 17 (1): 33-60.

Lee JL, and Kim MK (2004) Clinical performance and fitting characteristics with a multicurve lens for keratoconus. *Eye Contact Lens* 30 (1): 20-24.

Leung KK (1999) RGP fitting philosophies for keratoconus. *Clin Exp Optom* 82 (6): 230-235.

Li W, Vergnes JP, Cornuet PK, and Hassell JR (1992) cDNA clone to chick corneal chondroitin/dermatan sulfate proteoglycan reveals identity to decorin. *Arch Biochem Biophys* 296 (1): 190-197.

Lim N, and Vogt U (2002) Characteristics and functional outcomes of 130 patients with keratoconus attending a specialist contact lens clinic. *Eye* 26 (1): 54-59.

Luce D (2005) Determining in vivo biomechanical properties of the cornea with an ocular response analyser. *J Catract Refract Surg* 31: 156-162.

Mackie A (1993) Keratoconus. In: Mackie ed. *Medical contact lens practice-systematic approach.* (1st ed) Oxford: Butterworth-Heinemann.

Macsai MS, Varley GA, and Krachmer JH (1990) Development of keratoconus after contact lens wear. Patient characteristics. *Arch Ophthalmol* 108 (4): 534-538.

Maeda N, Klyce S, Smolek M, and Thompson H (1994) Automated keratoconus screening with corneal topography analysis. *Investigative Ophthalmology & Visual Science* 35 (6): 2749-2757.

Maguen E, Caroline P, Rosner IR, Macy JI, and Nesburn AB (1992) The use of the SoftPerm lens for the correction of irregular astigmatism. *CIAO J* 18 (3): 173-176.

Maguire LJ, and Bourne WM (1989) Corneal topography of early keratoconus. *Am J Ophthalmol* 108 (2): 107-112.

Maguire L, and Meyer R (1988) *The cornea.* Churchill Livingstone,New York.

Maguire L, Singer D, and Klyce S (1987) Graphic presentation of computer analyzed keratoscope photographes. *Arch Ophthalmol* 105: 223-230.

Maguire LJ, and Lowry JC (1991) Identifying progression of subclinical keratoconus by serial topography analysis. *Am J Ophthalmol* 112 (1): 41-45.

Mahmood M, and Wagoner M (2000) Penetrating keratoplasty in eyes with keratoconus and vernal keratoconjunctivitis. *Cornea* 23: 468-470.

Mandell R (1997) Contemporary management of keratoconus. *Int Contact Lens Clin* 24: 43-58.

Mannis J, and Zadnik K (1989) Contact lens fitting in keratoconus. *CIAO J* 15: 282-289.

Marin MJ, Sola Y, Tena F, Utrillas MP, Campmany E, de Cabo X, Lorente J, and Martinez-Lozano JA (2005) The UV Index on the Spanish Mediterranean coast. *Photochem Photobiol* 81 (3): 659-665.

Maruyama Y, Wang X, Li Y, Sugar J, and Yue B (2001) Involvement of Sp1 elements in the promoter activity of genes affected in keratoconus. *Investigate Ophthalmology & Visual Science* 42 (9): 1980-1985.

Mason J, Taylor A, Williiams G, Sage H, and Hogan M (1986) Evidence from molecular cloning that SPARC, a major product of mouse embryo parietal endoderm, is related to an endothelial cell "culture shock" glycoprotein. *EMBO J* 5: 1465-1472.

Maurice DM (1999) Some puzzles in the microscopic structure of the stroma. *J Ref Surg* 15: 692-694.

Maurice DM, and Monroe, F (1990) Cohesive strength of corneal lamellae. *Exp Eye Res* 50 (1): 59-63.

Maurice M (1984) The cornea and sclera. *In The Eye*. (3 (ed.H. Davson), Vol. 1. New York and London: Academic press, pp. 489-600.

Maurice M (1957) The transparency of the corneal stroma. *Vision Res* 10 (1): 107-108.

Maurice M (1969) The cornea and sclera. *In The Eye*. (3 (ed.H. Davson), Vol. 1. New York and London: Academic press, pp. 489-600.

McMonnies CW (2004) Keratoconus fittings: apical clearance or apical support? *Eye Contact Lens* 30 (3): 147-155.

McMonnies CW (2005) The biomechanics of keratoconus and rigid contact lenses. *Eye Contact Lens* 31 (2): 80-92.

McMonnies CW, and Boneham GC (2003) Keratoconus, allergy, itch, eye-rubbing and hand-dominance. *Clin Exp Optom* 86 (6): 376-384.

Meek KM, Blamires T, Elliott GF, Gyi TJ, and Nave C (1987) The organisation of collagen fibrils in the human corneal stroma: a synchrotron X-ray diffraction study. *Curr Eye Res* 6 (7): 841-846.

Meek KM, and Newton RH (1999) Organization of collagen fibrils in the corneal stroma in relation to mechanical properties and surgical practice. *J Refract Surg* 15 (6): 695-699.

Meek KM, Tuft SJ, Huang Y, Gill PS, Hayes S, Newton RH, and Bron A J (2005) Changes in collagen orientation and distribution in keratoconus corneas. *Investigative Ophthalmology & Visual Science* 46 (6): 1948-1956.

Michelacci YM (2003) Collagens and proteoglycans of the corneal extracellular matrix. *Braz J Med Biol Res* 36 (8): 1037-1046.

Ministry of Planning (2001) *Characteristics in the Kingdom of Saudi Arabia (demographic survey 2001)*. Riyadh: Ministry of Planning press.

Ministry of Planning (1985) *The fourth development plan, 1980-1990*. Riyadh, Saudi Arabia: Ministry of Planning.

Ministry of Planning (1999) *Population characteristics in the Kingdom of Saudi Arabia (Demographic survey 1999)*. Riyadh Saudi Arabia: Ministry of Planning.

Ministry of Planning (2000) *The seventh development plan, 2000-2004*. Riyadh, Saudi Arabia: Ministry of Planning.

Mishima H, Hibino T, Hara H, Murakami J, and Otori T (1998) SPARC from corneal epithelial cells modulates collagen contraction by keratocyte. *Investigative Ophthalmology & Visual Science* 39: 2547-2553.

Motamed K, and Sage H (1998) SPARC inhibits endothelial cell adhesion but not proliferation through a tyrosine phosphorylation-dependent pathway. *J Cell Biochem* 70: 543-552.

Muller L, and Vernsen G (1995) Novel aspects of the ultrastructure organization of human corneal keratocytes. *Investigative Ophthalmology & Visual Science* 37: 476-488.

Muller LJ, Pels E, and Vrensen GF (2001) The specific architecture of the anterior stroma accounts for maintenance of corneal curvature. *Br J Ophthalmol* 85 (4): 437-443.

Newton RH, and Meek KM (1998a) The integration of the corneal and limbal fibrils in the human eye. *Biophys J* 75 (5): 2508-2512.

Newton RH, and Meek KM (1998b) Circumcorneal annulus of collagen fibrils in the human limbus. *Investigative Ophthalmology & Visual Science* 39 (7): 1125-1134.

Norman C (2000) RGPs in the next decade: what will be their role? *Eye wittness* 2ed Quart: 1-3.

Norose K, Clark I, Syed A, Basu A, Heber-Katz E, Sage H, and Howe C (1998) SPARC deficiency leads to early-onset cataractogenesis. *Investigative Ophthalmology & Visual Science* 39 (13): 2674-2680.

Nottingham J (1854) Practical observations on conical cornea. In: Duke-Elder, S ed. *System of Ophthalomolgy, diseases of the outer eye*. Vol 2. pp. 964-976.

Oldberg A, Antonsson P, Lindblom K, and Heinegard D (1989) A collagen-binding 59-kd protein (fibromodulin) is structurally related to the small interstitial proteoglycans PG-S1 and PG-S2 (decorin). *EMBO J* 8 (9): 2601-2604.

Otsuka K, Yao L, Wasi S, Tung S, Aubin E, Sodek J, and Termine D (1984) Biosynthesis of osteonectin by fetal porcine calvarial cells in vitro. *J Biol Chem* 259: 9805-9812.

Owens H, and Gamble G (2003) A profile of keratoconus in New Zealand. *Cornea* 22 (2): 122-125.

Owens H, and Watters GA (1996) An evaluation of the keratoconic cornea using computerised corneal mapping and ultrasonic measurements of corneal thickness. *Ophthalmic Physiol Opt* 16 (2): 115-123.

Pearson R, Soneji B, Sarvanthan N, Sandford-Smith H (2000) Does ethnic origin influences the incidence or severity of keratoconus? *Eye* 14: 625-628.

Perez-Gomez IH, Morgan, P and Effron, N. (2000) A reference grid of the normal human cornea viewed with a confocal microscopy. *Optom. Vis. Sci* 77: S153.

Perry HD, Buxton JN, and Fine BS (1980) Round and oval cones in keratoconus. *Ophthalmology* 87 (9): 905-909.

Petrie A, and Sabin, C (2001) *Medical Statistics at a glance*. 2ed ed. London: Blachwell Science.

Petroll WM, Boettcher K, Barry P, Cavanagh HD, and Jester JV (1995) Quantitative assessment of anteroposterior keratocyte density in the normal rabbit cornea. *Cornea* 14 (1): 3-9.

Pfister R (1973) The normal surface of corneal epithelium: a scanning electron microscopic study. *Investigative Ophthalmology & Visual Science* 12 (9): 654-668.

Pierscionek BK, Popiolek-Masajada A, and Kasprzak H (2001) Corneal shape change during accommodation. *Eye* 15 (Pt 6): 766-769.

Polack FM (1976) Contributions of electron microscopy to the study of corneal pathology. *Surv Ophthalmol* 20 (6): 375-414.

Poncelet AC, and Schnaper HW (1998) Regulation of human mesangial cell collagen expression by transforming growth factor-beta1. *Am J Physiol* 275 (3 Pt 2): F458-466.

Pouliquen Y (1987) Doyen lecture keratoconus. *Eye* 1 (Pt 1): 1-14.

Pouliquen Y, Graf B, de Kozak Y, Bisson J, and Faure JP (1970) Morphological study of keratoconus. *Arch Ophtalmol Rev Gen Ophtalmol* 30 (6-7): 497-532.

Puolakkainen P, Bradshaw D, Kyriakides R, Reed M, Brekken R, Wight T, Bornstein P, Ratner B,and Sage H (2003) Compromised production of extracellular matrix in mice lacking secreted protein, acidic and rich in cysteine (SPARC) leads to a reduced foreign body reaction to implanted biomaterials. *Am J Pathol* 162 (2): 627-635.

Pullum K (2003) A keratoconus fitting system using the axial profile to establish optimum lens parameters. *CLAE* 26: 77-84.

Quantock A, Dennis S, Kinoshita S, Boote C, Meek K, Matsushima Y, and Tachibana M (2003) Annulus of collagen fibrils in mouse cornea and structural matrix alterations in a murine-specific keratopathy. *Investigative Ophthalmology & Visual Science* 44: 1906-1911.

Quantock AJ, Fullwood NJ, Thonar EJ, Waltman SR, Capel MS, Ito M, Verity SM, and Schanzlin DJ (1997) Macular corneal dystrophy type II: multiple studies on a cornea with low levels of sulphated keratan sulphate. *Eye* 11 (Pt 1): 57-67.

Quantock AJ, Meek KM, Fullwood NJ, and Zabel RW (1993) Scheie's syndrome: the architecture of corneal collagen and distribution of corneal proteoglycans. *Can J Ophthalmol* 28 (6): 266-272.

Quantock AJ, Sano Y, Young RD, and Kinoshita S (2005) Stromal architecture and immune tolerance in additive corneal xenografts in rodents. *Acta Ophthalmol Scand* 83 (4): 462-466.

Rabinowitz Y, Garbus J, and Mcdoonell P (1990) Computer-assisted corneal topography in family members of keratoconus. *Arch Ophthalmol* 108: 365-371.

Rabinowitz Y, Zu L, Yang H, Wang Y, Rotter J, and Pulst S (1999) Keratoconus: Non parametric linkage analysis suggests a gene locus near the centrome of chromosome 21. *Investigative Ophthalmology & Visual Science* 40 (4(suppl)): 2975.

Rabinowitz YS (1998) Keratoconus. *Surv Ophthalmol* 42 (4): 297-319.

Rabinowitz YS, Dong L and Wistow G (2005) Gene expression profile studies of human keratoconus cornea for NEIBank: a novel cornea-expressed gene and the absence of transcripts for aquaporin 5. *Investigative Ophthalmology Visual Science* 46 (4): 1239-1246.

Rabinowitz Y, and McDonnell PJ (1989) Computer-assisted corneal topography in keratoconus. *Refract Corneal Surg* 5 (6): 400-408.

Rada JA, Cornuet PK, and Hassell JR (1993) Regulation of corneal collagen fibrillogenesis in vitro by corneal proteoglycan (lumican and decorin) core proteins. *Exp Eye Res* 56 (6): 635-648.

Rada JA, Fini ME, and Hassell JR (1996) Regionalized growth patterns of young chicken corneas. *Investigative Ophthalmology & Visual Science* 37 (10): 2060-2067.

Radner W, and Mallinger R (2002) Interlacing of collagen lamellae in the midstroma of the human cornea. *Cornea* 21 (6): 598-601.

Radner W, Zehetmayer M, Aufreiter R, and Mallinger R (1998a) Interlacing and cross-angle distribution of collagen lamellae in the human cornea. *Cornea* 17 (5): 537-543.

Radner W, Zehetmayer M, Skorpik C, and Mallinger R (1998b) Altered organization of collagen in the apex of keratoconus corneas. *Ophthalmic Res* 30 (5): 327-332.

Rahi A, Davies P, Ruben M, Lobascher D, and Menon J (1977) Keratoconus and coexisting atopic disease. *Br J Ophthalmol* 61 (12): 761-764.

Rawe IM, Meek KM, Leonard DW, Takahashi T, and Cintron C (1994) Structure of corneal scar tissue: an X-ray diffraction study. *Biophys J* 67 (4): 1743-1748.

Reardon PL, and Lowther G (1973) Keratoconus: differential diagnosis and treatment. *J Optom Asso* 44 (8): 824-830.

Reed MJ, Vernon RB, Abrass IB, and Sage E H (1994) TGF-beta 1 induces the expression of type I collagen and SPARC, and enhances contraction of collagen gels, by fibroblasts from young and aged donors. *J Cell Physiol* 158 (1): 169-179.

Rhee D, Fariss RN, Brekken R, Sage H, and Russell P (2003) The matricellular protein SPARC is expressed in human trabecular meshwork. *Exp Eye Res* 77: 601-607.

Ridley F (1956) Contact lenses in treatment of keratoconus. *Br J Ophthalmol* 40 (5): 295-304.

Ridley F (1961) The role of contact lenses and shells. *Proc R Soc Med* 54: 110-111.

Ridley F (1966) The pathology of tropical diseases. *Dist Nurs* 9 (3): 69.

Rivera RK, and Polse KA (1991) Corneal response to different oxygen levels during extended wear. *CIAO J* 17: 96-101.

Sabiston W (1978) The crazy cone. *Austral J Ophthalmol* 6: 43-45.

Sage H, Johnson C, and Bornstein P (1984) Characterisation of a novel serum albumin-binding glycoprotein secreted by endothelial cells in culture. *J Biol Chem* 259: 3993-4007.

Sage H, Pritzl P, and Bornstein P (1981) Secretory phenotypes of endothelial cells in culture: comparison of aortic, venous, capillary and corneal endothelium. *Arteriosclerosis* 1: 422-427.

Sage H, Vernon B, Decker J, Funk S, and Iruela-Arispe L (1989) Distribution of the calcium-binding protein SPARC in tissues of embryonic and adult mice. *J Histochem Cytochem* 37: 819-829.

Saini G, Saroha V, Singh P, Sukhija J, Jain A (2004) Keratoconus in Asian eyes at a tertiary eye care facility. *Clin Exp Optom* 87 (2): 97-101.

Sallum J, and Erwenne C (1996) Clinical and topographical analysis of family members of keratoconus patients. *Investigative Ophthalmology & Visual Science* 37 (3): 4676.

Sandberg-Lall M, Hagg PO, Wahlstrom I, and Pihlajaniemi T (2000) Type XIII collagen is widely expressed in the adult and developing human eye and accentuated in the ciliary muscle, the optic nerve and the neural retina. *Exp Eye Res* 70 (4): 401-410.

Sawaguchi S, Fukuchi T, Abe H, Kaiya T, Sugar J, and Yue BY (1998) Three-dimensional scanning electron microscopic study of keratoconus corneas. *Arch Ophthalmol* 116 (1): 62-68.

Sawaguchi S, Twining SS, Yue BY, Wilson PM, Sugar J, and Chan SK (1990) Alpha-1 proteinase inhibitor levels in keratoconus. *Exp Eye Res* 50 (5): 549-554.

Sawaguchi S, Yue BY, Chang I, Sugar J, and Robin J (1991) Proteoglycan molecules in keratoconus corneas. *Investigative Ophthalmology & Visual Science* 32 (6): 1846-1853.

Schermer A, Galvin S, and Sun T (1986) Differentiation-related expression of a major 64K corneal keratin in vivo and in culture suggests limbal location of corneal epithelial stem cells. *J Cell Biol* 103 (1): 49-62.

Schmucker C, and Schaeffel F (2004) A paraxial schematic eye model for the growing C57BL/6 mouse. *Vision Res* 44 (16): 1857-1867.

Scott JE (1988) Proteoglycan-fibrillar collagen interactions. *Biochem J* 252 (2): 313-323.

Scott JE, and Bosworth TR (1990) A comparative biochemical and ultrastructural study of proteoglycan-collagen interactions in corneal stroma. Functional and metabolic implications. *Biochem J* 270 (2): 491-497.

Scott JE, and Haigh M (1985) 'Small'-proteoglycan: collagen interactions: keratan sulphate proteoglycan associates with rabbit corneal collagen fibrils at the 'a' and 'c' bands. *Biosci Rep* 5 (9): 765-774.

Scott JE, and Haigh M (1988) Identification of specific binding sites for keratan sulphate proteoglycans and chondroitin-dermatan sulphate proteoglycans on collagen fibrils in

cornea by the use of cupromeronic blue in 'critical-electrolyte-concentration' techniques. *Biochem J* 253 (2): 607-610.

Scroggs MW, and Proia A D (1992) Histopathological variation in keratoconus. *Cornea* 11 (6): 553-559.

Sharif W, and Casey, A (1991) Penetrating keratoplasty for keratoconus complications and long-term success. *British J Ophthalmology* 75 (3): 142-126.

Shaw EL, Rao GN, Arthur EJ, and Aquavella JV (1978) The functional reserve of corneal endothelium. *Ophthalmology* 85 (6): 640-649.

Sheldon H (1956) An electron microscope study of the epithelium in the normal mature and immature mouse cornea. *J Biophys Biochem Cytol* 2 (3): 253-262.

Sherwin T, Brookes NH, Loh IP, Poole CA, and Clover GM (2002) Cellular incursion into Bowman's membrane in the peripheral cone of the keratoconic cornea. *Exp Eye Res* 74 (4): 473-482.

Smiddy W, Hamburg T, Kracher G, and Stark W (1988) Keratoconus-contact lens or keratoplasty. *Ophthalmology* 95 (4): 487-492.

Smith R, John, S. Nishina, P. and Sundberg, J. (2002) *systematic evaluation of the mouse eye: Anatomy, pathology, and biomethods*. New York: CRC Press.

Smith V, and Easty D (2000) Matrix metalloproteinase-2: involvement in keratoconus. *Eur J Ophthalmol* 10 (3): 215-226.

Smolek MK (1993) Interlamellar cohesive strength in the vertical meridian of human eye bank corneas. *Investigative Ophthalmology & Visual Science* 34 (10): 2962-2969.

Smolek MK, and Beekhuis WH (1997) Collagen fibril orientation in the human corneal stroma and its implications in keratoconus. *Investigative Ophthalmology & Visual Science* 38 (7): 1289-1290.

Smolek MK, and McCarey BE (1990) Interlamellar adhesive strength in human eye bank corneas. *Investigative Ophthalmology & Visual Science* 31 (6): 1087-1095.

Song J, Lee Y, Houston J, Petroll W, Chakravati S, Cavanagh, H and Jester J (2003) Neonatal corneal stromal development in the normal and lumican-deficient mouse. *IOVS* 44 (2): 548-557.

Stenner D, Tracy R, Riggs B, and Mann K (1986) Human platelets contain and secrete osteonectin, a major protein of mineralised bone. *Proc Natl Acad Sci* 83: 6892-7001.

Sturbaum CW, and Peiffer RL (1993) Pathology of corneal endothelium in keratoconus. *Ophthalmologica* 206 (4): 192-208.

Swann G, and Waldron E (1986) Keratoconus: the clinical spectrum. *J Am Optom Asso* 57: 204-209.

Szczotka LB, Barr JT, and Zadnik K (2001) A summary of the findings from the Collaborative Longitudinal Evaluation of Keratoconus (CLEK) Study. CLEK Study Group. *Optometry* 72 (9): 574-584.

Tabbara KF (1999) Ocular complications of vernal keratoconjunctivitis. *Can J Ophthalmol* 34 (2): 88-92.

Tachibana M, Adachi W, Kinoshita S, Kobayashi Y, Honma Y, and Matsushima Y (2002a) Androgen-dependent hereditary mouse keratoconus: linkage to an MHC region. *Investigative Ophthalmology & Visual Science* 43 (1): 51-57.

Tachibana M, Okamoto M, Sakamoto M, and Matsushima Y (2002b) Hereditary keratoconus-like keratopathy in japanese wild mice mapped to mouse chrosome 13. *Mamm Genome* 13 (12): 692-695.

Takahashi A, Nakayasu K, Okisaka S, and Kanai A (1990) Quantitative analysis of collagen fiber in keratoconus. *Nippon Ganka Gakkai Zasshi* 94 (11): 1068-1073.

Tanihara H, Inatani M, Koga T, Yano T, and Kimura A (2002) Proteoglycans in the eye. *Cornea* 21 (7 Suppl): S62-69.

Teng C (1963) Electron microscope study of the pathology of keratoconus: I. *Am J Ophthalmol* 55: 18-47.

Termine D, Kleinman K, Whitson W, Conn M, McGarvey L, and Martin R (1981) Osteonectin, a bone-specific protein linking mineral to collagen. *Cell* 26: 99-105.

Theophanides S (1980) Contact Lens Clinical Experiences in Cyrus. *Contacto* 24 (3): 25-27.

Thoft RA, and Friend J (1983) The X, Y, Z hypothesis of corneal epithelial maintenance. *Investigative Ophthalmology & Visual Science* 24 (10): 1442-1443.

Totan Y, Hepsen IF, Cekic O, Gunduz A, and Aydin E (2001) Incidence of keratoconus in subjects with vernal keratoconjunctivitis: a videokeratographic study. *Ophthalmology* 108 (4): 824-827.

Tretter T, Rabinowitz Y, and Yang H (1995) Aetiological factors in keratoconus. *Ophthalmology* 102(supl): 156.

Tuft SJ, and Buckley RJ (1995) Iris ischemia following penetrating keratoplasty for keratoconus (Urrets-Zavalia syndrome). *Cornea* 14 (6): 618-622.

Tuft SJ, Gregory WM, and Buckley RJ (1994) Acute corneal hydrops in keratoconus. *Ophthalmology* 101 (10): 1738-1744.

Tsubota K, Mashima Y, Murata H, Sato N, and Ogata T (1995) Corneal epithelium in keratoconus. *Cornea* 14 (1): 77-83.

Ward A, Artunduaga G, and Thompson P (1995) Phototherapeutic keratectomy for the treatment of nodular subepithelial corneal scar in patients with keratoconus who are contact lens intolerant. *CIAO J* 21: 130-132.

Watsky MA (1995) Keratocyte gap junctional communication in normal and wounded rabbit corneas and human corneas. *Investigative Ophthalmology & Visual Science* 36 (13): 2568-2576.

Weed H, and McGhee J (1998) Referral patterns, treatment management and visual outcome in keratoconus. *Eye* 12: 663-668.

Wentz-Hunter K, Cheng L, and Ueda J (2001) Keratocan expression is increased in the stroma of keratoconus corneas. *Mol Med* 7: 470-477.

Westerhout D (1973) The combination lens and therapeutic uses of soft lenses. *The contact lens* 4: 3-24.

Wheeler C, Morantes M, Kristensen M, Pettit H, and Lee F (1992) Reliability coefficients of three corneal pachymeters. *Am J Ophthalmol* 113 (6): 645-651.

Willson G, Bell C, and Chotai S (1982) The effect of lifting the lids on corneal astigmatism. *Am J Optom Physiol Opt* 59 (8): 670-674.

Wilson SE (2000) Role of apoptosis in wound healing in the cornea. *Cornea* 19 (3 Suppl): S7-12.

Wilson SE, He YG, Weng J, Li Q, McDowall AW, Vital M, and Chwang EL (1996) Epithelial injury induces keratocyte apoptosis: hypothesized role for the interleukin-1 system in the modulation of corneal tissue organization and wound healing. *Exp Eye Res* 62 (4): 325-327.

Wilson SE, Lin DT, and Klyce SD (1991) Corneal topography of keratoconus. *Cornea* 10 (1): 2-8.

Wollensak G, Spoerl E, and Seiler T (2003) Riboflavin/ultraviolet-a-induced collagen crosslinking for the treatment of keratoconus. *Am J Ophthalmol* 135 (5): 620-627.

Wollensak J, and Buddecke E (1990) Biochemical studies on human corneal proteoglycans-a comparison of normal and keratoconic eyes. *Graefes Arch Clin Exp Ophthalmol* 228 (6): 517-523.

Woodward G (1984) Keratoconus - Epidemiology. *J Br Contact Lens Asso* 7: 64-76.

Woodward G (1997) Contact lens in abnormal ocular conditions - keratoconus. In: Speedwell. P ed. *A text book for practitioner and student.* (4th ed) London: Butterworth-Heinemann, pp. 693-705.

Yamani M (2000) *Aspects of drug misuse in the Kingdom of Saudi Arabia.* PhD Thesis, Cardiff University.

Yeniad B, Yigit B, Issever H, and Kozer Bilgin L (2003) Effects of contact lenses on corneal thickness and corneal curvature during usage. *Eye Contact Lens* 29 (4): 223-229.

Zadnik K, Barr JT, Gordon MO, and Edrington TB (1996) Biomicroscopic signs and disease severity in keratoconus. Collaborative Longitudinal Evaluation of Keratoconus (CLEK) Study Group. *Cornea* 15 (2): 139-146.

Zadnik K, Mannis MJ, and Johnson CA (1984) An analysis of contrast sensitivity in identical twins with keratoconus. *Cornea* 3 (2): 99-103.

Zadnik K, Steger-May K, Fink BA, Joslin CE, Nichols JJ, Rosenstiel CE, Tyler JA, Yu JA, Raasch TW, and Schechtman KB (2002) Between-eye asymmetry in keratoconus. *Cornea* 21 (7): 671-679.

Zhou L, Sawaguchi, S. Twining S, Sugar J, Feder RS, and Yue B Y (1998) Expression of degradative enzymes and protease inhibitors in corneas with keratoconus. *Investigative Ophthalmology & Visual Science* 39 (7): 1117-1124.

Zieske J D (1994) Perpetuation of stem cells in the eye. *Eye* 8 (Pt 2): 163-169.

SCIENTIFIC REPORT

Incidence and severity of keratoconus in Asir province, Saudi Arabia

A A Assiri, B I Yousuf, A J Quantock, P J Murphy

Br J Ophthalmol 2005;**89**:1403–1406. doi: 10.1136/bjo.2005.074955

Aim: To assess the incidence and associated signs and symptoms of patients with keratoconus in Asir Province, Saudi Arabia.

Methods: 125 new keratoconus patients (51 male, 74 female; mean age 18.5 (SD 3.8) years; range 8–28 years) were recruited from referrals to the department of ophthalmology, Asir Central Hospital, over a 1 year period. Age, visual acuity, and keratometry were recorded along with clinical signs and symptoms.

Results: The incidence of keratoconus in Asir Province is 20 cases per 100 000 population. Also, the disease severity is high, as indicated by an early mean age (17.7 (3.6) years) with advanced stage keratoconus. Visual acuity, with either spectacles or rigid contact lenses, was 6/12 or better in 98% of eyes measured. Just over half (56%) of patients had atopic ocular disease. 16% of patients had a positive family history of the disease and 16% had atopic dermatitis (eczema and/or vitiligo).

Conclusion: The incidence and severity of keratoconus in Asir Province, Saudi Arabia, is high with an early onset and more rapid progress to the severe disease stage at a young age. This might reflect the influence of genetic and/or environmental factor(s) in the aetiology of keratoconus.

Keratoconus is a non-inflammatory, acquired ectasia that causes progressive, changeable, myopic astigmatism. Mostly it occurs bilaterally but develops asymmetrically,[1] with an onset at puberty and progression over a period of 7–20 years.[2 3] Incidence ranges from 1.4 to 600 cases per year per 100 000 population.[4–9] Most reports have considered white populations, with some studies suggesting an influence of ethnic origin on the incidence and age at onset.[10 11]

Previous studies on keratoconus in Saudi Arabia are very limited.[12 13] This paper reports a prospective study that assesses the incidence rate and associated signs and symptoms of patients with keratoconus in Asir Province, Saudi Arabia.

METHODS

All patients attending the department of ophthalmology, Asir Central Hospital, Saudi Arabia, between May 2001 and April 2002, who were suspected of having keratoconus, were recruited, as were patients newly diagnosed with keratoconus but attending other tertiary hospitals in Asir Province. In total, 125 patients (240 eyes) were recruited, comprising 51 males and 74 females (mean age 18.5 (SD 3.9) years; range 8–28 years). All subjects were examined for case history, visual acuity, keratometry, refraction, and ocular signs. Diagnosis was made on the basis of changes in best corrected visual acuity, familial keratoconus, an irregular surface evidenced by distorted corneal curvature, keratometry, scissoring of the retinoscopic reflex, or irregularity in the red reflex on direct ophthalmoscopy. Clinical signs included at least one of the following: central corneal thinning, apical stromal scaring, Vogt's striae, Fleischer's ring, and Munson's sign. Unusual cases for which a diagnosis could not be established with confidence were excluded. All data were analysed using the statistical software package SPSS 12 (SPSS Inc, USA).

RESULTS

The incidence of keratoconus in Asir Province was calculated using the area population for those aged between 5 and 29 years (654 163),[14] because the disease usually develops within this age range, and because the study's age range was also of this order (8–28 years). With this calculation, the incidence was 20 cases per 100 000. Mean age at diagnosis was 17.7 (3.6) years for males (range 8–24 years) and 19.0 (3.8) years for females (range 12–28 years) (fig 1).

Visual acuity measurements indicated that uncorrected vision decreased with increasing disease severity and was classified on the basis of average keratometry reading (table 1). As corneal astigmatism and curvature increased vision decreased. However, visual acuity (VA) values were variable even for patients at the same disease stage. The data also show that the overall steepening of the cornea produces a greater change in VA than does any increase in astigmatism (fig 2).

Depending on the stage of the disease, VA was improvable for 108 eyes with spectacles, and 132 eyes with rigid contact lenses (table 2). With spectacles, 33% of eyes achieved a corrected VA of 6/6 or better, with 100% achieving 6/12 or

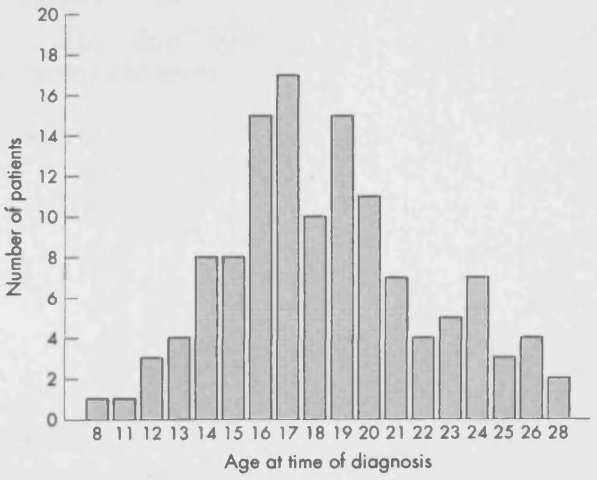

Figure 1 Age distribution of the patients enrolled in the study at the time of ophthalmological diagnosis.

Table 1 Vision varies with severity of keratoconus, but is influenced by the degree of astigmatism and myopia

	Average K reading		
Visual acuity	⩽48 D	> 48–54 D	> 54 D
⩽6/24	57	21	2
>6/24 ⩽6/60	34	68	18
> 6/60	3	13	24
Overall	94	102	44

better. With rigid contact lenses, 93% of eyes achieved 6/6 or better, and 97% 6/12 or better.

The severity of keratoconus was assessed from keratometry reading, in the worse affected eye, and patients' age at diagnosis.[15 16] Based on the keratometry results, the keratoconus population was divided into three groups: early ⩽48D, moderate 48–54D, and advanced >54D (fig 3).

Twenty of 125 (16%) patients had eczema, asthma, and/or vitiligo. Another 20 patients had a family history of keratoconus. There was no evidence of tapeto-retinal degeneration or Reiger's anomaly. Further, we encountered no systemic diseases such as Down's, Marfan's or Ehlers-Danlos syndromes. Seventy of 125 (56%) patients had a positive ocular history for one or more of the following keratoconus associated factors: eye rubbing, ocular allergy, tearing, ocular redness, or vernal keratoconjunctivitis (fig 4). Five patients between the ages of 6 and 12 years reported all five symptoms, and three of these also had a family history of keratoconus.

DISCUSSION

The ability to describe the incidence of a disease is important for predicting current and future clinical needs, and for establishing disease characteristics in a particular population. This study found an incidence of keratoconus in Asir Province, Saudi Arabia, to be 20 per 100 000 based on referrals to the provincial, tertiary level specialist clinic. This compares with 1 per 100 000 in the United Kingdom,[7] 2 per 100 000 in Minnesota (USA),[4] 2.2 per 100 000 in Finland,[5] 2.5 per 100 000 in Holland,[8] and 50 per 100 000 in New Zealand.[6]

The incidence of keratoconus in our cohort is comparable to that of 20–25 per 100 000 in Asian populations living in the United Kingdom but higher than for British white people.[10 11] Environmental influences for these groups will presumably be similar and the higher number of consanguineous marriages among Muslims has been proposed as a cause of the increased incidence.[10 11] Previous reported incidences for a family history of keratoconus in white populations are 6%,[17] 8.8%,[18] and 23.5%,[19] compared to 16% in this study. In one

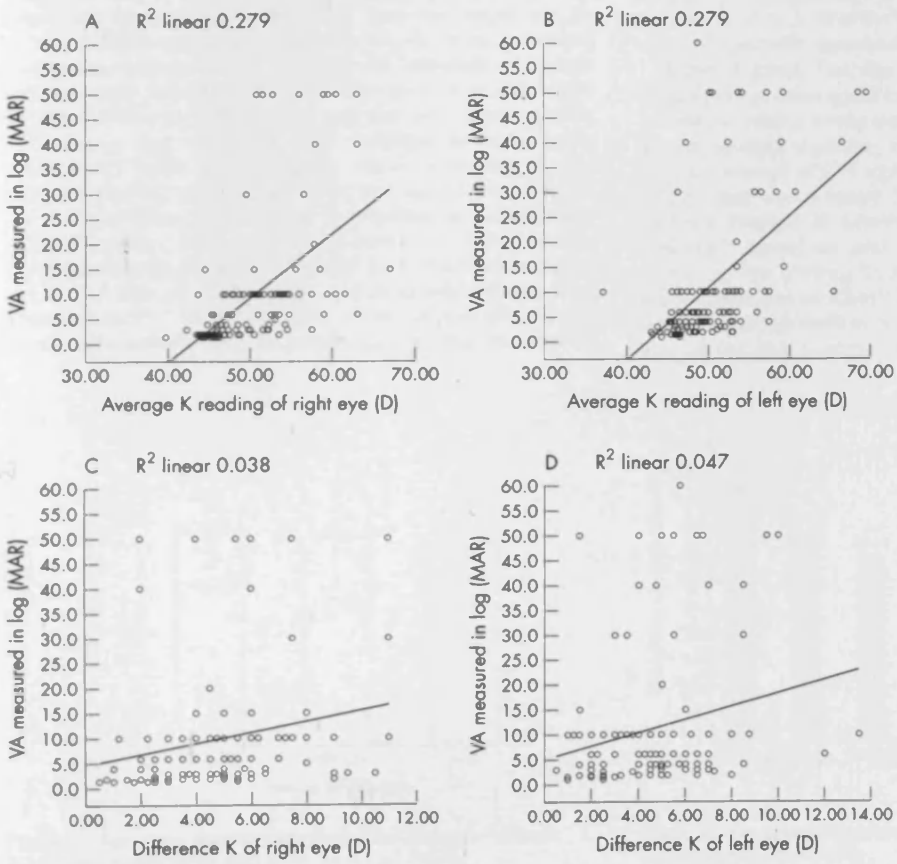

Figure 2 Scatter plot illustrating vision against keratometry measurements. (A, B) Vision decreases with increasing corneal curvature (r^2 =0.28). (C, D) Vision decreases with increasing corneal astigmatism, although with only a weak relation: right eye (r^2 = 0.04) left eye (r^2 = 0.05).

Table 2 Distribution of corrected visual acuity with spectacles and rigid contact lenses

Visual acuity level	With spectacle correction: No (eyes)	With spectacle correction: Cumulative	With rigid contact lenses: No (eyes)	With rigid contact lenses: Cumulative
6/4.5	–	0%	7	5.3%
6/5	–	0%	6	9.85%
6/6	36	33.3%	110	93.18%
6/7.5	8	40.7%	–	0%
6/9	22	61.1%	–	0%
6/12	42	100%	5	96.97%
6/15	–	0%	3	99.24%
6/18	–	0%	1	100%
Total	108 eyes	100%	132	100%

family reported here, of seven children, four had keratoconus in at least one eye.

We should consider the possibility that environmental or geographical factors may have contributed to the incidence and severity of keratoconus found in this study. Asir Province is a mountainous region and the majority of patients in our study (95%) live at an altitude of 3000 metres on average. Here, people are likely have a greater exposure to ultraviolet, given that levels increase with altitude by approximately 10% for every 1000 metres of elevation.[20] Ultraviolet light has previously been linked to keratoconus. Some investigators have proposed that keratoconic corneas have underlying defects in their ability to process accumulated reactive oxygen species, and that this might have a role in the disease pathogenesis.[21 22] The effect of ultraviolet light has also been used to explain the high incidence of keratoconus in New Zealand, which has a white population similar to the United Kingdom, but, because the ozone layer is thinner, a greater ultraviolet background.[19] This link, however, could not be proved definitively since it was not possible to assess actual ultraviolet dosage. Thus, the role of ultraviolet requires further study before it can be determined as a risk factor for keratoconus in patients from Asir Province, Saudi Arabia.

An early age of onset was recorded in this study (18.5 years) with approximately three quarters of our patients (74.4%) presenting before the age of 20 years (in the Collaborative Longitudinal Evaluation of Keratoconus (CLEK) study only 4% presented by this time[17]). Investigations in white populations have reported a higher age at the time of study (mean 27 years) suggesting a later disease onset.[4 10 11 23 24] Our results are comparable to the mean presentation age in Asian keratoconus patients of 20.2 years,[25] 21.5 years,[10] and 22.5 years.[11] Increased disease severity in our subjects is revealed by average keratometry readings, with 94 eyes (39.2%) in the early stage, 102 eyes (42.5%) in the moderate stage, and 44 eyes (18.3%) in the advanced stage. Moreover, 37 eyes in the advanced stage (84%) belonged to subjects 20 years or under, more than the 67% reported elsewhere.[25]

VA decreases as corneal curvature and astigmatism increase (fig 2). However, the correlations are not strong because of the variable influence of the amount, regularity, and obliqueness of the astigmatism, the level of progressive myopia, the scar type, morphology of the cone, and extent of any atopic disease. This indicates that the VA of a keratoconus patient does not present an accurate picture of the progress of the disease. Clinically this is seen when a keratoconic patient presents with an equal bilateral stage of the disease, with a VA in each eye that is manifestly different. Contact lenses generally provided the best means of improving vision, with 93% of eyes achieving 6/6 or better. Only one third of spectacle wearers achieved this level.

Atopic diseases (asthma and atopic dermatitis) have been suggested as aetiological components of keratoconus. Here, we did not find a strong pattern of association with only 16% of our patients reporting any form of atopy. This compares with an average of 35% reported by others.[26 27] A link between allergy and eye rubbing has been reported,[28] with atopic patients thought to develop keratoconus as a result of eye rubbing.[29] Karsersas and Ruben,[30] for example, found a history of eye rubbing in 66% of their keratoconus patients, while Weed and McGhee[31] indicated that 48% of keratoconus patients rubbed their eyes. In the current study, 49 (39.2%) and 56 (44.8%) patients complained of allergy and rubbing,

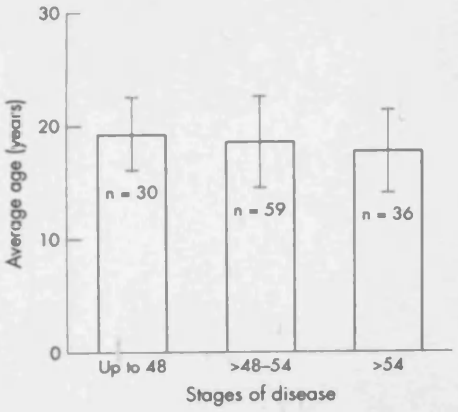

Figure 3 Age at the time of ophthalmological diagnosis for each keratometry group. Error bars show mean (±1.0 SD).

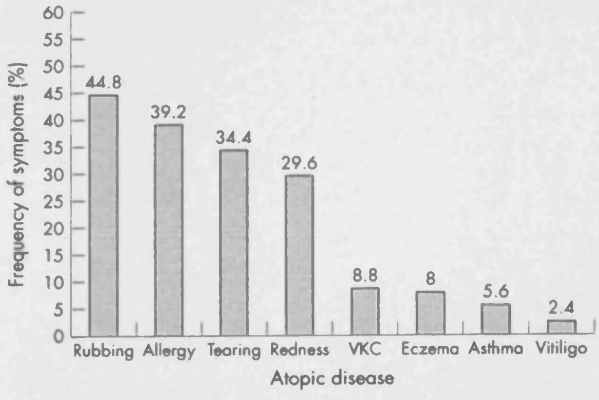

Figure 4 Percentage of patients with ocular signs and symptoms accompanying keratoconus.

respectively. In addition, 15 of 30 (50%) patients in the early stage, 32 of 59 (54%) patients in the moderate stage, and 23 of 36 (63.8%) patients in the advanced stage complained of both allergy and rubbing.

In conclusion, an early onset and increased severity of keratoconus was found in Asir Province, Saudi Arabia. This may be related to a combination of genetic and/or environmental factors. Clinically, contact lens correction should be considered earlier to maximise visual performance. The results have implications for keratoconus screening in Saudi Arabia, to improve early detection and treatment.

The work was done in accordance with the ethical rules of the Saudi Ministry of Health and Asir Central Hospital.

Authors' affiliations

A A Assiri, A J Quantock, P J Murphy, Cardiff University, School of Optometry and Vision Sciences, UK

A A Assiri, B I Yousuf, Asir Central Hospital, Department of Ophthalmology, Saudi Arabia

Supported by the Ministry of Health, and Asir Central Hospital, Department of Ophthalmology, Kingdom of Saudi Arabia.

Competing interests: none declared

Correspondence to: Abdullah M Assiri, Cardiff University, School of Optometry and Vision Sciences, Redwood Building, King Edward VII Avenue, Cathays Park, Cardiff CF10 3NB, UK; assiria@cf.ac.uk

Accepted for publication 6 June 2005

REFERENCES

1 **Zadnik K**, Steger-May K, Fink B, *et al*. Between-eye asymmetry in keratoconus. *Cornea* 2002;**2**:671–9.
2 **Bennett ES**. Keratoconus. In: Bennett ES, Grohe RM, eds. *Rigid gas permeable contact lenses*. New York: Professional Press, 1986:296–344.
3 **Zadnik K**. Keratoconus. In: Bennett ES, Weissman BA, eds. *Clinical contact lens practice*. Philadelphia: JB Lippincott. 1991;**45**:1–10.
4 **Kennedy RH**, Bourne WM, Dyer JA. A 48 year clinical and epidemiological study of keratoconus. *Am J Ophthalmol* 1986;**101**:267–73.
5 **Ihalainen A**. Clinical and epidemiological features of keratoconus: genetic and external factors in the pathogenesis of the disease. *Acta Ophthalmol* 1986;**178**(suppl):5–64.
6 **Sabiston DW**. The crazy cone. *Austral J Ophthalmol* 1978;**6**:43–5.
7 **Duke-Elder S**, Leigh AG. Keratoconus. In: Duke-Elder S, ed. *System of ophthalmology*, Vol 8, No 2. St Louis: Mosby, 1965:964–76.
8 **Woodward EG**. Keratoconus—epidemiology. *J Br Contact Lens Assoc* 1984;**7**:64–76.
9 **Hofstetter HW**. A keratoconic survey of 13,395 eyes. *Am J Optom Arch Am Acad Optom* 1959;**36**:3–11.
10 **Pearson AR**, Soneji B, Sarvananthan N, *et al*. Does ethnic origin influence the incidence of severity of keratoconus? *Eye* 2000;**14**:625–8.
11 **Georgiou T**, Funnell CL, Cassels-Brown A, *et al*. Influence of ethnic origin on the incidence of keratoconus and associated atopic disease in Asians and white patients. *Eye* 2004;**18**:379–83.
12 **Al-Towerki A**, El-Sayed G, Al-Rajhi A, *et al*. Changing indications for corneal transplantation at the King Khalid Eye Specialist Hospital (1983–2002). *Cornea* 2004;**23**:584–8.
13 **Mahmood M**, Wagoner M. Penetrating keratoplasty in eyes with keratoconus and vernal keratoconjunctivitis. *Cornea* 2000;**23**:468–70.
14 **Ministry of Planning, Central Department of Statistics Population and Vital Statistics**. Population Characteristics in the Kingdom of Saudi Arabia: demographic survey. Riyadh: Ministry of Planning, Central Department of Statistics Population and Vital Statistics, 2001:41.
15 **Fowler WC**, Belin MW, Chambers WA. Contact lenses in the visual correction of keratoconus. *CLAO J* 1988;**14**:203–6.
16 **Carmichael TR**, Ben-Smith GJ, Chopamba-Kamba A. Keratoconus associated with limbal vernal keratoconjunctivitis in African patients. *S Afr Optom* 2003;**62**:47–54.
17 **Zadnik K**, Barr JT, Mae O, *et al*. Bio-microscopic signs and disease severity in keratoconus. *Cornea* 1996;**15**:139–46.
18 **Swan PG**, Waldron HE. Keratoconus: the clinical spectrum. *J Am Optom Assoc* 1986;**57**:204–9.
19 **Owens H**, Gamble G. A profile of keratoconus in New Zealand. *Cornea* 2003;**22**:122–5.
20 **Marin MJ**, Sola Y, Tena F, *et al*. The UV index on Spanish Mediterranean coast. *Photochem Photobio* 2005; preprint. Published online Feb 2005.
21 **Kenney C**, Brown D. The cascade hypothesis of keratoconus. *Cont Lens Ant Eye* 2003;**26**:139–46.
22 **Buddi R**, Lin B, Atilano S, *et al*. Evidence of oxidative stress in human corneal diseases. *J Histochem Cytochem* 2002;**50**:341–51.
23 **Lim N**, Vogt U. Characteristics and functional outcomes of 130 patients with keratoconus attending a specialist contact lens clinic. *Eye* 2002;**16**:54–9.
24 **Owens H**, Watters GA. An evaluation of the keratoconic cornea using computerised corneal mapping and ultrasonic measurements of corneal thickness. *Ophthal Physiol Opt* 1994;**16**:115–23.
25 **Saini G**, Saroha V, Singh P, *et al*. Keratoconus in Asian eyes at a tertiary eye care facility. *Clin Exp Optom* 2004;**87**:97–101.
26 **Gasset AR**, Houde WL, Garcia-Bengochea M. Hard contact lens wear as an environmental risk in keratoconus. *Am J Ophthalmol* 1978;**85**:339–41.
27 **Rahi A**, Davies P, Ruben M, *et al*. Keratoconus and co-existing atopic disease. *Br J Ophthalmol* 1977;**61**:761–4.
28 **McMonnies CW**, Boneham GC. Keratoconus, allergy, itch, eye-rubbing and hand-dominance. *Clin Exp Optom* 2003;**86**:376–84.
29 **Barwazeer AM**, Hodge WG, Lorimer B. Atopy and keratoconus: a multivariate analysis. *Br J Ophthalmol* 2000;**84**:834–6.
30 **Karseras AG**, Ruben M. Aetiology of keratoconus. *Br J Ophthalmol* 1976;**60**:522–5.
31 **Weed KH**, McGhee CNJ. Referral patterns, treatment management and visual outcome in keratoconus. *Eye* 1998;**12**:663–8.